N° ordre : 4618

THÈSE

PRÉSENTÉE A

L'UNIVERSITÉ BORDEAUX 1

ÉCOLE DOCTORALE DES SCIENCES CHIMIQUES

Par Maréva FÈVRE

POUR OBTENIR LE GRADE DE

DOCTEUR

SPÉCIALITÉ : POLYMÈRES

PHOSPHINES, CARBÈNES *N*-HÉTÉROCYCLIQUES (NHCS) ET NOUVEAUX PRÉCURSEURS DE NHCS POUR LA CATALYSE ORGANIQUE DE RÉACTIONS (MACRO)MOLÉCULAIRES

Directeur de thèse : Pr. Daniel TATON

Soutenue le : 29 novembre 2012

Devant la commission d'examen formée de :

Mme. CHARLEUX, Bernadette	Professeur, Université de Lyon	Rapporteur
M. FREY, Holger	Professeur, University of Mainz	Rapporteur
M. BACEIREDO, Antoine	Directeur de recherche, Université de Toulouse	Examinateur
M. CRAMAIL, Henri	Professeur, Université de Bordeaux	Examinateur
M. LANDAIS, Yannick	Professeur, Université de Bordeaux	Examinateur
Mme. MIQUEU, Karinne	Chargée de recherche, Université de Pau	Examinateur
M. TATON, Daniel	Professeur, Université de Bordeaux	Directeur de thèse

Les travaux de thèse décrits dans ce manuscrit ont été effectués au Laboratoire de chimie des Polymères Organiques (LCPO) et cofinancés par le CNRS et la région Aquitaine. Je tiens donc tout d'abord à remercier Henri Cramail, notre dévoué et bien-aimé directeur, qui veille chaque jour au bon fonctionnement de ce laboratoire. Merci de m'avoir permis de travailler, un peu bruyamment parfois je vous l'accorde, dans de si bonnes conditions au cours de ces 3 ans. Enfin merci d'avoir accepté de présider mon jury de thèse.

Je tiens à remercier Mme Bernadette Charleux, Professeur à l'Université de Lyon et Mr Holger Frey, Professeur à l'Université de Mainz, qui m'ont fait l'honneur d'être rapporteurs de ce manuscrit. Merci à Mr Antoine Baceiredo, Directeur de recherche à l'Université de Toulouse, Mr Yannick Landais, Professeur à l'Université de Bordeaux et à Mme Karinne Miqueu, Chargée de recherche à l'Université de Pau qui ont eu la gentillesse de bien vouloir participer à mon jury de thèse.

Je tiens à remercier chaleureusement les nombreuses personnes avec qui j'ai eu l'occasion de collaborer pendant cette thèse : Valérie Héroguez, pour son savoir-faire en matière d'émulsions, Karinne Miqueu et Jean-Marc Sotiropoulos, pour avoir accepté de mettre des chiffres sur nos observations (on a encore du mal à prononcer M06-2X et B3LYP mais grâce à vous c'est déjà un peu moins flou !), Yannick Landais et Frédéric Robert, pour leur optimisme sans bornes et leur amour de la chimie (vive les réactions 1/1/1 mais ça ne nous donne toujours pas des polymères tout ça !), Brice Kauffmann, Odile Babot et Christelle Absalon.

Un immense merci à mon chef, Daniel Taton, pour ces trois années qui sont avant tout le fruit d'un vrai travail d'équipe. Merci d'avoir vu en moi (et surtout avant moi) la chimiste qui se cachait bien profondément, merci d'être amoureux de votre métier comme vous l'êtes, merci pour nos discussions (des fois à 3 avec votre Mac…), merci d'être l'architecte des polymères mais aussi des gens qui vous entoure, merci (quand même) à votre jumeau maléfique, merci d'avoir essayé de faire avec ma folie et ma voix "qui porte" (je remarque quand même que depuis que je vous crie dans les oreilles à longueur de journée, vous n'avez plus de pertes d'équilibre !), merci pour votre humour, surtout celui du vendredi soir, merci et encore merci… Quelques lignes ne suffiront jamais de toute façon ! Pour finir, je voulais vous dire que je suis quand même fière de nous, puisque même après les débuts difficiles, on ne s'en est pas trop mal sorti finalement !

Je tiens bien évidemment à remercier tous les membres du LCPO, qui au sein du labo, et en dehors d'ailleurs, contribuent à faire de cet endroit un lieu de travail (et de rigolades) hors pair. Un merci affectueux plus particulier à :

- Antoinette (alias Antoinette) et Katerina (alias Honey, uniquement valable avec une voix aigue !), mes deux comparses avec qui j'ai tout vécu pendant ces trois ans, et à Jules (alias le forain ou papy Jules ou encore au moins 24 surnoms !) qui a ensuite complété le quatuor de choc. Merci d'avoir été mes phares dans la tempête, merci pour nos discussions, nos rigolades merci tout simplement d'être les amis exceptionnels que vous êtes.
- Samira, ma sœur de cœur, pour son soutien inconditionnel et les barres de rire à s'en casser le ventre (et/ou à s'écrouler dans le couloir). Quelques lignes ne suffiront pas à décrire l'amitié que nous partageons, passez simplement en N1-04 ou N1-05 (enfin suivez la musique et les cris), prenez un café et venez partager !
- Nico (alias super carotte), le roi de la SEC, pour nous faire profiter de la mode made in Toulouse, Lebanon. Merci pour ton sens aigue de la patience avec nous, bande d'ânes bâtés de thésards.

- Paul, le dernier arrivé de la famille des craqués de la vie (surtout le vendredi et le jeudi et le mercredi et tous les jours en fait, "c'est un mec qui s'appelle on", le vrai début de la blague!), mon BFF pour ainsi dire. Merci d'avoir été là, merci pour ton humour toujours au rendez vous, merci à tes parents de t'avoir taillé dans le même grain de folie que moi ! Il est bien loin le temps du petit oiseau !
- Les autres membres de la "Team DT": Joan, l'expert de la chimie moléculaire (le roi des orbitales atomiques, du mouais, et des réflexions intenses les yeux fermés), Feng, l'encyclopédie de la chimie (merci pour les polymères qui grandissent dans mes poumons grâce aux agents RAFT qui y ont élu domicile !), Julien, le mec qui sait conjuguer chimie et nature à tous les temps, Jean, Na, Winnie et ses 14 pères, et ceux qui se cherchent encore entre 1er et 2ème : Camille, ma jumelle (courage plus qu'un an ou 2 !) et Dan ou Dany Boy, qui a emporté sa bonne humeur au pays des caribous. Merci aux membres "d'un jour" de cette équipe de choc : Gwen (Maréva, tu vas me tuer !), Leïla (la vérité, c'est chaud), Alexandre et Hélène.
- Les anciens : Bertrounet (Œil de Feu), Steph (j'ai toujours ton boy rose !), Anne-Laure, Aurélie, Célia, Maryline, Aurélien, Chantal (qui a rendu heureux un mec formidable) et tous ceux que j'oublie…
- Les présents : Vincent et Maud, les isolés du N0, Yannick et Karine, qui font pousser des plantes sur leur passage, Cédric, pour m'avoir retourné le cerveau juste avec des thermogrammes, Lise et Thomas, militants pour des polymères plus gras, Audrey, la sportive, même du dimanche, Silvia, pour sa joie de vivre italienne communicative, Charlotte, la reine des soirées déguisées, Maité, Colin, Hugo, Julie, Loïc, Floraine, Jun, le mec à 1g5 même à 13h, Usein, Carine et Chrystilla, les sourires du B8, Feifei, Dargie, Mumu, pour avoir supporté 3 nanas au N1-14 pendant 1 an et encore une fois tous ceux que ma mémoire a oubliés.
- Les futurs : Kévin, Elise (gooo petite fillotte !), Blandine, Estelle, Edgar & co qui sont la relève du LCPO !
- La greek team : Xristos (alias Kota), Eleni (alias Kotoula), et son +1 (alias la Creeete), Eftychia (Ness, Happiness), Maroula (alias Marouli) pour les repas (traditionnels) du vendredi soir, le partage de leur culture, les bars à vins et les week-ends entre potes. Merci à Guigui pour avoir vécu avec moi la vie d'expat' au sein de la communauté grecque de Bordeaux.
- A tous les permanents qui complètent joyeusement le tableau, ce qui ont d'abord été mes profs, et même les autres : Eric P (alias minichef, mister VP), pour son soutien et sa gentillesse sans égal, Seb, pour ses blagues un peu approximatives même à 8h du mat' et pour m'avoir permis de rester quelques mois de plus, (Mr) Eric, pour les conversations à 7h30, Babeth, wouwouwouwou !, Anne-Laure & Manu, mes deux voisins qui ont toujours le sourire aux lèvres, Mimi & Michel, les deux piliers du LCPO, Catherine, le maman adoptive de la moitié du labo (permanents compris), Corinne, Bernadette et Loïc qui œuvrent tous les jours pour le bon fonctionnement de cette machinerie capricieuse, et tous les autres.

Merci enfin à tous les extérieurs au LCPO qui ont, eux aussi, par leur soutien, œuvré à l'accomplissement de ce travail : Noura, Marine et la CP09 ; Samira, Sihame, Tito et la PCSI2 ; les girls du Studio : Mo, Carole et Made d'abord, puis Nat, Oph et Ana, le quatuor infernal. Merci enfin à ma famille, pour leur soutien inconditionnel malgré la distance.

“Our greatest weakness lies in giving up.
The most certain way to succeed is always to try just one more time.”
T. Edison

TABLE OF CONTENTS

Chapter 2. Azolium Hydrogen Carbonates and Azolium-2-Carboxylates as Genuine Sources of N-Heterocyclic Carbenes (NHCs): Applications to the Facile Preparation of NHC Metal Complexes and to NHC-Organocatalyzed Molecular and Macromolecular Syntheses

Chapter 3. Towards an Organic Multitask Activation: N-Heterocyclic Carbenes- Lewis Acids Pairs and their Uses for Polymerization Reactions

Chapter 4. Tris(2,4,6-trimethoxyphenyl)phosphine (TTMPP) as Potent Organocatalyst for Group Transfer Polymerization of Alkyl (Meth)acrylates

List of Abbreviations

ACEM : active chain end mechanism
AcOH : acetic acid
AMM : activated monomer mechanism
BED : (3*S*)-3-(2-{[(benzyloxycarbonyl)]oxy}suethyl)-1,4-dioxan-2,5-dione
BHET : bis(2-hydroxyethyl)terephthalate
β-BL : β-butyrolactone
BLA : boron Lewis acid
BnOH : benzyl alcohol
nBA : butyl acrylate
*t*BA : *tert*-butyl acrylate
t-BuP_4 : *tert*-butylimino)tris{[tris(dimethylamino)phosphoranylidene]amino}phosphorane
Bu_3P : tributylphosphine
C : catalyst
CA : continuous addition
ε-CL : ε-caprolactone
Cy_3P : tricyclohexylphosphine
D : dispersity
DBU : 1,5-diazabicyclo[5.4.0]undec-5-ene
DFT : density functional theory
DMA : *N*,*N*-dimethylacrylamide
DMAEA : 2-(dimethylamino)ethyl acrylate
DMAEMA : 2-(dimethylamino)ethyl methacrylate
DMAP : 4-(dimethylamino)pyridine
DMC : dimethylcarbonate
dMMLABz : [*R*,*S*]-4-benzyloxycarbonyl-3,3-dimethyl-2-oxetanone
DP : degree of polymerization
DSC : differential scanning calorimetry
D3 : hexamethylcyclotrisiloxane
D4 : octamethyltetracyclosiloxane
EO : ethylene oxide
ESI-MS : electron spray ionization mass spectrometry
FLP : frustrated Lewis pairs
GTP : group transfer polymerization (“polymérisation par transfert de groupe”)
HMDI : hexamethylene di-isocyanate
I : initiator
IL : ionic liquid
LA (Chap.1&2) : lactide
LA (Chap. 3) : Lewis acid
LB : Lewis base
M : monomer
M_n : number average molar mass
M_p : peak average molar mass
M_w : weight average molar mass
MALDI-ToF : matrix-assisted laser desorption/ionization-time of flight
MAN : methacrylonitrile

MBL : α-methylene-γ-butyrolactone
MMA : methyl methacrylate
MMBL : γ-methyl-α-methylene-γ-butyrolactone
MOP : multitask organocatalytic platform
MS : mass spectrometry
MTS : 1-methoxy-2-methyl-1-[(trimethylsilyl)oxy]prop-1-ene
NCA : *N*-carboxyanhydride
NHC : *N*-heterocyclic carbene (“carbène *N*-hétérocyclique”)
NHC-CO_2 : azolium-2-carboxylate
NHC-COS : azolium-2-thiocarboxylate
NHC-CS_2 : azolium-2-dithiocarboxylate
[NHC(H)][HCO_3] : azolium hydrogen carbonate
NMP : nitroxide mediated polymerization
NMR : nuclear magnetic resonance
OCA : *O*-carboxyanhydride
P : poly
PBL : poly(β-butyrolactone)
PBuOH : 4-(pyren-1-yl)butan-1-ol
P*t*BA : poly(*tert*-butyl acrylate)
PCL : poly(ε-caprolactone)
PDMS : poly(dimethylsiloxane)
PEO : poly(ethylene oxide)
PET : poly(ethylene terephthalate)
β-PL : β-propiolactone
PLA : poly(lactide)
PMMA : poly(methyl methacrylate)
PO : propylene oxide
PPh_3: triphénylphosphine
PPO : poly(propylene oxide)
PS : poly(styrene)
PVL : poly(δ-valerolactone)
RAFT : reversible addition-fragmentation chain transfer
RI : refractive index
ROP : ring-opening polymerization (“polymérisation par ouverture de cycle”)
RT : room temperature
SAXS : small-angle X-ray scattering
SEC : size exclusion chromatography
SiLA : silicon Lewis acid
SKA : silyl ketene acetal
$TASF_2SiMe_3$: tris(dimethylamino)sulfonium difluorotrimethylsilicate
TBAF : tetrabutylammonium fluoride
TBD: 1,5,7-triazabicyclo[4.4.0]dec-5-ene
TGA : thermogravimetric analysis
TiBP : proazaphosphatrane 2,8,9-triisobutyl-2,5,8,9-tetraaza-1-phosphabicyclo[3.3.3]undecane
T_m : melting temperature
TMC : trimethylene carbonate
TMOSC : 2,2,5,5-tetramethyl-1-oxa-2,5- disilacyclopentane

TMS : trimethylsilyl
TMSCN : trimethylsilylcyanide
TOF : turnover frequency
TS : transition state
TTMPP : tris(2,4,6-trimethoxyphenyl)phosphine
UV : ultraviolet
δ-VL: δ-valerolactone
WL : weight loss
ZROP : zwitterionic ring-opening polymerization

Introduction Générale

La plupart des avancés en chimie des polymères au 20ème siècle ont été dominées par la catalyse organométallique. Mis à part dans les procédés radicalaires, en effet, des espèces organométalliques sont le plus souvent nécessaires pour catalyser ou amorcer les réactions de polymérisation, que celles-ci procèdent en chaine ou par étapes. Il en va de même s'agissant de la modification chimique des polymères. Une telle catalyse métallique permet de conjuguer sélectivité et cinétique rapide. Toutefois, la toxicité des métaux, au sens général, reste problématique dans des domaines sensibles comme le biomédical, l'emballage ou l'électronique.

Les catalyses enzymatique et organique semblent aujourd'hui des alternatives viables à la catalyse organométallique pour la synthèse macromoléculaire. L'organocatalyse, dans son acception générale, s'inscrit dans un contexte de chimie verte. En plus de rivaliser avec les sélectivités et les cinétiques réactionnelles observées avec les catalyseurs métalliques, les polymérisations organocatalysées peuvent être effectuées dans des conditions douces (température modérée, tolérance vis-à-vis des groupements fonctionnels, …).[1-2]

Parmi ces espèces non-métalliques, les carbènes *N*-hétérocycliques ("*N*-heterocyclic carbenes" (NHCs)),[3] ont reçu une attention particulière en synthèse moléculaire, et plus récemment en chimie des polymères. Les carbènes sont des espèces divalentes neutres dotées de six électrons périphériques.

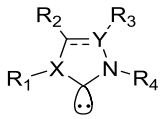

X = N, S ; Y = C, N
Structure des NHCs

Alors que quatre d'entre eux sont impliqués dans une liaison σ, les deux électrons restants sont appariés dans une orbitale non-liante σ. Les NHCs ne sont pas électrophiles à cause de l'interaction forte existant entre les deux orbitales des atomes d'azote et l'orbitale p_π du centre carbénique. Ce sont, au contraire, d'excellentes bases de Lewis et/ou de Bronsted. L'intérêt pour les réactions de chimie moléculaire catalysées par les NHCs s'est considérablement accru au cours des vingt dernières années, en raison de la polyvalence et de l'efficacité de ces catalyseurs pour la construction de liaisons C-C et C-X (X=hétéroatome).[4] Les NHCs sont, en effet, des catalyseurs de choix pour un certain nombre de transformations : réactions de condensation, d'addition 1,2- et 1,4-, de transestérification, d'ouverture de cycles, etc... Plus récemment, le potentiel catalytique des NHCs a été appliqué avec succès en synthèse

macromoléculaire, non seulement dans des réactions de polymérisation en chaine mais aussi de (dé)polymérisation par étapes.[1-2]

Malgré l'incroyable potentiel des NHCs en tant que catalyseurs, un certain nombre de défis restent encore à relever en chimie (macro)moléculaire. Par exemple, leur sensibilité à l'air et à l'humidité limitent encore la généralisation de leur utilisation. De plus, leur synthèse requiert souvent l'utilisation d'une base forte, souvent à basse température, et des étapes de purification compliquées. En chimie des polymères, un panel relativement limité de monomères a été examiné, les monomères polaires comportant des groupements carbonyle (esters, carbonates, anhydrides cycliques) restant les plus étudiés par polymérisation par ouverture de cycle. Enfin, les masses molaires des polymères issus des NHCs sont limitées dans la plupart des exemples rapportés (généralement M_n < 50 000 g/mol).

Dans ce travail de thèse, plusieurs approches ont été développées pour palier certaines de ces limitations. Pour comprendre le succès des NHCs, les caractéristiques essentielles des polymérisations organocatalysées et les mécanismes associés seront d'abord présentés dans le **chapitre 1** de ce manuscrit. L'accent sera mis sur l'utilisation des NHCs pour la synthèse "de précision" de polymères. Les propriétés stériques et électroniques, ainsi que les méthodes de synthèse et de manipulation des NHCs, seront préalablement présentées. Leur potentiel à activer des groupements fonctionnels (e. g. aldéhydes, esters, hétérocycles, silyl cétène acetals, alcools) sera discuté dans un contexte de chimie moléculaire, puis illustré en chimie macromoléculaire. Les polymères ainsi obtenus incluent les polyesters, les polyéthers, les poly(α-peptoide)s, les poly(méth)acrylates d'alkyle, les polyuréthanes, ou encore les polysiloxanes.

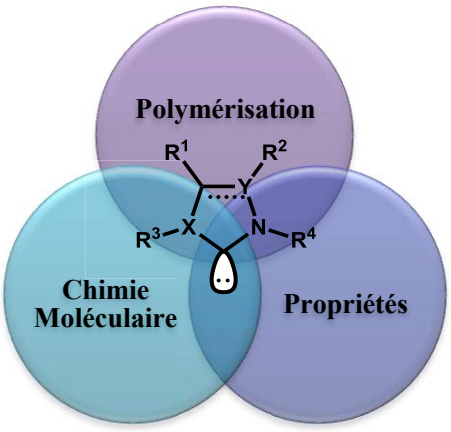

Le **chapitre 2** de ce manuscrit est consacré à la conception de nouveaux précurseurs de carbènes stables à l'air, en l'occurrence les hydrogénocarbonates d'azolium, notés [NHC(H)][HCO_3]. La synthèse de ces composés peut être effectuée en une seule étape à partir de précurseurs commerciaux. Nous montrerons de quelle manière ces précurseurs [NHC(H)][HCO_3] permettent de générer des

NHCs libres. Dans un premier temps, le comportement de ces composés en solution et en phase solide sera discuté. Nous montrerons ensuite comment ils ont été utilisés pour diverses transformations (macro)moléculaires. Leur efficacité catalytique sera comparée avec celle des adduits zwittérioniques homologues de NHC avec le CO_2, notés NHC-CO_2. Enfin, des résultats obtenus par calculs théoriques (Density Functional Theory) seront présentés, dans le but d'élucider les mécanismes mis en jeu lors de la libération du NHC depuis leurs précurseurs [NHC(H)][HCO_3].

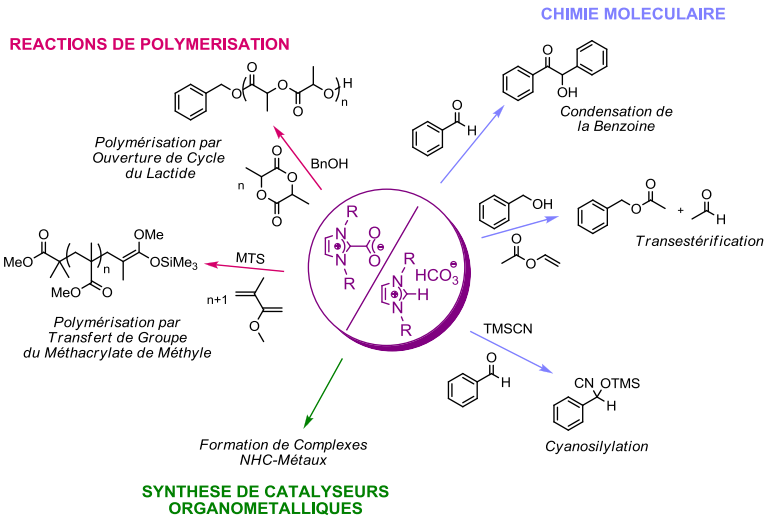

Dans la suite de ce travail de thèse, nous avons choisi d'utiliser un co-activateur afin d'activer des réactions impliquant des substrats tels que le méthacrylate de méthyle et l'oxyde de propylène. Ainsi le **chapitre 3** de ce manuscrit traitera du concept de "catalyse coopérative". Divers acides de Lewis à base de silicium et de bore ont été sélectionnés pour une utilisation en tant que co-catalyseurs électrophiles en sus du NHC, jouant le rôle de nucléophile. Les interactions mises en jeu entre ces deux types de composés ont tout d'abord été étudiées. L'efficacité de telles "paires de Lewis" pour des réactions en synthèse organique et en chimie des polymères a alors été examinée.

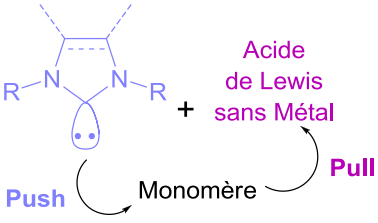

Au-delà des NHCs, nous nous sommes intéressés à des catalyseurs disponibles commercialement, susceptibles de déclencher diverses reéactions de polymérisation. Ainsi, la capacité des phosphines commerciales à catalyser la polymérisation par transfert de groupe ("group transfer polymerization" (GTP)) des (méth)acrylates d'alkyle est présentée dans le **chapitre 4**. Bien que les phosphines soient souvent comparées aux NHCs et que leur utilisation en chimie moléculaire soit bien établie, elles n'ont été que très peu étudiées dans un contexte de polymérisation organocatalysée. L'efficacité d'une

phosphine particulière, la tris(2,4,6-triméthoxyphényl)phosphine (TTMPP), à polymériser le méthacrylate de méthyle (MMA) et l'acrylate de *tert*-butyle (*t*BA) par un mécanisme de type GTP sera démontrée dans ce dernier chapitre. La cinétique de polymérisation du MMA ainsi que la synthèse d'un copolymère à bloc PMMA-*b*-P*t*BA seront enfin présentées.

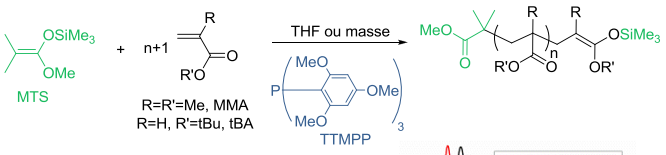

PMMA, PtBA et copolymères à blocs bien définis

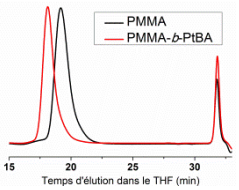

Références :

1. Fèvre, M.; Vignolle, J.; Gnanou, Y.; Taton, D., In *Polymer Science: A Comprehensive Reference*, Editors-in-Chief:; Matyjaszewski, K.; Möller, M., Eds. Elsevier: Amsterdam, 2012; p 67.
2. Kiesewetter, M. K.; Shin, E. J.; Hedrick, J. L.; Waymouth, R. M., *Macromolecules* **2010,** *43*, 2093.
3. Bourissou, D.; Guerret, O.; Gabbai, F. P.; Bertrand, G., *Chem. Rev.* **2000,** *100*, 39.
4. Enders, D.; Niemeier, O.; Henseler, A., *Chem. Rev.* **2007,** *107*, 5606.

Chapitre 1

Etude Bibliographique: Potentiel des Carbènes *N*-Hétérocycliques en tant qu'Organocatalyseurs de Réactions de Polymérisation

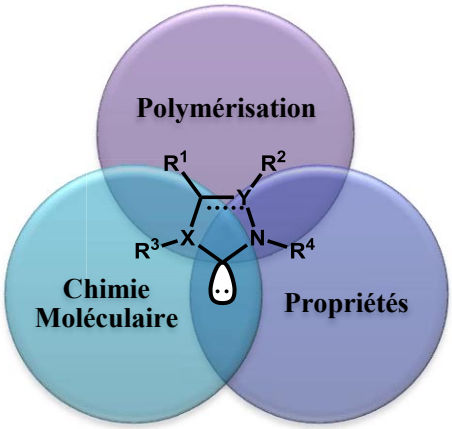

Mots clés: Organocatalyse, Carbènes *N*-hétérocycliques, Polymérisation par étapes, Polymérisation par ouverture de cycle, Polymérisation par transfert de groupe, Mécanisme du monomère activé, Mécanisme du bout de chaine activé.

Keywords: Organocatalysis, *N*-heterocyclic carbenes, Step-growth polymerization, Ring-opening polymerization, Group transfer polymerization, Activated monomer mechanism, Activate chain-end mechanism.

Résumé: Ce chapitre résume les avancées récentes en polymérisation organocatalysée par les carbènes *N*-hétérocycliques ("*N*-heterocyclic carbenes" = NHCs). Dans un contexte où la demande en réactifs et procédés plus respectueux de l'environnement est sans cesse croissante, l'organocatalyse ouvre de nouvelles opportunités en chimie des polymères, par exemple en augmentant les vitesses de polymérisation et en permettant l'accès à des polymères "sur mesure" sans métaux. Les catalyseurs organiques induisent aussi des mécanismes spécifiques pour contrôler les réactions de polymérisation, suivant des modes d'activation différents de ceux généralement observés avec les métaux. Les avantages liés à l'utilisation de ces organocatalyseurs sont discutés dans un premier temps. Les composés organiques susceptibles de catalyser des réactions de polymérisation ainsi que les monomères polymérisables par ces techniques sont brièvement passés en revue.

L'accent est ensuite mis sur les NHCs. Depuis l'isolation des premiers carbènes stables par Bertrand *et al.* et Arduengo *et al.* dans les années 90, l'utilisation des carbènes en chimie a largement été exploitée ces 20 dernières années. En particulier, les NHCs sont devenus non seulement des ligands de choix pour les métaux de transition, mais aussi de véritables catalyseurs organiques en chimie moléculaire et plus récemment, en synthèse de polymères. Leurs voies de synthèse, leurs propriétés et leur potentiel catalytique pour des réactions de chimie moléculaire, à la lumière d'une transposition possible en chimie macromoléculaire, sont ensuite présentés dans ce chapitre.

L'utilisation des NHCs pour des réactions de polymérisation par étapes et en chaine –incluant principalement la polymérisation par ouverture de cycle ("ring-opening polymerization" = ROP) de monomères cycliques, la polymérisation par transfert de groupe ("group transfer polymerization" = GTP) des (méth)acryliques ainsi que certaines polymérisations par étapes (synthèses de polyuréthanes, du poly(éthylène téréphtalate), de polysiloxanes ou de polybenzoines)– est enfin décrite. Les mécanismes putatifs impliqués dans ces réactions de polymérisation sont aussi discutés.

This chapter focuses on organocatalyzed polymerizations. In particular, it discusses how N-heterocyclic carbenes (NHCs) were successfully utilized in this context. The aim of this chapter is neither a comprehensive review on organocatalyzed polymerization reactions nor a complete description of synthesis, properties and use of NHCs in molecular chemistry. It aims at providing the reader the basics to better understand the objectives and the achievements of this PhD work.

This chapter is actually part of a chapter of volume 4 of Polymer Science: a Comprehensive Reference entitled "Organocatalyzed Ring Opening Polymerizations" edited by S. Penczek and R. Grubbs[1] and of a review recently submitted to Chem. Soc. Rev.[2] For further information on the topic of "organocatalyzed polymerization reactions", the reader can refer to this chapter but also to the two previous reviews by Hedrick and Waymouth et al.[3-4]

Excellent reviews can also be found regarding the synthetic developments to carbenes as well as, the electronic properties of these compounds, their reactivity and the means to manipulate them.[5-9] Here, molecular reactions that have inspired their use as organic catalysts for polymer synthesis are presented. For more information on NHC-catalyzed reactions in molecular chemistry, the reader is referred to review articles by Enders et al.,[7,10] Nolan et al.,[11] Rovis et al.,[12] and Glorius et al.[13] In the same vein, the use of NHCs as ligands of catalytically active metallic complexes in (macro)molecular chemistry, as well as structural components for polymer synthesis, will not be covered and can be found elsewhere.[14-17]

Chapter 1

Bibliographic Study: The Potential of *N*-Heterocyclic Carbenes as Organocatalysts of Polymerization Reactions

TABLE OF CONTENTS

Introduction

Polymer chemistry has been dominated in the 20th century by radical processes, on one hand, and by metal-based catalysis, on the other. Besides polymers obtained by radical polymerization standing for about 50% of polymeric materials produced industrially,[18] most of other synthetic polymers require metallic species to catalyze, activate or initiate elementary reactions that bring about their synthesis.[19-20] In most cases, the metallic catalyst (typically, organometallic complexes based on transition metals or metal-based ionic species) represents minute amounts and remains in the final polymer. To prevent hazards due to the presence of toxic metallic species that can freely migrate out of the polymeric material when in service, a purification process is sometimes required which adds to the cost of the polymer produced. Besides this, in sensitive domains such as biomedical, packaging, and microelectronics, metal-based catalysts are prohibited.

Organic and enzymatic catalysis appear today as reliable alternatives to metal-mediated catalysis for polymer synthesis.[3-4,21-22] Organocatalysis, in its general sense, is a part of the general concept of catalysis and is categorized as Green Chemistry. Organocatalysis is actually known for a while, since Justus Liebig reported, as early as 1859, the synthesis of oxamide employing acetaldehyde as organic catalyst (Scheme 1).[23-24] A few decades later, Emil Fischer developed the glycosidation process using acids as catalysts (Scheme 1).[25-27]

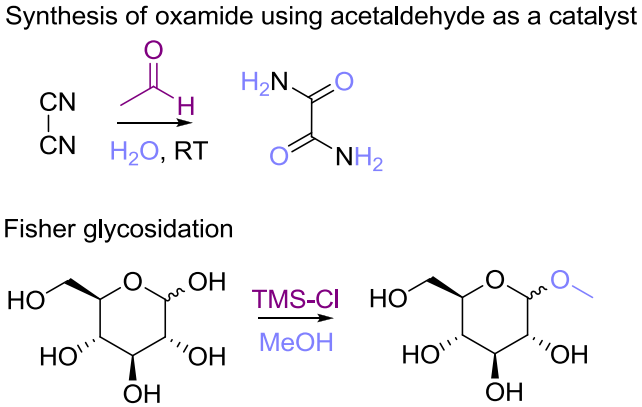

Scheme 1. First molecular reactions involving an organic species as catalysts: synthesis of oxamide using acetaldehyde[23-24] and Fisher glycosidation with TMS-Cl.[25-27]

Other significant examples of organocatalytic approaches have been reported in the 1970s.[28-30] However, not less than a century passed before organocatalysis could be finally recognized as the third pillar of catalysis,[3] besides metallic catalysis and enzymatic catalysis.

In the last decade, tremendous efforts have been made in molecular chemistry to develop powerful organocatalysts for a variety of transformations. Most of the work has focused on enantioselective processes using chiral organocatalysts, taking inspiration from the *modus operandi* of enzymes to catalyze reactions in a biomimetic fashion. In this regard, organocatalysts are sometimes viewed as "minimal enzymes" possessing advantages of biocatalysts, such as selectivity and mild reaction conditions, without their drawbacks, such as the complexity of their structure/conformation, their lack of availability and their lack of robustness due to possible deactivation/denaturation.[31] In molecular chemistry, most of the organocatalyzed enantioselective transformations can be classified as follows:

i) asymmetric C-C bond and C-X-forming reactions (X=O,N,H…; e.g. Michael additions, Mannich reactions, aldol additions, vinylogous aldol additions, allylation reactions, α-alkylation of amino acids, α-halogenation or α-amination of carbonyl compounds, protonation, etc.);

ii) enantioselective oxidation-reduction processes: epoxidations, sulfoxidations of thioethers, enantioselective reduction processes, α-hydroxylation of carbonyl compounds.

Numerous reviews and book chapters have already been reported on the general topic of organocatalysis in molecular chemistry.[7,11,32-48] It is not yet viewed as a mature field and it is far from being applied in the chemical industry. A representative example, however, is the synthesis of the Wieland-Miescher ketone developed in 1970 on industrial scale, *via* an enantioselective organocatalytic aldol process employing L-proline as a chiral organocatalyst (Scheme 2).[49-50]

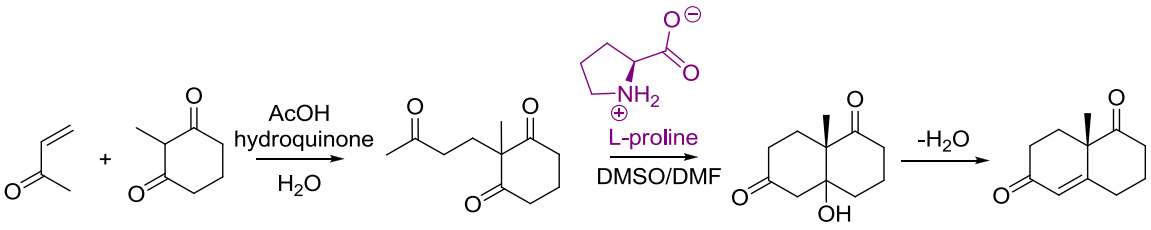

Scheme 2. Example of an organocatalytic molecular reaction developed at the industrial scale: synthesis of Wieland-Miescher ketone using **L**-proline.[49-50]

In the last decade, organocatalysis has also been applied to a few polymerization reactions, in an attempt to replace metal-based catalysts and to enhance the rate of polymerization through activation of monomers and/or polymer chain ends.[3-4]

Use of organic promoters in polymerization reactions is actually known for a while. For instance, polyurethane synthesis by step-growth polymerization of multi-hydroxy compounds with multi-isocyanates can be catalyzed with tertiary amines, such as 1,5-diazabicyclo[5.4.0]undec-5-ene (DBU) or triethylamine.[51] The group transfer polymerization (GTP) of methacrylic monomers can be also categorized, to some extent, as organocatalyzed polymerization when a metal-free nucleophilic catalyst (Lewis base) is employed.[51] Finally, works by the group of Penczek in the late 80s regarding the cationic ROP of cyclic ethers by acids such as BF_3, HPF_6 or trifluoromethanesulphonic acid can also be mentioned as first examples of a metal-free approach for precision polymer synthesis.[52]

However, the (re)emergence of the field of organocatalyzed polymerizations dates back to 2001 with reports by Hedrick (IBM), Waymouth (Stanford) and coworkers who employed dialkylaminopyridines for the ring opening polymerization (ROP) of lactones and lactide.[53-54]

This chapter covers past and recent achievements related to polymerization reactions employing organic catalysts, with a special emphasis on *N*-heterocyclic carbenes (NHCs). This field -including chain and step-growth polymerizations- has been reviewed in 2007 and at the beginning of 2010 by Hedrick, Waymouth *et al.*[3-4] Roughly, two hundreds of papers have been published in peer-reviewed journals in the past 15 years. In the introduction, the meaning of "organocatalyzed polymerization" will be specified. This will be followed by an overview of main catalysts and monomer candidates that have been employed to this end. General polymerization mechanisms encountered will be also discussed. As mentioned, this chapter focuses on the use of NHCs in metal-free polymer synthesis, with a short introduction on their synthesis, properties and reactivity in molecular chemistry. Their use in polymerization reactions, including chain-growth, mainly by ring opening polymerization and by group transfer polymerization, and step-growth processes will be overviewed.

1. Metal-free initiated versus metal-free organocatalyzed polymerizations

Beyond radical processes accounting for about 50% of polymeric materials produced industrially,[18] the use of organic promoters for the purpose of metal-free polymer synthesis is well-documented.[4] A distinction should be made, however, between metal-free polymerizations triggered by organic initiators, with truly organocatalyzed polymerizations, where an organic promoter is used in the presence of a chain length regulator as the other component.

For instance, the ROP of *N*-carboxyanhydrides can be readily initiated with amines, as reported in the early 1970s.[55] Another example is the ROP of *β*-lactones that can be triggered with amines, phosphines, or tetraalkyl ammonium carboxylates as organic initiators.[56-57] The same is true for the ROP of epoxides in the presence of organic amino-containing initiators.[56] The cationic ROP of 2-alkyl oxazolines generally employs organic benzyl halides or alkyl tosylates.[58] Initiation of the zwitterionic chain-growth polymerization of cyanoacrylates can be achieved with phosphines,[59] etc. In all cases, the organic initiator is part of the polymer being formed (Scheme 3). In contrast, an organic catalyst should be regenerated at the completion of the polymerization process and, ideally, it is employed in sub-stoichiometric amounts relatively to the initiator.

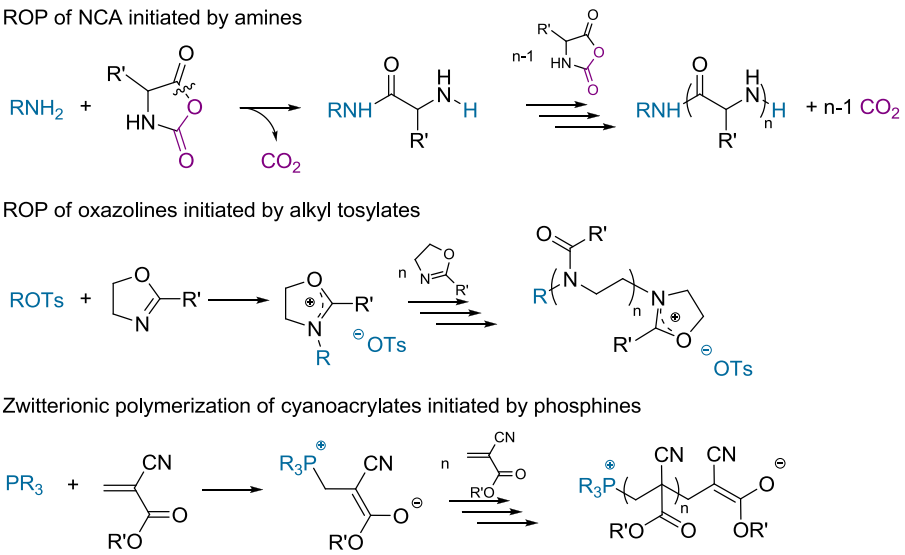

Scheme 3. Examples of metal-free initiated -but not catalyzed- polymerizations.

2. Organocatalytic platforms, monomer candidates and related mechanisms

2.1. The different organic catalysts

Only organocatalysts employed in polymerization reactions are here considered (Figure 1). *N*-heterocyclic carbenes will be discussed in more details in section 3.

Organic catalysts include Bronsted acids, from weak carboxylic derivatives (e.g. CF_3COOH, lactic acid, alanine, etc.) to stronger acids (e.g. CF_3SO_3H, CH_3SO_3H, etc.) and so-called "superstrong" acids (e.g. $(CF_3SO_2)_2NH$ and $(C_4F_9SO_2)_2NH$), Bronsted bases (e.g. phosphazenes such as (tert-butylimino)tris{[tris(dimethylamino)phos phoranylidene]amino}phosphorane *t*BuP_4, pyridine derivatives, NHCs, etc.), Lewis bases (mostly phosphines, 4-(dimethylamino)pyridine, guanidines, NHCs, etc.) and bifunctional systems, as a result of the combination of two antagonist catalytic moieties, within the same molecule or not. In the latter case, however, the strength of each antagonistic reactive center has to be moderate enough not to quench the system (e.g. a strong Bronsted acid combined with a strong Bronsted base will react together preventing any monomer activation). Such organic catalytic systems lead to cooperative activation of the monomer and initiator (see section 2.3.4). In this respect, bifunctional organocatalysts find analogies with multi-centered enzymatic catalysts, which allow synergistic interactions with the different reaction partners with high selectivities. Typical example of a dual activation by hydrogen bonding is provided by the bicyclic guanidine 1,5,7-triazabicyclo[4.4.0]dec-5-ene (TBD),[60-61] or by combination of a thiourea moiety with an amino group, in a mono- or a bicomponent catalytic system (see Scheme 8).[62]

2.2. Monomer candidates

Figure 2 shows the different families of monomers that were subjected to an organocatalyzed polymerization pathway, with their name and abbreviation as will be used hereafter. In their vast majority, monomers amenable to organocatalyzed polymerizations are heterocyclics. In particular, carbonyl-containing heterocyclics were employed in ring opening polymerization (ROP) by almost all categories of the organic catalysts.[1] Carbonylated heterocycles include lactide (both in its racemic and

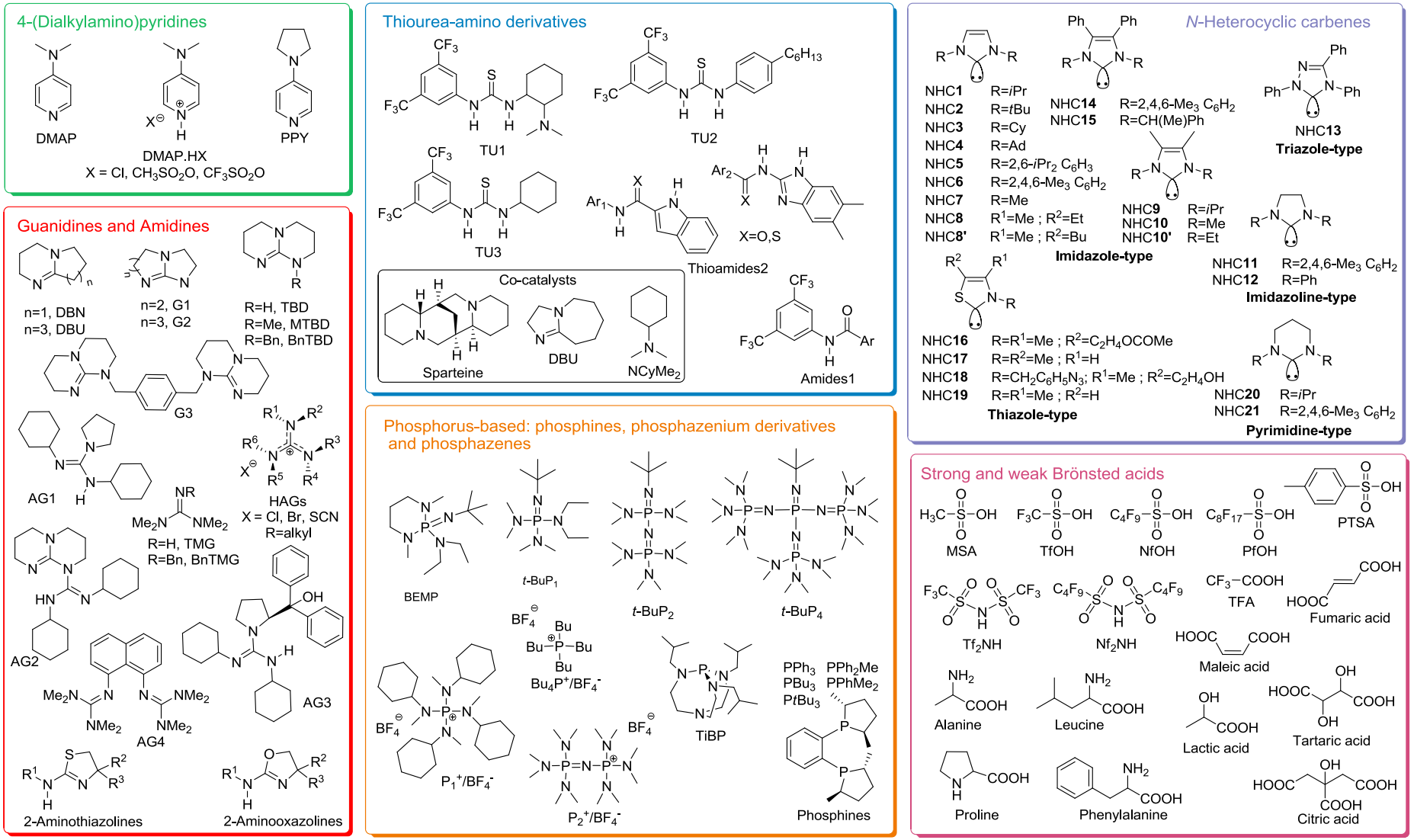

Figure 1. Organic catalysts used for polymerization reactions

enantiopure versions, *rac*-LA and D- or L-LA, respectively), lactones, cyclic carbonates, *N*-carboxyanhydrides, and 1,3-dioxolane-2,4-diones, referred to as *O*-carboxyanhydrides (OCAs). In the two latter cases, the driving force of the polymerization is the evolution of a CO_2 molecule in each propagation step. For instance, the ROP of L-Lac-OCA proved a competitive synthetic route to poly(lactide) (PLA) compared to the ROP of LA.[63]

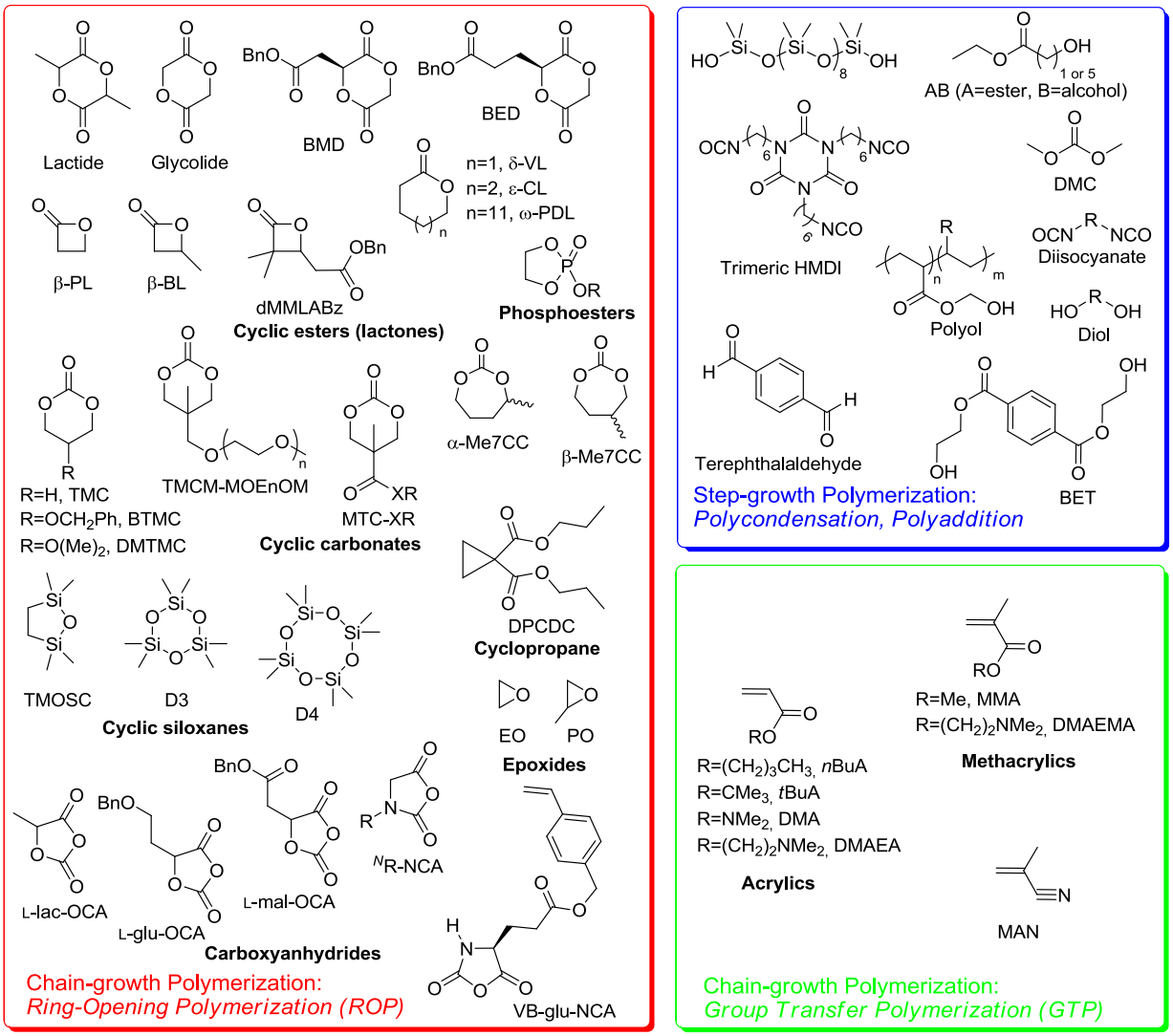

Figure 2. Monomers polymerized *via* an organocatalytic pathway.

Many of these heterocycles are commercially available. They arise from petroleum as resource, except LA. Methyl substituted seven-membered ring carbonates (7CCs), namely, 4-methyl- and 5-methyl-1,3-dioxepan-2-one (R-Me7CC and β-Me7CC), have been synthesized by cyclization of the corresponding α,ω-diols drawn from green renewable acids.[64] Specific monomers incorporating functional groups in a protected form, e.g. protected functional cyclic carbonates or L-Glu-OCA or

(3*S*)-3-(2-{[(benzyloxycarbonyl)]oxy}suethyl)-1,4-dioxan-2,5-dione (BED) were purposely designed, sometimes *via* multi-step synthetic methods.[65-67] Introduction of pendant functional groups in the resulting polymers was aimed at bestowing better degradation properties, and greater hydrophilicity of these materials. Less polar cyclic monomers, such as ethylene oxide, and propylene oxide, cyclosiloxanes and cyclocarbosiloxanes have also been reported to undergo a metal-free ROP, in particular using NHCs as organocatalysts.

Besides, some organocatalysts, including NHCs and strong Bronsted acids, were shown to bring about the group transfer polymerization of both acrylic and methacrylic monomers.[68-71] A few examples of polymers obtained by step-growth polymerizations were also described, including poly(ester)s, poly(ethylene terephthalate) (PET), poly(benzoin) and poly(siloxane)s.[72-74] Interestingly, NHCs,[75] and more recently 1,5,7-triazabicyclo[4.4.0]dec-5-ene (TBD),[76] proved efficient to trigger depolymerization processes, opening avenues for an organocatalytic pathway to polymer degradation/recycling.

2.3. General polymerization mechanisms

Since organic catalysts may operate differently as compared to metal-based ones, they may offer a diversity of mechanistic pathways to control the polymerization. In the particular case of the ROP of heterocycles, four distinct mechanisms can be singled out, depending upon the nature of the active center of the organocatalyst used: acid *vs* base and/or electrophilic *vs* nucleophilic.[4] In the presence of a purposely added "chain regulator", i.e. an initiator controlling the resulting polymer chain length – typically an alcohol in the following examples–, the organocatalyst can activate either the latter initiator then the polymer chain ends after repetitive propagation steps, or the monomer substrate. However, some organic catalysts can provide dual activation, that is, in a cooperative fashion (see further).

Polymerization proceeding by activation of the monomer refers to as the *activated monomer mechanism* (AMM) –following either a nucleophilic or an electrophilic pathway–, whereas polymerization by activation of the initiator/polymer chain ends refers to as the *active chain end mechanism* (ACEM). In some cases, it is unclear whether polymerization occurs solely by monomer

activation, initiator activation or both. Sometimes, one mechanism is exclusive (as in the case of bulky non-nucleophilic phosphazenes, which operate as strong bases to activate the initiator) but, different mechanisms may be operative concomitantly.

2.3.1. Nucleophilic activated monomer mechanism

AMM has been suggested in the early 70s for several polymerizations involving organometallic species. A typical example is the ROP of ε-caprolactam by lithium amides, as illustrated in Scheme 4.[77] With the recently developed nucleophilic organic catalysts, the nucleophilic AMM proceeds by a direct attack of the cyclic monomer by the catalyst (Nu, Scheme 5). This ring opening generates a zwitterionic intermediate, typically an alkoxide featuring a bulky and soft counter-cation, e.g. pyridinium, imidazolinium when 4-(dimethylamino)pyridine (DMAP) or a NHC is used, respectively. Protonation of this zwitterionic "activated monomer" by the alcohol initiator (ROH), and subsequent displacement of the bound catalyst by the alkoxide arising from the initiator (RO^-), generates a ring-opened alcohol mono-adduct, with concomitant release of the organic catalyst. The next propagation step proceeds in the same way, i.e., by activation of the monomer, except that, this is the alcohol mono-adduct which reacts with the activated monomer. This nucleophilic AMM mechanism has been proposed for miscellaneous nucleophilic organocatalysts, such as DMAP, 4-pyrrolidinopyridine (PPY), trialkyl- and triarylphosphines, and NHCs.

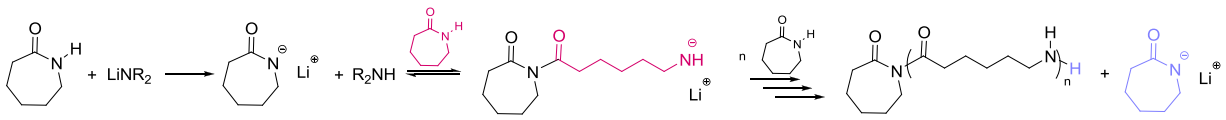

Scheme 4. ROP of ε-caprolactam by lithium amides (nucleophilic activated monomer).[77]

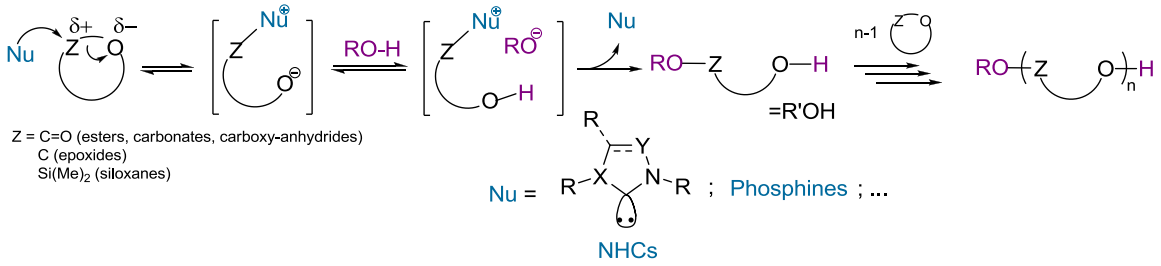

Scheme 5. Activated monomer mechanism (AMM) *via* nucleophilic monomer activation.

2.3.2. Acidic activated monomer mechanism

As already mentioned, the AMM induced by Lewis or Bronsted acids has been established by Penczek *et al.* for the ROP of cyclic ethers.[78-79] However, only Bronsted acids will be considered in this section, as they are involved in most of the organocatalytic pathways which are thought to proceed *via* AMM. In this case, the catalyst (noted "H^+") activates the cyclic monomer through protonation of the heteroatom: the oxygen of the carbonyl group for cyclic esters or the oxygen atom of cyclic ethers (Scheme 6). The resulting activated monomer undergoes ring-opening by nucleophilic attack of the oxygen of the alcohol initiator –or polymer chain end–, leading to the formation of the mono-adduct alcohol, while the acidic catalyst is regenerated. Strong and weak acids have been reported to induce such an acidic AMM in the case of the ROP of epoxides, LA, lactones or cyclic carbonates (Scheme 6).[1]

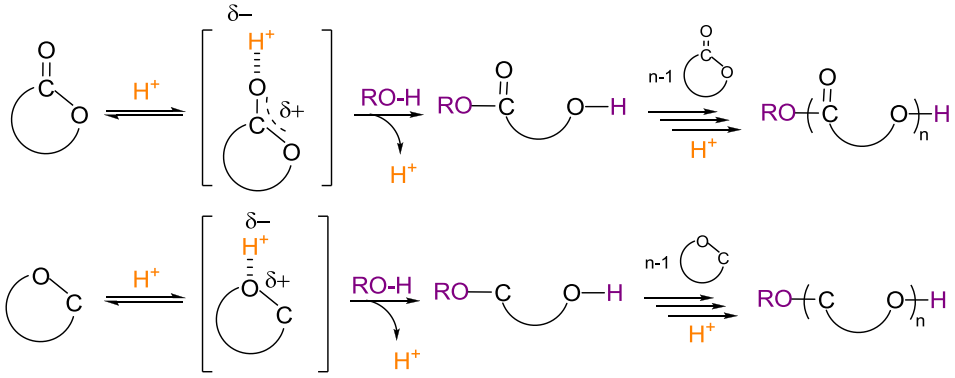

Scheme 6. Activated monomer mechanism (AMM) *via* acid (H^+) monomer activation (top: case of cyclic esters; bottom: case of cyclic ethers).

2.3.3. Active chain-end mechanism

ACEM occurs in the anionic or ionic coordinated ROP of many heterocycles mediated by organometallic species. Propagation occurs by the direct attack of the active chain end (an alkoxide, a carboxylate, a silanolate or a thiolate) on the cyclic monomer. With metal-free organic catalysts, a similar mechanism can operate but under milder conditions. The basic catalyst typically activates the initiator (or the polymer chain end), most often by hydrogen bonding thereby increasing its nucleophilicity, which favors the attack on the cyclic monomer (Scheme 7). Depending on the pK_a

difference between the initiating alcohol and the Bronsted base, the RO-H proton can be completely transferred to the basic site, thus generating an alkoxide.

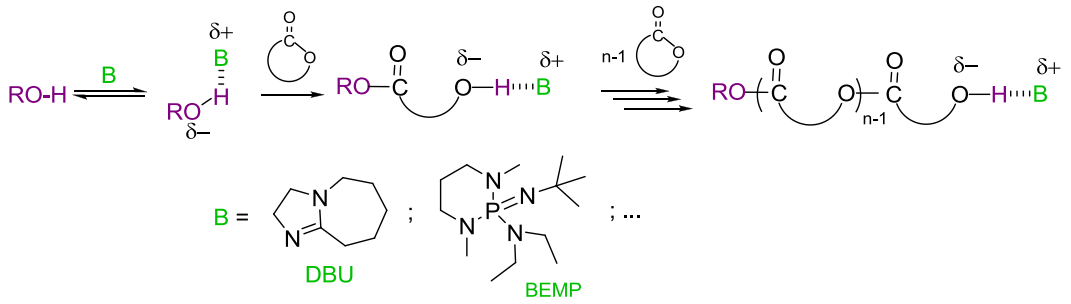

Scheme 7. Basic activated initiator/chain end mechanism (ACEM).

2.3.4. Dual Activation of monomer and initiator/chain end

Cooperative dual activation of both the monomer and the initiator/polymer chain end can be operative with specific catalysts (e.g. thiourea-amino derivatives, 1,5,7-triazabicyclo[4.4.0]dec-5-ene (TBD) or even DMAP) as a means to trigger the ROP of cyclic esters (Scheme 8). Here also, analogies can be found with some metal-based or enzymatic catalysts which have been suggested to behave by such a dual activation.[56] Using true organic catalysts for ROP implies that an electrophilic moiety (typically a proton) activates the heteroatom of the cyclic monomer, while a basic moiety (e.g. an amino-type function) interacts with the proton of the alcohol initiator, increasing its nucleophilicity.

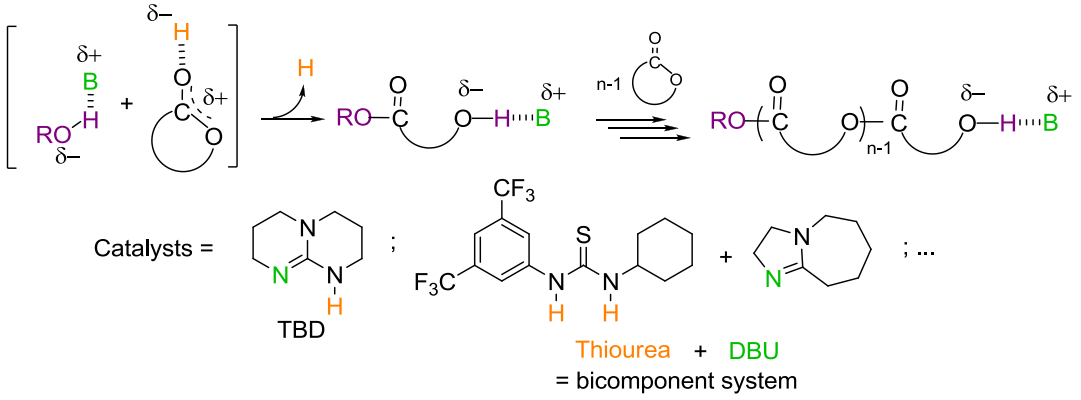

Scheme 8. Dual cooperative activation of both the monomer (by an H-bond donor, noted H) and the alcohol initiator (by an H-bond acceptor, noted B).

Many of the aforementioned organic catalysts provide high rates and selectivities, tolerance to functional groups, easy handling, environment-friendliness, and sometimes offer opportunities for new synthetic strategies and precision polymer synthesis.[3-4]

3. *N*-Heterocyclic carbenes (NHCs)

NHCs are a specific subgroup of carbenes. The first isolated stable carbene was actually an acyclic non-NHC, i.e. a (phosphinosilyl)carbene, synthesized by Bertrand *et al.* in 1988.[80] A few years later, Arduengo *et al*. succeeded in the isolation of the first NHC, namely 1,3-diadamantylimidazol-2-ylidene.[81] Variation of R^1-R^4 substituents of NHCs (Figure 3) offers opportunities to tune both the electronic and steric properties, hence to modulate their reactivity/nucleophilicity.

Since these pioneering works on stable carbenes, these species have received a considerable attention in molecular synthesis,[7,11-12] and more recently, in macromolecular chemistry as well.[3-4] Stable singlet carbenes, and in particular NHCs, have not only become versatile ligands for transition metals,[9,14-15,82-83] but also powerful organocatalysts for a variety of organic transformations.

Many of these NHC-catalyzed reactions are based on the activation of the carbonyl group (e.g. benzoin condensation, Stetter reaction, transesterification, etc.),[7,12] though other electrophilic groups such as trimethylsilyl can be activated (e. g. cyanosilylation or (trifluoromethyl)silylation reactions).[84]

After a summary on synthetic methods to NHCs, properties and means to manipulate them, this section briefly discusses the use of NHCs as organocatalysts for molecular chemistry, regarding elementary reactions that may be transposed, to some extent, to polymer synthesis. Finally, the potential of NHCs as organocatalysts for polymerization reactions, including step-growth (de)polymerizations and chain-growth polymerizations (i.e. ring opening polymerization and group transfer polymerization) will be highlighted.

3.1. Properties, synthesis and manipulation

3.1.1. Properties

Carbenes are neutral divalent species of carbon, possessing six peripheral electrons in their valence shell. Four of them are involved in two σ-bonds with the two adjacent substituents, while the two non-bonding electrons remain at the central carbon. When the carbene center is not properly substituted, these species are highly reactive with lifetime typically under 1s (0,1-1 ns).[85]

The geometry of the carbenic atom is most of the time bent -as for NHCs- instead of linear.[8] In the case of a bent geometry, the carbon atom adopts an sp^2-type hybridization. The p_y orbital is then called p_π as it is almost unchanged, whereas the p_x orbital is stabilized by acquiring some s-character and is then called σ. Depending on the ground state multiplicity, two main electronic configurations can be considered :[8]

- Triplet state: $\sigma^1 p_\pi^1$, where the two electrons have parallel spins (one electron is located in each orbital). These carbenes are thought to behave as diradical species.
- Singlet states: σ^2 and p_π^2, where the two electrons are paired in the same orbital. As the σ orbital is generally the most stable, the σ^2 configuration is then favored. As these carbenes have one filled (σ) and one empty (p_π) orbitals, they should possess an ambiphilic character.

As depicted in Figure 3,[8] the two non-bonding electrons of NHCs, and of diaminocarbenes in general, adopt a σ^2 configuration. NHCs are thermodynamically stabilized by inductive and mesomeric effects. Indeed, the N atoms surrounding the carbon center are σ-electron-withdrawing but π-electron-donating substituents:

- Inductive effect: The σp_π gap is increased because the σ-electron-withdrawing N,X atoms stabilize the σ orbital by increasing its s-character.
- Push-push mesomeric effect: The σp_π gap is increased because of the mesomeric interaction of the lone pairs of the π-electron-donating N atoms with the p_π orbital that increase the p_π orbital energy level.

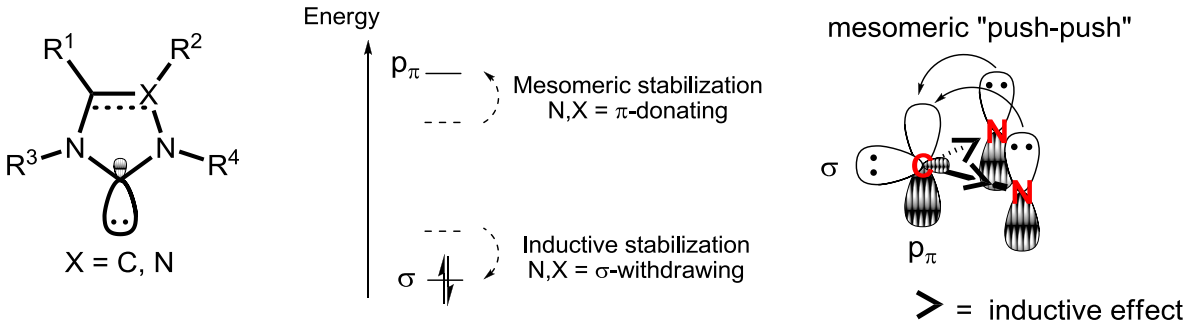

Figure 3. General structure of NHCs and electronic stabilization of NHCs.[8]

Finally, the more bulky the substituents (R^3, R^4) are, the more –kinetically– stabilized the NHC is; because the carbon center is less accessible.

Recent studies have shown that NHC**6** and NHC**11** (Figure 1) are much better Lewis bases than DMAP, DBU and PPh_3 (Figure 1).[86] NHCs can also behave as strong Bronsted bases. The pK_a of corresponding conjugated acid of some carbenes were determined both experimentally[87] and theoretically;[88] they range between 15 and 39 depending on the solvent (pK_a values of corresponding azolium salts in water at 25 °C: NHC**2**~25, NHC**5** and NHC**6**~21, see Figure 1).

The existence of the "Wanzlick equilibrium" (Scheme 9), that is, the equilibrium between the free NHC and its dimer, has been the subject of a debate.[89-92] However, it is generally admitted that dimerization of imidazole-type NHCs is thermodynamically unfavorable, whereas imidazoline and benzimidazole-type NHCs have strong tendency to dimerize.[93] The latter property has been used by the group of Bielawski to synthesize conjugated polymers from the dimerization of bis(NHC)s used, in this case, as bifunctional monomers in step growth polymerization.[17,94]

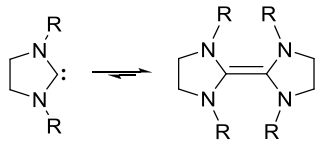

Scheme 9. Wanzlick's equilibrium of imidazolin-2-ylidenes.

3.1.2. Synthesis

NHCs are generally obtained *via* one of the four following routes (Scheme 10): deprotonation of imidazol(in)ium salts,[95] chemical reduction of imidazol-2(3H)-thiones,[96] electrochemical reduction of azolium precursors in a one-electron solution process, or generation from "masked" NHCs, mainly by thermolysis.

Synthetic access to NHCs by deprotonation of imidazol(ni)um salts utilizes a strong base (NaH, *t*-BuOK, *n*BuLi, …) in an aprotic solvent (THF, Et_2O or toluene), as shown in Scheme 10a.[95] This method potentially gives access to a wide range of imidazole- and imidazoline-type NHCs, as most of their corresponding imidazol(in)ium salts, often referred to as ionic liquids,[97] are commercially

available.[98] This technique can lead to chemically pure "naked" NHCs, free of any metallic residues, – e.g. by distillation/sublimation or crystallization–. This strategy can be also applied, however, for the *in-situ* generation of NHCs, although in this case, the metallic contaminants may remain in the reaction media. Polymer-supported versions referred to as "poly(NHC)s" have also been investigated.[82,99-103]

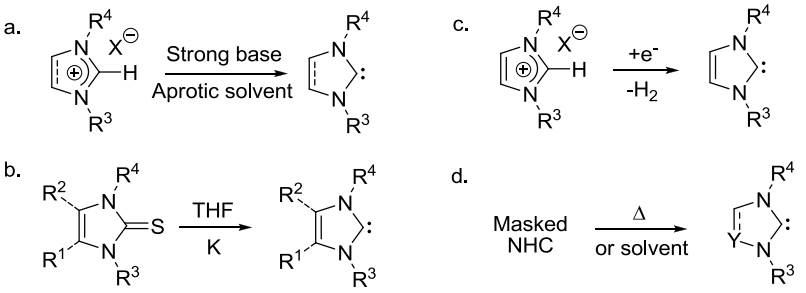

Scheme 10. Generation of NHCs *via*: a. deprotonation of an imidazol(in)ium salt with a strong base, b. reduction of an imidazol-2(3H)-thione, c. electrochemical reduction of an azolium salt, d. thermolysis of "masked" NHCs (see Figure 4).

Alternatively, Kuhn and co-workers developed a synthetic approach to alkyl-substituted NHCs (R^1-$R^2 \neq H$), thus overcoming one of the limitations of the deprotonation technique (R^1-R^2=H).[96] This method relied on the reduction of imidazol-2(3H)-thiones with potassium in boiling THF (Scheme 10b).

The *in-situ* generation of NHCs can also be conveniently performed by electrochemical reduction of azolium precursors in a one-electron solution process, forming molecular H_2 as a by-product (Scheme 10c).[104-106]

Finally, various NHC adducts have been derived, the activation of which generates free NHCs *in situ* (Scheme 10d). For instance, the group of Enders isolated NHC**13** from its 5-methoxy adduct.[107] Since then, several NHC adducts serving as NHC precursors have been developed: NHC-Ag(I) complexes (**M1**),[108-109] alkoxy- (**M2**),[107,110-112] amino-,[107,113-114] trichloromethyl- (**M3**),[115] pentafluorophenyl- (**M4**),[115] carboxylic acid- (**M5**),[116-117] NHC-thioisocyanates (NCS, **M6**),[118] NHC-CO_2 adducts (**M7**)[5,119] and, very recently, imidazolium hydrogen carbonates (**M8**, Figure 4).[120] Upon heating, such precursors undergo an α-elimination reaction, affording NHCs without the need for a

strong base. Most of these adducts have been successfully applied in organometallic chemistry to transfer the carbene fragment to some transition metals, but also as latent pre-catalysts for molecular and/or macromolecular synthesis.[3-4,117-118,120-126]

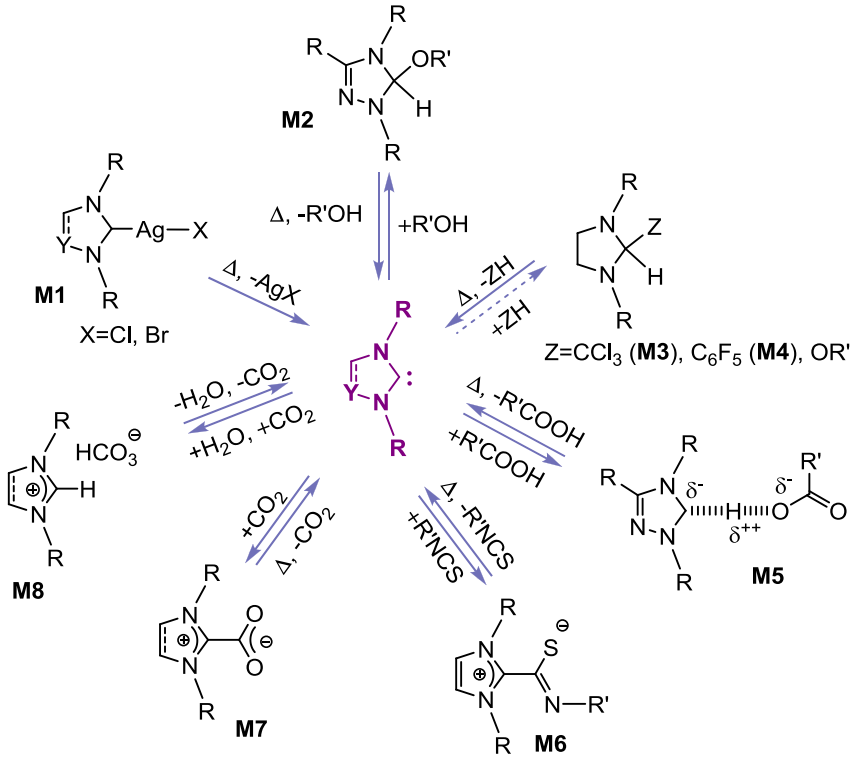

Figure 4. Overview of NHC precursors under their masked form.

3.1.3. Manipulation

Most of NHCs are air and moisture sensitive, hence they have to be handled under an inert atmosphere. However, increasing the bulkiness of R^3-R^4 substituents provides a better stability. NHCs are prone to oxidation[127] and hydrolysis,[128-130] which can lead to distinct compounds as a function of the NHC type and the water content. Thus, hydrolysis of imidazoline-type NHCs is fast, forming ring opened structure (Scheme 11a). In contrast, hydrolysis of imidazole-type NHCs is slow owing to their aromatic character, the structure of the degradation species depending on the water content. While traces of water yields a similar degradation product to that observed with imidazoline-type NHCs, a large excess of water leads to the formation of an imidazolium hydroxide (Scheme 11b). [129]

Several techniques have been proposed to better handle NHCs. For instance, Baceiredo *et al.* have encapsulated NHCs in poly(dimethylsiloxane), allowing the storage and manipulation of NHCs in air

for a few weeks.[127] As highlighted in section 3.1.2., another strategy is to convert the NHC into its masked form. Carboxylation of NHCs is particularly versatile since all NHCs can virtually react with CO_2 in a reversible manner. NHC-CO_2 adducts (**M7**) have yet been reported to progressively hydrolyze in air forming related azolium hydrogen carbonates (**M8**).[131-132] In contrast, the latter salts have proven relatively stable.[120]

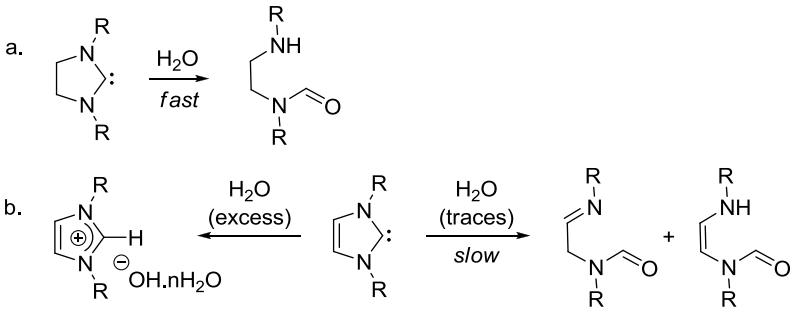

Scheme 11. Hydrolysis of NHCs: a. imidazoline-type, b. imidazole-type.[129]

3.2. Organocatalysts in molecular chemistry

Organic transformations catalyzed by NHCs have received a great deal of interest in the past fifteen years.[7,10-12] This is due to the versatility and high activity of NHCs for the construction of C-C and C-X (X=O, N) bonds, under relatively mild reaction conditions. Transformations catalyzed by NHCs include condensation, 1,2-, 1,4-additions, transesterification, ring-opening reactions, etc.[7]

NHCs can provide different modes of activation (Figure 5), which correlates with their electronic and/or steric effects. As strong nucleophiles, for instance, NHCs can react with aldehyde or ester substrates. Nucleophilic attack of the NHC onto one aldehyde molecule yields the so-called "Breslow intermediate" after proton transfer (Figure 5a). The electrophilic carbonyl group is virtually transformed into a nucleophilic one, a process called "Umpolung" ("polarity inversion" in German). Such Umpolung reactions occur both in the benzoin condensation and the Stetter reactions (section 3.2.1.).

In contrast, nucleophilic addition of NHCs onto esters (Figure 5b) leads to an acyl-imidazolium intermediate by nucleophilic substitution of the -OR group by the NHC (σ-donor). This intermediate is

thus more electrophilic than the starting ester, which is of particular interest for transesterification reactions (section 3.2.2.).

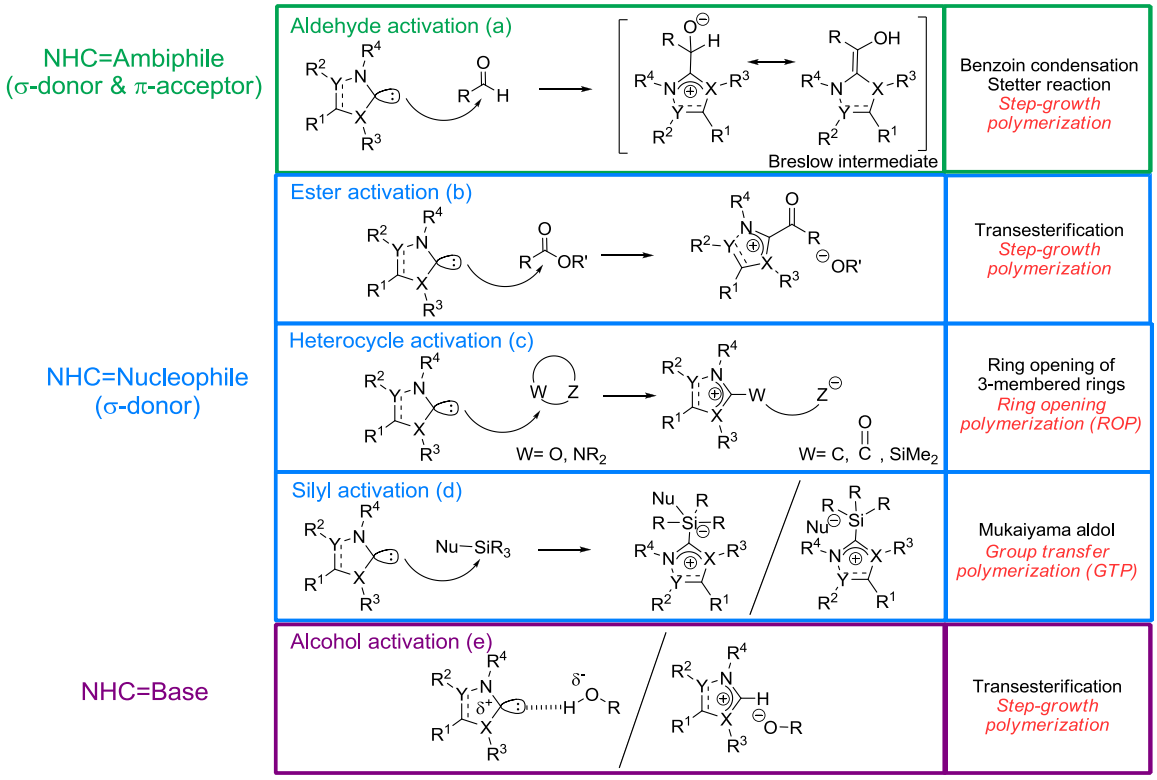

Figure 5. Different modes of substrate activation by NHCs applied in molecular chemistry (in black) and in polymer synthesis (in red).

NHCs have also proven to trigger ring opening of three-membered ring epoxides and aziridines (Figure 5c, section 3.2.3). The high Lewis basicity of NHCs also explains their potential as activators of silylated substrates.[84,86] This has been applied to the Mukaiyama-aldol reaction (Figure 5d, section 3.2.4). Finally the Bronsted basicity of NHCs allows activating alcohols (Figure 5e) and amines *via* hydrogen bonding, representing another reaction pathway for transesterification reactions (section 3.2.2.).

3.2.1. Benzoin condensation and Stetter reactions

Pioneer works on NHC-catalyzed benzoin condensation by Breslow date back to 1958.[133] Since then, various NHCs, including thiazol-2-ylidenes, imidazol(in)-2-ylidenes, benzimidazol-2-ylidenes and triazol-5-ylidenes, and their masked versions, have served to catalyze this C-C bond forming

reaction. Benzoin condensation transforms aromatic aldehyde molecules into benzoin derivatives (Scheme 12a).[7] The first step involves the formation of the "Breslow intermediate" discussed above, whose carbonyl center is stabilized by negative hyper-conjugation with the thia/imidazolium cation.[134-135] This nucleophilic species further attacks the electrophilic carbon of a second aldehyde molecule. After proton transfer, benzoin is obtained while the NHC catalyst is regenerated.

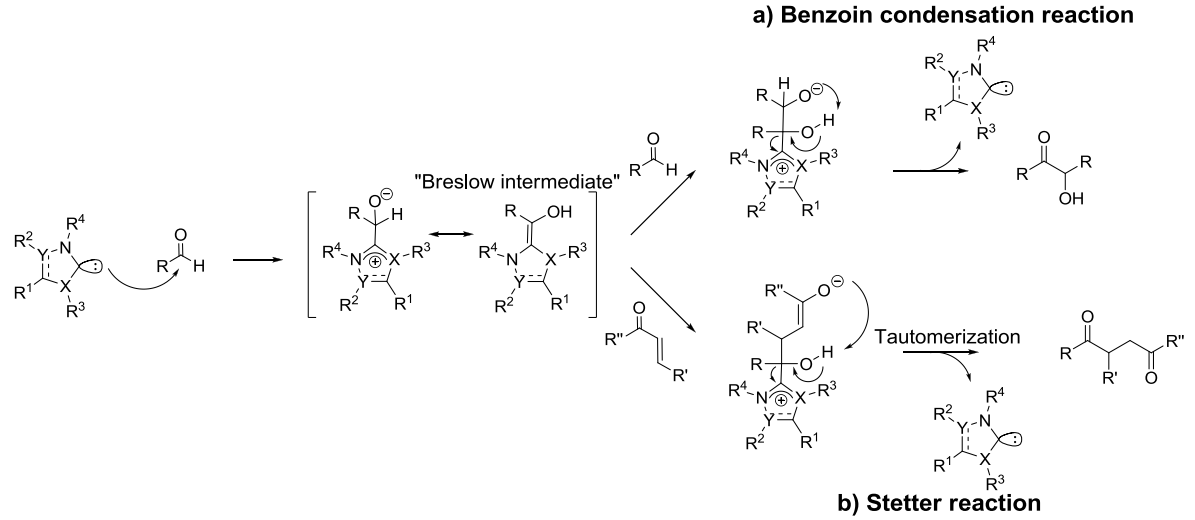

Scheme 12. Mechanisms of: a) the benzoin condensation, b) the Stetter reaction.

In the presence of a Michael acceptor, the "Breslow intermediate" reacts *via* a 1,4-addition, which refers to as the Stetter reaction (Scheme 12b), giving access to 1,4-diketones. More information on this reaction can be found elsewhere.[7,13,136-137]

3.2.2. Transesterification reaction

Both Hedrick, Waymouth *et al.*[73] and Nolan *et al.*[138-139] have used NHCs as catalysts of transesterification reactions. Some masked NHCs, namely imidazolium-2-carboxylates (NHC-CO_2 adducts, **M7**) and their polymer-supported homologues, can efficiently trigger this reaction.[102] High yields can be reached with a low catalyst loading under mild reaction conditions. As NHCs are nucleophiles but can also behave as Bronsted bases, they can activate either the ester or the alcohol moieties (Scheme 13).[140]

Computational studies have suggested that NHCs play the role of proton transfer agents from the alcohol to the carbonyl oxygen (path B).[141] However, it is highly likely that the involved mechanism strongly depends on both the catalyst and the overall reaction conditions.

The transesterification reaction has been applied in polymer chemistry through the synthesis of polyesters and polycarbonates by step-growth polymerization of bifunctional monomers (see section 3.3.1.). In this context, it is worth mentioning that, due the ester/carbonate nature of the repetitive units obtained from such monomers, transesterification may be seen as a side reaction (by intra- or intermolecular transfer).

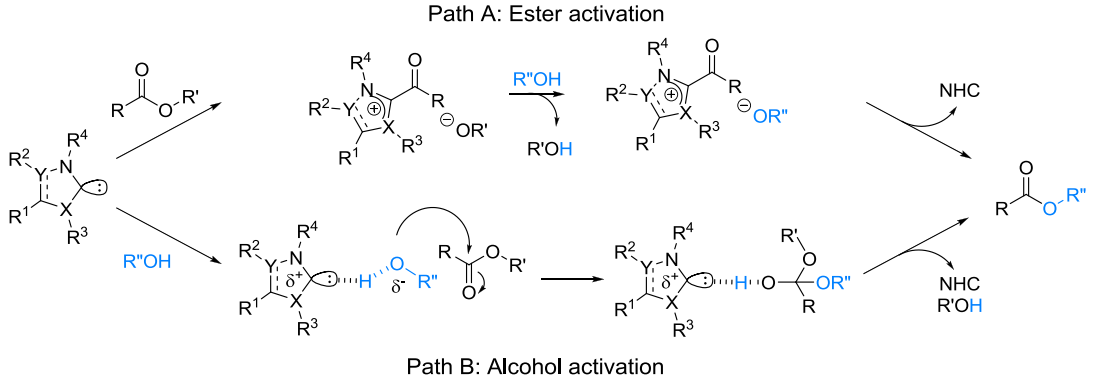

Scheme 13. Putative mechanisms of the transesterification reaction: path A, *via* ester activation; path B, *via* alcohol activation.

3.2.3. Ring opening reaction of 3-membered rings

NHCs can bring about the ring opening of epoxides and activated aziridines. However, their role towards epoxides remains unclear. They have been applied to catalyze the ring opening of epoxides, forming aliphatic polyethers (section 3.3.2.).[142-144] In contrast, their potential as catalysts for ring opening of aziridines has never been applied to polymer chemistry. Detailed information on these particular reactions can be found elsewhere.[7,145-147]

3.2.4. Mukaiyama-aldol reaction

The Mukaiyama aldol reaction involves a silyl enol ether and an aldehyde (or a ketone) and results, after quenching, in the formation of a β-keto-alcohol (Scheme 14).[39,148] Catalysts of this

reaction include Lewis acids, which activate the carbonyl group by coordination, and Lewis bases (e.g. fluoride ions and NHCs) which are thought to interact with the silicon center, forming transient hypervalent siliconates.[149] However, whether or not a true enolate is formed during this step remains unclear (see also section 3.3.3.).

Similarly, the Mukaiyama-Michael reaction is based on the addition of a silyl enol ether on an α,β-carbonyl-containing substrate in a 1,4 fashion, leading to 1,5-bisketo product. Although this molecular reaction has not been catalysed by NHCs, Hedrick, Waymouth *et al.* on one hand,[69] and Taton, Gnanou *et al.* on the other,[68,150-153] have reported the so-called group transfer polymerization (GTP)[154] of (meth)acrylic monomers, involving repeated Mukaiyama-Michael reactions through successive additions of silyl ketene acetal (SKA) moieties onto an incoming (meth)acrylic monomer (see section 3.3.3).

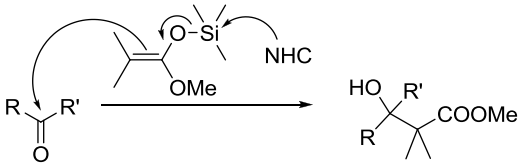

Scheme 14. Mukaiyama aldol reaction between an aldehyde (or a ketone) and an NHC-activated silyl ketene acetal (SKA).[39,148]

3.3. Organocatalysts in polymer synthesis

Among organocatalysts, carbenes have been the most investigated for the purpose of polymerization.[1,4] In particular, NHCs have served to catalyze different polymerization reactions, including step-growth and chain-growth polymerizations. An overview is given in Figure 6 and main results reported in the last decade are summarized in Table 1. NHCs are advantageous for polymerizing a variety of monomers, including heterocycles (lactones, lactide, cyclic carbonates, cyclic siloxanes and carbosiloxanes, epoxides, *N*-carboxyanhydrides), (meth)acrylic monomers but also bis-aldehydes, diols with multiisocyanates, bis-silanols, etc.[1,4]

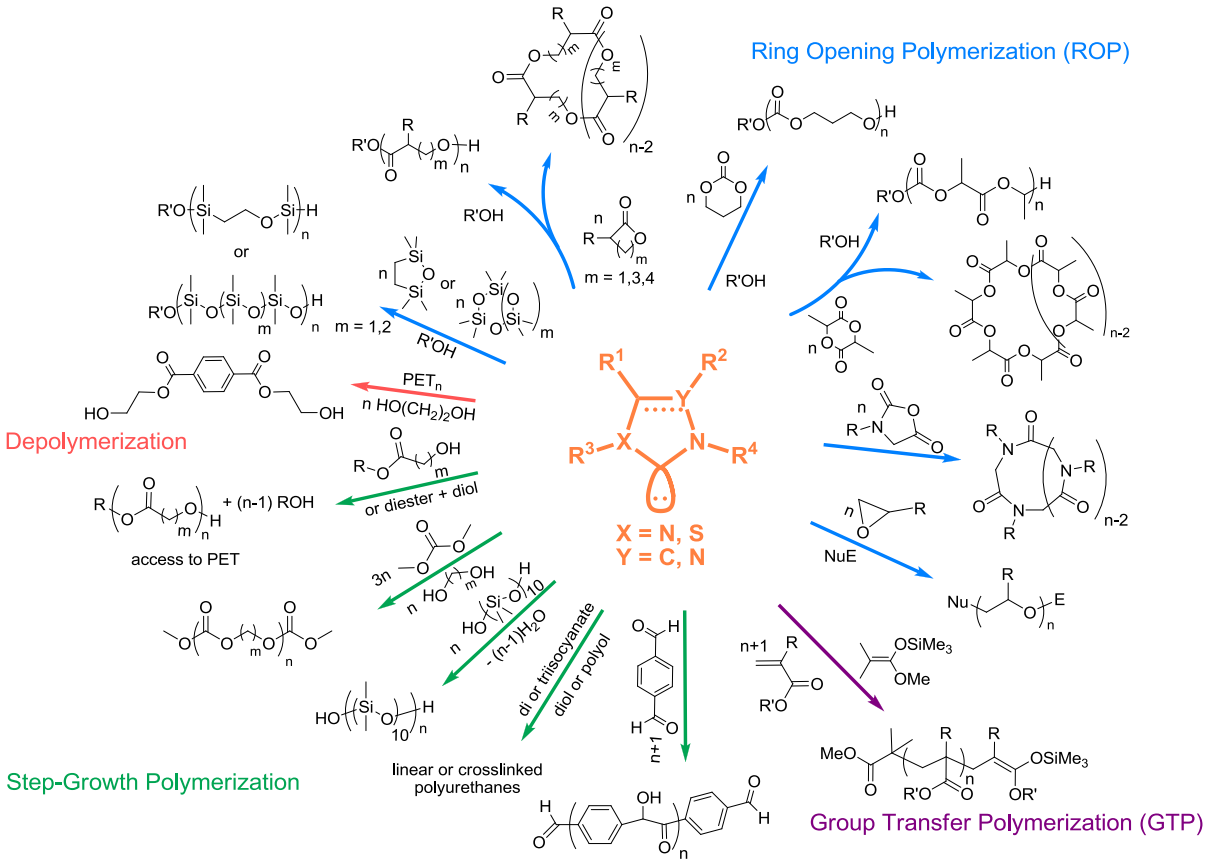

Figure 6. Overview of polymers obtained from *N*-heterocyclic carbenes as catalysts.

3.3.1 Step-growth polymerization

Polymer synthesis *via* a NHC organocatalysis was actually first reported by Jones *et al.* in the late 1990s.[155-156] These authors elegantly applied the principle of the Stetter reaction (section 3.2.1.) to the step-growth polymerization of diformylarenes and bis-Mannich bases used as bifunctional monomers, in the presence of NHC **18** (Scheme 15). Polymeric 1,4-diketones were synthesized in this way, after few hours at 85 °C in DMF. Subsequent ring closure of resulting polyketones, by the so-called Paal-Knorr reaction, gave conjugated alternating copolymers bearing pyrrole, furyl or thienyl moieties.

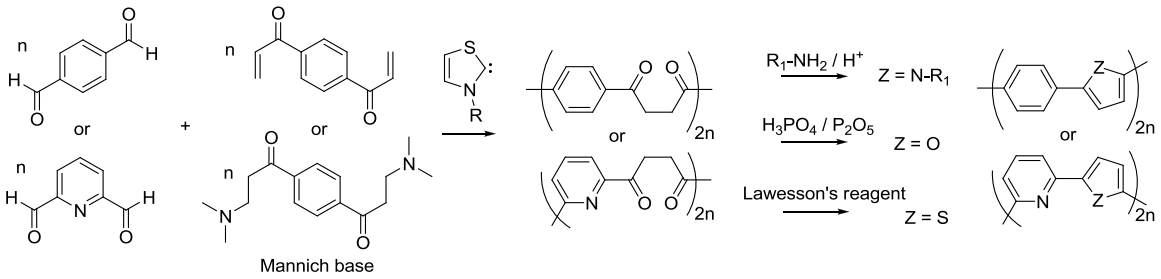

Scheme 15. Synthesis of polymeric 1,4-diketones by thiazolylidene**18**-catalyzed step-growth polymerization and subsequent ring-closure.[129, 130]

Table 1. Representative examples of the polymer syntheses catalyzed by *N*-heterocyclic carbenes.

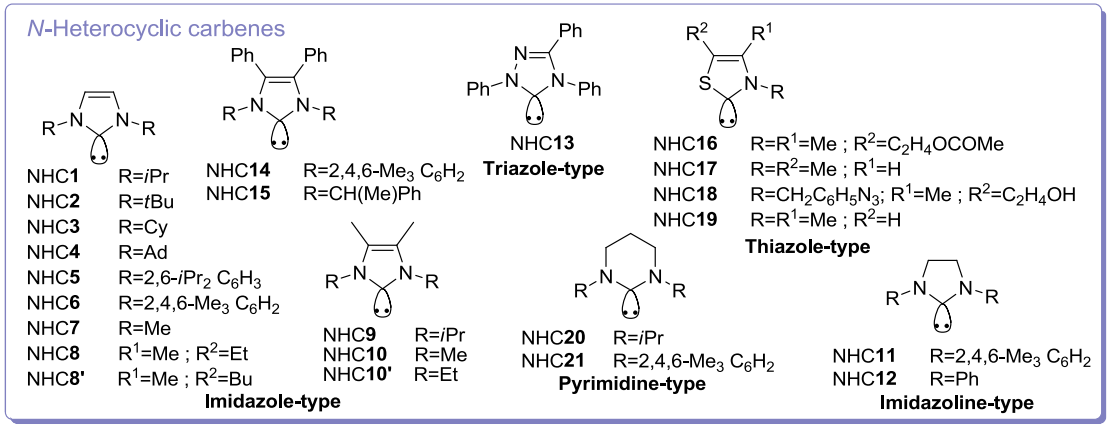

Entry	Catalyst (NHC)	Monomer	Bulk/Solvent	Initiator	$[C]/[I]_0$	*t*	*T* (°C)	conv	M_n (g/mol)	*D*	Ref
1	**7**[a]	AB or AA+BB (A=ester, B=alcohol)	THF	-	0.0003% to M	24	60 to 65	80-95%	8,000-21,000	1.57-1.80	[73]
	7, **10**	BHET	bulk	-	7% to M	1.5 h	250	81%	n.m.	n.m.	
2	**2**, **3**, **6**	$HO(SiMe_2O)_{10}H$	bulk	-	0.25-1% to M	16 h	80	86-94%	48,000-300,000	1.6-1.9	[72]
3	**1**, **2**, **4**, **13**	Terephthalaldehyde	THF, DMSO or THF/DMSO mixture	-	0.5 -5% to M	3-170 h	40	3-93%	up to 3,000	1.3-1.52	[74]
4	**6**,[b] **8**,[b] **11**,[b] **20**,[b] **21**[b]	Polyol+trimeric HMDI (NCO/OH=1/1)	Butylacetate, bulk	-	0.0035% to NCO	75 min	65	40-80%	n.m. (3D network)	n.m.	[157-158]
5	**2**	Diols+aliphatic diisocyanate	THF	-	1%	1 h	30-50	75-99%	1,600-4,200	1.3-11.4	[159]
6	**8'**[b]	Diols+DMC	bulk	-	1%	15 min then 1 h	100 then 150	n.m.	1,700-6,700	1.4-2.2	[160]
7	**6**	Lactide, ε-CL, β-BL	THF	BnOH, PBuOH	0.0083-1.5	2 h	25	60-99%	1,600-17,000	1.05-1.33	[161]
8	**10**, **7**,[a] **12**[a]	ε-CL, δ-VL, β-BL	THF	BnOH	0.5-1.8	0.5-6 h	25	>98%	2,900-28,000	1.04-1.55	[162]
	5,[a] **6**,[a] **7**,[a]	Lactide		BnOH	0.25-1.5	0.25-1 h	25	60-99%	17,700-28,000	1.15-	

	8,[a] PS-**8**,[a] **11**,[a] **12**[a]								1.52	
	16,[a] **17**,[a] **18**,[a] PS-**19**[a]	Lactide		BnOH, PBuOH	<0.005	48-72 h	25 to 38	80-85%	6,900-14,400	1.07-1.35	
9	**11** adducts[c]	Lactide	THF	$R(OH)_x$	X	10 min	RT	84-99%	12,000-25,500	1.16-1.34	111
10	**13**[d]	Lactide	toluene	MeOH/PBuOH / PEO-OH/bis-MPA =$R(OH)_x$	X	19-113 h	90	35-97%	2,600-19,000	1.06-1.36	110
11	**13**[d,e]	β-BL	THF toluene	PBuOH	n.m.	3-24 h	50 90	81-95%	4,400-15,500	1.09-1.19	112
12	**13**[d,e]	dMMLABz+β-BL[e]	toluene/*t*BuOH mixture	Ethylene glycol	2	2 d	80	<95%	~10,000 $f_{dMMLABz}$=0.1-0.58	<1.27	163
13	**13**[d]	Lactide	benzene	$R(OH)_x$ or $R(NH_2)_y$	x or 2y	18-71 h	90	70-100%	8,000-18,000	1.07-1.24	164
14	**13**	β-BL	*t*BuOH, bulk	MeOH, 1-pyreneacetic acid, PTMC with pendant COOH moities	1	0.75-97 h	80-90	20-99%	3,250-34,900	1.09-1.32	116-117
15	**11**, **12** adducts[f]	Lactide	THF, toluene or o-xylene	BnOH	1.5	3-24 h	65 to 144	30-83%	3,200-10,000	1.10-1.52	115
16	**2**, **5**, **6**	D,L Lactide	dichloromethane	BnOH	0.5-2	20-30 min	-20 to 25	71-98%	7,000-17,000	1.23-1.39	165
17	**14**, **15**	*rac*- or *meso*-Lactide[g]	dichloromethane	PBuOH	1	1-240 min	-70 to 25	>88%	~14,000	1.18-1.48	166
18	**9**, **10**	ε-CL	THF	BnOH, $R(OH)_x$	0.5-1	2 min-5 h	RT	18-77%	1,000-14,500	1.11-1.3	167
19	**5**, **9**	TMC	benzene	BnOH	0.05	0.1-30 min	25	>99%	4,500	1.04->2	168
20	-	Lactide	THF	NHC**6**[h]	-	10-900 s	25	32-92%	7,000-26,000	1.15-1.35	169-170
21	-	(*R*)β-BL β-BL	THF, benzene	NHC**11**[h]	-	4 h 10 min	RT	24%	4,900 5,800	1.42 1.16	171
22	-	ε-CL, δ-VL[i]	THF, toluene	NHC**9**, NHC**10**, NHC**10'**[j]	-	20-390 min	RT	30-97%	41,000-114,000	1.36-2.4	172-173
23	-	^{N}Bu-NCA, ^{N}Me-NCA, ^{N}De-NCA,	THF	NHC**5**[k]	-	8-48 h	50	79-100%	3,000-43,200	1.03-1.3	174-

		^{N}Propargyl-NCA[i]									[177]
24	**2**, **3**	D4	bulk	BnOH/ MeOH/ *t*BuOH	0.014-1	16 h	80	~85%	20,000-220,000	~1.6	[178]
25	**6**, **9**	TMOSC	benzene	PBuOH	1	1-30 min	RT	80-99%	10,000-13,000	1.14-1.19	[179]
	9	D3	toluene	n.m.	1	n.m.	n.m.	n.m.	n.m.	>1.4	
26	-	EO	DMSO	NHC**1**[l]	-	3 d	50	100%	2,400-13,000	<1.14	[142]
27	**1**, **2**	EO	DMSO	Chain Regulator Nu-E	0.1	4 d	50	>90%	2,000-12,000	<1.15	[143]
28	**1**	PO	bulk	Chain Regulator Nu-E	0.1	3 d	50	30-40%	1,800-7,300	<1.18	[144]
29	**1**, **2**	MMA, *t*BA, *n*BA	THF, toluene	MTS	0.01-0.05	1-16 h	25	100%	2,600-110,000	1.08-1.6	[68, 152]
30	**9**	MMA, *t*BA	THF	MTS	0.0003-0.032	0.1-17 h	RT	81->95%	4,000-19,000	1.14-1.72	[69]
31	**1**, **2**	MMA, *t*BA, nBA, DMAEA, DMAEMA, DMA, MAN[i]	THF, toluene, DMF	MTS	0.016-1	1-70 h	25	90-100%	5,000-42,000	1.07-1.51	[151,180]

[a]= *in-situ* generated with *t*BuOK (triethylamine for thiazole-based carbenes)
[b]= *in-situ* generated from the corresponding NHC-CO_2 adducts
[c]= adducts with $R(OH)_x$ ($R(OH)_x$ is further used as the initiator) (equilibrium between NHC and adduct at RT)
[d]= forms adducts with alcohols and amines (stable at RT)
[e]= *t*BuOH used to decrease the NHC activity (by adduct formation)
[f]= adducts with $CHCl_3$ or $C_6H_xF_{(6-x)}$ (x>1) (stable at RT)
[g]= *rac*-Lactide leading predominantly to isotactic polymers (*RRR* or *SSS*); *meso*-L-lactide leading predominantly to heterotactic polymers (*RRSSRRSS*)
[h]= terminated with CS_2, leading to cyclics
[i]= miscellaneous homo and copolymers
[j]= terminated with 4-nitrophenol, leading to cyclics
[k]= terminated with dithranol, leading to cyclics
[l]= terminated with NuE, leading to α,ω difunctionalized PEO
n.m.=not mentioned

Hedrick, Waymouth *et al.* reported the synthesis of poly(ethylene terephthalate) referred to as PET (entry 1, Table 1).[73] The two-step procedure using NHCs **7** or **10** as single catalytic components consisted in the preparation of bis(2-hydroxyethyl)terephthalate (BHET) first, followed by its self-condensation (Scheme 16). Quantitative conversions were obtained after 1 h at 250 °C. The reaction proved reversible in the presence of methanol.

The same NHCs were also effective for chemical degradation of PET (Scheme 16) under mild conditions (typically at 80 °C or even less), providing the first example of a depolymerization reaction by an organocatalytic pathway.[75,181]

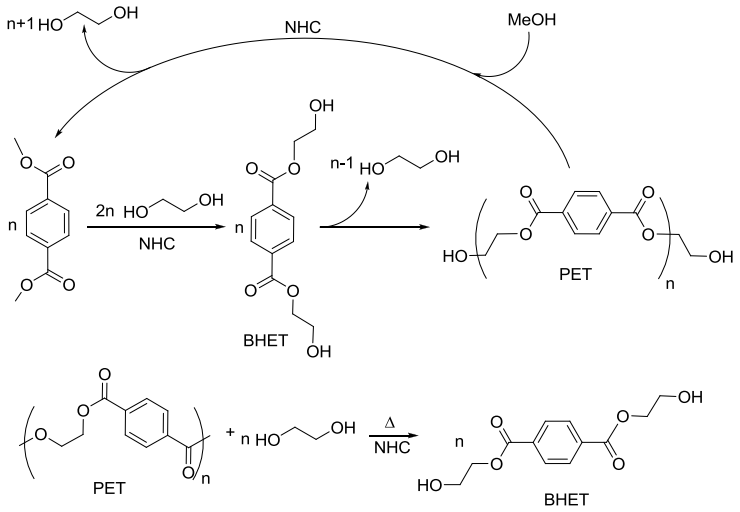

Scheme 16. Synthesis of PET by step-growth polymerization, and depolymerization of PET *via* transesterification with a NHC (NHCs**7** and **10**).[73,75,181]

The same group described the synthesis of structural analogues of poly(ε-caprolactone) (PCL) and poly(glycolide), by self-condensation of ethyl 6-hydroxyhexanoate and ethyl glycolate.[75] The reactions were performed in bulk at 60 °C under vacuum for 24 h, leading to aliphatic polyesters with molar masses, M_n, ranging from 8,000 to 20,000 g/mol. A statistical copolymer was also obtained from the condensation of the two monomer types.

Another example of a NHC-catalyzed step-growth polymerization was reported by Baceiredo *et al.*: the polycondensation of α,ω-dihydroxy disilanol oligomers led to polydimethylsiloxane (PDMS, entry 2, Table 1 and Scheme 17).[72] Though water was generated during polymerization, the catalytic activity of NHCs remained unchanged despite their moisture sensitivity. This was explained by the

fact that the catalyst was non-miscible with PDMS. The α,ω-dihydroxy disilanol oligomer was thus heated at 80 °C for 16 h, in the presence of 2500 ppm of NHCs, causing an increase in viscosity of the reaction mixture.

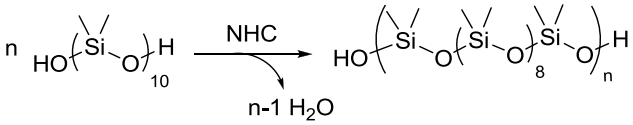

Scheme 17. Polycondensation of a α,ω-dihydroxy disilanol oligomer by NHCs**2**, **3** and **6**.[72]

Taking inspiration of the mechanism operating in the benzoin condensation (section 3.2.1.), Taton, Gnanou *et al.* employed a commercially available bis-aldehyde, namely, terephtalaldehyde (entry 3, Table 1).[74] The latter monomer was polymerized by a NHC-catalyzed step-growth polymerization (Scheme 18) under relatively mild conditions (THF or DMSO at 40 °C), leading to the formation of poly(1,4-phenylene-1-oxo-2-hydroxyethylene)s, referred to as polybenzoins, of relatively low molar masses ($M_n \approx$ 2,000 g/mol). 1,3,4-triphenyl-1,2,4-triazol-5-ylidene (NHC**13**) was the most active among all tested NHCs. Formation of cyclic polymers during the polymerization was however noticed. The content in cyclics was found to vary as a function of the polarity of reaction medium and the monomer conversion reached.

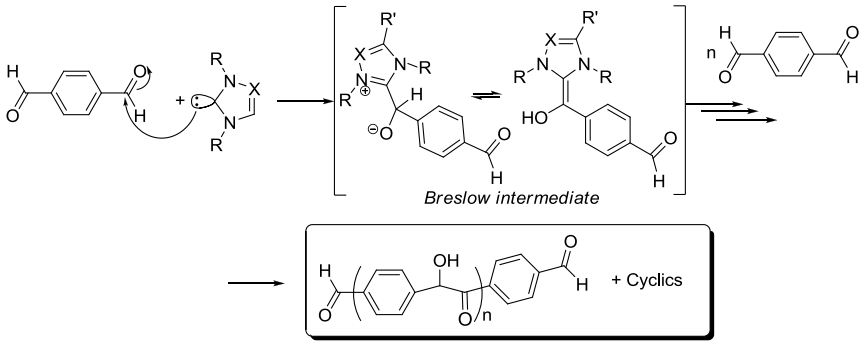

Scheme 18. NHC-catalyzed benzoin condensation in step-growth polymerization (NHCs**1**, **2**, **4** and **13**).[135]

NHCs also proved efficient for the synthesis of polyurethanes by step-growth polymerization of polyols and a multiisocyanates. Buchmeiser *et al.* first employed NHC-CO_2 adducts as pre-catalysts to access insoluble polyurethane 3D networks, by reacting trimeric hexamethylene di-isocyanate (HMDI) with a polyol (entry 4, Table 1).[157-158] Only 3.5 mmol% of CO_2-protected imidazole-, imidazoline- and

pyrimidine-type NHCs with respect to isocyanate led to 40 to 80% conversion after 75 min. In this case, NHC-CO_2 adducts served as latent catalysts, as the reaction only proceeded upon raising the temperature at 65 °C. As NHCs are also efficient catalysts for isocyanate cyclotrimerization,[182] the final polymeric materials might consist of isocyanurate and/or urethane linkages (Scheme 19a).

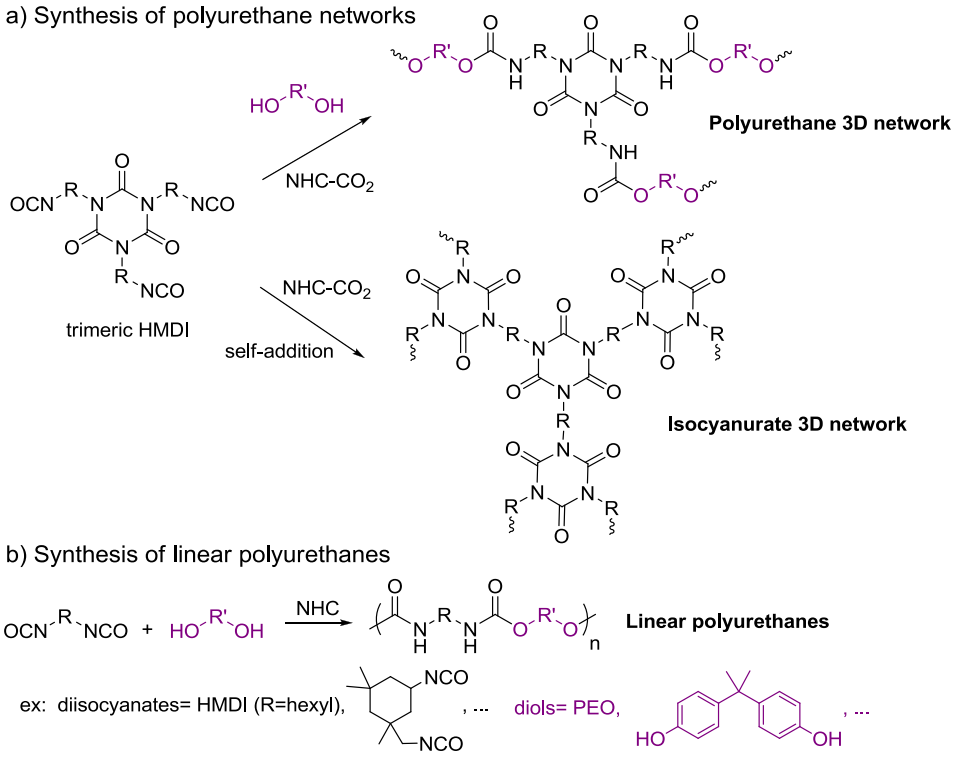

Scheme 19. Synthesis of a) polyurethane networks (NHCs**6**, **8**, **11**, **20** and **21**),[157-158] b) linear polyurethanes by NHC catalysis (NHC**2**).[159]

More recently, Destarac *et al.* described the synthesis of linear and soluble polyurethanes using diols and alkyl isocyanates (entry 5, Table 1).[159] It was noticed that the proportion of dimers and trimers obtained by cyclodi/trimerization remained at a traces level with alkyl isocyanates, whereas aryl isocyanates formed cyclodi/trimers almost quantitatively. Based on different orders of addition of monomers, the proposed mechanism for the formation of the urethane bond was suggested to involve the activation of the alcohol by the basic NHC catalyst (basic mechanism), followed by the alkoxide attack on the isocyanate moiety (Scheme 19b). Several linear polyurethanes could thus be derived, the molar masses of which were in the range 1,600-4,200 g/mol.

Plasseraud, Picquet *et al.* also used a CO_2-masked NHC to catalyze the synthesis of aliphatic polycarbonates, from dimethylcarbonate and various diols (entry 6, Table 1 and Scheme 20).[160]

Heating the NHC**8'**-CO_2 adduct released the free carbene for activation of the diol/alcohol chain end. The formed alkoxide further attacked the carbonate moiety, resulting in the formation of an alcohol-terminated polycarbonate after release of a MeOH molecule. Miscellaneous polycarbonates were thus obtained by varying the structure of the diol. Corresponding molar masses M_n were between 1,700 and 6,700 g/mol, with dispersities lower than 2.2.

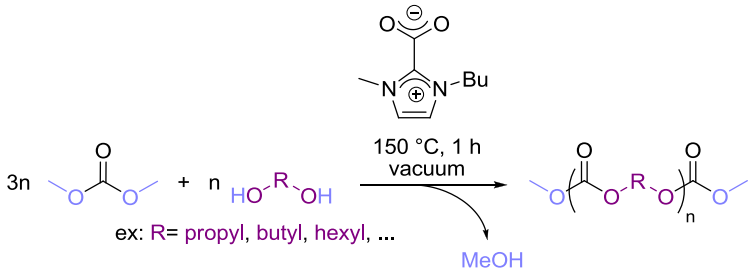

Scheme 20. NHC-catalyzed synthesis of aliphatic polycarbonates from dimethylcarbonate and diols.[160]

3.3.2. Ring-opening polymerization (ROP)

Besides their use in step-growth polymerization reactions, NHCs were mainly used as organic catalysts in chain-growth polymerizations, mainly for ROP of cyclic esters, to produce linear as well as cyclic aliphatic polyesters.[3-4]

The first report dates back to 2002 and exploited the ability of the NHC**6** (IMes) to catalyze the ROP of cyclic esters. Poly(lactide) (PLA), poly(ε-caprolactone) (PCL), poly(β-butyrolactone) (PBL) and poly(δ-valerolactone) (PVL) with controlled molar masses, high chain end fidelity and a dispersity close to unity were synthesized by the ROP of corresponding cyclic esters in THF solution (1-2M) at 25 °C, in the presence of benzyl alcohol or 4-(pyren-1-yl)butan-1-ol playing the role of initiator (entry 7, Table 1).[161] A chain extension experiment employing a PLA precursor yielded a PLA of molar mass of 39,500 g/mol and a dispersity of 1.17. A well-defined star PCL was even synthesized from six-arm poly(propylene glycol), PPG (M_n=3,000 g/mol), as macromolecular hexafunctional initiator. Compared with DMAP, the ROP of LA catalyzed by IMes proved much faster (TOF~18 s^{-1} *vs.* ~0.8 h^{-1} with DMAP).

Since this first report, several other NHCs, either in their "naked" or under a masked form, were tested for the ROP of cyclic esters. In most cases, OH-containing precursors were employed as (macro)initiators (Figure 7). [3-4]

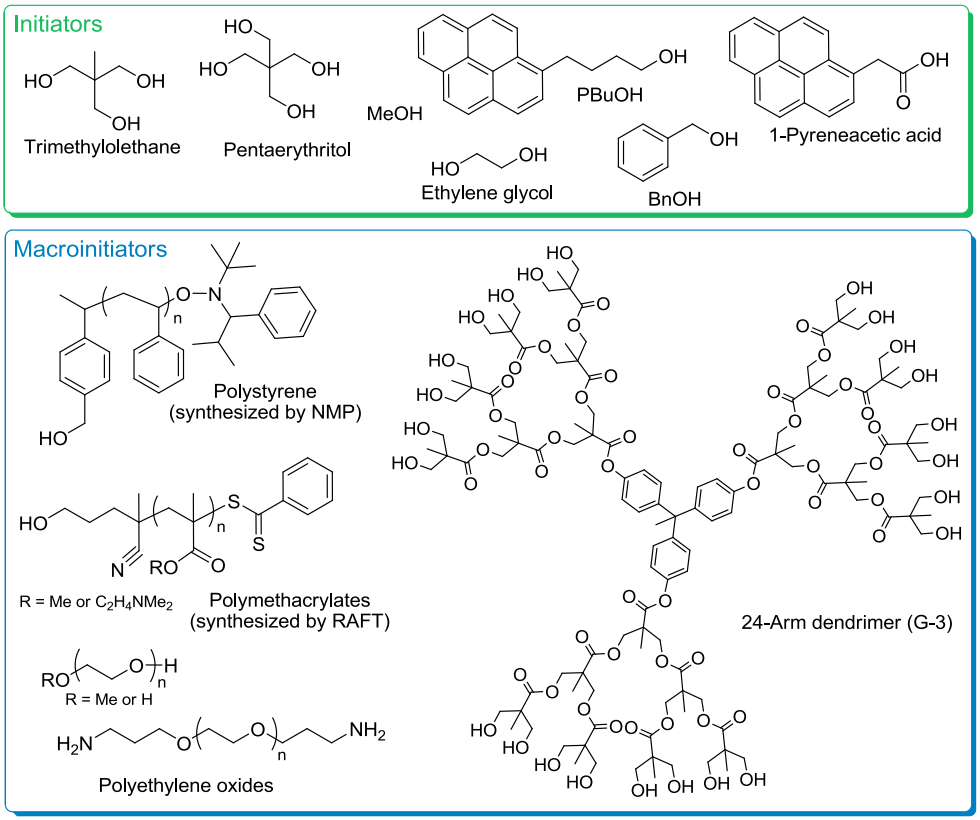

Figure 7. Alcohol (macro)initiators employed for ROP of cyclic esters.

In a systematic study, Hedrick, Waymouth *et al.* reported that NHCs derived from imidazolium- and thiazolium ionic liquid salts (pre-catalysts) could be generated *in situ* using a strong Bronsted base.[162] This allowed screening of different pre-catalysts to investigate the structure-catalytic activity relationship of NHCs toward the ROP of different lactones. ROPs of lactide (LA), β-butyrolactone (β-BL), δ-valerolactone (δ-VL) and ε-caprolactone (ε-CL) were investigated (Table 1, entry 8). For instance, imidazole-based NHC catalysts (e.g. NHC**6**) exhibited a higher reactivity than thiazole-based catalysts. Imidazol-2-ylidene and imidazolin-2-ylidene showed similar catalytic activity. IMes was found the most active for the ROP of LA, even with low catalyst loading (0.5 mol%). Molar masses could be varied by a change of the initial monomer to initiator ratio (DP= [M]/[I]) without changes in dispersity (D < 1.2).

In the same report, the authors developed an attractive interfacial polymerization process where the ionic liquid pre-catalyst served as a reservoir, forming a two-phase reaction mixture, with a THF solution containing both the monomer and the initiator. Subsequent *in situ* activation of the ionic liquid allowed the NHC to be generated. Being neutral, the catalyst could migrate to the THF phase to trigger ROP. At the completion of the reaction, the IL precursor could be regenerated by acidic treatment.

Pre-catalysts supported on PS beads were also employed to catalyze the ROP of cyclic esters. The versatility of this approach was demonstrated through the synthesis of well-defined homopolyesters, macromonomers as well as block and graft copolymers.

As described in literature of molecular chemistry,[183] alternatives to *in situ* generation of NHCs with strong bases consists in the thermolysis of masked NHCs (see section 3.1.2.). For instance, upon heating the NHC**13**-alcohol monoadduct **M2** at 80 °C under vacuum (0.1 mbar), methanol is released, forming the corresponding 1,2,4-triazol-5-ylidene.[107] Other adducts, obtained from a 1:1 reaction between imidazolin-2-ylidene and alcohols can also be cleaved to release the free NHC, as illustrated in Figure 4.[7,111,184] However, it is worth noticing that masking NHCs with alcohols cannot be applied to generate imidazol-2-ylidenes (unsaturated NHCs).

The above-mentioned methods were exploited by Hedrick, Waymouth *et al.* for generating NHCs and trigger the organocatalyzed ROP of various cyclic esters.[110-112,115,162-164] For instance, a series of primary and secondary alcohol adducts of imidazolin-2-ylidenes were designed and used as single-component latent catalyst/initiator systems for the ROP of LA. Thus PLA's of controlled molar masses were synthesized in THF solution at room temperature, within 10 min (entry 9, Table 1).[111] Such NHC adducts were found quite stable in the solid state at room temperature, but readily released both the alcohol and the free saturated NHC in solution. Di- and tri-functional adducts were also prepared to access, respectively, two-arm linear and three-arm stars based on PLA (Scheme 21).

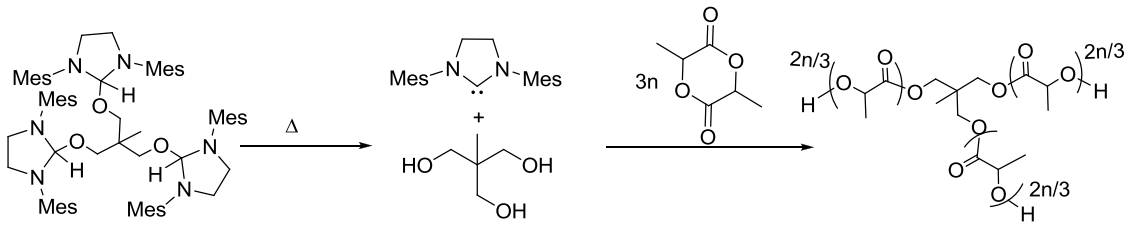

Scheme 21. ROP of LA employing a tri-NHC**11**-alcohol adduct and leading to three-arm star PLAs.[111]

Similarly, Dubois, Hedrick, Waymouth *et al.* designed alkoxytriazolines, deriving from the commercially available 1,3,4-triphenyl-4,5-dihydro-1*H*-1,2,4-triazol-5-ylidene carbene (NHC **13**), as latent unimolecular catalyst/initiator systems.[110,112] These triazole carbene precursors exhibited low activity at room temperature for the ROP of LA, because of the stability of the alcohol adducts under these conditions. However, nearly quantitative monomer conversion was observed in ~50 h and PLAs of controlled molar masses and low dispersities were obtained by polymerisation of LA at 90 °C, in the presence of a variety of alcohol initiators, in 1 M toluene solution (entries 10 and 11). An interesting feature of these polymerizations was that the hydroxy-terminated PLA and the free triazole carbene reacted reversibly, forming a dormant polymer adduct. This reversible termination helped in minimizing the concentration of propagating alkoxides, thus preventing the occurrence of side transesterification reactions between polymer chains. In this way, activation/deactivation of polymer chain ends was possible simply by heating/cooling the reaction mixture on demand. This high level of control also facilitated chain extension experiments: after full conversion of a first load of monomer, the NHC-catalyzed ROP of a second monomer readily occurred.

This strategy was next applied to macromolecular engineering, through the design of block copolymers and "hybrid dendrimer/star" copolymer made of a dendritic core surrounded by 24 PLA branches.[112] For block copolymer synthesis, adducts of hydroxy-functionalized oligomers or bifunctional "double-headed" initiators were employed, by combining different polymerization techniques (typically NMP or RAFT with the NHC-catalyzed ROP). A multifunctional hydroxylated three-generation dendrimer derived from 2,2'-bis(hydroxymethyl)propianoic acid served as multifunctional macroinitiator to access the hybrid dendrimer/star copolymer.

The same group reported the synthesis of amphiphilic ABA-type triblocks based on PLA and poly(dimethyl malic acid) (poly(dMMLA)), *via* the triazole carbene organocatalysis.[163] A statistical poly(dMMLABz-*co*-β-BL) was first prepared by NHC-catalyzed ring-opening copolymerization of [*R*,*S*]-4-benzyloxycarbonyl-3,3-dimethyl-2-oxetanone (dMMLABz) and β-BL, in a toluene/*t*-BuOH solvent mixture at 80 °C, in the presence of ethylene glycol as initiator (entry 12, Table 1). Under such conditions, the dMMLABz monomer was preferentially incorporated in the resulting aliphatic polyester chains. This precursor was further employed as a difunctionalized macroinitiator for the ROP of LA at 90 °C. After a deprotection step by catalytic hydrogenation of pendant benzylic ester groups of poly(dMMLABz), the expected PLA-*b*-poly(dMMLA-*co*-β-BL)-*b*-PLA triblock copolymer was obtained (Scheme 22). Investigations into the self-assembling properties in aqueous solutions of these amphiphilic compounds revealed the formation of "flower-like" micelles at 4 °C. Increasing the temperature to 25 °C induced microgelation of the micelles, which upon further increase in temperature to 40 °C, led to a disruption of the microgel. This demonstrated the temperature-dependent reversible sol-gel transition of the self-assembled ABA-type triblock copolymers.

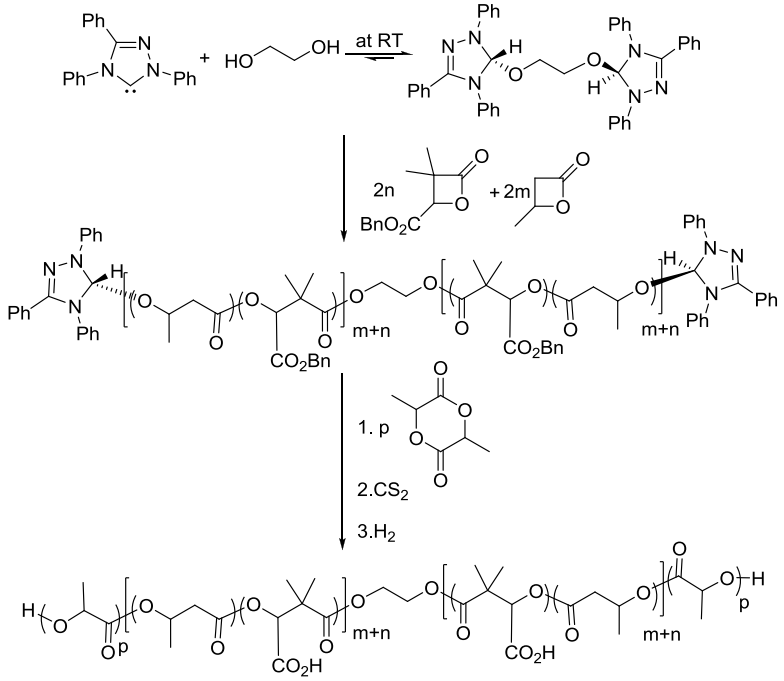

Scheme 22. Synthesis of PLA-*b*-poly(dMMLA-*co*-β-BL)-*b*-PLA triblock copolymer *via* the triazole carbene (NHC**13**) organocatalysis.[163]

Besides alcohols, primary amines are also suitable initiators in NHC catalysis.[164] In this case, however, the primary amino-function acts as a bifunctional initiating site for the ROP of LA, in the presence of the triazole carbene (entry 13, Table 1).

By making use of multifunctional (macro)initiators based on PEO and featuring multiple primary amino-functionalities, "H-shaped" and "super-H-shaped" architectures based on PEO/PLA could indeed be synthesized. Initiation from each primary amine, indeed, creates imide-type branching points (two chains per initiating amine, Scheme 23). A model primary amine initiator, namely, 1-aminomethylpyrene, was first employed for the ROP of LA using the triazole carbene as a catalyst in benzene. Initiation of LA at both N-H groups of the initiator (i.e., both the amine and resulting amide functionality) was established. The ability of an amido-group to initiate the ROP of LA was then verified using ε-caprolactam as initiator. Using a telechelic tetrakis-amino-functionalized PEO precursor allowed the authors to synthesize "super-H shaped" copolymers.

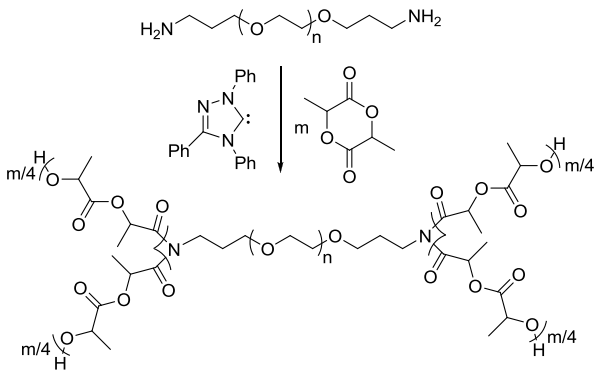

Scheme 23. Synthesis of H-shaped PEO/PLA-based block copolymers by NHC**13**-catalyzed ROP of LA.[164]

Dubois *et al.* noticed that the ROP of β-BL initiated by MeOH and catalyzed by NHC**13**, can proceed both *via O*-alkyl (64%) and *O*-acyl (36%) cleavage (Scheme 24).[116] Thus, NHC**13** can form RT-stable adducts with a carboxylic acid moiety (adducts **M5**, Figure 4), as shown by NMR analysis of a 1/1/1 mixture of NHC**13**, β-BL and MeOH.[116-117] 1-Pyreneacetic acid was then used as an initiator leading to poly(β-BL)s with M_n between 4,000 and 32,000 g/mol and dispersities lower than 1.15 (Table 1, entry 14). PEO-*b*-PBL diblock copolymers were obtained using a PEO-COOH initiator. This strategy was further applied to the synthesis of polycarbonates grafted with PBL blocks. First, a cyclic

carbonate with a pendant carboxylic acid moiety was mixed with an equivalent of NHC**13**. After copolymerization of the corresponding carbonate-NHC monomer adduct with trimethylene carbonate (TMC) using another organocatalytic system (sparteine/chlorophenol), β-BL was polymerized at 90 °C in bulk, leading to a polycarbonate backbone bearing PBL pendant blocks.[117]

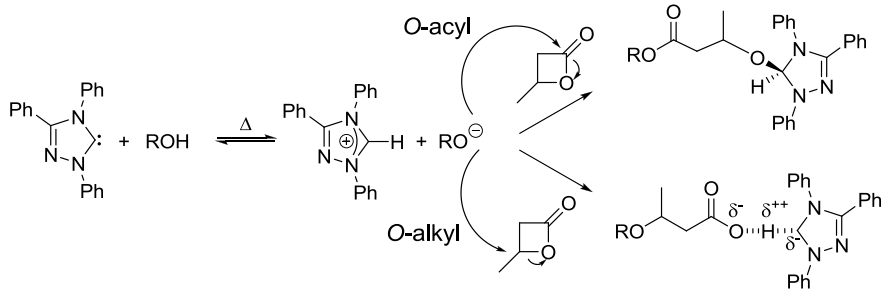

Scheme 24. Polymerization of β-BL with NHC**13** *via O*-acyl and *O*-alkyl cleavages.[116-117]

Hedrick, Waymouth *et al.* synthesized NHC-adducts featuring fluorinated substituents at C-1 (**M4**, Figure 4), by condensation of diamines with properly substituted benzaldehydes.[115] Such adducts were successfully employed as organic pre-catalysts for the ROP of LA (Scheme 25) in THF, toluene or *o*-xylene solution (Table 1, entry 15), though elevated temperatures were required to release the carbene catalyst (between 60 and 144 °C, as a function of the structure of the pre-catalyst).

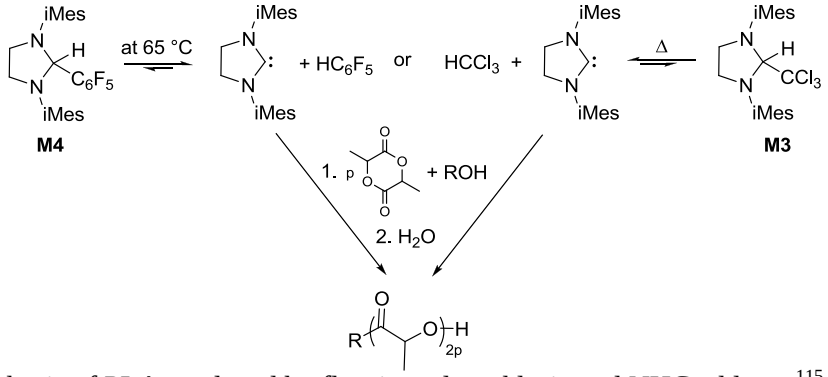

Scheme 25. Synthesis of PLA catalyzed by fluorinated or chlorinated NHC adducts.[115]

In 2004, Hillmyer, Tolman *et al.* showed that the free achiral NHC**6**, 1,3-dimesitylimidazol-2-ylidene, could trigger the stereoelective polymerization of *rac*-LA (Table 1, entry 16).[165] While the bimetallic Zn-based complex, formed by addition of benzyl alcohol to the (1,3-dimesitylimidazol-2-ylidene)-$ZnEt_2$ complex, produced heterotactic PLA, the metal-free catalyzed ROP of *rac*-LA mediated by the NHC alone led to isotactic enriched PLA under similar conditions (CH_2Cl_2, 25 °C).

Actually, other NHCs, namely, 1,3-di-*tert*-butylimidazol-2-ylidene (NHC**2**) and 1,3-bis(2,6-diisopropylphenyl)imidazol-2-ylidene (NHC**5**) also formed isotactic enriched PLA with semi-crystalline properties. However, no clear explanation was provided to account for the different behavior of the free NHCs and the metal-based complex.

Later on, Hedrick, Waymouth *et al.* reported that sterically hindered unsaturated free NHCs catalyzed the polymerization of *rac*-LA or *meso*-LA (entry 17), leading to highly isotactic PLA or heterotactic PLA, respectively, at low temperature (from -70 °C to -15 °C).[166] Both chiral and achiral versions of these NHCs were purposely designed. These catalysts exhibited a very high activity (95 min^{-1}) at room temperature, affording PLA of controlled molar mass and low dispersity (entry 16). Highly isotactic PLA, with blocks of (*R*,*R*)-LA and (*S*,*S*)-LA units were generated at low temperature, with an increase in the probability of isotactic enrichment (P_i), from 0.59 at room temperature to 0.90 at -70 °C, as suggested by NMR characterization. The high level of stereoselectivity with this NHC was ascribed to the steric hindrance brought by both phenyl groups at C4 and C5 of the imidazole backbone of this catalyst.

The ROP of *rac*-LA using the chiral NHC**15** also formed a highly isotactic PLA at low temperature. It was suggested that stereocontrol originated from the steric congestion of the active site, rather than by the chirality of the catalyst. The polymerization of *meso*-LA mediated by a chiral NHC yielded a heterotactic PLA. All these observations (highly isotactic polymer formed from *rac*-LA, and heterotactic polymer with *meso*-LA) were eventually in agreement with a chain end control mechanism, for both achiral and chiral NHCs, despite the presence of chiral groups close to the active site. In the case of *rac*-LA, both D- and L-LA should be subjected to a stereoselective attack by the terminal alkoxide of the last inserted monomer unit, leading to isotactic enrichment. In the case of heterotactic-enriched PLA obtained from *meso*-LA, the oxygen adjacent to the last chiral center of the PLA chain end (either *R* or *S*) might attack the activated monomer with the same stereogenic configuration adjacent to it.

While the aforementioned NHCs were highly active in the ROP of LA, they showed less efficiency toward the ROP of ε-CL.[161-162] More electron-rich and less bulky substituents carbenes such as 1,3-

diisopropyl-4,5-dimethylimidazol-2-ylidene (NHC**9**) and 1,3,4,5-tetramethylimidazol-2-ylidene (NHC**10**) proved more active organocatalysts for the synthesis of well-defined PCL's, again corroborating that the catalytic activity was sensitive to the steric and electronic properties of the carbene (entries 7, 8 and 18 in Table 1).[167] The ROP of ε-CL was performed at room temperature in THF solution (0.5-2.0 M), in the presence of BnOH and 4-pyren-1-ylbutan-1-ol as monofunctional initiators, or multihydroxylated initiators such as ethylene glycol, 1,1,1-tris(hydroxymethyl)propane, and pentaerythritol. Heterodifunctionalized PCL and three- and tetra-arm PCL stars were thus synthesized. Low NHC/ε-CL ratios (typically 1/400) were employed to obtain PCL of low molar masses, preventing the occurrence of transesterification reactions and formation of cyclic oligomers.

The NHC-catalyzed ROP of TMC was also shown to be a controlled process (Table 1, entry 19).[168] NHC catalysis (5 mol%) allowed for a fast conversion (>99% after 30 min). The resulting polymers were characterised by a low dispersity, which competed with that obtained for the best other organocatalysts used (guanidines, amidines and thioureas). However, the more reactive NHC**9** did not provide a good control of the polymerisation.

The two mechanisms discussed above for the transesterification reaction (section 3.2.2.) were eventually proposed for these NHC-catalyzed ROP's of cyclic esters.

In the activated monomer mechanism (AMM), the carbonyl group of the cyclic ester substrate first undergoes a nucleophilic attack by the carbene catalyst (Path A, Scheme 26). This ring-opening generates a zwitterionic intermediate, typically an alkoxide featuring an imidazoli(ni)um-type counter-cation. After proton transfer from the alcohol initiator and subsequent displacement of the bound catalyst by the as generated alkoxide (RO^-), a ring-opened alcohol mono-adduct is generated, with concomitant release of the NHC. Propagation then proceeds in the same way, i.e. by activation of the monomer, and reaction of the alcohol mono-adduct with the activated monomer.

The activate initiator/chain end mechanism (ACEM) involves interaction of the O-H group of the alcohol initiator with the NHC (Path B, Scheme 26). This is followed by the nucleophilic attack of the monomer by the oxygen of this alcohol. Propagation then occurs by direct ring-opening of the active chain end on the cyclic monomer. Depending on the pKa difference between the initiating alcohol and

the NHC, the RO-H proton can be completely transferred to the basic site, thus generating an alkoxide. In other words, the NHC behaves as a Bronsted base in this case as ACEM can be viewed as a "basic" mechanism.

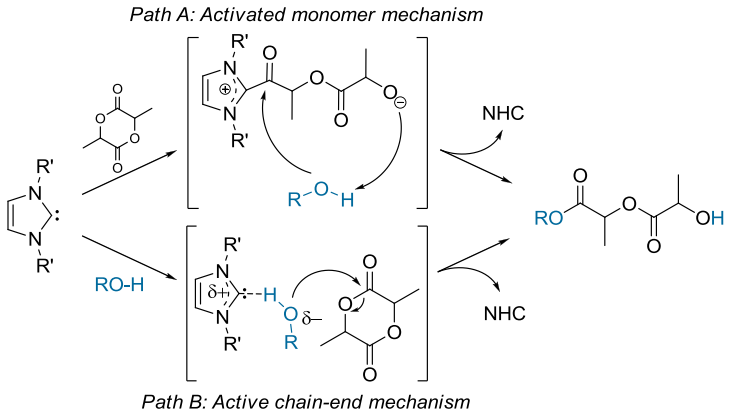

Scheme 26. Initiation of the ROP of LA and subsequent propagation to form PLA.

Firstly, Hedrick, Waymouth *et al.* suggested that, due to the higher pK_a of the alcohol initiator compared to that of the conjugated acid of NHC**6** in DMSO (pK_a(alcohol)=29 *vs* pK_a(NHC)=24), a direct attack of the monomer by the nucleophilic NHC (Path A, Scheme 26) was the most likely pathway.[161] However, theoretical calculations performed on the NHC-catalyzed transesterification reaction predicted that the NHC behave more as a proton transfer agent than as a nucleophilic agent, which was thus in favor of the basic ACEM involving H-bond.[141]

Interactions between IMes (NHC**6**) and the alcohol were studied by NMR spectroscopy and by X-ray crystallography. Structures of ensuing adducts proved to be greatly sensitive to the solvent and to the structure/nature of the alcohol: the more sterically hindered the alcohol was, the weaker the interaction with the carbene was.[185] Moreover, the pK_a of the alcohol had also a great importance, a low pK_a leading to a greater involvement of imidazolium alkoxides.

Evidence of a direct attack of the nucleophilic NHC IMes onto the cyclic ester was yet reported, when polymerizing LA in total absence of an alcohol initiator.[169-170] In this case, cyclic PLA's could be obtained by a kinetically controlled zwitterionic ROP mechanism (referred to as the ZROP mechanism). In this case, deactivation of polymeric zwitterionic species occurred intramolecularly (Scheme 27), even at relatively high monomer concentrations (0.6–1.0 M in THF). Under such conditions, molar masses were directly controlled by the initial monomer to NHC ratio (entry 20,

Table 1). In other words, NHC played in this case the role of initiator, though released after intramolecular cyclization (macrolactonization reaction). These polymerization reactions were very fast (k_p = 48.7 L/mol/s), yielding high molar masses cyclic PLAs (M_n = 5,000 and 30,000 g/mol) with narrow dispersities (D < 1.32) in only a few seconds (5-900 s). Polymerization reactions were quenched by adding carbon disulfide (CS_2) in order to irreversibly trap the NHC within a zwitterionic NHC-CS_2 adduct.

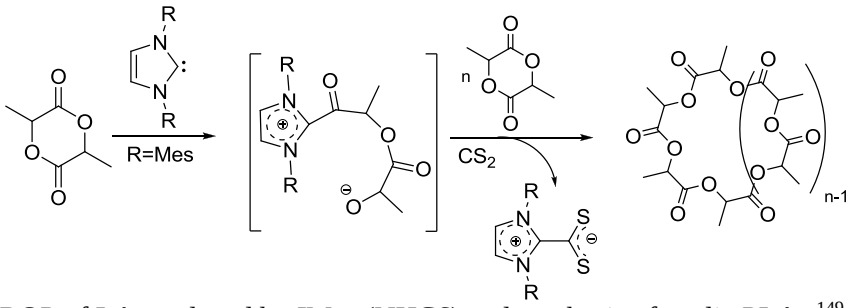

Scheme 27. ZROP of LA catalyzed by IMes (NHC**6**) and synthesis of cyclic PLAs.[149, 150]

The cyclic architecture was supported by a combination of techniques, including NMR, MALDI-ToF MS, and viscometry of the cyclic polymers in comparison with the linear homologues of the same molar mass (prepared in the presence of alcohol initiators). In addition, thermogravimetric analysis (TGA) suggested that cyclic PLAs were more thermally stable than the respective linear polymers. When IMes-mediated ROP was applied to optically pure L-LA, a crystalline isotactic cyclic PLA was formed, indicating that the polymerization occurred without epimerization of the chiral center.

Investigations into the kinetics of these ZROPs mediated by NHC**6** (IMes) allowed the authors to account for these experimental observations.[170] If the rate of cyclization was of the same order than the rate of propagation, cyclization would be the result of an intramolecular chain-transfer, releasing the NHC that would create new chains. In the latter case, the molar masses should not evolve linearly but should remain constant with monomer conversion, while the dispersity should be equal to 2.0. Since this was not observed experimentally, it was proposed that the IMes-mediated ZROP involved a slow initiation step (which was second order in monomer concentration, k_i = 0.274 L^2 mol^{-2} s^{-1}), a propagation step (first order in monomer concentration) that was found much faster than initiation, cyclization (k_c = 0.0575 s^{-1}), and depropagation (k_d = 0.208 s^{-1}). As a matter of fact, few chains could be re-initiated by the carbenes released upon cyclization. The fact that the dispersity increased at high

conversions was explained by the occurrence of either competitive transesterification reactions of the propagating zwitterions, or transesterification reactions of the cyclic polymers by the zwitterions or the carbene molecules. Kinetic data were supported by numerical and stochastic simulations.

In complement to the previous studies, reaction of the saturated homologue of IMes, i.e. 1,3-dimesitylimidazolin-2-ylidene (NHC**11**) with four-membered lactones (β-butyrolactone, β-BL and β-propiolactone, β-PL) was investigated (entry 21, Table 1).[171] This particular carbene first generated zwitterionic species by a direct nucleophilic attack of the carbene to the lactone monomer, followed by ring-closure, forming a neutral and stable imidazolidine spirocycle. The latter intermediate could be isolated and characterized by crystallography. Interestingly, propagation occurred in the presence of excess β-BL monomer upon using the imidazolidine spirocycle thus operating as a latent initiating system. In other words, the controlled ROP of both β-PL and β-BL operated by reversible opening and closure of the labile spirocyclic imidazolidine intermediate, affording well-defined aliphatic poly(β-BL) and poly(β-PL), as illustrated in Scheme 28. The use of CS_2 allowed quenching these polymerizations and releasing the cyclic polyesters.

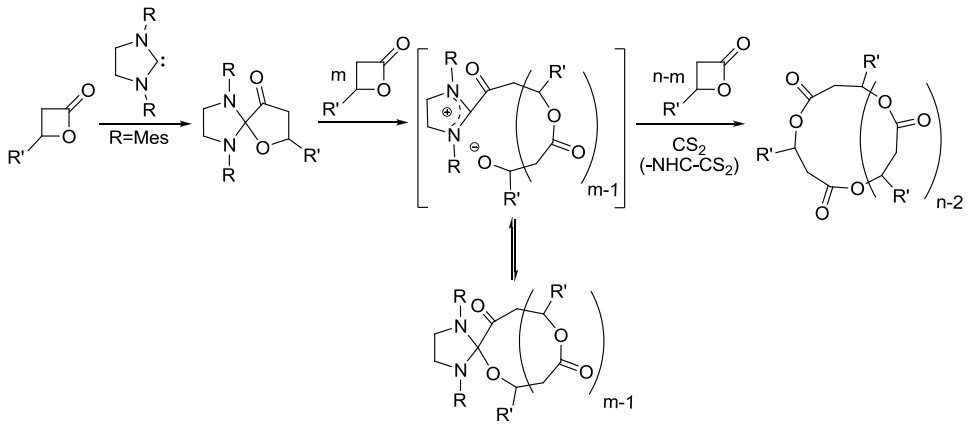

Scheme 28. Formation of a spirocycle from β-butyrolactone (R'= CH_3) and the saturated NHC 1,3-dimesitylimidazolin-2-ylidene (R= mesityl; NHC**11**).[171]

This technique was recently applied by Hedrick, Waymouth *et al.* to synthesize high molar mass cyclic PCLs and cyclic gradient copolymers of PVL and PCL (Table 1, entry 22).[172-173] Using NHCs **9**, **10** or **10'** in THF or toluene afforded high molar masses cyclic PCL's (up to 114,000 g/mol) *via* ZROP.[173] The cyclic topology of the obtained polymers was checked by NMR and viscosity measurements. SAXS and DSC analyses showed that cyclic PCL's and linear homologues display the

same crystalline organization although, for high molar masses (higher than 75,000 g/mol), the crystallization was faster for cyclic polymers.

The synthesis of cyclic gradient copolymers was also reported by batch copolymerization of δ-valerolactone (VL) and ε-caprolactone (CL). The two monomers were found to exhibit different reactivities (r_{VL}=9.0 and r_{CL}=0.24, as determined by the Fineman-Ross method with NHC**10** as catalyst and benzyl alcohol as initiator in THF).[172] Such difference in the reactivity ratios is usually not observed with metal-based alkoxides as initiating systems (with $Sn(Oct)_2$ at 160 °C: r_{VL} = 0.49 and r_{CL} = 0.25), thus highlighting the organocatalytic effect for the production of specific (co)polymers. Several cyclic copolymers with various VL/CL compositions and dispersities lower than 2.4 were thus derived. Kinetics study highlighted that, 5 min after mixing all reactants, the consumption of the VL monomer was almost complete (94%), while CL monomer required about 1 h to reach the same conversion, attesting of the gradient topology of the as-obtained copolymer. Finally, the cyclic gradient copolymers exhibited similar melting temperatures as VL or CL-based homopolymers (T_{mPVL}= 57 °C, T_{mPCL}= 56 °C *vs.* $T_{mgradient}$= 38-44 °C), as substantiated by DSC analysis.

Zhang *et al.* reported the synthesis of poly(α-peptoid)s that are structural mimics of poly(α-peptide)s, *via* the direct NHC-initiated ROP of R-substituted *N*-carboxyanhydrides (^{N}R-NCA) (Table 1, entry 23).[174-177] In contrast to poly(α-peptide)s whose well-defined secondary structures are stabilized through hydrogen bonding interactions, poly(α-peptoid)s are free of such interactions. As with regular NCA monomers, ^{N}R-NCA can be polymerized through a nucleophilic chain growth pathway that entails regioselective insertion of a nucleophilic initiator (e.g., primary amine) into the anhydride carbonyl group, followed by elimination of CO_2 reforming an amino propagating chain-end.

^{N}R-NCA monomers could be polymerized in the presence of NHC**5** as direct initiator (ZROP mechanism). It is interesting to note that the activated functional group (i.e., anhydride) of the ^{N}R-NCA monomer is different from that of the polymer backbone (i.e., amide). As NHCs have not been reported to trigger transamidation reactions, it is likely that *inter*- and *intra*-chain transfer (side) reactions, if existing, are *de facto* reduced. This situation differs from that of aliphatic polyesters discussed above, which can be subjected to NHC-catalyzed transesterifications.

Analysis by mass spectroscopy revealed that the carbene moiety was retained as spirocycle adduct (Scheme 29) when precipitated in hexane. Chain-extension could be performed upon addition of a second batch of ^{N}R-NCA monomer. Analysis by MALDI-ToF MS showed that the resulting polymers mainly consisted of cyclic poly(α-peptoid)s formed by ZROP, followed by intramolecular cyclization and release of the NHC moiety (Scheme 29).[177] The cyclic architecture was confirmed by viscometric measurements. Interestingly, control over polymer molar masses and dispersities could be maintained even at relatively high concentrations of monomer, in contrast to common synthetic strategies for cyclic polymers that generally require dilute conditions.[186-188]

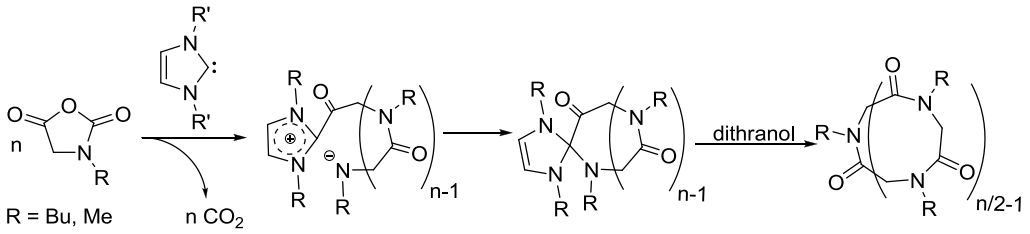

Scheme 29. NHC**5**-initiated ROP of *N*-carboxyanhydrides.[174]

Cyclic copoly(α-peptoid)s could be derived by sequential ZROP of ^{N}Me-NCA, ^{N}Bu-NCA, ^{N}De-NCA, ^{N}Propargyl-NCA monomers. For instance, the sequential copolymerization of ^{N}Me-NCA and ^{N}De-NCA afforded amphiphilic cyclic diblock copolypeptoids which were found to self-assemble into spherical micelles that reorganized into micrometer-long cylindrical micelles, as shown by cryo-TEM.[176] Cyclic brush-like copolymers were derived by grafting of PEG-N_3 chains to random cyclic poly(^{N}propargylglycine)-*r*-poly(^{N}-butylglycine). [175]

NHCs were also employed to catalyze the ROP of cyclosiloxanes (hexamethylcyclotrisiloxane and octamethyltetracyclosiloxane, referred to as D_3 and D_4, respectively) and carbosiloxanes, in the presence of initiating alcohols.[178] For instance, Baceiredo *et al.* reported the ROP of D_4 in THF solution at 25 °C, using NHC**2** or NHC**3** as catalyst, in the presence of methanol, *tert*-butyl alcohol or benzyl alcohol as initiator (Scheme 30a). Poly(dimethyl siloxane) (PDMS) of dispersities in a range 1.58-1.70 were obtained (Table 1, entry 24), likely due to undesirable intra- (back-biting) and intermolecular transfer reactions. The authors also observed faster polymerization as the amount of NHC catalyst increased. This might be attributed to the affinity of carbenes to the silicon atom and the

propensity of Si to hypervalency,[84] favoring ring-opening of D_4. Thus, either the AMM or the ACEM is plausible in these polymerizations.

The ROP of 2,2,5,5-tetramethyl-1-oxa-2,5- disilacyclopentane (TMOSC) catalyzed by the strongly basic NHC**9** in the presence of an initiating alcohol was found to be very fast (99% conversion in 1 min, k = 1.65 s^{-1}), forming poly(carbosiloxane) having a molar mass of 10,200 g/mol and a dispersity equal to 1.19 (Table 1, entry 25, Scheme 30b).[179] The polymerization was slower with the NHC**6** (80% after 30 min, k = 0.044 s^{-1}). An initiator (of the alcohol-type)/chain end (of the silanol-type) activation mechanism was proposed (ACEM). However, activation of the silicon atoms of the monomer (AMM) could be envisaged in this case also.

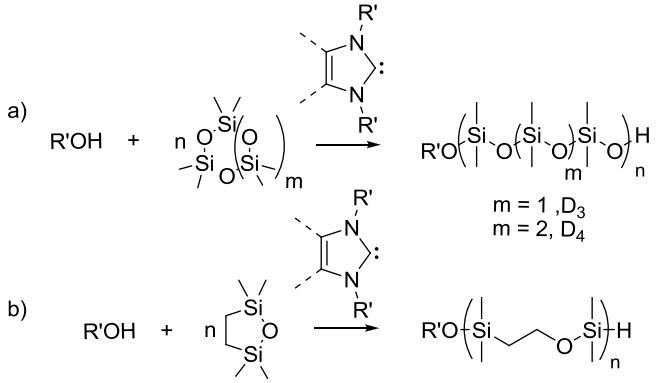

Scheme 30. NHC-catalyzed ROPs of a) D_3 and D_4 (R'=*t*Bu (NHC**2**), Cy (NHC**3**), *i*Pr (NHC**9**)),[178-179] b) carbosiloxanes (R'=iMes (NHC**6**), *i*Pr (NHC**9**)).[179]

Gnanou, Taton *et al.* reported that NHCs could trigger the ROP of ethylene oxide (EO),[142] not only as direct initiators (*via* a ZROP mechanism), but also as organocatalysts when used in conjunction with chain regulators of the NuE-type, where Nu and E are the nucleophilic and electrophilic moieties, respectively, (e.g. Nu = $PhCH_2O$, $HC{\equiv}CCH_2O$, N_3 and E = H, $SiMe_3$). In both cases, linear α,ω-heterodifunctionalized PEOs were achieved (entries 26 and 27). For instance, 1,3-diisopropylimidazol-2-ylidene (NHC**1**) directly initiated the metal-free ROP of EO at 50 °C in DMSO, in absence of any other reagents. The PEO chain length was thus controlled by the EO to the NHC molar ratio (typically, [EO]/[NHC] = 100/1). No competitive intra- or intermolecular transfer reactions are expected during anionic ROP of EO, the possible side reactions being transfer reactions to protic impurities, or cyclization of the growing zwitterionic PEO chains.

The resulting polymer was quenched at the completion of the ZROP by a NuE functionalizing terminator, leading to linear α-Nu,ω-OH (or α-Nu,ω-$OSiMe_3$)-difunctionalized PEOs exclusively, unlike the zwitterionic polymerization of LA described above forming cyclics. The quantitative introduction of the Nu moiety in α- position and of OH (or $OSiMe_3$) in ω-position of PEO chains occurred through the nucleophilic substitution of the imidazolium moiety by $Nu^{\delta-}$ and the concomitant reaction of the ω-growing alkoxide of PEO chain with $H^{\delta+}$ (or $Me_3Si^{\delta+}$), as illustrated in Scheme 31. In particular, difunctionalized α,ω-dihydroxy-telechelic, α-benzyl,ω-hydroxy and α-azido,ω-hydroxy-PEOs could be synthesized by NHC-initiated ZROP, using H_2O, $PhCH_2OH$ and N_3SiMe_3 as terminating agents. A well-defined PEO-*b*-PCL diblock copolymer could also be directly synthesized by sequential ZROP in DMSO, using the same NHC as organic initiator, without isolation of the zwitterionic PEO block intermediate.

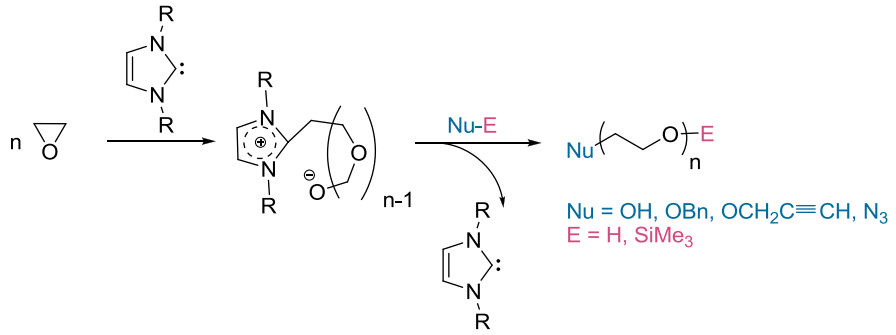

Scheme 31. Functionalizing terminators in the ZROP of ethylene oxide initiated by NHC**1** (R=*i*Pr).[142]

Instead of using NHCs as direct initiators, the same group also reported the ROP of EO with NHCs as organocatalysts, in conjunction with not only alcohol but also trimethylsilylated initiators (the same NuE-type compounds mentioned above) introduced at the beginning.[143] Typical amounts of NHC catalyst equal to 10 mol% relative to NuE were employed in this case, leading to PEOs with molar masses in the range 1,800-10,500 g/mol and dispersities lower than 1.15.

Similarly to ROP of cyclic esters, the two mechanisms (AMM, Path A and ACEM, Path B) of initiation and chain growth were proposed (Scheme 32).

The two methods discussed above, i.e. NHC**1** employed either as direct initiator in ZROP or as true organocatalyst in the presence of the NuE-type reagents, was applied to the ROP of propylene oxide (PO).[144] In this way, α,ω-difunctionalized PPOs were derived using NHC**1** under metal-free

and solvent-free conditions, whereas PPO is generally obtained by anionic ROP in low polar media from alkali metal-based initiators.[56] When NHC**1** was used as a direct organic initiator, the polymerization was simply quenched by H_2O, leading to dihydroxytelechelic PPO's with molar masses up to 4,500 g/mol (Table 1, entry 28). Targeting a PPO of higher molar masses, however, showed the presence of a small extent of allyl-ended PPO chains, as observed by ^{1}H NMR, which was characteristic of the occurrence of the chain transfer of active PPO chains to the monomer.[56] With NHC**1** as catalyst, and the hydroxylated or trimethylsilylated reagents as initiators, the ROP of PO at 50 °C permitted the synthesis of PPO's of molar masses up to 8,000 g.mol^{-1} with a dispersity lower than 1.18. Both routes implied PO polymerization in bulk and incomplete monomer conversion (≤ 40% in all experiments), allowing an easy removal -and possible recycling- of the residual low-boiling monomer by simple distillation.

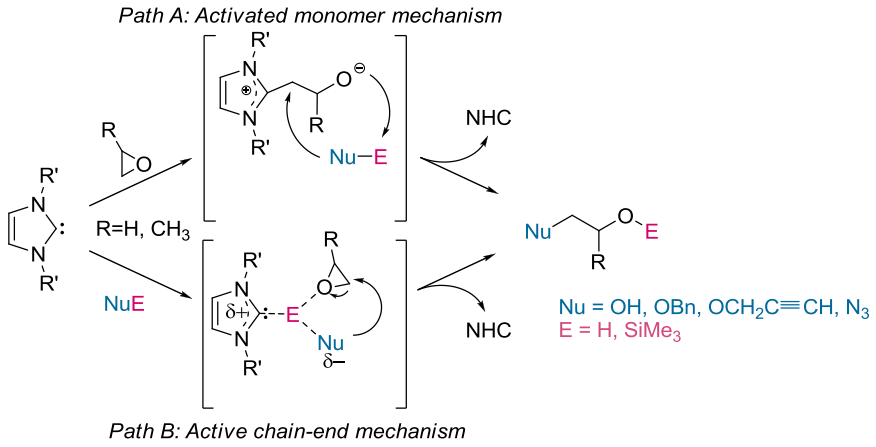

Scheme 32. AMM (path A) and ACEM (path B) in ROP of ethylene oxide (R'=H) and propylene oxide (R'=CH_3) catalyzed by NHCs**1** and **2**.[154,155]

3.3.3. Group transfer polymerization (GTP)

Organocatalysis has been used in other polymerization methods than ROP. For instance, Hedrick, Waymouth *et al.*[69] on one hand and Taton, Gnanou *et al.*,[68] on the other, reported that the group transfer polymerization (GTP) of (meth)acrylic monomers can advantageously be catalyzed by NHCs.

GTP was proposed in the mid 1980s as a convenient method to control the polymerization of (meth)acrylic monomers at ambient temperature and above.[189] It is based on the repetition of

Mukaiyama-Michael reactions[190] involving the addition of silyl ketene acetal (SKA) onto an incoming (meth)acrylic monomer. GTP is generally catalyzed by a metal-free nucleophile (Lewis base) or a metal-based Lewis acid, for methacrylic or acrylic monomers, respectively.[191] The absence of a unique catalytic system that could be generalized for both families of monomers did not permit, however, the synthesis of block copolymers featuring both monomer units by sequential GTP.[154] However, new developments in GTP *via* an organocatalysis pathway have been recently disclosed. [70-71,192-199]

Webster *et al.* originally suggested the name "group transfer polymerization" to account for the fact that the trimethylsilyl group remained at the end of the *chain it created with throughout polymerization.*[154] In other words, an associative (concerted) mechanism of GTP involving the transfer of the trialkylsilyl group from the polymer chain-end to the inserted monomer was originally put forward. However, this pathway was further questioned. In particular, Quirk proposed that GTP occurred by a dissociative mechanism through minute amounts of propagating enolates.[200] These anionic species would be the real active centers and be temporarily trapped by the silyl ketene acetals (SKAs), forming dormant trimethylsilyl bis-enolates (Scheme 33). In fact, the mechanism of GTP seems to strongly depend on the overall polymerization conditions and, in particular, on the nature of the catalyst.[201] NHCs were themselves reported to induce either the dissociative or the associative mechanism, depending upon the substituent on the imidazole ring (Scheme 33).

The NHC-catalyzed GTP of (meth)acrylic monomers was typically performed at room temperature, using 1-methoxy-2-methyl-1-[(trimethylsilyl)oxy]prop-1-ene (MTS) as initiator, in polar (THF) or non-polar (toluene) medium. In this way, polymethacrylates and polyacrylates with molar masses in the range 10,000-300,000 g/mol, corresponding to the initial [monomer]/[MTS] ratio and with dispersities lower than 1.2 were obtained in quantitative yields.

While Hedrick *et al.* postulated a dissociative mechanism forming enolate-type species from NHC**9** as catalyst (Table 1, entry 30),[69] Taton, Gnanou *et al.* provided a series of experimental evidences suggesting that GTP occurred by an associative (concerted-like) mechanism, when catalyzed by NHC**1** or NHC**2** (Table 1, entry 29 and Scheme 33).[152] This difference was explained by the varying nucleophilicity/siliconphilicity of the NHCs tested. NHC**9** is indeed slightly more nucleophilic than

NHC**1** and NHC**2** due to the presence of two extra methyl groups on the imidazole backbone. Though both mechanisms lead to the same polymer, the polymerization kinetics as well as the properties of the final polymers associated with each of them might be different.[191,201]

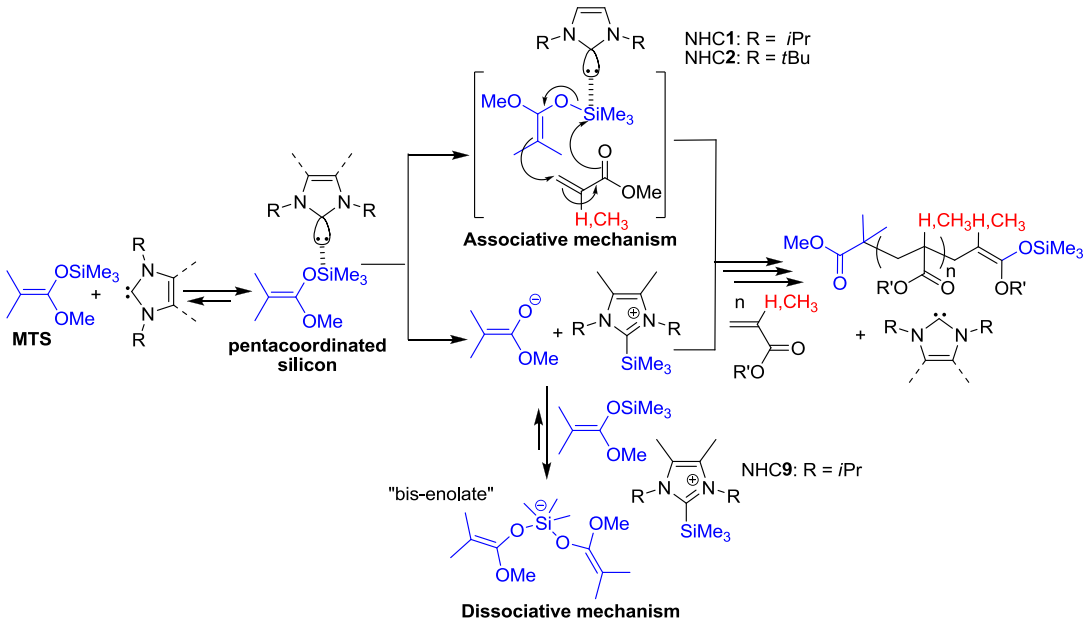

Scheme 33. Associative and dissociative mechanisms for NHC-mediated GTP.[69,152]

The existence of the associative mechanism with NHC**1** and **2**, involving the formation of hypervalent siliconate intermediates, was supported by the following observations:

- Though the first-order kinetic plot $\ln[M]_0/[M]$ *versus* time deviated from linearity at high monomer conversions, no inhibition period was noted at low monomer conversion. Moreover, the polymerization rate dramatically increased as the concentration of initiator increased, with first-order kinetic dependence of the initiator.

- When mixed in 1:1 molar ratio, MTS and NHC**1** did not reveal the formation of enolate-type species by ^{29}Si or ^{13}C NMR spectroscopy.

- The production of well-defined poly(methyl methacrylate)s using the 1:1 adducts of NHC**1** and MTS as initiating system.

- The controlled polymerization of n-butyl and *tert*-butyl acrylates in the presence of NHC**1** or NHC**2**, suggesting that back-biting and internal isomerisation could be minimized, likely because no enolates were generated.

- The preparation of block copolymers based on acrylate-type and methacrylate-type monomer units, irrespective of the order of addition of the two monomers, which would not be possible from pure enolates formed by a dissociative mechanism.[151]

It is very likely, however, that the more slightly nucleophilic NHC**9** used by Hedrick and Waymouth brought about the GTP of (meth)acrylics *via* a dissociative pathway.

Gnanou, Taton *et al.* also exploited the potential of NHC**1** and NHC**2** to catalyze the MTS-initiated GTP of a variety of monomers in THF or toluene at room temperature.[151,180] Monomers include not only acrylics (i.e. butyl acrylate, *tert*-butyl acrylate, and 2-(dimethylamino)ethyl acrylate), methacrylics (methyl methacrylate and 2-(dimethylamino)ethyl methacrylate), but also an acrylamide-type monomer, namely, *N*,*N*-dimethylacrylamide. The NHC-catalyzed MTS-initiated GTP of methacrylonitrile using DMF as solvent was also reported.

Recently, Chen *et al.* employed NHC**2** to directly trigger the zwitterionic polymerization of some methacrylic monomers, such as MMA, γ-methyl-α-methylene-γ-butyrolactone (MMBL), α-methylene-γ-butyrolactone (MBL) and furfuryl methacrylate (FMA), in absence of any other initiator.[202] Polymerizations were performed with NHC**2** in DMF. Using other NHCs such as NHC**6** or NHC**13** (Scheme 34) or performing the reaction in toluene and THF resulted in lower efficiencies. For instance, NHC**6** was shown to form a very stable 1/1 adduct with MMA, while NHC**13** only allowed the tail-to-tail dimerization of two MMA molecules. The authors suggested that such "organopolymerizations" occurred through iterative 1,4-conjugate additions of the propagating ester enolate to the incoming monomer (Scheme 34). As no initiating or terminating end groups could be detected by MALDI-ToF MS of low-molecular weight PMMBL, the polymerization was thought to terminate by intramolecular chain-end coupling, forming cyclic polymethacrylics.

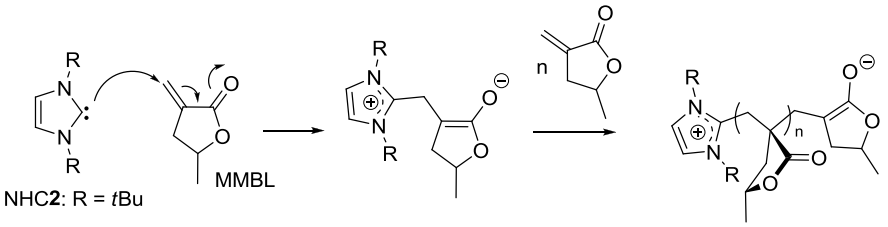

Scheme 34. Direct NHC-initiated polymerization of γ-methyl-α-methylene-γ-butyrolactone.[202]

Conclusion

Tremendous research efforts are currently made in organic synthesis for the development of more sustainable processes, taking into account mild conditions, energy savings, high selectivities, reduced by-products and wastes. In this regard, both enzymatic catalysis and organocatalysis offer new opportunities for activating miscellaneous substrates and accessing functional building blocks. In the past decade, concepts of organocatalysis have been applied to polymer synthesis, allowing significant breakthroughs such as enhancement of polymerization rates and high selectivity of propagation relative to adverse chain breaking by termination or transfer reactions. Moreover, biocompatible polymers free of metal residues can now be accessed by an organocatalytic pathway.

In this context, NHCs have proven particularly versatile for various organocatalyzed polymerization reactions, owing to their unique electronic properties. NHCs have mainly served to trigger the ring-opening polymerization (ROP) of cyclic esters for the production of both cyclic and linear aliphatic polyesters. However, the scope of NHCs has been expanded to other chain-growth polymerization reactions, including ROP of both ethylene and propylene oxides, *N*-substituted NCA's, cyclosiloxanes, group transfer polymerization of (meth)acrylic monomers, and to some step growth polymerization reactions as well (e.g. for the metal-free synthesis of polyurethanes, polysiloxanes or polybenzoins).

It is worth mentioning that, taking benefit of their broad range of reactivity, NHCs have also been employed as structural components, i.e. side chain functionalizing reagents of pre-formed polymers featuring pendant azide groups (not discussed in this chapter). Their reactivity towards azides, isothiocyanates and their ability to dimerize have also enabled the synthesis of conjugated polymers through step-growth polymerizations involving bis(NHC) monomer substrates.[94,203-205]

Owing to their inherent structural modularity and their extremely diverse chemistry, NHCs are expected to provide selective polymerization reaction pathways as a function of the monomer substrate to be activated. Yet, challenges still remain in the utilization of NHCs either as reagents or as catalysts in macromolecular synthesis. For instance, their air and moisture sensitivities still limit the widespread adoption of NHCs in (macro)molecular synthesis, though they can be generated *in situ*

(e.g. upon heating or addition of a base), from readily accessible precursors. Moreover, only a limited number of monomer candidates have actually been investigated so far, carbonyl-containing monomers such as cyclic esters and cyclic carbonates being the most studied in the context of ROP. Also polymer molar masses of polymers are somehow limited in most examples reported. On the other hand, asymmetric polymerizations using chiral catalysts have to be investigated in much more details.

The next chapter addresses some of these points, in particular through the design of novel air-stable NHC precursors for a use in (macro)molecular synthesis (chapter 2). In chapter 3, use of NHCs in conjunction with organic Lewis acids as a possible means to induce a cooperative dual activation mechanism is described. Chapter 4 discusses the utilization of a particular commercial trialkylphosphine for GTP as an alternative to NHC catalysis.

References

1. Fèvre, M.; Vignolle, J.; Gnanou, Y.; Taton, D., In *Polymer Science: A Comprehensive Reference*, Editors-in-Chief:; Matyjaszewski, K.; Möller, M., Eds. Elsevier: Amsterdam, 2012; p 67.
2. Fèvre, M.; Pinaud, J.; Gnanou, Y.; Vignolle, J.; Taton, D., *submitted to Chem. Soc. Rev.*
3. Kamber, N. E.; Jeong, W.; Waymouth, R. M.; Pratt, R. C.; Lohmeijer, B. G. G.; Hedrick, J. L., *Chem. Rev.* **2007,** *107*, 5813.
4. Kiesewetter, M. K.; Shin, E. J.; Hedrick, J. L.; Waymouth, R. M., *Macromolecules* **2010,** *43*, 2093.
5. Delaude, L., *Eur. J. Inorg. Chem.* **2009,** *2009*, 1681.
6. de Frémont, P.; Marion, N.; Nolan, S. P., *Coord. Chem. Rev.* **2009,** *253*, 862.
7. Enders, D.; Niemeier, O.; Henseler, A., *Chem. Rev.* **2007,** *107*, 5606.
8. Bourissou, D.; Guerret, O.; Gabbai, F. P.; Bertrand, G., *Chem. Rev.* **2000,** *100*, 39.
9. Dröge, T.; Glorius, F., *Angew. Chem. Int. Ed.* **2010,** *49*, 6940.
10. Grossmann, A.; Enders, D., *Angew. Chem. Int. Ed.* **2012,** *51*, 314.
11. Marion, N.; Díez-González, S.; Nolan, S. P., *Angew. Chem. Int. Ed.* **2007,** *46*, 2988.
12. Moore, J.; Rovis, T., In *Asymmetric Organocatalysis*, List, B., Ed. Springer Berlin / Heidelberg: 2009; Vol. 291, p 77.
13. Bugaut, X.; Glorius, F., *Chem. Soc. Rev.* **2012,** *41*, 3511.
14. Glorius, F., In *N-Heterocyclic Carbenes in Transition Metal Catalysis*, Springer Berlin / Heidelberg: 2007; Vol. 21, p 1.
15. Díez-González, S.; Marion, N.; Nolan, S. P., *Chem. Rev.* **2009,** *109*, 3612.
16. Samojłowicz, C.; Bieniek, M.; Grela, K., *Chem. Rev.* **2009,** *109*, 3708.
17. Williams, K.; Neilson, B.; Bielawski, C., In *Synthesis of Polymers*, Wiley-VCH Verlag GmbH & Co. KGaA.: 2012; Vol. 2, p 973.
18. Matyjaszewski, K., In *Controlled and Living Polymerizations*, Wiley-VCH Verlag GmbH & Co. KGaA: 2010; p 103.
19. Odian, G., In *Principles of Polymerization*, 4th ed.; John Wiley & Sons, Inc.: Hoboken, NJ, USA, 2004; p i.
20. Percec, V., *Chem. Rev.* **2009,** *109*, 4961.
21. Platel, R. H.; Hodgson, L. M.; Williams, C. K., *Polym. Rev.* **2008,** *48*, 11
22. Kobayashi, S.; Makino, A., *Chem. Rev.* **2009,** *109*, 5288.
23. von Liebig, J., *Justus Liebigs Ann. Chem.* **1860,** *113*, 246.
24. *J. Prakt. Chem.* **1873,** *8*, 428.
25. Fischer, E., *Ber. Dtsch. Chem. Ges.* **1893,** *26*, 2400.
26. Fischer, E., *Ber. Dtsch. Chem. Ges.* **1895,** *28*, 1145.
27. Fischer, E.; Beensch, L., *Ber. Dtsch. Chem. Ges.* **1894,** *27*, 2478.
28. Steglich, W.; Höfle, G., *Angew. Chem. Int. Ed.* **1969,** *8*, 981.
29. Eder, U.; Sauer, G.; Wiechert, R., *Angew. Chem. Int. Ed.* **1971,** *10*, 496.
30. Overberger, C. G.; Dixon, K. W., *J. Polym. Sci. Polym. Chem. Ed.* **1977,** *15*, 1863.
31. Domínguez de María, P., *ChemCatChem* **2010,** *2*, 487.
32. Dalko, P. I.; Moisan, L., *Angew. Chem. Int. Ed.* **2004,** *43*, 5138.
33. Barbas, C. F., *Angew. Chem. Int. Ed.* **2008,** *47*, 42.
34. Seayad, J.; List, B., *Org. Biomol. Chem.* **2005,** *3*, 719.
35. Zhang, Z.; Schreiner, P. R., *Chem. Soc. Rev.* **2009,** *38*, 1187.
36. Bertelsen, S.; Jorgensen, K. A., *Chem. Soc. Rev.* **2009,** *38*, 2178.
37. Bella, M.; renzi, p., *Chem. Commun.* **2012**.
38. Marinetti, A.; Voituriez, A., *Synlett* **2010**, 174.
39. Pansare, S. V.; Paul, E. K., *Chem. Eur. J.* **2011,** *17*, 8770.
40. Schreiner, P. R., *Chem. Soc. Rev.* **2003,** *32*, 289.
41. Pellissier, H., *Adv. Synth. Catal.* **2012,** *354*, 237.
42. Bradshaw, B.; Bonjoch, J., *Synlett* **2012,** *2012*, 337.
43. Renzi, P.; Bella, M., *Chem. Commun.* **2012,** *48*, 6881.
44. Zhang, W., Horváth, I. T., Ed. Springer Berlin / Heidelberg: 2012; Vol. 308, p 175.
45. Briere, J.-F.; Oudeyer, S.; Dalla, V.; Levacher, V., *Chem. Soc. Rev.* **2012,** *41*, 1696.
46. Taylor, J. E.; Bull, S. D.; Williams, J. M. J., *Chem. Soc. Rev.* **2012,** *41*, 2109.
47. Lu, L.-Q.; An, X.-L.; Chen, J.-R.; Xiao, W.-J., *Synlett* **2012,** *23*, 490.
48. Hernandez, J. G.; Juaristi, E., *Chem. Commun.* **2012,** *48*, 5396.
49. Hajos, Z. G.; Parrish, D. R. DE 2102623, 1971.
50. Bui, T.; Barbas, C. F., *Tetrahedron Lett.* **2000,** *41*, 6951.

51. Chattopadhyay, D. K.; Raju, K. V. S. N., *Prog. Polym. Sci.* **2007,** *32*, 352.
52. Penczek, S.; Kubisa, P.; Matyjaszewski, K., *Adv. Polym. Sci.* **1980,** *37*, 1.
53. Nederberg, F.; Connor, E. F.; Möller, M.; Glauser, T.; Hedrick, J. L., *Angew. Chem. Int. Ed.* **2001,** *40*, 2712.
54. Nederberg, F.; Connor, E. F.; Glausser, T.; Hedrick, J. L., *Chem. Commun.* **2001**, 2066.
55. Kricheldorf, H. R., *Angew. Chem. Int. Ed.* **2006,** *45*, 5752.
56. Penczek, S.; Cypryk, M.; Duda, A.; Kubisa, P.; Slomkowski, S., *Prog. Polym. Sci.* **2007,** *32*, 247.
57. Odian, G., In *Principles of Polymerization*, 4th ed.; John Wiley & Sons, Inc.: Hoboken, NJ, USA, 2004; p 544.
58. Aoi, K.; Okada, M., *Prog. Polym. Sci.* **1996,** *21*, 151.
59. Cronin, J. P.; Pepper, D. C., *Makromol. Chem.* **1988,** *189*, 85.
60. Simón, L.; Goodman, J. M., *J. Org. Chem.* **2007,** *72*, 9656.
61. Chuma, A.; Horn, H. W.; Swope, W. C.; Pratt, R. C.; Zhang, L.; Lohmeijer, B. G. G.; Wade, C. G.; Waymouth, R. M.; Hedrick, J. L.; Rice, J. E., *J. Am. Chem. Soc.* **2008,** *130*, 6749.
62. Schreiner, P. R.; Wittkopp, A., *Org. Lett.* **2002,** *4*, 217.
63. Thillaye du Boullay, O.; Marchal, E.; Martin-Vaca, B.; Cossío, F. P.; Bourissou, D., *J. Am. Chem. Soc.* **2006,** *128*, 16442.
64. Brignou, P.; Priebe Gil, M.; Casagrande, O.; Carpentier, J.-F. o.; Guillaume, S. M., *Macromolecules* **2010,** *43*, 8007.
65. Sanders, D. P.; Fukushima, K.; Coady, D. J.; Nelson, A.; Fujiwara, M.; Yasumoto, M.; Hedrick, J. L., *J. Am. Chem. Soc.* **2010,** *132*, 14724.
66. Thillaye du Boullay, O.; Bonduelle, C.; Martin-Vaca, B.; Bourissou, D., *Chem. Commun.* **2008**, 1786.
67. du Boullay, O. T.; Saffon, N.; Diehl, J.-P.; Martin-Vaca, B.; Bourissou, D., *Biomacromolecules* **2010,** *11*, 1921.
68. Raynaud, J.; Ciolino, A.; Baceiredo, A.; Destarac, M.; Bonnette, F.; Kato, T.; Gnanou, Y.; Taton, D., *Angew. Chem. Int. Ed.* **2008,** *47*, 5390.
69. Scholten, M. D.; Hedrick, J. L.; Waymouth, R. M., *Macromolecules* **2008,** *41*, 7399.
70. Fuchise, K.; Sakai, R.; Satoh, T.; Sato, S.-i.; Narumi, A.; Kawaguchi, S.; Kakuchi, T., *Macromolecules* **2010,** *43*, 5589.
71. Kakuchi, R.; Chiba, K.; Fuchise, K.; Sakai, R.; Satoh, T.; Kakuchi, T., *Macromolecules* **2009,** *42*, 8747.
72. Marrot, S.; Bonnette, F.; Kato, T.; Saint-Jalmes, L.; Fleury, E.; Baceiredo, A., *J. Organomet. Chem.* **2008,** *693*, 1729.
73. Nyce, G. W.; Lamboy, J. A.; Connor, E. F.; Waymouth, R. M.; Hedrick, J. L., *Org. Lett.* **2002,** *4*, 3587.
74. Pinaud, J.; Vijayakrishna, K.; Taton, D.; Gnanou, Y., *Macromolecules* **2009,** *42*, 4932.
75. Kamber, N. E.; Tsujii, Y.; Keets, K.; Waymouth, R. M.; Pratt, R. C.; Nyce, G. W.; Hedrick, J. L., *J. Chem. Educ.* **2010,** *87*, 519.
76. Fukushima, K.; Coulembier, O.; Lecuyer, J. M.; Almegren, H. A.; Alabdulrahman, A. M.; Alsewailem, F. D.; McNeil, M. A.; Dubois, P.; Waymouth, R. M.; Horn, H. W.; Rice, J. E.; Hedrick, J. L., *J. Polym. Sci., Part A: Polym. Chem.* **2011,** *49*, 1273.
77. Hashimoto, K., *Prog. Polym. Sci.* **2000,** *25*, 1411.
78. Kubisa, P.; Penczek, S., *Prog. Polym. Sci.* **1999,** *24*, 1409.
79. Penczek, S., *J. Polym. Sci., Part A: Polym. Chem.* **2000,** *38*, 1919.
80. Igau, A.; Grutzmacher, H.; Baceiredo, A.; Bertrand, G., *J. Am. Chem. Soc.* **1988,** *110*, 6463.
81. Arduengo, A. J.; Harlow, R. L.; Kline, M., *J. Am. Chem. Soc.* **1991,** *113*, 361.
82. Poyatos, M.; Mata, J. A.; Peris, E., *Chem. Rev.* **2009,** *109*, 3677.
83. Crabtree, R. H., *Coord. Chem. Rev.* **2007,** *251*, 595.
84. Fuchter, M. J., *Chem. Eur. J.* **2010,** *16*, 12286.
85. M. B. Smith; J. March, In *March's Advanced Organic Chemistry: Reactions, Mechanisms, and Structure*, 6th ed.; John Wiley & Sons, Inc.: Hoboken, NJ, USA, 2007; p 234.
86. Maji, B.; Breugst, M.; Mayr, H., *Angew. Chem. Int. Ed.* **2011,** *50*, 6915.
87. Higgins, E. M.; Sherwood, J. A.; Lindsay, A. G.; Armstrong, J.; Massey, R. S.; Alder, R. W.; O'Donoghue, A. C., *Chem. Commun.* **2011,** *47*, 1559.
88. Magill, A. M.; Cavell, K. J.; Yates, B. F., *J. Am. Chem. Soc.* **2004,** *126*, 8717.
89. Alder, R. W.; Blake, M. E.; Chaker, L.; Harvey, J. N.; Paolini, F.; Schütz, J., *Angew. Chem. Int. Ed.* **2004,** *43*, 5896.
90. Liu, Y.; Lindner, P. E.; Lemal, D. M., *J. Am. Chem. Soc.* **1999,** *121*, 10626.
91. Lemal, D. M.; Lovald, R. A.; Kawano, K. I., *J. Am. Chem. Soc.* **1964,** *86*, 2518.
92. Winberg, H. E.; Carnahan, J. E.; Coffman, D. D.; Brown, M., *J. Am. Chem. Soc.* **1965,** *87*, 2055.
93. Denk, M. K.; Thadani, A.; Hatano, K.; Lough, A. J., *Angew. Chem. Int. Ed.* **1997,** *36*, 2607.
94. Kamplain, J. W.; Bielawski, C. W., *Chem. Commun.* **2006**, 1727.

95. Arduengo, A. J.; Dias, H. V. R.; Harlow, R. L.; Kline, M., *J. Am. Chem. Soc.* **1992,** *114*, 5530.
96. Kuhn, N.; Kratz, T., *Synthesis* **1993,** *1993*, 561.
97. Hallett, J. P.; Welton, T., *Chem. Rev.* **2011,** *111*, 3508.
98. Benhamou, L.; Chardon, E.; Lavigne, G.; Bellemin-Laponnaz, S.; César, V., *Chem. Rev.* **2011,** *111*, 2705.
99. Zhang, Y.; Zhao, L.; Patra, P. K.; Hu, D.; Ying, J. Y., *Nano Today* **2009,** *4*, 13.
100. Tan, M.; Zhang, Y.; Ying, J. Y., *Adv. Synth. Catal.* **2009,** *351*, 1390.
101. Pawar, G. M.; Buchmeiser, M. R., *Adv. Synth. Catal.* **2010,** *352*, 917.
102. Pinaud, J.; Vignolle, J.; Gnanou, Y.; Taton, D., *Macromolecules* **2011,** *44*, 1900.
103. Powell, A. B.; Suzuki, Y.; Ueda, M.; Bielawski, C. W.; Cowley, A. H., *J. Am. Chem. Soc.* **2011,** *133*, 5218.
104. Orsini, M.; Chiarotto, I.; Sotgiu, G.; Inesi, A., *Electrochim. Acta* **2010,** *55*, 3511.
105. Orsini, M.; Chiarotto, I.; Feeney, M. M. M.; Feroci, M.; Sotgiu, G.; Inesi, A., *Electrochem. Commun.* **2011,** *13*, 738.
106. Feroci, M.; Chiarotto, I.; Orsini, M.; Pelagalli, R.; Inesi, A., *Chem. Commun.* **2012,** *48*, 5361.
107. Enders, D.; Breuer, K.; Raabe, G.; Runsink, J.; Teles, J. H.; Melder, J.-P.; Ebel, K.; Brode, S., *Angew. Chem. Int. Ed.* **1995,** *34*, 1021.
108. Wang, H. M. J.; Lin, I. J. B., *Organometallics* **1998,** *17*, 972.
109. Lin, J. C. Y.; Huang, R. T. W.; Lee, C. S.; Bhattacharyya, A.; Hwang, W. S.; Lin, I. J. B., *Chem. Rev.* **2009,** *109*, 3561.
110. Coulembier, O.; Dove, A. P.; Pratt, R. C.; Sentman, A. C.; Culkin, D. A.; Mespouille, L.; Dubois, P.; Waymouth, R. M.; Hedrick, J. L., *Angew. Chem. Int. Ed.* **2005,** *44*, 4964.
111. Csihony, S.; Culkin, D. A.; Sentman, A. C.; Dove, A. P.; Waymouth, R. M.; Hedrick, J. L., *J. Am. Chem. Soc.* **2005,** *127*, 9079.
112. Coulembier, O.; Lohmeijer, B. G. G.; Dove, A. P.; Pratt, R. C.; Mespouille, L.; Culkin, D. A.; Benight, S. J.; Dubois, P.; Waymouth, R. M.; Hedrick, J. L., *Macromolecules* **2006,** *39*, 5617.
113. Hocker, J.; Merten, R., *Angew. Chem. Int. Ed.* **1972,** *11*, 964.
114. Enders, D.; Balensiefer, T., *Acc. Chem. Res.* **2004,** *37*, 534.
115. Nyce, G. W.; Csihony, S.; Waymouth, R. M.; Hedrick, J. L., *Chem. Eur. J.* **2004,** *10*, 4073.
116. Coulembier, O.; Delva, X.; Hedrick, J. L.; Waymouth, R. M.; Dubois, P., *Macromolecules* **2007,** *40*, 8560.
117. Coulembier, O.; Moins, S.; Dubois, P., *Macromolecules* **2011,** *44*, 7493.
118. Norris, B. C.; Sheppard, D. G.; Henkelman, G.; Bielawski, C. W., *J. Org. Chem.* **2010,** *76*, 301.
119. Delaude, L.; Demonceau, A.; Wouters, J., *Eur. J. Inorg. Chem.* **2009,** *2009*, 1882.
120. Fèvre, M.; Pinaud, J.; Leteneur, A.; Gnanou, Y.; Vignolle, J.; Taton, D.; Miqueu, K.; Sotiropoulos, J.-M., *J. Am. Chem. Soc.* **2012,** *134*, 6776.
121. Tommasi, I.; Sorrentino, F., *Tetrahedron Lett.* **2009,** *50*, 104.
122. Sauvage, X.; Demonceau, A.; Delaude, L., *Adv. Synth. Catal.* **2009,** *351*, 2031.
123. Piermattei, A.; Karthikeyan, S.; Sijbesma, R. P., *Nat Chem* **2009,** *1*, 133.
124. Delaude, L., *Eur. J. Inorg. Chem.* **2009**, 1681.
125. Zhou, H.; Zhang, W.-Z.; Liu, C.-H.; Qu, J.-P.; Lu, X.-B., *J. Org. Chem.* **2008,** *73*, 8039.
126. Voutchkova, A. M.; Feliz, M.; Clot, E.; Eisenstein, O.; Crabtree, R. H., *J. Am. Chem. Soc.* **2007,** *129*, 12834.
127. Bonnette, F.; Kato, T.; Destarac, M.; Mignani, G.; Cossío, Fernando P.; Baceiredo, A., *Angew. Chem. Int. Ed.* **2007,** *46*, 8632.
128. Denk, M. K.; Rodezno, J. M.; Gupta, S.; Lough, A. J., *J. Organomet. Chem.* **2001,** *617-618*, 242.
129. Hollóczki, O.; Terleczky, P.; Szieberth, D.; Mourgas, G.; Gudat, D.; Nyulászi, L., *J. Am. Chem. Soc.* **2010,** *133*, 780.
130. Amyes, T. L.; Diver, S. T.; Richard, J. P.; Rivas, F. M.; Toth, K., *J. Am. Chem. Soc.* **2004,** *126*, 4366.
131. Van Ausdall, B. R.; Glass, J. L.; Wiggins, K. M.; Aarif, A. M.; Louie, J., *J. Org. Chem.* **2009,** *74*, 7935.
132. Bridges, N. J.; Hines, C. C.; Smiglak, M.; Rogers, R. D., *Chem. Eur. J.* **2007,** *13*, 5207.
133. Breslow, R., *J. Am. Chem. Soc.* **1958,** *80*, 3719.
134. Breslow, R., *J. Am. Chem. Soc.* **1958,** *80*, 3719.
135. Lapworth, A., *J. Chem. Soc., Trans.* **1903,** *83*, 995.
136. Moore, J. L.; Rovis, T., *Top. Curr. Chem.* **2010,** *291*, 77.
137. Marion, N.; Diez-Gonzalez, S.; Nolan, S. P., *Angew. Chem. Int. Ed.* **2007,** *46*, 2988.
138. Grasa, G. A.; Güveli, T.; Singh, R.; Nolan, S. P., *J. Org. Chem.* **2003,** *68*, 2812.
139. Singh, R.; Kissling, R. M.; Letellier, M.-A.; Nolan, S. P., *J. Org. Chem.* **2003,** *69*, 209.
140. Movassaghi, M.; Schmidt, M. A., *Org. Lett.* **2005,** *7*, 2453.
141. Lai, C.-L.; Lee, H. M.; Hu, C.-H., *Tetrahedron Lett.* **2005,** *46*, 6265.

142. Raynaud, J.; Absalon, C.; Gnanou, Y.; Taton, D., *J. Am. Chem. Soc.* **2009,** *131*, 3201.
143. Raynaud, J.; Absalon, C.; Gnanou, Y.; Taton, D., *Macromolecules* **2010,** *43*, 2814.
144. Raynaud, J.; Ottou, W. N.; Gnanou, Y.; Taton, D., *Chem. Commun.* **2010,** *46*, 3203.
145. Sun, X.; Ye, S.; Wu, J., *Eur. J. Org. Chem.* **2006,** *2006*, 4787.
146. Zhou, H.; Campbell, E. J.; Nguyen, S. T., *Org. Lett.* **2001,** *3*, 2229.
147. Yadav, L. D. S.; Rai, V. K.; Singh, S.; Singh, P., *Tetrahedron Lett.* **2010,** *51*, 1657.
148. Carreira, E. M., In *Comprehensive Asymmetric Catalysis I-III*, Jacobsen, E. N.; Pfaltz, A.; Yamamoto, H., Eds. Springer-Verlag: Berlin, Germany, 1999; Vol. 3, p 997.
149. Song, J. J.; Tan, Z.; Reeves, J. T.; Yee, N. K.; Senanayake, C. H., *Org. Lett.* **2007,** *9*, 1013.
150. Raynaud, J.; Liu, N.; Fevre, M.; Gnanou, Y.; Taton, D., *Polym. Chem.* **2011,** *2*, 1706.
151. Raynaud, J.; Liu, N.; Gnanou, Y.; Taton, D., *Macromolecules* **2010,** *43*, 8853.
152. Raynaud, J.; Gnanou, Y.; Taton, D., *Macromolecules* **2009,** *42*, 5996.
153. Raynaud, J.; Ciolino, A.; Baceiredo, A.; Destarac, M.; Bonnette, F.; Kato, T.; Gnanou, Y.; Taton, D., *Angew. Chem. Int. Ed.* **2008,** *47*, 5390.
154. Webster, O. W., *J. Polym. Sci., Part A: Polym. Chem.* **2000,** *38*, 2855.
155. Alan Jones, R.; Karatza, M.; Voro, T. N.; Civeir, P. U.; Franck, A.; Ozturk, O.; Seaman, J. P.; Whitmore, A. P.; Williamson, D. J., *Tetrahedron* **1996,** *52*, 8707.
156. Jones, R. A.; Civcir, P. U., *Tetrahedron* **1997,** *53*, 11529.
157. Bantu, B.; Pawar, G. M.; Decker, U.; Wurst, K.; Schmidt, A. M.; Buchmeiser, M. R., *Chem. Eur. J.* **2009,** *15*, 3103.
158. Bantu, B.; Pawar, G. M.; Wurst, K.; Decker, U.; Schmidt, A. M.; Buchmeiser, M. R., *Eur. J. Inorg. Chem.* **2009,** *2009*, 1970.
159. Coutelier, O.; El Ezzi, M.; Destarac, M.; Bonnette, F.; Kato, T.; Baceiredo, A.; Sivasankarapillai, G.; Gnanou, Y.; Taton, D., *Polym. Chem.* **2012,** *3*, 605.
160. Naik, P. U.; Refes, K.; Sadaka, F.; Brachais, C.-H.; Boni, G.; Couvercelle, J.-P.; Picquet, M.; Plasseraud, L., *Polym. Chem.* **2012,** *3*, 1475.
161. Connor, E. F.; Nyce, G. W.; Myers, M.; Möck, A.; Hedrick, J. L., *J. Am. Chem. Soc.* **2002,** *124*, 914.
162. Nyce, G. W.; Glauser, T.; Connor, E. F.; Mock, A.; Waymouth, R. M.; Hedrick, J. L., *J. Am. Chem. Soc.* **2003,** *125*, 3046.
163. Coulembier, O.; Mespouille, L.; Hedrick, J. L.; Waymouth, R. M.; Dubois, P., *Macromolecules* **2006,** *39*, 4001.
164. Coulembier, O.; Kiesewetter, M.; Mason, A.; Dubois, P.; Hedrick, J.; Waymouth, R., *Angew. Chem. Int. Ed.* **2007,** *46*, 4719.
165. Jensen, T. R.; Breyfogle, L. E.; Hillmyer, M. A.; Tolman, W. B., *Chem. Commun.* **2004**, 2504.
166. Dove, A. P.; Li, H.; Pratt, R. C.; Lohmeijer, B. G. G.; Culkin, D. A.; Waymouth, R. M.; Hedrick, J. L., *Chem. Commun.* **2006**, 2881.
167. Kamber, N. E.; Jeong, W.; Gonzalez, S.; Hedrick, J. L.; Waymouth, R. M., *Macromolecules* **2009,** *42*, 1634.
168. Nederberg, F.; Lohmeijer, B. G. G.; Leibfarth, F.; Pratt, R. C.; Choi, J.; Dove, A. P.; Waymouth, R. M.; Hedrick, J. L., *Biomacromolecules* **2006,** *8*, 153.
169. Culkin, D.; Jeong, W.; Csihony, S.; Gomez, E.; Balsara, N.; Hedrick, J.; Waymouth, R., *Angew. Chem. Int. Ed.* **2007,** *46*, 2627.
170. Jeong, W.; Shin, E. J.; Culkin, D. A.; Hedrick, J. L.; Waymouth, R. M., *J. Am. Chem. Soc.* **2009,** *131*, 4884.
171. Jeong, W.; Hedrick, J. L.; Waymouth, R. M., *J. Am. Chem. Soc.* **2007,** *129*, 8414.
172. Shin, E. J.; Brown, H. A.; Gonzalez, S.; Jeong, W.; Hedrick, J. L.; Waymouth, R. M., *Angew. Chem. Int. Ed.* **2011,** *50*, 6388.
173. Shin, E. J.; Jeong, W.; Brown, H. A.; Koo, B. J.; Hedrick, J. L.; Waymouth, R. M., *Macromolecules* **2011,** *44*, 2773.
174. Guo, L.; Zhang, D., *J. Am. Chem. Soc.* **2009,** *131*, 18072.
175. Lahasky, S. H.; Serem, W. K.; Guo, L.; Garno, J. C.; Zhang, D., *Macromolecules* **2011,** *44*, 9063.
176. Lee, C.-U.; Smart, T. P.; Guo, L.; Epps, T. H.; Zhang, D., *Macromolecules* **2011,** *44*, 9574.
177. Li, X.; Guo, L.; Casiano-Maldonado, M.; Zhang, D.; Wesdemiotis, C., *Macromolecules* **2011,** *44*, 4555.
178. Rodriguez, M.; Marrot, S.; Kato, T.; Stérin, S.; Fleury, E.; Baceiredo, A., *J. Organomet. Chem.* **2007,** *692*, 705.
179. Lohmeijer, B. G. G.; Dubois, G.; Leibfarth, F.; Pratt, R. C.; Nederberg, F.; Nelson, A.; Waymouth, R. M.; Wade, C.; Hedrick, J. L., *Org. Lett.* **2006,** *8*, 4683.
180. Raynaud, J.; Liu, N.; Fevre, M.; Gnanou, Y.; Taton, D., *Polym. Chem.* **2011**.
181. Hedrick, J. L.; Nyce, G. W.; Waymouth, R. M. US7053221, 2006.
182. Duong, H. A.; Cross, M. J.; Louie, J., *Org. Lett.* **2004,** *6*, 4679.

183. Arduengo, A. J.; Calabrese, J. C.; Davidson, F.; Rasika Dias, H. V.; Goerlich, J. R.; Krafczyk, R.; Marshall, W. J.; Tamm, M.; Schmutzler, R., *Helv. Chim. Acta* **1999,** *82*, 2348.
184. Wanzlick, H. W., *Angew. Chem. Int. Ed.* **1962,** *1*, 75.
185. Schmidt, M. A.; Müller, P.; Movassaghi, M., *Tetrahedron Lett.* **2008,** *49*, 4316.
186. Kricheldorf, H. R., *J. Polym. Sci., Part A: Polym. Chem.* **2010,** *48*, 251.
187. Yamamoto, T.; Tezuka, Y., *Polym. Chem.* **2011,** *2*, 1930.
188. Jia, Z.; Monteiro, M. J., *J. Polym. Sci., Part A: Polym. Chem.* **2012,** *50*, 2085.
189. Webster, O. W.; Hertler, W. R.; Sogah, D. Y.; Farnham, W. B.; RajanBabu, T. V., *J. Am. Chem. Soc.* **1983,** *105*, 5706.
190. Mukaiyama, T., *Angew. Chem. Int. Ed.* **2004,** *43*, 5590.
191. Brittain, W. J., *Rubber Chem. Technol.* **1992,** *65*, 580.
192. Chen, Y.; Fuchise, K.; Narumi, A.; Kawaguchi, S.; Satoh, T.; Kakuchi, T., *Macromolecules* **2011,** *44*, 9091.
193. Kakuchi, T.; Chen, Y.; Kitakado, J.; Mori, K.; Fuchise, K.; Satoh, T., *Macromolecules* **2011,** *44*, 4641.
194. Hsu, J.-C.; Chen, Y.; Kakuchi, T.; Chen, W.-C., *Macromolecules* **2011,** *44*, 5168.
195. Zhang, Y.; Lay, F.; García-García, P.; List, B.; Chen, E. Y. X., *Chem. Eur. J.* **2010,** *16*, 10462.
196. Takada, K.; Fuchise, K.; Chen, Y.; Satoh, T.; Kakuchi, T., *J. Polym. Sci., Part A: Polym. Chem.* **2012,** *50*, 3560.
197. Zhang, Y.; Chen, E. Y. X., *Macromolecules* **2007,** *41*, 36.
198. Zhang, Y.; Chen, E. Y. X., *Macromolecules* **2008,** *41*, 6353.
199. Miyake, G. M.; Zhang, Y.; Chen, E. Y. X., *Macromolecules* **2010,** *43*, 4902.
200. Quirk, R. P.; Kim, J.-S., *J. Phys. Org. Chem.* **1995,** *8*, 242.
201. Webster, O. W., In *New Synthetic Methods*, Springer Berlin / Heidelberg: 2004; Vol. 167, p 257.
202. Zhang, Y.; Chen, E. Y. X., *Angew. Chem. Int. Ed.* **2012,** *51*, 2465.
203. Coady, D. J.; Khramov, D. M.; Norris, B. C.; Tennyson, A. G.; Bielawski, C. W., *Angew. Chem. Int. Ed.* **2009,** *48*, 5187.
204. Tennyson, A. G.; Kamplain, J. W.; Bielawski, C. W., *Chem. Commun.* **2009**, 2124.
205. Norris, B. C.; Bielawski, C. W., *Macromolecules* **2010,** *43*, 3591.

Chapitre 2

Hydrogénocarbonates et Carboxylates d'Azolium comme Nouveaux Précurseurs de NHCs : Applications à la Préparation de Complexes Organométalliques et aux Réactions (Macro)moléculaires Catalysées par les NHCs

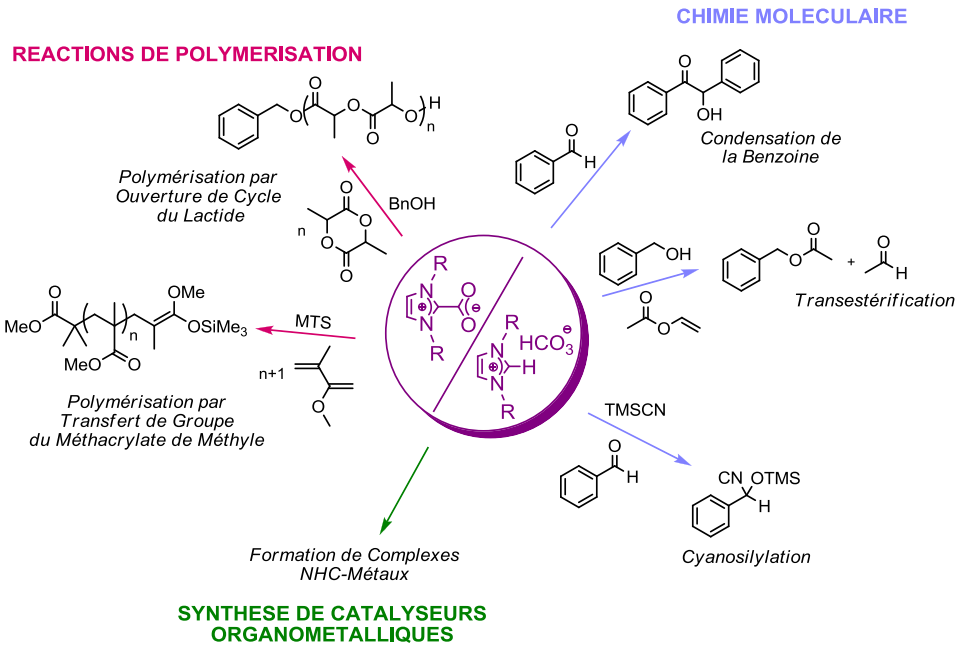

Mots clés: Organocatalyse, Carbènes *N*-hétérocycliques, Hydrogénocarbonates d'Azolium, Carboxylates d'imidazolium.

Keywords: Organocatalysis, *N*-heterocyclic carbenes, Imidazolium-2-carboxylates, Azolium hydrogen carbonates.

Résumé: Ce chapitre est consacré à la synthèse et à l'utilisation en chimie (macro)moléculaire de nouveaux carbènes masqués. En tant que précurseurs de NHCs, les adduits zwitterioniques obtenus par carboxylation des NHCs avec le CO_2, notés NHC-CO_2, ont été très étudiés car leur structure est facilement modulable. Cependant, leur synthèse nécessite le plus souvent la préparation préalable du NHC correspondant. De plus, leur stabilité à l'air est quelque peu limitée. En effet, ces composés peuvent s'hydrater et former des espèces de type hydrogénocarbonates d'azolium, notées [NHC(H)][HCO_3]. De tels sels n'avaient jamais été considérés comme précurseurs de NHCs. Dans ce chapitre, nous démontrerons, d'une part, qu'ils peuvent être synthétisés en une seule étape, sans la synthèse préalable du NHC, et d'autre part, que ces espèces sont stables à l'air et peuvent générer des NHCs libres par simple effet de solvatation. L'analyse par RMN de ces composés a en réalité mis en évidence un équilibre entre [NHC(H)][HCO_3] et adduits NHC-CO_2. Plusieurs méthodes ont été mises en oeuvre pour montrer que ces hydrogénocarbonates d'azolium peuvent servir de précurseurs de NHCs. Tout d'abord, le comportement en phase solide de ces composés a été éxaminé. Les analyses thermogravimétriques (TGA) ont montré que la dégradation de la plupart des [NHC(H)][HCO_3] s'effectue en plusieurs étapes, avec un départ d'eau et de CO_2 concomitant ou indépendant, en fonction de la nature de l'azolium et de ses substituents. Ces [NHC(H)][HCO_3] ont ensuite été employés comme pré-catalyseurs pour diverses réactions de chimie (macro)moléculaire. L'efficacité catalytique des [NHC(H)][HCO_3], mais aussi de leurs homologues NHC-CO_2 a ainsi pu être étudiée. La libération des NHCs depuis ces deux types de précurseurs a pu être effectuée à température ambiante, probablement par un effet de solvatation, bien qu'aucun intermédiaire n'ait pu être isolé. Il a été montré que l'activité catalytique des (pré)-catalyseurs testés suivait l'évolution suivante : [NHC(H)][HCO_3] < adduits NHC-CO_2 < NHCs libres. Enfin, des calculs théoriques par DFT ont montré que la libération du NHC, à partir du [NHC(H)][HCO_3], procède par perte formelle de H_2CO_3 (H_2O + CO_2). Le mécanisme correspondant est concerté et met en jeu des barrières énergétiques faibles (<10 kcal/mol).

This chapter is dedicated to the use of azolium hydrogen carbonates as NHC precursors. Results described have been partly published[1] *and/or submitted recently.*[2]

Chapter 2

Azolium Hydrogen Carbonates and Azolium-2-Carboxylates as Genuine Sources of *N*-Heterocyclic Carbenes (NHCs): Applications to the Facile Preparation of NHC Metal Complexes and to NHC-Organocatalyzed Molecular and Macromolecular Syntheses

TABLE OF CONTENTS

Introduction

In the last 20 years, stable carbenes, in particular *N*-heterocyclic carbenes (NHCs) have emerged not only as versatile ligands for transition metals[3-8] but also as powerful organocatalysts in molecular chemistry for a variety of transformations[9-11] and, more recently, in macromolecular chemistry for precision polymer synthesis.[12-19] NHCs are generally prepared by deprotonation of azolium salts with a strong base.[20] Because this method not only necessitates dry and air-free conditions, but also provides limited tolerance to various functionalities, different approaches have been developed to circumvent these limitations. Apart from the encapsulation of free NHCs into hydrophobic silicon polymers allowing their handling in air,[21] most efforts have been focused toward the design of masked NHCs,[22] whose thermal activation can *in-situ* generate the free carbene. Several masked NHCs such as 2-alkoxy,[23-29] 2-trichloromethyl,[26,30] 2-pentafluorophenyl imidazolidine,[30-31] 5-alkoxytriazoline,[29,32] imidazolium-2-carboxylates -referred to as NHC-CO_2 adducts-[33-40] imidazolium-2-thiocarboxylates,[41] imidazolium-2-isothiocyanates[42] and NHC-Ag(I) complexes[43-44] have been developed (see Figure 1). Most of such NHC precursors have been successfully applied as NHC-transfer agents for transition metals,[23-26,30-31,37,45-51] and as (pre)catalysts for molecular[30,42,52-59] and macromolecular synthesis.[17,27-30,42,60-64]

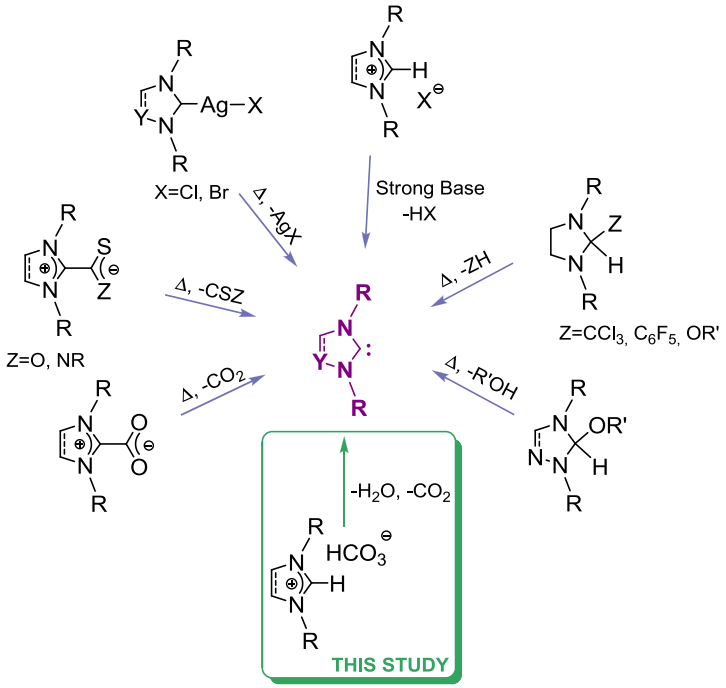

Figure 1. Masked NHC precursors reported in the literature and those described in this work.

Among these masked NHCs, NHC-CO_2 adducts, namely imidazol(in)ium-2-carboxylates, have attracted a great deal of attention. This is due to the fact that (*i*) any types of structures are virtually accessible by reaction of free NHCs with CO_2,[34-36,38-39] (*ii*) NHC-CO_2 adducts are relatively stable in the solid state under air exposure,[50] and (*iii*) CO_2 is the only by-product upon NHC generation. However, synthesis of NHC-CO_2 adducts generally requires the corresponding NHC to be prepared prior to the carboxylation step. Free NHCs are thought to be *in situ* generated upon heating the NHC-CO_2 adducts, typically between 60 and 90 °C.[35,37-39,46-51,65-67] In the context of organometallic chemistry, however, Crabtree *et al.* [37,46] and Sauvage *et al.*[51] have noticed successful NHC transfer onto transition metal fragments at room temperature (RT). Such imidazol(in)ium-2-carboxylates, and some polymer-supported versions, have been utilized as NHC and poly(NHC) precursors, respectively, for the purpose of organocatalysis. Related (macro)molecular reactions include transesterification,[54,57] benzoin condensation,[57,68] cyanosilylation,[56] cyclotrimerization of isocyanates,[56,69] and synthesis of polyurethanes[60-61] and polycarbonates[64] by step-growth polymerization.

In the presence of water, decomposition of some masked NHCs has been observed in solution. In particular, Rogers *et al.*[70] and Louie *et al.*[39] have evidenced that the $C_{carbene}$-CO_2 bond of NHC-CO_2 adducts can hydrolyze, forming stable imidazolium hydrogen carbonate salts, denoted as [NHC(H)][HCO_3] (eq.1, Scheme 1). Interestingly, this hydrolysis reaction proves reversible, suggesting a non-innocent role of the HCO_3^- counter-anion toward the imidazolium cation. This behavior is reminiscent to that observed for basic anions such as AcO^- in imidazolium-based ionic liquids (ILs), which are capable to reversibly deprotonate the imidazolium cation, generating the corresponding NHC.[71-74] By analogy, and from a mechanistic point of view, we hypothesized that in the case of [NHC(H)][HCO_3] **4**, the NHC could be reversibly generated by formal loss of H_2CO_3 (eq.3, Scheme 1). It might also be anticipated that subsequent reaction of the NHC **2** with CO_2 (formed by decomposition of H_2CO_3) would afford the corresponding NHC-CO_2 adduct **3** (eq.2, Scheme 1).

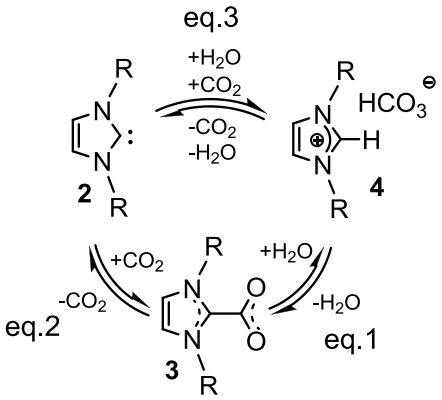

Scheme 1. Reversible transformation of NHC-CO_2 adducts into [NHC(H)][HCO_3] salts *via* the generation of NHCs.

To the best of our knowledge (see chapter 1 of this manuscript, sections 3.1.2., 3.2., 3.3.), no report has mentioned about the NHC-like behavior of imidazolium hydrogen carbonates in (macro)molecular chemistry.[75,76-77] In this thesis work, we wish to report the facile synthesis of such [NHC(H)][HCO_3] salt precursors by a simple anion metathesis from commercially available imidazolium chlorides, [NHC(H)][Cl], using $KHCO_3$. Characterization by thermogravimetric analysis (TGA) of [NHC(H)][HCO_3] salts is also described. TGA results evidence that, in the solid state, most of these precursors release H_2O and CO_2 molecules upon heating before they degrade. Next, we show that such precursors can be used as stoichiometric transfer agents of NHCs toward organic and organometallic substrates.

Formation of the NHC from its [NHC(H)][HCO_3] precursor, *via* formal loss of H_2CO_3, has also been investigated by Density Functional Theory (DFT) calculations. Given the small energetic barriers obtained in the gas phase at 25 °C for NHC generation from both [NHC(H)][HCO_3] salts **4** and NHC-CO_2 adducts **3**, we also wish to compare the ability of each precursor to generate the NHC **2** in solution, especially at room temperature. The catalytic efficiencies of both types of precursors (**3** and **4**) are thus compared in several reactions including, cyanosilylation, benzoin condensation, and transesterification. Both solvent and temperature effects have been studied.

Finally, we show that both imidazolium-2-carboxylates (NHC-CO_2 adducts) and azolium hydrogen carbonates ([NHC(H)][HCO_3]) of various structures can serve as pre-catalysts for two distinct chain-

growth polymerization reactions, including the ROP of D,L-lactide and the GTP of methyl methacrylate.

1. Synthesis and properties of azolium hydrogen carbonates

1.1. Synthesis and properties in solution

The synthesis of imidazolium hydrogen carbonates, [NHC(H)][HCO_3], has been scarcely investigated in the literature.[78-82] They can be prepared by reacting free NHCs with NH_4HCO_3, as reported by Kuhn *et al.*,[83] or by hydrolysis of NHC-CO_2 adducts.[39,70,80] Both methods involve the prior preparation of the free NHC. To avoid the manipulation of air-sensitive free carbene intermediates, and thus provide an easy access to [NHC(H)][HCO_3] salts, we turned to the salt metathesis of commercially available imidazolium halide precursors, [NHC(H)][Cl], using $KHCO_3$. This method has been employed for the synthesis of molecular,[76-78] polymeric [NHC(H)][HCO_3]-based ILs[82] and for the surface modification of IL-functionalized gold nanoparticles,[81] using NH_4CO_3,[78] $NaHCO_3$[77,81] or $KHCO_3$[82] as HCO_3^- source and *i*-PrOH or water as reaction medium.[84] For this study, we resorted to a modified procedure of the anion metathesis methods based on the aforementioned literature.

Thus, reacting 1,3-di-isopropylimidazolium bromide, [IiPr(H)][Br], **1a**, with 1.05 eq. of $KHCO_3$ in MeOH for 2 days led, after workup, to a white powder in 71% yield (Scheme 2b). Analysis of the crude powder by ^{1}H NMR in CD_3OD revealed the presence of one product (Figure S1). As expected, the chemical shifts of the different protons of the imidazolium backbone were similar to that of the starting material **1a**, thus precluding its identification. However, in the ^{13}C NMR spectrum, the characteristic signals of both the N_2CH carbon and the HCO_3^- quaternary carbon atoms were clearly detected at 134.4 and 161.3 ppm respectively, in agreement with data from the literature (Figure S2).[70,80] The absence of the ^{1}H NMR signal corresponding to the N_2CH proton was attributed to the rapid exchange of this proton with the deuterated solvent, on the NMR time scale.[80] Absence of the signal due to the more acidic HCO_3^- proton is likely due to the same phenomenon.

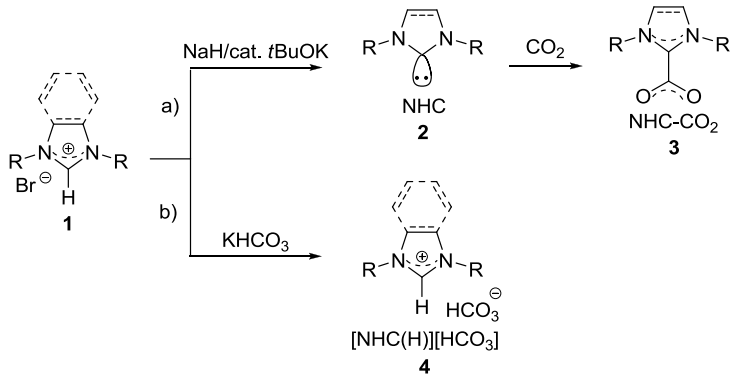

Scheme 2. a) Synthesis of NHCs **2a** and **2b** by deprotonation of corresponding imidazolium bromides (**1**) with a strong base, and of related imidazolium-2-carboxylates **3a** and **3b** by subsequent carboxylation; b) Synthesis of imidazol(in)ium/benzimidazolium hydrogen carbonates **4a-f** by anion exchange, see also Figure 3 for a representation of all the tested precursors.

Crystals of **4a** suitable for X-ray diffraction analysis could be obtained by cooling a solution of **4a** in a MeOH/Et_2O mixture. The modest quality of the crystallographic data precludes a thorough discussion of the geometric parameters, but the connectivity of the complex could be unambiguously established (see Figures S3-S4). In particular, the asymmetric unit cell consists of one imidazolium cation and one HCO_3^- anion, the HCO_3^- anions forming hydrogen-bonded dimers around crystallographic centers of inversions, consistently with previous observations for similar structures.[70,78,83]

In contrast to CD_3OD, **4a** was found to co-exist with a minor compound, **3a**, (3:1 ratio in favor of **4a**) in dry DMSO-d_6, as deduced from the presence of a new set of signals in the ^{1}H NMR spectrum. Compound **3a** was eventually identified as being the corresponding NHC-CO_2 adduct, by comparing its ^{1}H NMR spectrum with an authentic sample prepared by reacting the free NHC with CO_2 (see Figure 2 for a comparison between ^{1}H NMR spectra of **4a** in CD_3OD, dry or wet DMSO-d_6 and **3a** in dry DMSO-d_6). Consistent with observations made by Rogers *et al.*[70,80] with some [NHC(H)][HCO_3] ILs, **4a** and **3a** are eventually in equilibrium in DMSO. Interestingly, the equilibrium can be totally shifted toward the formation of **4a** by adding a few drops of water in DMSO or by letting stand the sample in air, while in CD_3OD, the equilibrium is totally shifted toward the formation of **4a**.

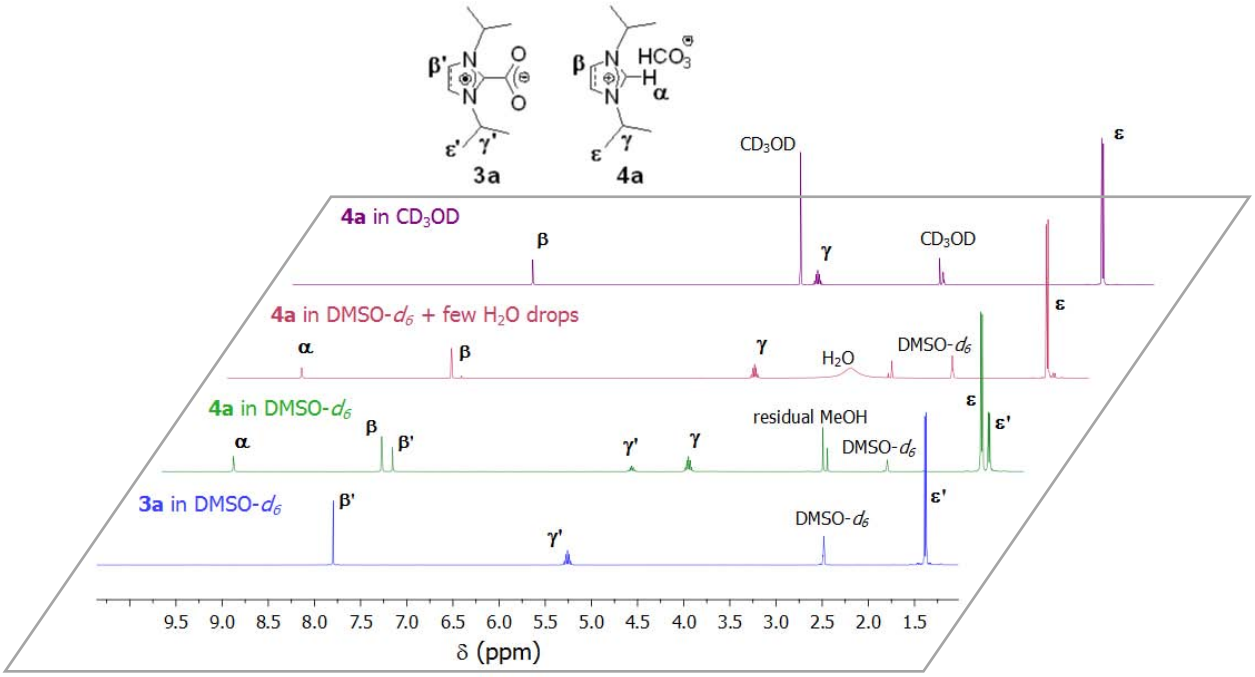

Figure 2. ^{1}H NMR spectra of **4a** in CD_3OD, DMSO-d_6 where few drops of water were added, dry DMSO-d_6 (leading to an equilibrium between compounds **4a** and **3a**) and ^{1}H NMR spectrum of **3a** in dry DMSO-d_6 synthesized by carboxylation of the corresponding free NHC.

This anion metathesis method was next applied to precursors featuring aryl substituents on the nitrogen atoms, namely, 1,3-bis(mesityl)imidazolium chloride [IMes(H)][Br], **1b**, and its saturated counterpart, namely, 1,3-bis(dimesityl)imidazolinium chloride [SIMes(H)][Br], **1b'** (Figure 3). Subjecting the two latter salts to anion metathesis in dry MeOH yielded, after usual workup, **4b** and **4b'** as off-white and white solids, in 76 % and 88 % yield, respectively. Given that **4b** is sparingly soluble in dry DMSO-d_6 and that **4b'** is in equilibrium with **3b'** in this solvent, their characterization was performed in MeOD by ^{1}H and ^{13}C NMR spectroscopy (Figures S5-S8).

In particular, both the H*C*O_3^- anion and the N_2*C*H carbon atoms could be identified by ^{13}C NMR spectroscopy through the presence of signals at 159.4 and 130.5 ppm, respectively, for **4b**, and at 160.3 and 160.1 ppm, respectively, for **4b'**(Figures S6 and S8). As in the case of **4a** discussed above, shifting the equilibrium toward the quantitative formation of the imidazolium hydrogen carbonates could be achieved by adding a few drops of water. Thus, co-existence in solution of [NHC(H)][HCO_3] and NHC-CO_2 strongly depends on the nature of the solvents and on the presence of water.

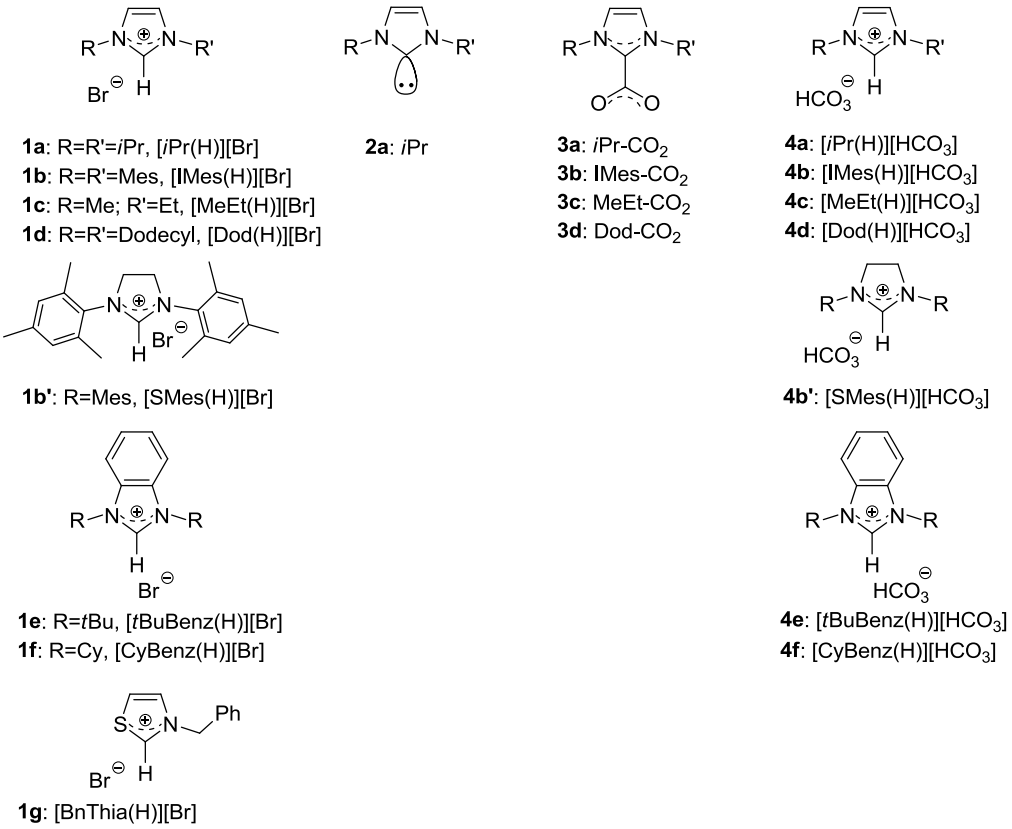

Figure 3. [NHC(H)][Br] salt precursors **1**, NHCs **2**, NHC-CO_2 adducts **3** and [NHC(H)][HCO_3] salts **4** used in this study.

To generalize the synthesis of imidazolium hydrogen carbonates from imidazolium halides, the anion metathesis method was applied to various precursors (**c**-**d**, Figure 3). Characterization of compounds **4c**-**d** by ^{1}H and ^{13}C NMR spectroscopy confirmed the expected structures (Figures S9-S12). This synthetic method could also be applied to benzimidazolium hydrogen carbonates, **4e**,**f**, from corresponding benzimidazolium bromides **1e**,**f** (see Figures S13-S16 in Annexes for a characterization by ^{1}H and ^{13}C NMR spectroscopy). In contrast, attempt to synthesize a thiazolium hydrogen carbonate from the thiazolium bromide salt **1g** was unsuccessful: a methanolic solution of **1g** in the presence of $KHCO_3$ turned red within a few minutes, a viscous red-to-black insoluble paste progressively forming. This might be explained by the more acidic character of thiazolium salts, compared to their imidazolium counterparts (pK_a([*i*Pr(H)][Br], **1a**)=22 *vs.* pK_a([MeThia(H)][Br], **1g**)=14.5, in DMSO).[85] It is thus likely that, instead of anion metathesis, $KHCO_3$ mediated the deprotonation of **1g**, generating the corresponding NHC, which further decomposed.

Solution behaviors of imidazolium/benzimidazolium hydrogen carbonates **4c-f** were also studied. As previously mentioned, [NHC(H)][HCO_3] and their NHC-CO_2 counterparts can co-exist in solution, in particular as a function of the water content of the solvent analysis. For instance, mixtures of NHC-CO_2 adducts and [NHC(H)][HCO_3] salts were observed, roughly in a molar ratio of 1:4, in the ^{1}H and ^{13}C NMR spectra of imidazolium hydrogen carbonates **4a-c** in DMSO-d_6. Analyses in MeOD showed a single population of signals attributed to the pure [NHC(H)][HCO_3] salt. In contrast, NMR spectra of imidazolium hydrogen carbonates **4d** and benzimidazolium hydrogen carbonates **4e**,**f** revealed the presence of the sole [NHC(H)][HCO_3] compound, irrespective of the solvent analysis (DMSO-d_6, MeOD or CD_2Cl_2).

It is worth mentioning that compounds **4** -with the exception of **4d**- were hardly soluble in THF, which was the main solvent used for the organocatalyzed reactions of the present study (see section 3). Complete solubilization of the precursors did however occur upon addition of the substrate (e.g. benzaldehyde, vinyl acetate and benzyl alcohol, etc).

1.2. Properties at the solid state

It is well documented that thermal degradation of imidazolium-based ionic liquids proceeds first by dealkylation of the imidazole ring.[86-87] Likewise, study of the thermal behavior of some NHC-CO_2 (and NHC-COS) adducts have shown that decarboxylation (or release of COS) strongly depends on the bulkiness of the substituents on the nitrogen atoms.[39,41] In contrast, and to the best of our knowledge, no report has described the thermal properties of [NHC(H)][HCO_3] salts. The thermal behavior of **4a-f** was thus investigated simultaneously by thermogravimetric analysis (TGA) and differential scanning calorimetry (DSC), as summarized in Table 1.

Except for **4c**,**d**, no phase transition was noted on the DSC curves before these compounds started to decompose, as observed by TGA. It should be noted, however, that, DSC results correspond to one heating cycle only. Hence, endotherms observed by DSC may be due to a weight loss, as seen by TGA at the same temperatures, rather than to melting peaks. In the case of **4a**, for instance, endotherms

observed between 150 and 200 °C by DSC (Figure 4a) may be attributed either to the melting of **4a**, or to the melting of degradation compounds, or to a loss of H_2O/CO_2/alkyl chains.

In contrast, the DSC curve of **4d** showed two distinct endothermic peaks below the degradation temperature (Figure 4b), owing to its liquid crystalline character. The peak observed at 42 °C can indeed be ascribed to a solid/liquid crystalline transition (S/LC), while that at 126 °C is due to a liquid crystalline/liquid transition (LC/L). A similar thermotropic behavior has already been reported for imidazolium halide homologues (1,3-di-hexadecylimidazolium bromide: $T_{S/LC}$ = 46 °C and $T_{LC/L}$ = 143 °C).[88-90] As for precursor **4c**, its DSC analysis showed a single melting peak at 77 °C, similarly to its imidazolium bromide homologue **1c** (T_m = 79 °C). Compounds **4c-d** are thus in their melt state before they decompose, above 142 and 280 °C, respectively.

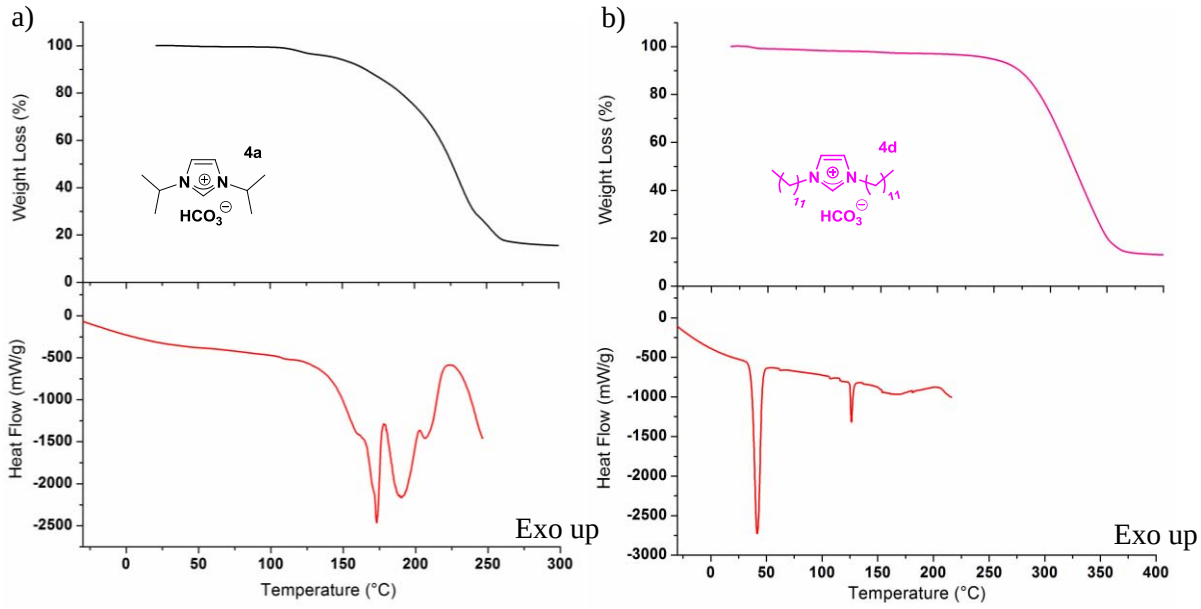

Figure 4. a) TGA (black) and DSC (red) curves of **4a**, b) TGA (pink) and DSC (red) curves of **4d**.

All [NHC(H)][HCO_3] **4** precursors proved stable at least up to 100 °C in the solid state (Table 1 and Figure 5). Typical thermograms obtained by TGA/MS are provided in Figure 6 (case of precursors **4c** and **4f**). With the exception of **4d** featuring dodecyl chains, all compounds **4** showed a minor weight loss prior to their degradation at higher temperature.

Table 1. Results of TGA and DSC analyses of [NHC(H)][HCO_3] salts **4a-f**.

Entry	Compound	T_{onset} (°C)	WL_{exp} (%)[a]	-H_2O_{th} (%)[b]	-CO_{2th} (%)[c]	T_{deg} (°C)[d]	T_m (°C)[e]
1	**4a**	110	3.1	8.4	20.6	190	77
2	**4b**	134/218[f]	1.8/15.4	4.9	12.0	310	-
3	**4c**	142	N.D.[g]	-	-	238	-
4	**4d**	-	-	-	-	280	42/126
5	**4e**	142	20.6	6.2	15.3	232	-
6	**4f**	108	18.0	5.3	12.9	243	-

[a] Experimental weight loss measured on TGA curves (heating rate: 10 °C/min, N_2 atmosphere). [b] Theoretical weight loss for the loss of H_2O from the initial compounds **4**: -H_2O_{th} (%)= M_{H2O}/M_4*100. [c] Theoretical weight loss for the loss of CO_2 from the initial compounds **4**: -CO_{2th} (%)= M_{CO2}/M_4*100. [d] Degradation temperature measured on TGA curves at the onset of their major weight losses. [e] Experimental endothermic peak temperature measured on DSC curves (when observed below T_{onset} and/or T_{deg}, heating rate: 10 °C/min, N_2 atmosphere). [f] Two weight losses were observed before degradation. [g] N.D.= not determined because of the overlapping of the first weight loss with the major degradation.

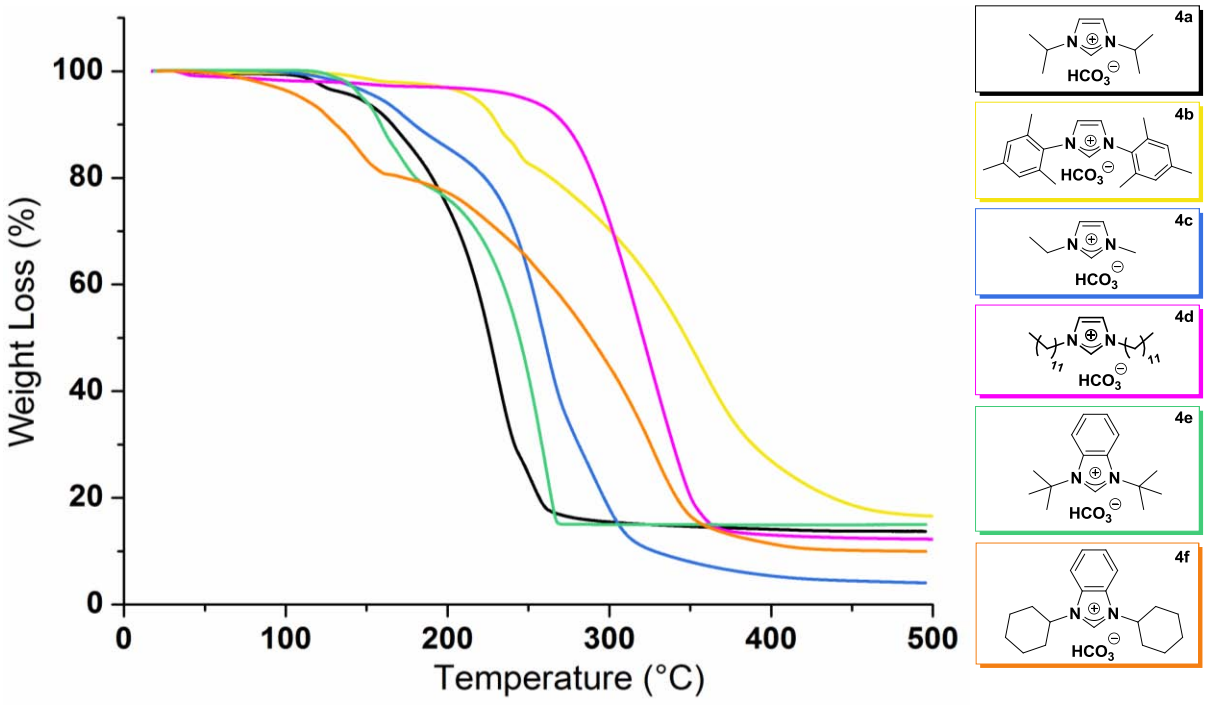

Figure 5. TGA curves of the thermal degradation of [NHC(H)][HCO_3] salts **4a-f**.

In particular, an initial weight loss is observed at 142 °C and 108 °C, respectively, for both benzimidazolium hydrogen carbonates, **4e** and **4f**, followed by their degradation at 230-240 °C. The initial weight loss can be ascribed to the loss of both H_2O and CO_2, as supported by TGA coupled with mass spectrometry (MS) analysis. In both cases, the loss of H_2O molecules (leading to mass to charge ratios at *m/z*=18 and *m/z*=17) occurred at a slightly lower temperature than that due to the departure of

CO_2 (at *m/z*=44 and 22). In addition, experimental weight loss (WL_{exp}) results for **4e-f** were found very close to expected values (WL_{calc}) by considering a loss of (H_2O + CO_2). In the case of **4e**, for instance, results were as follows: WL_{exp}=20.6% *vs.* $WL_{calc}(H_2O+CO_2)$=21.5%, while for **4f**: WL_{exp}=18.0% *vs.* $WL_{calc}(H_2O+CO_2)$=17.2%).

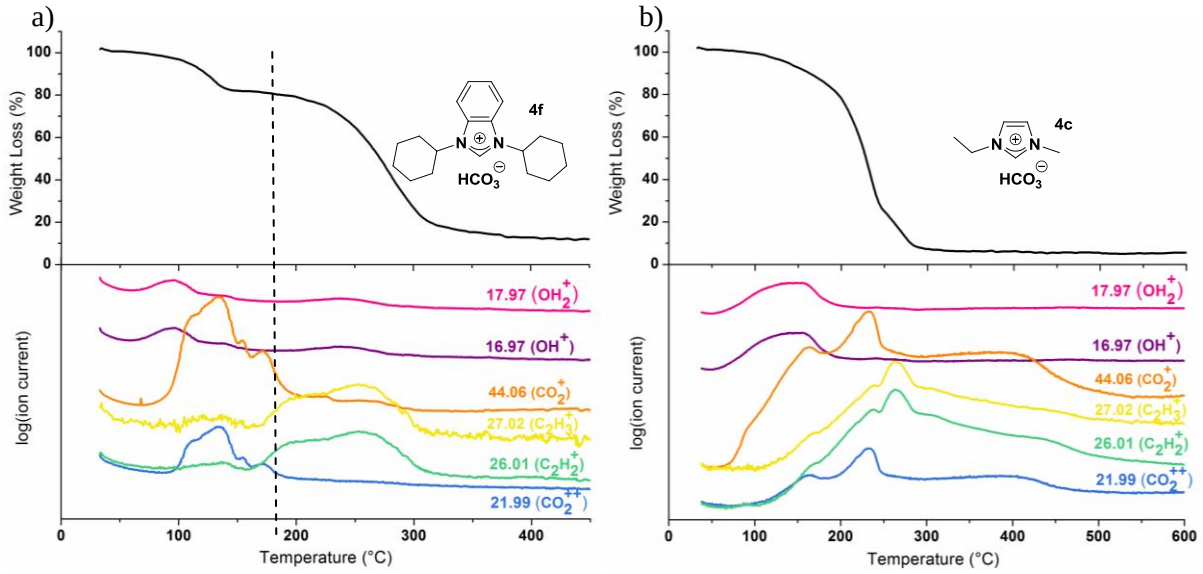

Figure 6. TGA-MS analyses (heating rate: 5 °C/min, Ar atmosphere) of a) **4f** (dotted line= end of the H_2O+CO_2 loss and beginning of loss of alkyl chains), b) **4c**; log(ion current) were recorded for several mass to charge ratios corresponding to the loss of: H_2O (pink and purple), CO_2 (orange and blue) and alkyl chains (yellow and green).

Of particular interest, a pale yellow solid could eventually be obtained after heating **4f** for 5 min at 130 °C, under a high dynamic vacuum (<10^{-7} bar). Analysis of this compound by ^{1}H NMR and ^{13}C NMR spectroscopy revealed characteristic signals of both the free benzimidazol-2-ylidene and its dimeric form, along with other signals likely attributable to degradation compounds (Figures 7-8).[91-92] Indeed, as can be seen on the TGA-MS curve of **4f** (Figure 6a), dealkylation of the benzimidazole backbone (yellow and green curves) starts after **4f** has lost its CO_2 moiety (blue and orange curves). This result nonetheless evidences that, for the first time, a free NHC can be spectroscopically detected upon heating a benzimidazolium hydrogen carbonate precursor in the solid state.

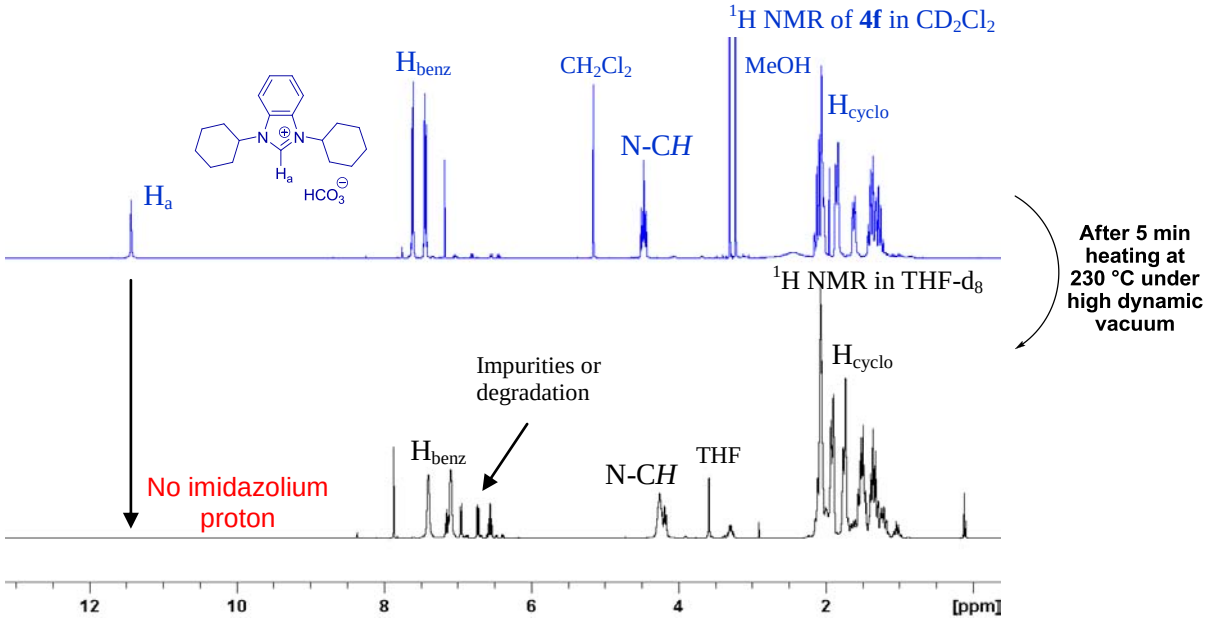

Figure 7. ^{1}H NMR spectra of: **4f** in CD_2Cl_2, in blue, and of the product obtained after 5 min of heating **4f** in the solid state at 230 °C under high dynamic vacuum, in black; NMR performed in THF-d_8, showing the disappearance of the imidazolium proton signal.

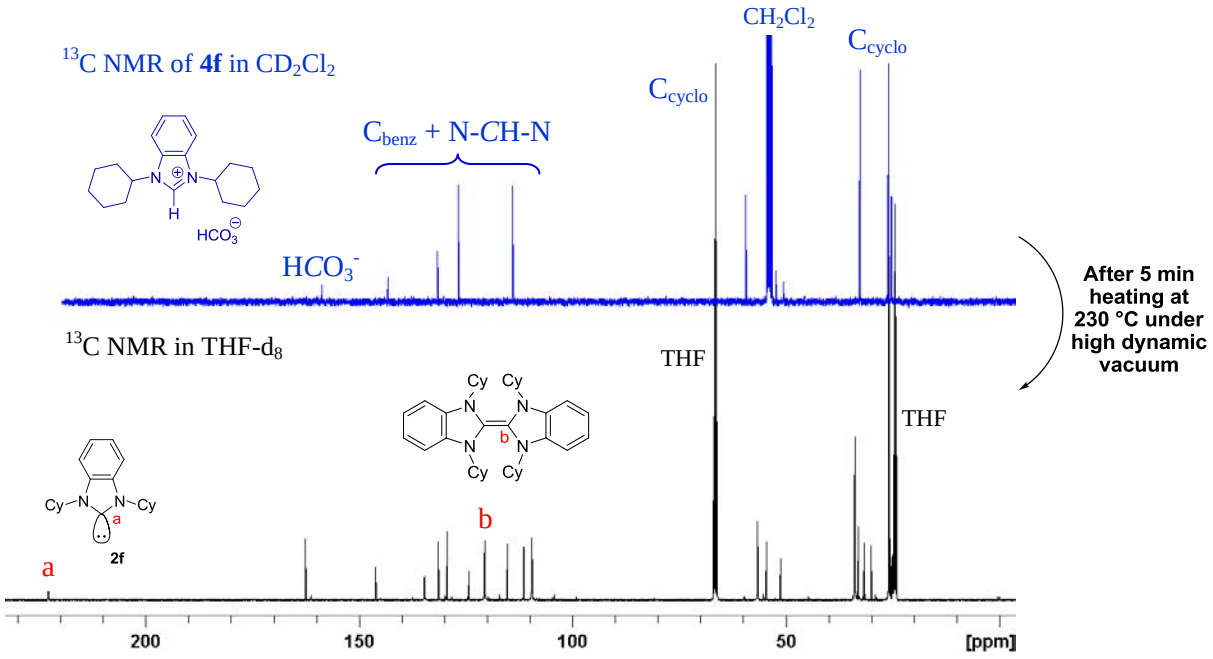

Figure 8. ^{13}C NMR spectra of: **4f** in CD_2Cl_2, in blue and of the product obtained after 5 min of heating **4f** in the solid state at 230 °C under high dynamic vacuum, in black; NMR performed in THF-d_8, showing the appearance of the signal ($C_{carbene}$) corresponding to the carbene **2f** and its dimer form at δ=223 and 121 ppm respectively.

As anticipated, the size and the nature of the substituents on the nitrogen atoms significantly influence the thermal stability of imidazolium-based salts, **4a-d**. In contrast to **4b**, the loss of H_2O/CO_2 moieties for **4a**,**c**,**d** could not be clearly distinguished from their thermal degradation (see Figure 6b, case of precursor **4c**). Similar observations were made with NHC-CO_2 adducts **3a-c** undergoing decarboxylation upon heating.[39] For instance, loss of CO_2 from **3b** could be discriminated from the degradation phenomenon. Conversely, **3a**,**c** showed concomitant degradation and loss of CO_2.[39] This difference may be explained by the aromatic nature of the mesityl groups in **3b**, compared to primary or secondary alkyl substituents in **3c** and **3a**.

Experimental initial weight loss of **4a** was found lower than the expected value (3.0% *vs.* 8.4% for -H_2O_{th} and 29.0% for -$(H_2O+CO_2)_{th}$) and may be explained by the loss of adsorbed water. Likewise, a decomposition in stages was not observed for **4c**,**d**.

In addition, the longer the substituents of the alkyl chains, the higher the onset temperature: T_{onset}=142 *vs.* 280 °C, for **4c** and **4d** respectively. In contrast, due to the higher stability of secondary cations compared to primary ones (iPr$^+$ *vs.* Me$^+$ or Et$^+$), **4a** exhibited a lower degradation temperature than **4c**, consistently with data reported for imidazolium bromide homologues, **1a** and **1c**.[86-87,93]

Compound **4b** exhibited the higher thermal stability in this series, which may be attributed to the aromatic nature of its aryl substituents. Similarly to benzimidazolium hydrogen carbonates, TGA curves of **4b** showed a concomitant dehydration/decarboxylation (WL_{exp}=15.4% *vs.* $WL_{calc}(H_2O+CO_2)$=16.9%), corresponding to the weight loss observed at 218 °C, followed by thermal degradation above 310 °C. The initial minor weight loss (134 °C, 1.8%) is most probably due to adsorbed water.

In summary, the solid state behavior of [NHC(H)][HCO_3] precursors strongly depends on the nature of the azolium backbone and of the substituents on the nitrogen atoms. Benzimidazolium backbones, and more bulky substituents, lead to concomitant or stepwise losses of H_2O and CO_2 before the degradation stage, while such changes in the thermal properties cannot not be differentiated for compounds featuring short alkyl substituents.

2. Evidence for the NHC generation from [NHC(H)][HCO_3] by DFT calculations

All DFT calculations were performed by the group of Karinne Miqueu and Jean-Marc Sotiropoulos at the Institut pluridisciplinaire de recherche sur l'environnement et les matériaux (IPREM, Université de Pau & des pays de l'Adour). These results are mentioned in this section as they were particularly useful to account for the ability of [NHC(H)][HCO_3] to behave as a genuine source of NHC.

The reactions **4** → **2** were found reversible (Scheme 3), regardless of the nature of the substituents on the nitrogen atoms. Indeed, very small energetic differences between **4** and **2** were calculated for the three transformations ($\Delta G_{4\rightarrow 2}$ = (-)0.2-(-)2.6 kcal/mol, Table 2).

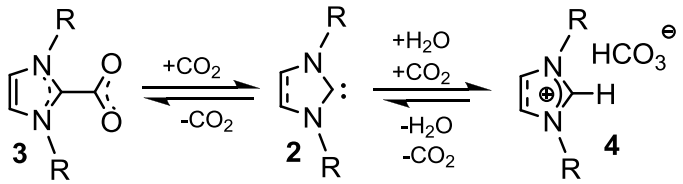

Scheme 3. Transformation of NHC-CO_2 adducts and [NHC(H)][HCO_3] onto NHCs.

For each reaction, a transition state $TS_{4\rightarrow 2}$, connecting directly **4** and **2** and lying at 10.0, 7.5 and 10.2 kcal/mol above **4a**, **4b** and **4c**, respectively, could be located on the potential energy surface (Figure 9 and Table 2). The geometry of the TS (Figure 11) indicates that the process is concerted for the 3 transformations and quasi synchronous for **4b** → **2b** and **4c** → **2c**. In the case of **4a** → **2a**, the transformation is asynchronous, the breaking of the C5-O2 bond being more advanced than the proton transfer of H1 from C to O2 in $TS_{4a\rightarrow 2a}$.

The reactions **3** → **2** were also investigated by DFT calculations (Scheme 3 and Table 2, see also Figures S17-S18 in Annexes). The energetic barriers found were: 6.1 kcal/mol for **3a** → **2a** and 5.1 kcal/mol for **3b** → **2b**. Small energetic differences between **3** and **2** were observed for these transformations ($\Delta G_{3a\rightarrow 2a}$ = -3.5 kcal/mol and $\Delta G_{3b\rightarrow 2b}$ = -1.6 kcal/mol). These values highlight that NHC **2** is more easily generated from NHC-CO_2 **3** than from [NHC(H)][HCO3] **4**, the activation barriers of the **4a** → **2a** and **4b** → **2b** transformations being 10 and 7.5 kcal/mol respectively.

Table 2. Results of DFT calculations for **4 → 2**, subsequent **2 → 3 (**with H_2O) and **3 → 2**.

Transformation	Activation barrier (kcal/mol)	ΔG_{trans} (kcal/mol)
4a → 2a	10	-0.2
2a → 3a (+H_2O)	5.6	-4.3
3a → 2a	6.1	-3.5
4b → 2b	7.5	-2.5
2b → 3b (+H_2O)	6.3	-3.7
3b → 2b	5.1	-1.6

The low energy barrier associated with the reversibility of these transformations thus agrees well with the NHC behavior of both NHC-CO_2 **3** and [NHC(H)][HCO_3] **4** observed in solution, at room temperature.

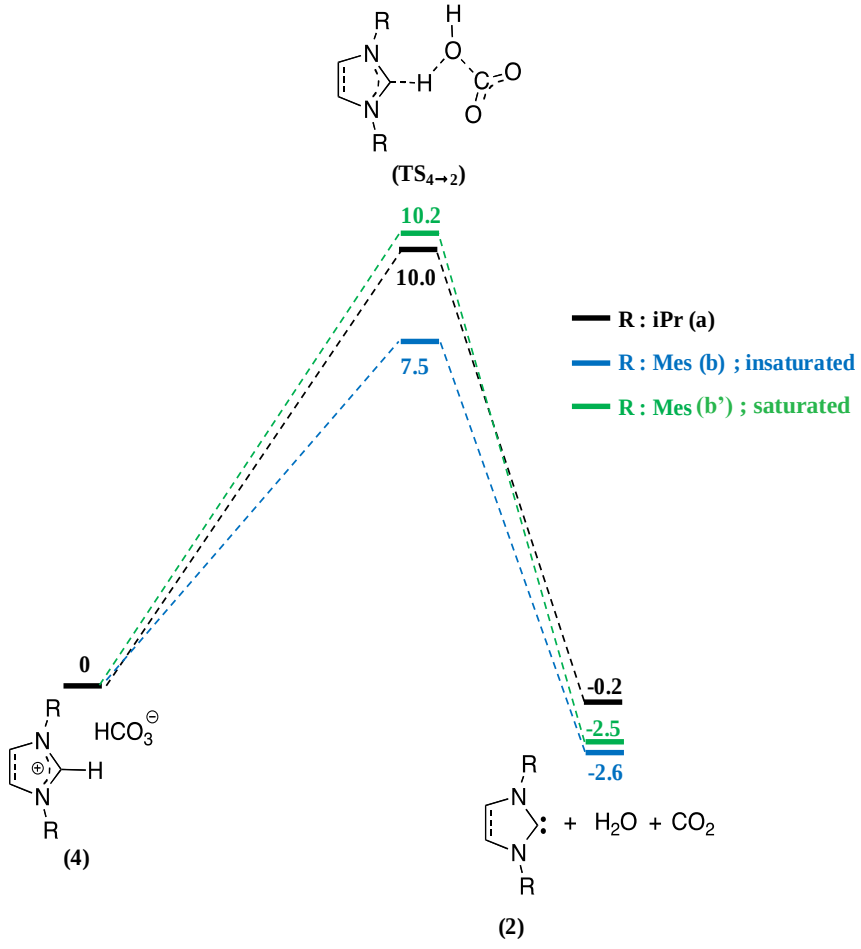

Figure 9. Energy profile computed at the B3LYP/6-31G** level (free energies G at 25°C including ZPE correction in kcal/mol, distances in Å) for the rearrangement **4→2 + CO_2 + H_2O**, noted **4→2** in the text.

The reactions of CO_2 with free NHCs **2**, in the presence of H_2O, were also investigated computationally (Figure 10). Here again, the rather small differences calculated for the three transformations ($\Delta G_{2\rightarrow 3}$ = (-)3.7-(-)8.0 kcal/mol) indicate the reversibility of the process, regardless of the nature of the substituents on the nitrogen atoms. For each reaction, a transition state $TS_{2\rightarrow 3}$ connecting directly **2** and **3** and lying at 5.6, 6.3 and 2.7 kcal/mol above **2a**, **2b** and **2c**, respectively, could be located on the potential energy surface (Figure 10 and Figure 12 for geometrical parameters).

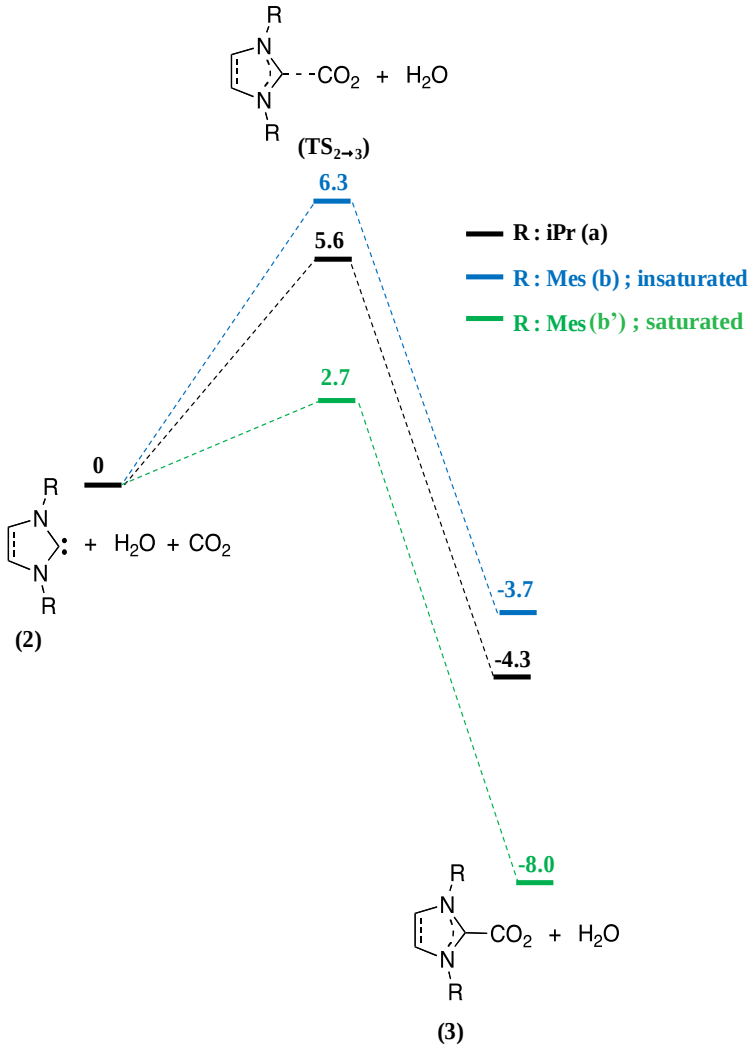

Figure 10. Energy profile computed at the B3LYP/6-31G** level (free energies G at 25°C including ZPE correction in kcal/mol, distances in Å) for the rearrangement **2 + CO_2 + H_2O → 3 + H_2O**.

Hence, the low energy barrier associated with the reversibility of the reaction accounts for the facile inter-conversion of [NHC(H)][HCO_3] **4** into NHC-CO_2 **3** through the intermediacy of NHC **2**. The generation of NHC **2** from NHC-CO_2 **3** (in dry conditions) was however found slightly more

favorable than from [NHC(H)][HCO_3] **4**. This is also consistent with the fact that NHCs could not be observed in solution neither from NHC-CO_2 nor from [NHC(H)][HCO_3]. It may be indeed assumed that free NHCs react very fast with CO_2 or (H_2O and CO_2), yielding the respective NHC-CO_2 and [NHC(H)][HCO_3] compounds, which are in equilibrium.

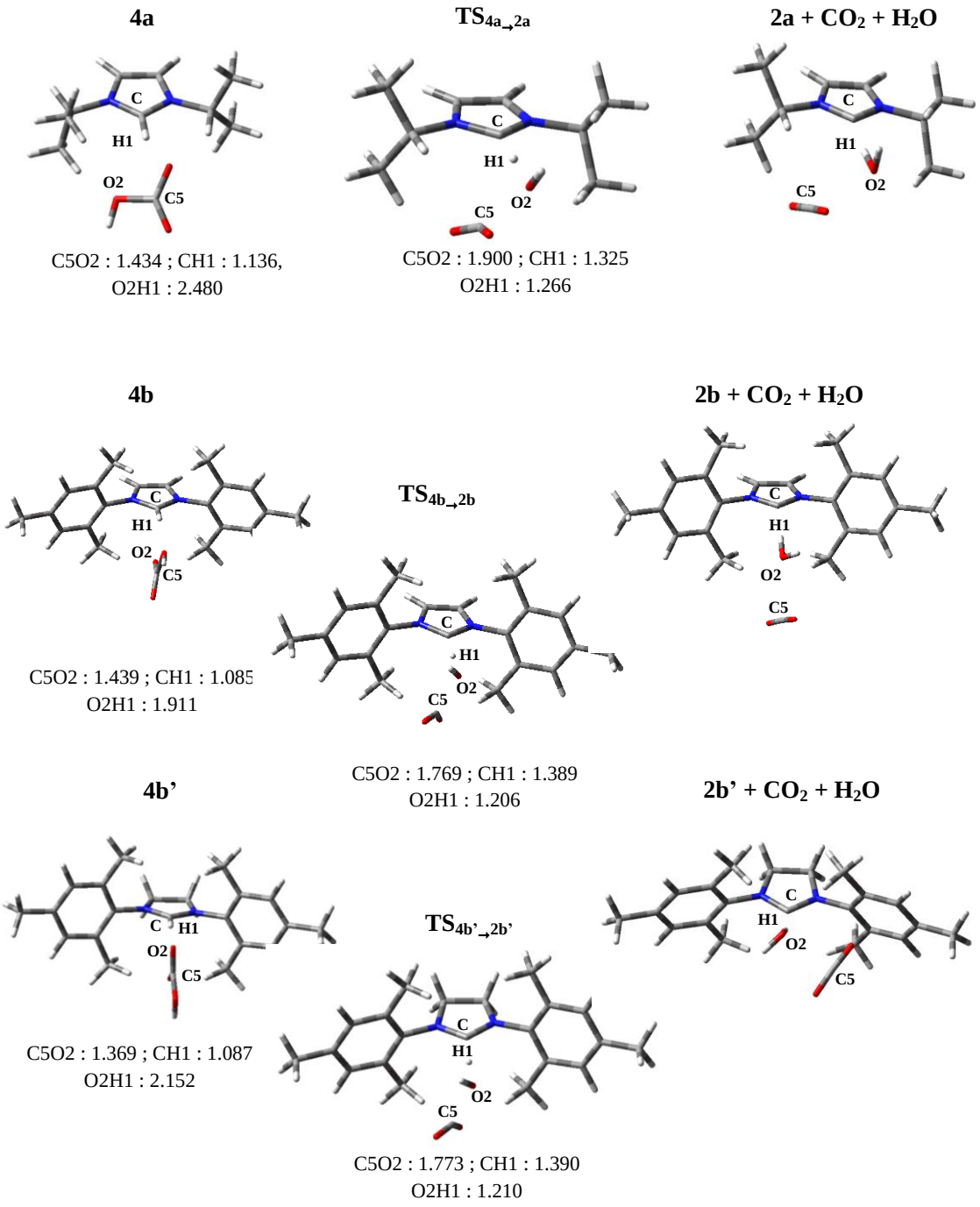

Figure 11. Geometrical structures and main bond lengths for all the compounds involved in the **4→2** rearrangement.

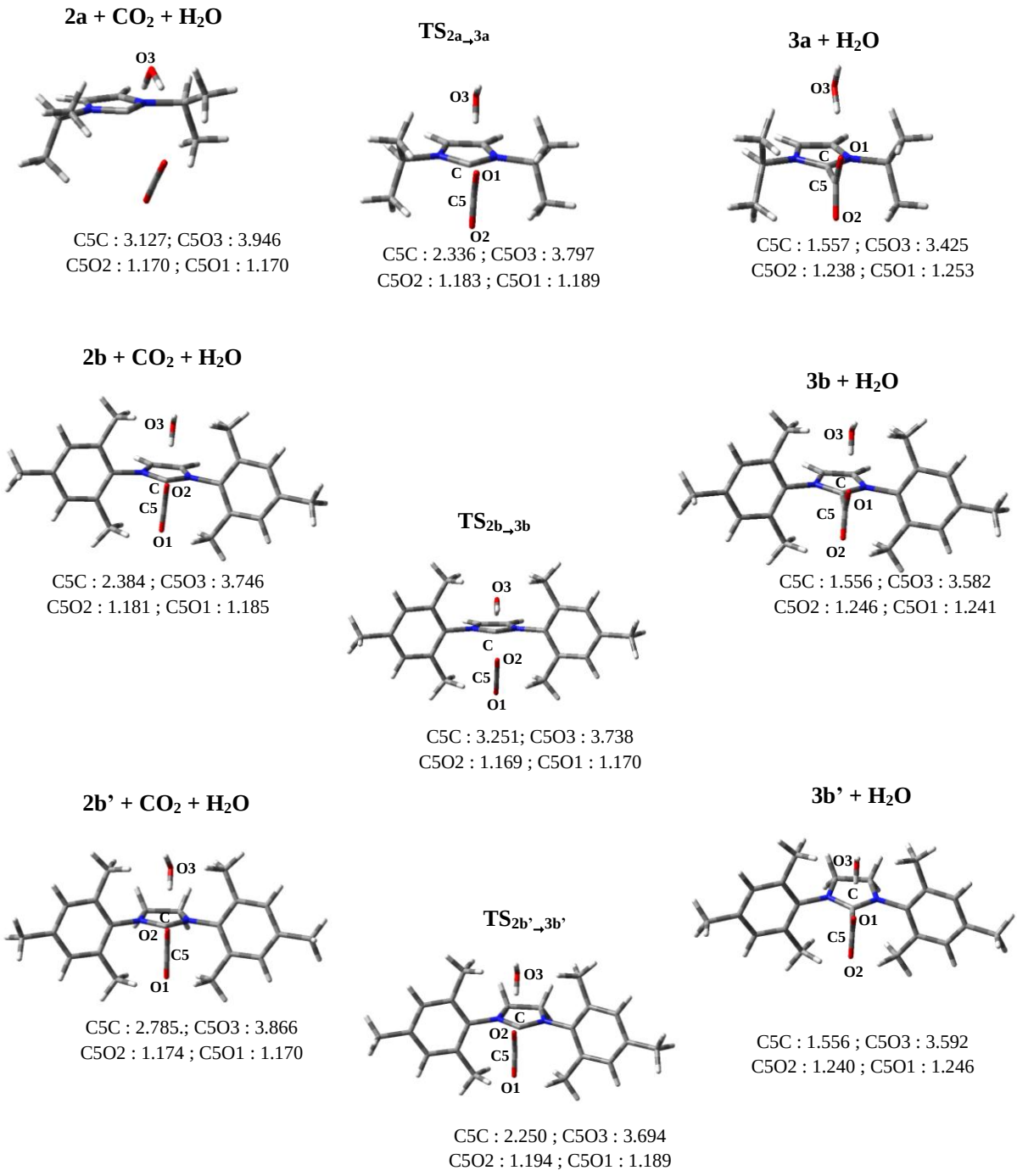

Figure 12. Geometrical structures and main bond lengths for the all the compounds involved in the **2→3** rearrangement.

3. Catalytic tests: azolium hydrogen carbonates *vs.* imidazolium-2-carboxylates

This section is dedicated to the use of imidazolium hydrogen carbonates as NHC precursors in solution. First, The [NHC(H)][HCO_3] salts are shown to behave as masked NHCs, allowing for the NHC moiety to be readily transferred to both organic and organometallic substrates, without the need for dry and oxygen-free conditions. Such [NHC(H)][HCO_3] precursors were next successfully investigated as pre-catalysts for several reactions in molecular chemistry and polymer synthesis. Given the small energetic barriers obtained in the gas phase at 25 °C for NHC generation from both [NHC(H)][HCO_3] salts **4** and NHC-CO_2 adducts **3**, the ability of each precursor to generate the NHC **2** was compared, especially at room temperature.

Mechanisms of the five tested (macro)molecular reactions catalyzed by NHCs are depicted in supporting information (see Schemes S1-S5).

3.1. Transfer of the NHC moiety onto transition metals and CS_2

We first examined whether [NHC(H)][HCO_3] **4** could be of some practical use as a source of NHCs to be transferred, in a stoichiometric fashion, to organic substrates and to transition metals. For instance, in the presence of CS_2, an organic substrate known to readily react with free NHCs,[38,94] imidazolium hydrogen carbonates **4b**,**b'** afforded the corresponding highly colored azolium dithiolate-type betaines, denoted as NHC-CS_2 adducts **5b**,**b'**, in high yield (92-96%; see Experimental). Reactions of **4** with an excess of CS_2 were carried out in THF at 50 °C for 1 to 6 h (Scheme 4). The structure of NHC-CS_2 adducts **5b-b'** were authenticated by comparing their ^{1}H NMR spectra with those reported in the literature.[94] Although this reaction involving CS_2 has a limited synthetic utility, it clearly established that [NHC(H)][HCO_3] **5** could deliver the free carbene in solution.

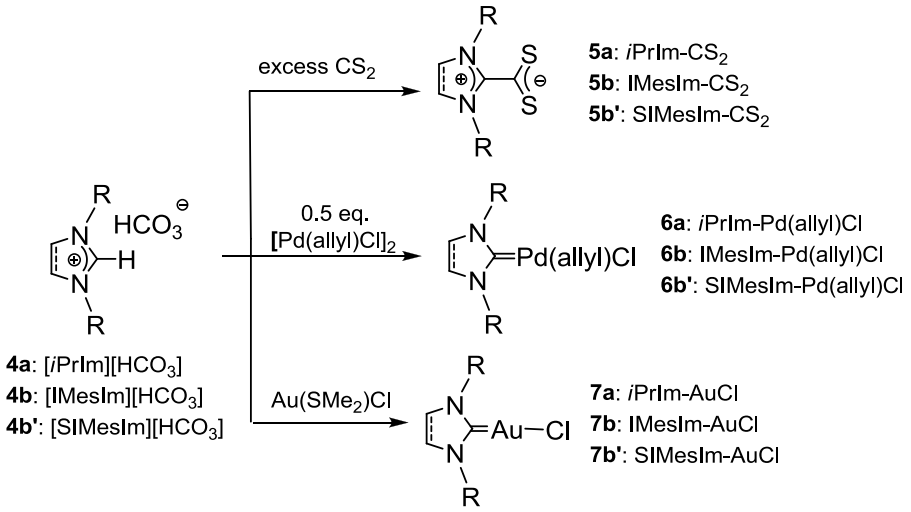

Scheme 4. Transfer of the NHC from [NHC(H)][HCO_3] salts **4** to CS_2, [Pd(allyl)Cl]$_2$ and $Au(SMe_2)Cl$.

To further illustrate their potential as NHC precursors, the reactivity of [NHC(H)][HCO_3] salts **4** toward transition metals was investigated (Scheme 4). It is worth mentioning that these transfer reactions were performed in air with non-purified solvents. Thus, 1.2 eq. of **4a**,**b**,**b'** was reacted with 0.5 eq. of [Pd(allyl)Cl]$_2$ in THF. The corresponding NHC-Pd(II) complexes **6a**,**b**,**b'** were isolated in excellent yield (>87%), after 24 h of stirring at RT for compound **6a**, and 1 h for **6b**,**b'**. The two latter compounds were identified by comparing their ^{1}H NMR spectra with those already reported,[95-96] while compound **6a** was completely characterized by ^{1}H and ^{13}C NMR spectroscopy.

The ^{1}H NMR spectrum of **6a** exhibited 5 different signals corresponding to the allyl fragment, indicating a dissymmetric structure around the palladium center. In the ^{13}C NMR spectrum, the characteristic signal of the carbene center was observed at 177.2 ppm, in agreement with that observed for analogous palladium-NHC complexes (δ = 175.6-188.5 ppm).[95-96]

Similarly, transfer of the NHC moiety from **2** to $AuCl(SMe_2)$ was successfully accomplished in air, giving excellent yields of the corresponding NHC-Au complexes **7**, after 1 h of stirring in $CHCl_3$ at 50 °C for **7a**, and at RT for **7b**,**b'**. Excellent agreement between the ^{1}H NMR spectra of **7a**,**b**,**b'** synthesized from [NHC(H)][HCO_3] **2** and data reported in the literature was noted.[97-98]

Catalytic activities of selected precursors (**3a**,**b** and **4a**,**c-f**, Figure 1) were next evaluated in several molecular reactions, including cyanosilylation, benzoin condensation and transesterification

reactions. All these reactions were carried out under different experimental conditions so as to investigate both solvent and temperature effects. Precursors **4a-f** being thought to generate free NHCs **2** by releasing H_2CO_3 (=H_2O + CO_2; Scheme 1),[2] molecular sieves (3Å) were systematically added in the reaction vessel. Control experiments were also implemented from the corresponding bare NHC **2a** which was purposely synthesized. Only **3a** and **4a** were tested as pre-catalysts for transesterification reaction, in order to highlight the solvent effect on the ability of imidazolium hydrogen carbonates and their NHC-CO_2 counterparts to generate corresponding NHCs.

NHC-CO_2 adducts **3**, were synthesized following slightly modified reported procedures.[35,39] Briefly, 1,3-di-isopropyl-imidazolium-2-carboxylate, **3a**, and 1,3-di-mesityl-imidazolium-2-carboxylate, **3b**, were obtained by direct carboxylation of corresponding free NHCs **2** in THF (Scheme 2a), and characterized by ^{1}H and ^{13}C NMR spectroscopy (Figures S19-S22). It is worth pointing out that unlike **2a**, **3a** was easily isolated by simple filtration of the reaction mixture. Moreover, neat **3a** was found relatively stable when exposed to air at RT, whereas its related NHC had to be stored at -30 °C under dry and inert conditions.

3.2. Molecular reactions

3.2.1. Benzaldehyde and benzophenone cyanosilylation reaction

Hermann *et al.*,[99] then both Song *et al.*[100] and Suzuki *et al.*[101] have employed NHCs as organocatalysts for cyanosilylation reactions of carbonyl-containing substrates. When aldehydes or ketones react with trimethylsilylcyanide (TMSCN) in the presence of catalytic loadings of NHC, high conversions are obtained. Although the mechanism that may involve either the activation of the carbonyl group or the silicon atom remains unclear (see Scheme S1), this is a general method to access α-hydroxyamines, α-hydroxyacids and α-hydroxyaldehydes after derivatization.[102-103] Polymer-supported versions of NHC-CO_2 adducts have also been reported for organocatalyzed cyanosilylation reactions.[56]

Here, we examined the catalytic activity of both molecular imidazolium hydrogen carbonates **4a,c-f** and NHC-CO_2 adduct **3a** toward the cyanosilylation reaction of benzaldehyde or benzophenone with TMSCN, both at RT and at 80 °C. Most significant results are collected in Table 3. Reaction conversions were calculated by ^{1}H NMR, in the case of benzaldehyde as substrate, as illustrated in Figure 13. In the case of benzophenone, aliquots of the crude mixture were periodically analyzed by ^{13}C NMR, until complete disappearance of the ketone signal at δ=196 ppm (conversion= 100%).

Table 3. Cyanosilylation of benzaldehyde or benzophenone with TMSCN in THF, in the presence of **2a**, **3a** or **4a,c-f** (see Scheme S1 for the putative mechanism).

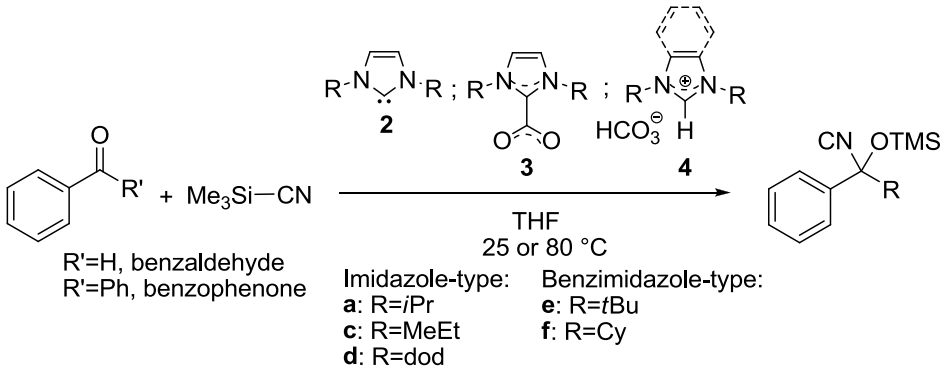

Entry	Catalyst	%mol catalyst	Substrate	*T* (°C)	*t* (min)	Conv (%)[a]	TOF[b] (h^{-1})
1	**2a**	0.02	benzaldehyde	25	10	56	16800
				80	10	95	28500
2	**3a**	0.02	benzaldehyde	25	10	86	25800
				80	10	100	30000
3[c]	**4a**	0.02	benzaldehyde	25	30	86	8600
				80	30	100	10000
4[c]	**4c**	0.1	benzaldehyde	25	10	93	5580
5[c]	**4d**	0.1	benzaldehyde	25	60	100	1000
6[c]	**4e**	0.1	benzaldehyde	25	10	99	5940
7[c]	**4f**	0.1	benzaldehyde	25	10	100	6000
8	**2a**	0.02	benzophenone	25	20	100	15000
				80	20	100	15000
9	**3a**	0.02	benzophenone	25	20	100	15000
				80	20	100	15000

[a] Conversion was calculated by ^{1}H NMR in $CDCl_3$. [b] Turnover frequency. [c] 3Å molecular sieves were added.

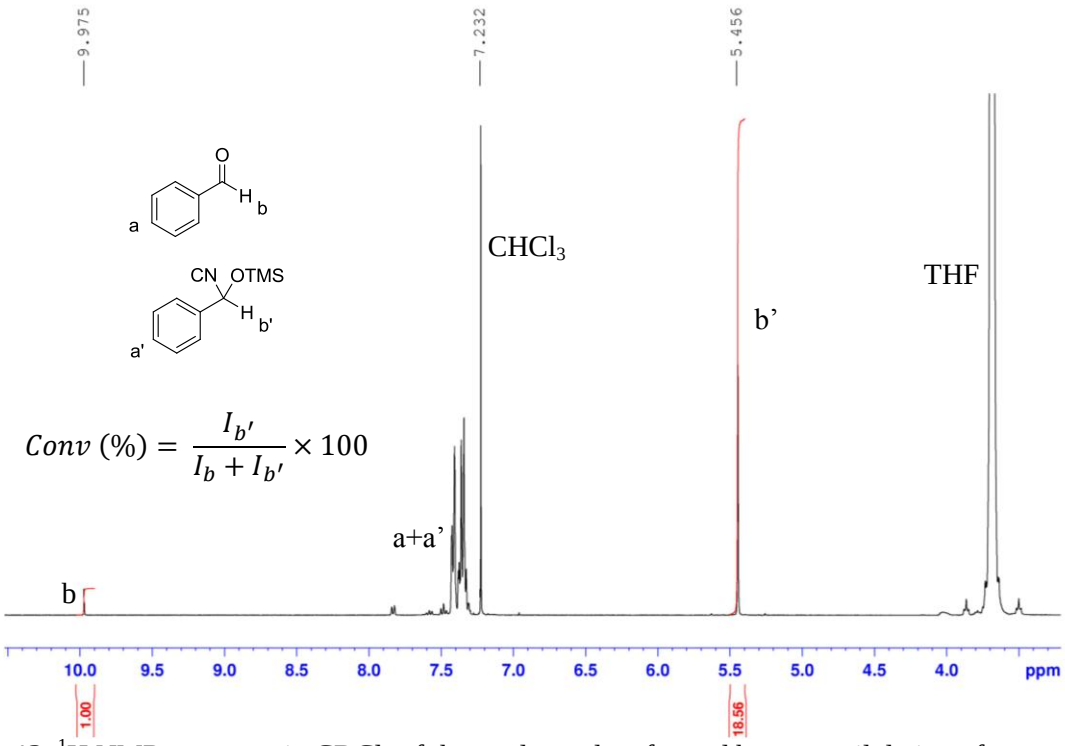

Figure 13. ^{1}H NMR spectrum in $CDCl_3$ of the crude product formed by cyanosilylation of benzaldehyde with TMSCN in THF, calculation of the conversion is shown in the inserted formula.

In the case of benzaldehyde as substrate, 0.02 mol% of **3a** gave almost quantitative conversions, both at RT and 80 °C, only after 10 min of reaction (entry 2). A control experiment employing the free NHC **2a** gave similar results (entry 1). Interestingly, the use of **4a** as NHC precursor only divided the turn over frequency (TOF) by a factor of 3 (entry 3), attesting that both **3a** and **4a** could generate NHC at RT and 80 °C. These experimental results are in agreement with the reversibility and relatively low energetic barriers which were discussed in section 2: 6.1 and 10 kcal/mol, calculated for the transformation **3a** → **2a** and **4a** → **2a**, respectively.[2]

Imidazolium hydrogen carbonates **4c,d** were also efficient to trigger the cyanosilylation of benzaldehyde at RT (entries 4-5), though **4d** bearing more bulky substituents gave a lower TOF. Benzimidazole-type salts **4e,f** were also successfully used as pre-catalysts at RT (entries 6-7) witnessing, for the first time, that such precursors could generate corresponding NHCs in solution at RT, likely by a simple solvation effect.

Song *et al.* have noticed that NHC-catalyzed cyanosilylation of ketones -compared to aldehydes- requires longer reaction times using 1,3-di-*tert*butyl-imidazol-2-ylidene as catalyst, the reaction being

favored in DMF compared to THF.[100] Here, both **2a** and **3a** catalyzed the cyanosilylation of benzophenone quantitatively, after 20 min in THF, both at room and at higher temperatures (entries 8 and 9). Hence, high temperatures are not needed to achieve high yields, suggesting in that case again that solvation effect, associated with the favorable kinetics and thermodynamics of the transformations **3a** → **2a** and **4a** → **2a**,[2] can drive the generation of the NHC catalyst from NHC-CO_2 adducts and [NHC(H)][HCO_3] precursors.

3.2.2. Benzoin condensation reaction

Pioneer works on NHC-catalyzed benzoin condensation by Breslow date back to 1958.[104] Since then, various NHCs, including thiazol-2-ylidenes, imidazol(in)-2-ylidenes, benzimidazol-2-ylidenes and triazol-5-ylidenes, as well as NHC-COS adducts,[41] have served to catalyze this C-C bond forming reaction that transforms aromatic aldehyde molecules into benzoin derivatives. The reaction intermediate is a resonance-stabilized enaminol-type intermediate called the "Breslow intermediate" (see Scheme S2).[9] Application of this elementary reaction to polymer synthesis, that is, the NHC-catalyzed step-growth polymerization of an aromatic bis-aldehyde, namely terephtaldehyde, forming "polybenzoin" has also been reported.[105] Besides, polymer-supported NHC precursors, such as poly(NHC-CO_2) adducts[57] and poly(imidazolium salt)s,[68] have been used to catalyze the benzoin condensation, the *in situ* generation of poly(NHC)s being triggered by a temperature increase or the addition of a base, respectively.

Masked NHCs **3a** and **4a-f** were thus tested as organic pre-catalysts for the benzoin condensation reaction (Table 4). Reaction conversions were calculated by ^{1}H NMR, as illustrated in Figure 14.

In contrast to cyanosilylation, temperature has a strong impact on the reaction conversion. For instance, a temperature increase, from 25 °C to 80 °C, led to more than twice higher yields upon using **3a** as precursor (Table 4, entry 2). However, this pre-catalyst gave approximately 30 % conversion after 24 h at RT, that was twice lower than the result obtained with its free NHC homologue **2a**. The use of **4a** at RT resulted in even poorer conversions. At 80 °C, similar kinetics and yields were noted both with the free NHC **2a** and the NHC-CO_2 adduct **3a**, attesting for the quantitative generation of the

NHC at this temperature. As already observed in the cyanosilylation, reaction using **4a** led to similar conversions, but divided the TOF by a factor of 3 at 80 °C.

Table 4. Benzoin condensation reaction in THF using **2a**, **3a** or **4a-f** (see Scheme S2 for the putative mechanism).

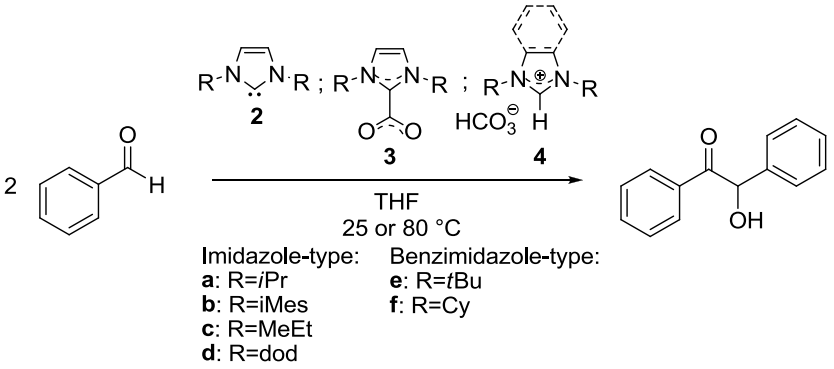

Entry	Catalyst	%mol catalyst	Solvent	*T* (°C)	*t* (h)	Conv (%)[a]	TOF[b] (h^{-1})
1	**2a**	1	THF	25	24	52	2.17
				80	24	72	3
2	**3a**	1	THF	25	21	28	1.3
					48	45	0.94
				80	24	72	3
3[c]	**4a**	3	THF	25	21	6	0.09
					48	11	0.08
				80	24	72	1
4	**4b**	10	THF	60	24	88	0.37
4'	**4b'**	10	THF	60	24	83	0.35
5[c]	**4c**	10	THF	25	24	44	0.2
				80	24	72	0.3
6[c]	**4d**	10	THF	25	24	17	0.07
				80	24	79	0.3
7[c]	**4e**	10	THF	25	24	0	-
				80	24	0	-
8[c]	**4f**	10	THF	25	24	71	0.3
				80	24	75	0.3

[a] Conversion was calculated by ^{1}H NMR in $CDCl_3$. [b] Turnover frequency. [c] 3Å molecular sieves were added.

While relatively high amounts of free NHCs are required to achieve high yields (up to 10-30 mol% for asymmetric condensations),[9] only 1 mol% of precursor **2a** gave a rather good catalytic efficiency at RT (entry 1). However, complete conversion was not achieved at 80 °C from **2a**, **3a** or **4a**, after 24h, even with higher amounts of (pre)-catalysts. This is presumably due to the temperature sensitivity of **2a**. Similar results were observed upon using 10%mol of **4b** or **4b'** as NHC precursors

(entries 4 and 4'). Changing the substituents of the imidazole ring for less bulky (**4c**) or for more bulky (**4d**) ones did not improve TOF values.

Finally, benzimidazolium hydrogen carbonate **4f** exhibited catalytic efficiency similar to **4a-d**, whereas **4e** showed no activity at all. Indeed, the steric hindrance of *t*Bu substituents as compared to cyclohexyl ones (**4e** *vs.* **4f**) may slower the NHC generation by a solvation effect.

Both categories of masked NHCs **3a** and **4a-f** are nonetheless capable to catalyze the benzoin condensation by generating NHCs in solution, better results being achieved at 80 °C.

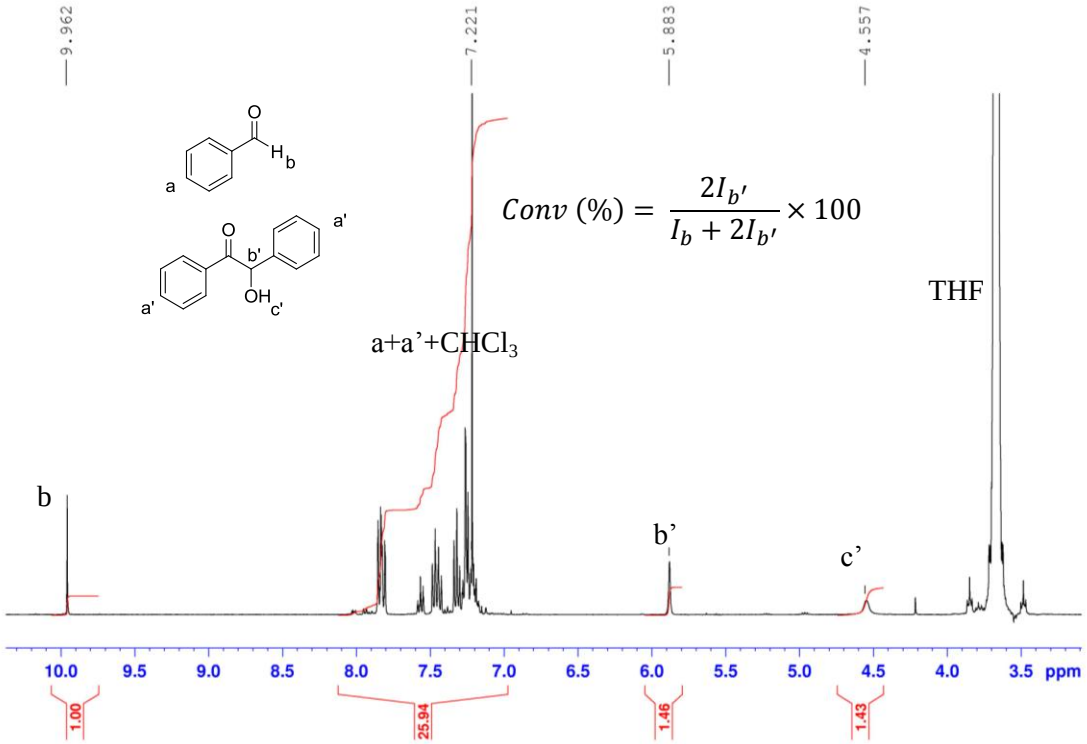

Figure 14. ^{1}H NMR spectrum in $CDCl_3$ of the crude product formed by benzoin condensation in THF, calculation of the conversion is shown in the inserted formula.

3.2.3. Transesterification reaction

Free NHCs,[106-107] and some masked NHCs such as imidazol(in)ium-2-thiocarboxylates (NHC-COS adducts)[41] or polymer-supported versions of imidazolium-2-carboxylates (poly(NHC-CO_2) adducts),[57] are known to efficiently catalyze transesterification reactions (for the mechanism, see Scheme S3). However, neither NHC-CO_2 adducts nor [NHC(H)][HCO_3] salt precursors have been evaluated as pre-catalysts for such reactions at RT.

Reaction between benzyl alcohol and vinyl acetate, a typical transesterification reported as being catalyzed by NHCs,[107] was thus performed in the presence of **3a** or **4a**. Non polar solvents such as cyclohexane and toluene, and polar solvents such as THF or DMSO, both at room temperature and at 80 °C were employed. Results obtained with the two types of NHC precursors are summarized in Table 5. The catalytic potential of free NHC **2a** was also evaluated for a comparison purpose since, to the best of our knowledge, this particular NHC has never been tested in transesterification reaction. Reaction conversions were calculated by ^{1}H NMR, as illustrated in Figure 15.

Table 5. Transesterification between benzyl alcohol and vinyl acetate using **2a**, **3a** or **4a** (see Scheme S3 for the putative mechanism).

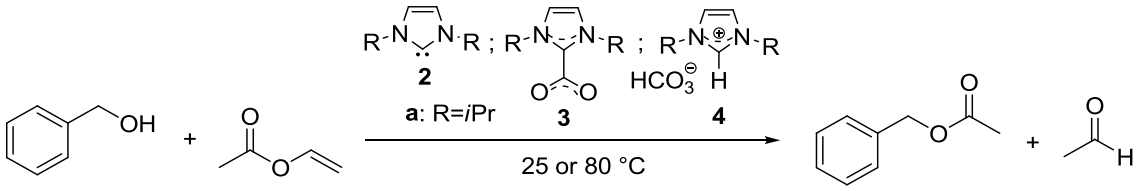

Entry	Catalyst	%mol catalyst	Solvent	*T* (°C)	*t* (min)	Conv (%)[a]	TOF[b] (h^{-1})
1	**3a**	0.5	THF	25	10	100	1200
				80	10	100	1200
2[c]	**4a**	0.5	THF	25	10	81	980
				80	10	93	1120
3	**3a**	0.1	THF	25	10	30	1800
				80	10	60	3600
4	**2a**	0.1	THF	25	10	100	6000
				80	10	100	6000
5	**3a**	0.1	Toluene	25	10	37	2220
				80	10	77	4620
6	**2a**	0.1	Toluene	25	10	94	5640
				80	10	100	6000
7	**3a**	0.1	Cyclohexane	25	10	4	240
				80	10	15	900
8	**2a**	0.1	Cyclohexane	25	10	79	4740
				80	10	100	6000
9	**3a**	0.1	DMSO	25	10	0	-
				80	10	7	420
10	**2a**	0.1	DMSO	25	10	5	300
				80	10	19	1140
11	**3a**	0.1	none	25	10	7	420
				80	10	10	600
12	**2a**	0.1	none	25	10	32	1920
				80	10	30	1800

[a] Conversion was calculated by ^{1}H NMR in $CDCl_3$. [b] Turnover frequency. [c] 3Å molecular sieves were added.

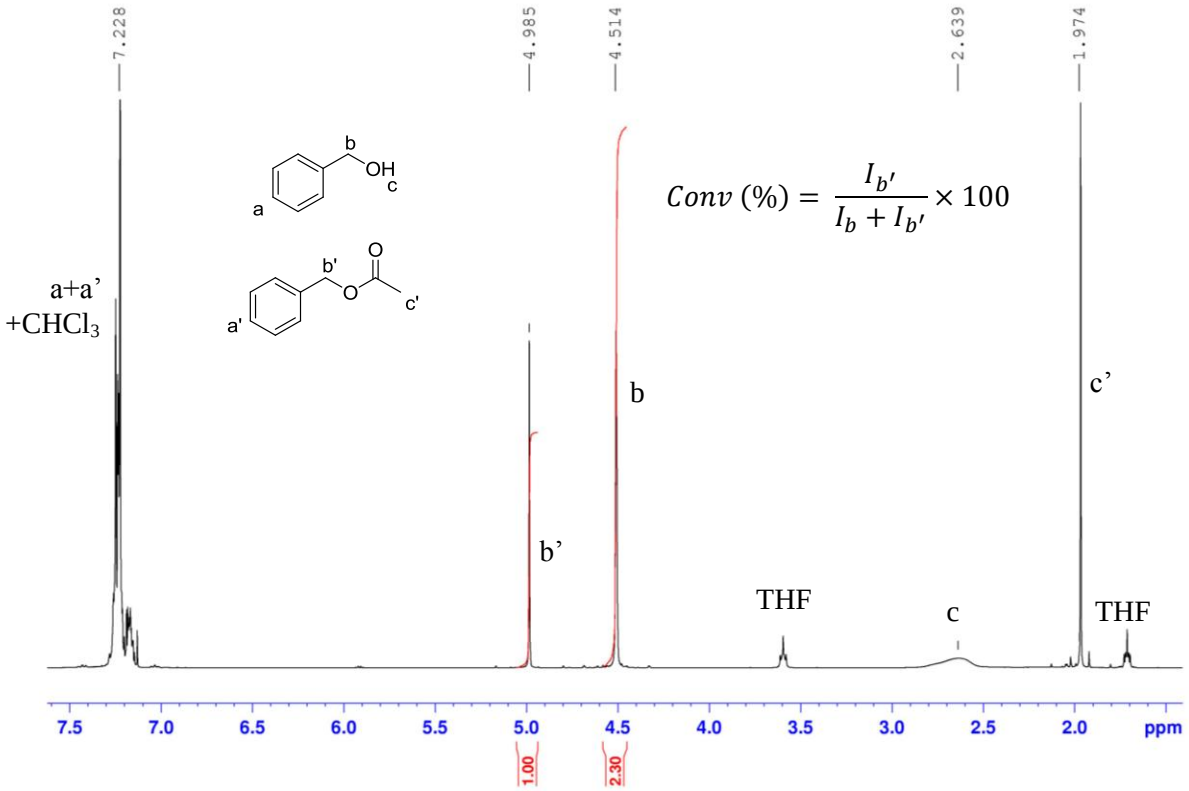

Figure 15. ^{1}H NMR spectrum in $CDCl_3$ of the crude product formed by transesterification of benzyl alcohol with vinyl acetate in THF, calculation of the conversion is shown in the inserted formula.

When 0.5 mol% of 1,3-di-isopropyl-imidazolium-2-carboxylate, **3a**, was used in THF, quantitative yields were achieved within only 10 min at 80 °C and, more strikingly, at room temperature as well (Table 5, entry 1). Interestingly, **4a** could also serve as a pre-catalyst of transesterification at RT, although twice a lower TOF value was noted compared to its carboxylate homologue, **3a**, under the same conditions (entry 2 *vs.* entry 3). These results are again consistent with the facile generation of NHC from both types of precursors at RT. Lower TOF values but high conversions observed with **3a** and **4a** compared to free NHC **2a** are also in agreement with the fact that **2a** has to be generated from its masked forms, prior to enter the catalytic cycle.

At a pre-catalyst **3a** concentration of 0.1 %mol, increasing the temperature from 25 to 80 °C gave twice higher conversions, regardless of the nature of the solvent, while almost no temperature effect was noted with the bare NHC **2a**. For example, TOF values increased from 1800 h^{-1} to 3600 h^{-1} in THF, from RT to 80 °C, using **3a** as pre-catalyst (entry 3). These results again support that NHC **2a** is

the true catalytically active species, the rate of CO_2 release from **3a** being increased by increasing the temperature.

Lower conversions were noted in THF compared to toluene, both from the NHC precursor **3a** and the free NHC **2a** (entries 3-4 *vs.* 5-6). In addition, NHC-CO_2 **3a** gave almost no conversion in cyclohexane, most probably due to its insolubility in this solvent. DMSO gave lower yields than all the other tested solvents despite of its high polarity, irrespectively of the catalyst (entries 9 and 10). A control experiment in absence of solvent was also attempted, which led to only poor yields, both at RT and at 80 °C, in the presence of either **2a** or **3a** (entries 11 and 12). Consistent with observations made by Delaude *et al.*[51] concerning NHC transfer to metal complexes, the solvent thus plays a crucial role during decarboxylation of NHC-CO_2 adducts.

The catalytic activity of **2a** in the tested solvents was as follows: DMSO < none << cyclohexane ≈ toluene ≈ THF, while in the case of **3a**, it varied as follows: DMSO ≈ none ≈ cyclohexane << toluene ≈ THF. Thus, the influence of the solvent on the transesterification reaction is similar upon using NHC-CO_2 **3a** or its corresponding bare NHC **2a** as catalysts, except when cyclohexane is employed, owing to the poor solubility of **3a** in this solvent.

Both NHC-CO_2 adducts and [NHC(H)][HCO_3], including those of benzimidazole-type, proved efficient for the transesterification and cyanosilylation reactions, giving excellent TOF at RT in THF. Both categories of NHC precursors could also trigger the benzoin condensation, preferentially at 80 °C.

As already mentioned, NHC-CO_2 adducts were widely used as ligand precursors in organometallic chemistry[37,48,50,108] or as pre-catalysts for molecular reactions.[53,55-57,59] Surprisingly, they remain poorly studied for a polymerization purpose (see also the bibliographic chapter –chapter 1– of this manuscript). Buchmeiser *et al.* have described the preparation of polyurethanes by step-growth polymerization between aliphatic triisocyanates and polyols.[60-61] The investigated NHC-CO_2 adducts displayed a latent behavior, as the polymerization only occurred above 65 °C. In a most recent study, Picquet, Plasseraud *et al.* showed that 1-butyl-3-methylimidazolium-2-carboxylate could trigger the polytransesterification of dimethyl carbonate with diols.[64] Aliphatic polycarbonates could be derived

in this way. The *in situ* formation of the NHC was achieved through heating of its CO_2-masked precursor. In contrast, and to the best of our knowledge, no report mentioned about the generation of NHCs from NHC-CO_2 adducts to catalyze chain growth polymerization reactions. In the two next sections, the ability of imidazolium-2-carboxylates and several azolium hydrogen carbonates to trigger the ring opening polymerization (ROP) of D,L-lactide and the group transfer polymerization (GTP) of methyl methacrylate is evaluated.

3.3. Polymer synthesis

3.3.1. Ring opening polymerization of D,L-lactide

Masked NHCs **3a**,**b**,**d** and **4a-f** were tested as organic pre-catalysts for the ROP of D,L-lactide (Table 6). As already mentioned, 3Å molecular sieves were added to the reaction mixture to avoid competitive initiation of the polymerization by H_2O generated from the [NHC(H)][HCO_3] pre-catalyst (see Scheme 3). Benzyl alcohol was employed as initiator. Reaction conversions were calculated by ^{1}H NMR, as illustrated in Figure 16.

Precursors **3** and **4a-d** led to polymers exhibiting experimental molar masses (M_n), as determined by size exclusion chromatography (SEC), in close agreement with expected values (based on initial $[D,L\text{-LA}]_0/[BnOH]_0$). Low dispersities (*D*) were obtained (<1.23), accounting for the quality of control of the polymerization.

Pre-catalysts **3a** and **3b** showed similar catalytic activities (TOFs around 700 h^{-1}, both at RT and 80 °C in THF, for an initial ratio $[M]_0/[I]_0$=27; Table 6, entries 2 and 5). However, values were lower than those observed with the free NHC **2a** (entry 1). As for [NHC(H)][HCO_3] precursors **4a** and **4b** (Table 6, entries 3 and 6), they gave three times lower catalytic activities, compared to their NHC-CO_2 adduct homologues. It turns out that NHC generation from imidazolium hydrogen carbonates, **4a** and **4b**, both at RT and 80 °C, is somehow less favored than upon using imidazolium-2-carboxylates, **3a** and **3b**, as also observed in the tested molecular reactions (section 3.2.). The catalytic activity of **2a** *vs.* **3a** *vs.* **4a** was thus as follows: [NHC(H)][HCO_3] **4a** < NHC-CO_2 adduct **3a** < free NHC **2a**.

This trend is confirmed through the evolution of the monomer conversion and of $\ln([M]_0/[M])$ with time, as depicted in Figure 17. Neither **3a** nor **4a** exhibited an induction period while catalyzing the ROP of LA, evidencing that the NHC generation from these two precursors can readily occur at RT. However, the formation of **2** is somehow kinetically and thermodynamically less favored in the case of **4** than in the case of **3**, as already supported by DFT calculations ($\Delta G_{\mathbf{3a} \rightarrow TS\mathbf{3a}\rightarrow\mathbf{2a}}$ = 6.1 kcal/mol *vs.* $\Delta G_{\mathbf{4a} \rightarrow TS\mathbf{4a}\rightarrow\mathbf{2a}}$ = 10 kcal/mol, and $\Delta G_{\mathbf{3a} \rightarrow \mathbf{2a}}$ = -3.5 kcal/mol *vs.* $\Delta G_{\mathbf{4a} \rightarrow \mathbf{2a}}$ = -0.2 kcal/mol, see also section 2 and Scheme 3).

Table 6. Ring opening polymerization of D,L-lactide in THF or toluene catalyzed by free NHC **2a**, imidazolium-2-carboxylates **3a** and **3b**, and (benz)imidazolium hydrogen carbonates **4a-f** (see Scheme S4 for the putative mechanism).

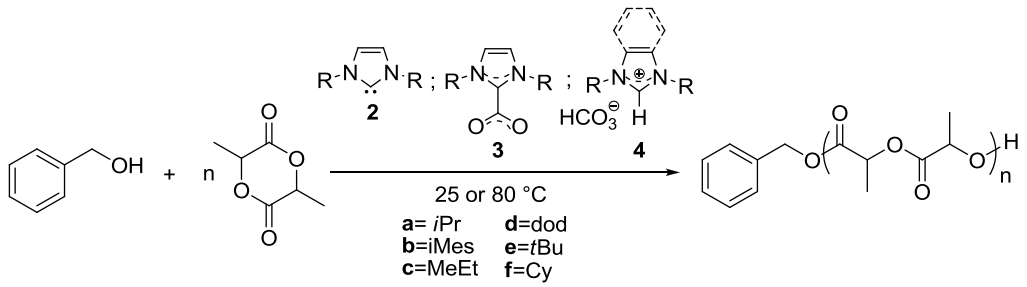

Entry	Catalyst	Solvent	[M]/[I]/[C]	*T* (°C)	*t* (min)	Conv[a] (%)	M_{nSEC}[b] (g/mol)	*D*[b]	TOF (h^{-1})
1	**2a**	THF	27/1/0.03	25	5	88	3,500	1.18	9504
2	**3a**	THF	27/1/0.03	25	60	84	3,700	1.13	756
				80	60	75	3,200	1.13	675
3[c]	**4a**	THF	27/1/0.1	25	60	95	4,600	1.23	257
				80	60	88	4,100	1.18	238
4	**3b**	THF	27/1/0.03	25	60	86	4,200	1.08	774
				80	60	79	3,700	1.09	711
5[c]	**4b**	THF	27/1/0.1	25	60	94	4,700	1.09	254
6[c]	**4b'**	THF	26/1/0.1	25	180	87	4.000	1.07	78
7	**3b**	THF	72/1/0.1	25	120	90	10,600	1.07	324
				80	120	69	7,500	1.06	249
8[from109]	**2b**[d]	THF	200/1/1.5	25	15	85	25,000	1.18	453
9	**4c**	THF	27/1/0.1	25	120	88	4,000	1.10	60
10[from109]	**2c**[d]	THF	200/1/1.5	25	15	97	28,000	1.31	517
11[c]	**4d**	THF	27/1/0.5	25	1440	0	-	-	-
12[c]	**4e**	THF	27/1/0.2	25	420	92	4,000	1.10	18
13[c]	**4f**	THF	27/1/0.05	25	5	96	5,100	1.17	1555

[a] Conversion was calculated by ^{1}H NMR in $CDCl_3$. [b] SEC in THF calibrated with polystyrene standards was used for characterization. [c] 3Å molecular sieves were added. [d] **2b,c** were *in situ* generated by exposure of **1b**,**c** to 0.875 eq. of *t*-BuOK for 10 min.

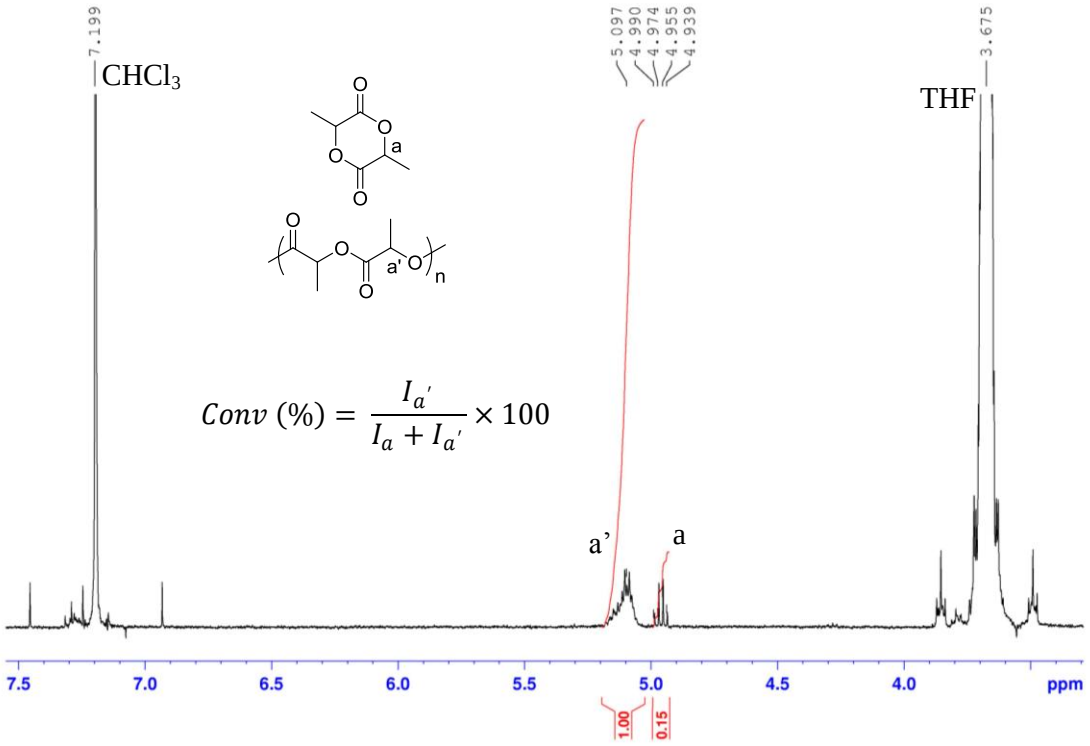

Figure 16. ^{1}H NMR spectrum in $CDCl_3$ of the crude product formed by ring opening polymerization of lactide in THF, calculation of the conversion is shown in the inserted formula.

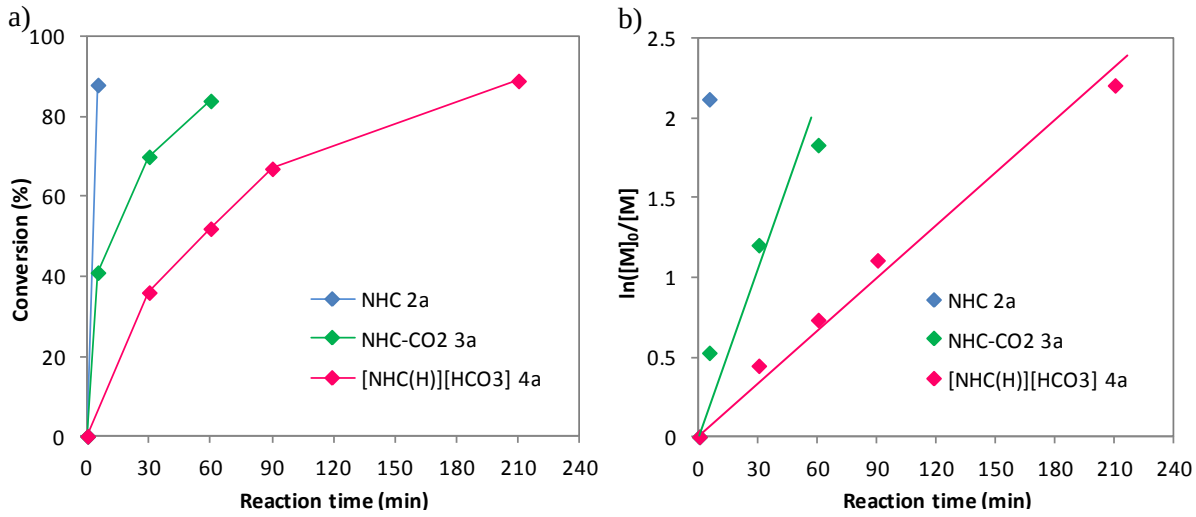

Figure 17. Conversion (a) and ln($[M]_0$/[M]) (b) *vs.* reaction time during the ROP of D,L-lactide catalyzed by: 3 %mol of NHC **2a** (in blue), 3 %mol of NHC-CO_2 **3a** (in green) or 5 %mol of [NHC(H)][HCO_3] **4a** (in pink).

The catalytic activity of the imidazolium hydrogen carbonate **4c** was approximately two times lower than the one of **4a**,**b** at RT (entry 9). Precursor **4d** featuring long alkyl chains on the

imidazolium ring showed no efficiency at all, despite the fact that reaction was performed for one day using 50%mol of pre-catalyst (entry 11).

These differences in TOF values highlight that the ability of NHC precursors to generate their corresponding free NHCs is very sensitive to the size of the alkyl substituents: in THF at 25 °C, TOF_{4a}=257 > TOF_{4c}=119 > TOF_{4d}=0 h^{-1}. This trend was already established while using these precatalysts for molecular syntheses in solution. Stability studies performed in the solid state also revealed that the temperature of CO_2+H_2O release from these compounds was as follows: $T_{4a} > T_{4c} > T_{4d}$ (see section 1.2.). Thus, the ability of **4d** to generate its corresponding NHC in solution is lower compared to other tested [NHC(H)][HCO_3], most probably owing to the bulkiness of its dodecyl substituents, that somehow decreased the accessibility of the imidazolium moiety of **4d**. This finding is also in agreement with the fact that the NMR spectrum of imidazolium hydrogen carbonates **4d** revealed the presence of the sole [NHC(H)][HCO_3] compound, irrespective of the solvent analysis. In contrast, NMR analyses of **4a-c** evidenced an equilibrium with their corresponding NHC-CO_2 adducts (**3a-c**).

Importantly, SEC traces did not show any side population attributable to a loss of control (see, for instance, Figure 18a for the SEC trace corresponding to entry 5). As depicted in Figure 19 (kinetic study corresponding to entry 3), the molar mass increases linearly with conversion. Increasing the initial monomer to the initiator ratio, from 27 to 72, in the presence of **3b** as a pre-catalyst in THF, led to 2.5 times higher M_n values, as expected, with no noticeable loss of control (Table 6, entry 7 and Figure 18b).

It is worth mentioning that TOF values observed using NHC-CO_2 adduct **3b** as pre-catalyst are comparable to those reported by Hedrick *et al.* when the NHC was *in situ* generated using *t*-BuOK as a base to deprotonate the imidazolium halide precursor[109] (entries 4 and 7 *vs.* 8). In their case, however, a TOF value about two to ten times higher than that obtained with our [NHC(H)][HCO_3] precursor was noted. In conclusion, although less catalytically efficient that free NHC homologues, both imidazolium hydrogen carbonates, **4a-c**, and imidazolium-2-carboxylates, **3a** and **3b**, prove useful pre-catalysts for the ROP of D,L-lactide, both at RT and 80 °C. To the best of our knowledge, this is the

first time that NHC-CO_2 adducts are employed in the context of a chain-growth polymerization process.

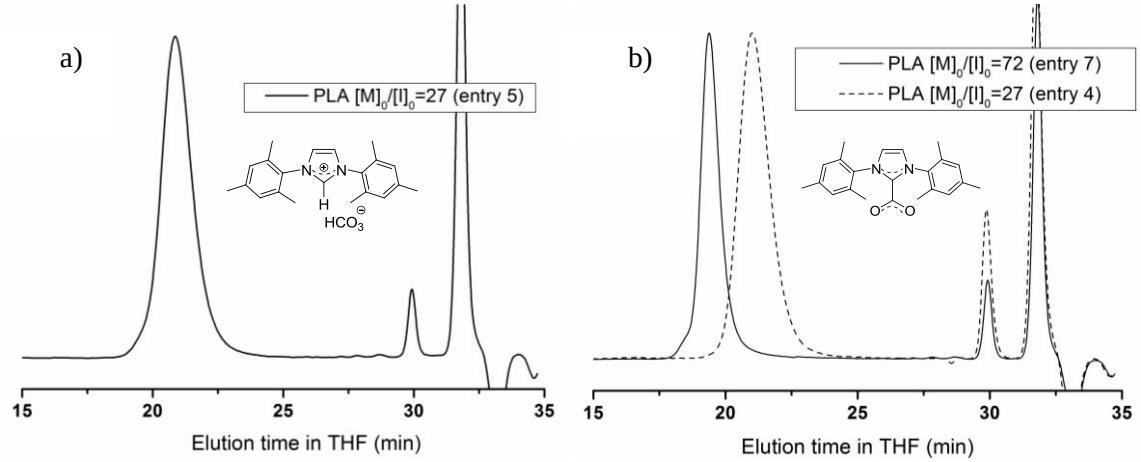

Figure 18. SEC traces (RI detector) of PLA obtained by ROP of D,L-lactide in THF at RT using benzyl alcohol as initiator, and: a) **4b** as pre-catalyst (Table 6, entry 5) ; b) **3b** as pre-catalyst (entry 4, dashed line and entry 7, solid line).

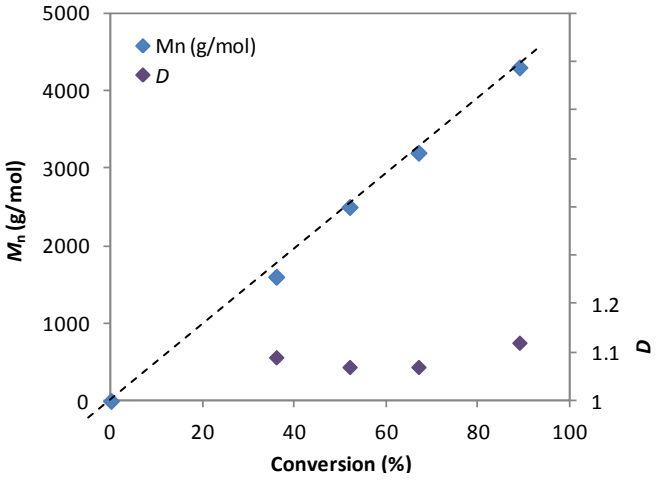

Figure 19. Molar masses (M_n, in blue) and dispersities ($D = M_w/M_n$, in purple) (determined by SEC in THF calibrated with PS standards) *versus* conversion (determined by ^{1}H NMR in $CDCl_3$) during the ROP of D,L-lactide catalyzed by **4a** at RT (Table 6, entry 3).

MALDI-ToF MS analysis was run on a PLA obtained using 1,3-di-mesityl-imidazolinium hydrogen carbonate, **4b'**, as NHC precursor (entry 6). On the corresponding MALDI-ToF mass spectrum ([LA]/[BnOH]/[C] = 26/1/0.1), only one series of peaks was observed at m/z = 108.14 + 144.13 n + 23, where 108.14 is the molar mass of the benzyloxy and H end-groups, and 23 the molar

mass of sodium ion. These values perfectly matched the expected molar masses of the targeted BnOH-initiated **4b'**-catalyzed PLA synthesis (Figure 20).

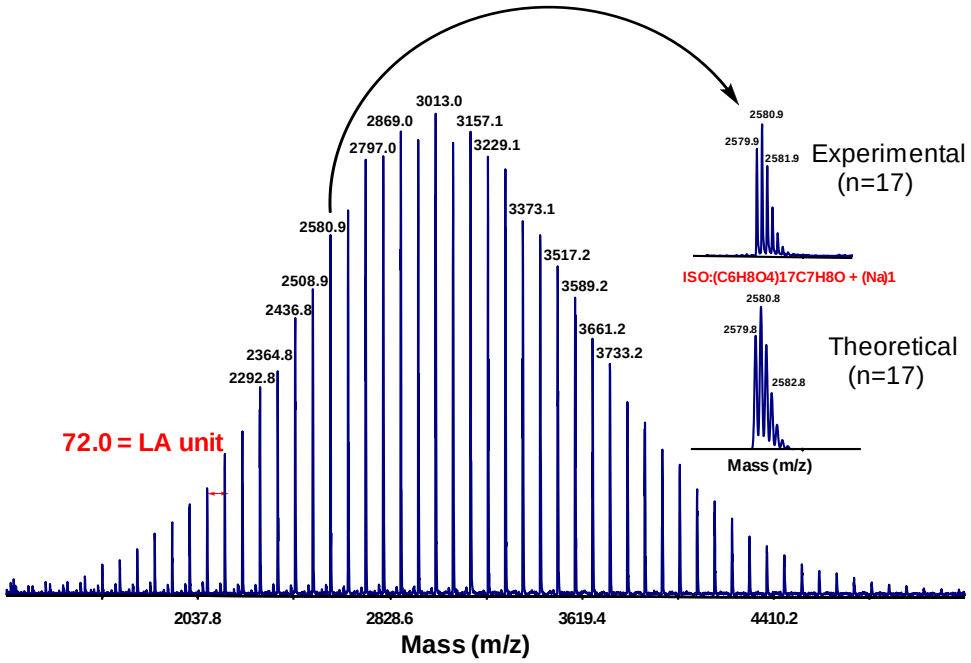

Figure 20. MALDI-ToF MS spectra in reflector mode of PLA ([LA]/[BnOH]/[**4b'**] = 26/1/0.1, Table 6, entry 6).

Benzimidazolium hydrogen carbonates **4e**,**f** were also tested as potent pre-catalysts for the ROP of D,L-lactide at RT (entries 12-13). While few examples in molecular chemistry have already unlighted the potential of benzimidazol-2-ylidenes as organocatalysts (mainly for the benzoin condensation reaction),[9] such NHCs have never been employed for a polymerization purpose. As for their imidazolium homologues, **4e**,**f** gave polymers with low dispersities and experimental M_n (determined by SEC in THF) close to expected values. The precursor **4e** showed, however, a low catalytic efficiency (entry 12) compared to other [NHC(H)][HCO_3] salts **4**. This result can be likely explained by the bulkiness of its *tert*-butyl substituents that decrease the rate of the formation of the corresponding NHC **2e**. In contrast, **4f** was the most powerful NHC precursor of this study. Indeed, the TOF value (1555 h^{-1}) with this pre-catalyst was two times higher than those observed with imidazolium-2-carboxylates used under similar experimental conditions (750 and 774 h^{-1} for **4a** and **4b** respectively). Thus, benzimidazole-type precursors can trigger the ROP of D,L-lactide in THF at RT, pre-catalysts bearing less bulky substituents being more efficient.

Masked NHCs **3a** and **4a** were also tested as pre-catalysts for the ROP of ε-caprolactone (εCL) and trimethylene carbonate (TMC, Table 7), as some NHCs have been established to catalyze such polymerizations (see Chap.1).[110-111] Both precursors proved efficient for the ROP of TMC. The masked NHC **4a** was found approximately 6 times less active than its carboxylate homologue **3a** (entries 3-4), again in good concordance with previous results comparing the catalytic activities of NHC-CO_2 adducts **3** and [NHC(H)][HCO_3] **4**.

However, **3a** exhibited a quite low catalytic efficiency toward the ROP of ε-CL, while **4a** was not able to trigger the polymerization of this monomer (entries 1-2). It is worth mentioning that only NHCs bearing methyl groups in 4- and 5-positions of their backbone –being more nucleophilic– efficiently catalyze the ROP of ε-CL.[18-19] For instance, NHC **2b** cannot trigger the ROP of this monomer.[110] Thus, the poor catalytic activity of **3a** and **4a** toward the ROP of ε-CL may be explained by the limited efficiency of related bare NHCs. The obtained PTMC and P(ε-CL) nonetheless exhibited low dispersities and experimental M_n (determined by SEC in THF) close to expected values.

Table 7. Ring opening polymerization of εCL and TMC in THF at 25 °C catalyzed by imidazolium-2-carboxylate **3a** and imidazolium hydrogen carbonate **4a**.

Entry	Catalyst	Monomer	[M]/[I]/[C]	*t* (h)	Conv[a] (%)	$M_{n\mathrm{SEC}}$[b] (g/mol)	D[b]	TOF (h^{-1})
1	**3a**	εCL	27/1/0.5	96	25	1,700	1.09	0.14
2[c]	**4a**	εCL	27/1/0.5	96	3	-	-	-
3	**3a**	TMC	28/1/0.1	1	91	3,500	1.07	255
4[c]	**4a**	TMC	28/1/0.1	5	73	3,300	1.07	41

[a] Conversion was calculated by ^{1}H NMR in $CDCl_3$. [b] SEC in THF calibrated with polystyrene standards was used for characterization. [c] 3Å molecular sieves were added.

3.3.2. Group transfer polymerization of methyl methacrylate

Group transfer polymerization (GTP) has been proposed in the mid 1980s as a convenient method to control the polymerization of (meth)acrylic monomers at ambient temperature and above.[112] It is based on the repetition of Mukaiyama-Michael reactions[113] involving the addition of silyl ketene acetal (SKA) onto an incoming (meth)acrylic monomer. NHCs have advantageously been used as GTP catalysts, which allowed polymerizing both acrylic and methacrylic monomers overcoming some of

the drawbacks of previous catalysts.[16,114-117] Other organic catalysts useful in GTP, including Bronsted phosphazene bases,[118-120] and strong Bronsted acids,[121-124] have also been reported.

Here, the GTP of methyl methacrylate (MMA) was performed at RT and at 80 °C, using 1-methoxy-2-methyl-1-[(trimethylsilyl)oxy]prop-1-ene (MTS) as initiator and **3a**,**d** or **4a**,**c-f** as pre-catalysts, in THF or in bulk. Table 8 summarizes main results obtained. Reaction conversions were calculated by ^{1}H NMR, as illustrated in Figure 21. As 1,3-di-mesityl-imidazol-2-ylidene **2b** is a poor GTP catalyst (kinetics about 12 times lower than **2a**),[125] none of its precursors has been tested for this particular polymerization reaction.

Table 8. Group transfer polymerization of methyl methacrylate catalyzed by **3a**,**d** and **4a**,**c-f** in THF or in bulk (see Scheme S5 for the putative mechanism).

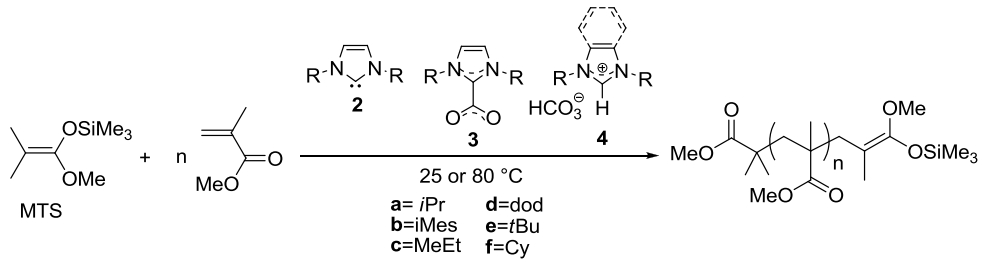

Entry	Catalyst	Solvent	[M]/[I]/[C]	*T* (°C)	*t* (h)	Conv (%)[a]	$M_{n\text{SEC}}$ (g/mol)[b]	*D*[b]	TOF (h^{-1})
1	**3a**	THF	38/1/0.05	25	48	77	3,200	1.12	12
				80	48	95	3,900	1.27	15
2	**3a**	bulk	38/1/0.03	25	0.5	60	2,700	1.27	1520
3[c]	**4a**	THF	38/1/0.3	25	20	50	2,500	1.09	3.2
4[c]	**4a**	bulk	38/1/0.09	25	24	90	4,900[d]	1.14	16
5[from 116]	**2a**	THF	30/1/0.01	25	16	100	2,900	1.25	188
6[c]	**4c**	THF	38/1/0.1	25	20	0	-	-	-
7	**3d**	bulk	76/1/0.15	25	0.5	63	6,300	1.37	320
8[c]	**4d**	bulk	76/1/0.15	25	20	0	-	-	-
9[c]	**4e**	THF	38/1/0.1	25	20	0	-	-	-
10[c]	**4f**	THF	38/1/0.1	25	20	36	1,600[d]	1.14	7

[a] Conversion was calculated by ^{1}H NMR in $CDCl_3$. [b] SEC in THF calibrated with polystyrene standards was used for characterization. [c] 3Å molecular sieves were added. *d* Second population in the high molar mass region (≈ 10% of the total distribution).

Although higher conversion was noted after 48 h at 80 °C compared to RT, a slight increase of the dispersity was observed along with a side population (≈ 2.5% of the total distribution) in the high molar mass region (Table 5, entry 1 and Figure 22a). The same was true when catalyzing the GTP of

MMA with **3a**,**d** in bulk. To avoid the presence of this side population, likely due to a few uncontrolled polymer chains, the reaction was stopped at 60% conversion (entry 2 and Figure 22b).

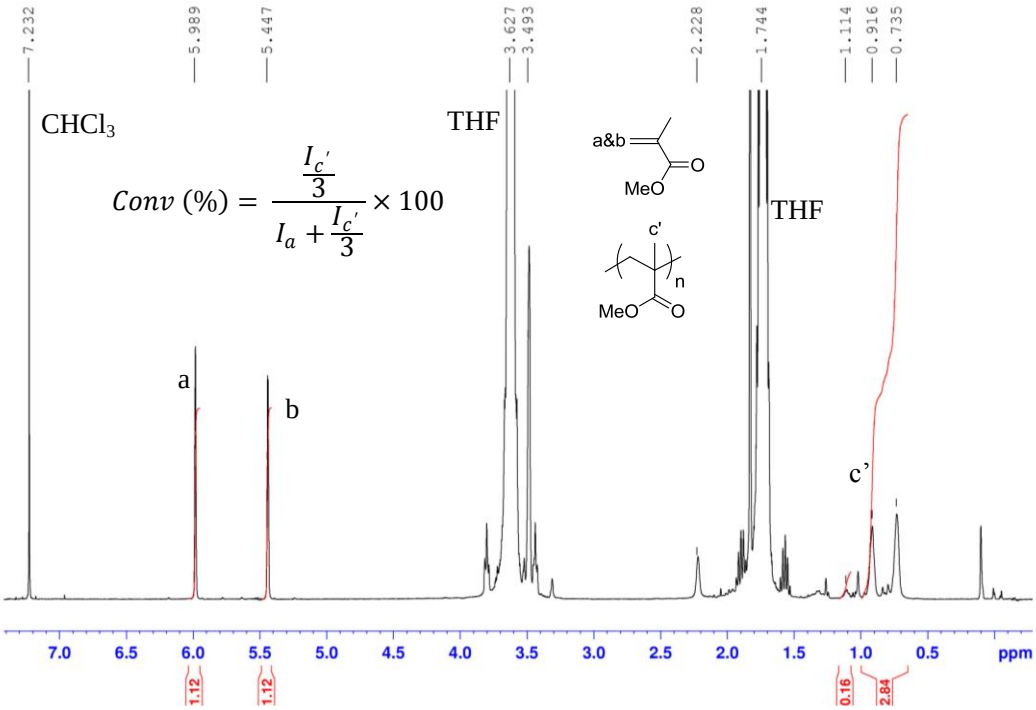

Figure 21. ^{1}H NMR spectrum in $CDCl_3$ of the crude product formed by group transfer polymerization of methyl methacrylate in THF, calculation of the conversion is shown in the inserted formula.

Under such conditions, relatively good control over M_n and D was observed, at RT, both under solventless conditions (bulk) and in THF solution. These results support that NHC-CO_2 adducts allow for a NHC-catalyzed GTP of MMA.

A catalytic activity about 15 times higher was noted with the free NHC **2a** compared to **3a** (entry 5), similarly to results prevailing for the ROP of D,L-lactide. As the bulk GTP of (meth)acrylics is hardly controlled using NHC catalysts because of their high activities, the good control over the polymerization upon using 3 mol% of pre-catalyst **3a** in bulk (D=1.27), may be ascribed to the fact that **3a** generates only a part of the related NHC in the polymerization timescale (30 min). In general terms, the catalytic activity of NHC-CO_2 adducts is thus more moderate than that of free NHCs.

Interest in employing [NHC(H)][HCO_3] precursors **4** as GTP pre-catalyst of MMA might be limited here. Indeed, these precursors were found hardly soluble in the MMA monomer substrate. As a

matter of fact, lower TOF values and a progressive loss of control were noted when polymerizing MMA in bulk (entries 3-4,6,8-10).

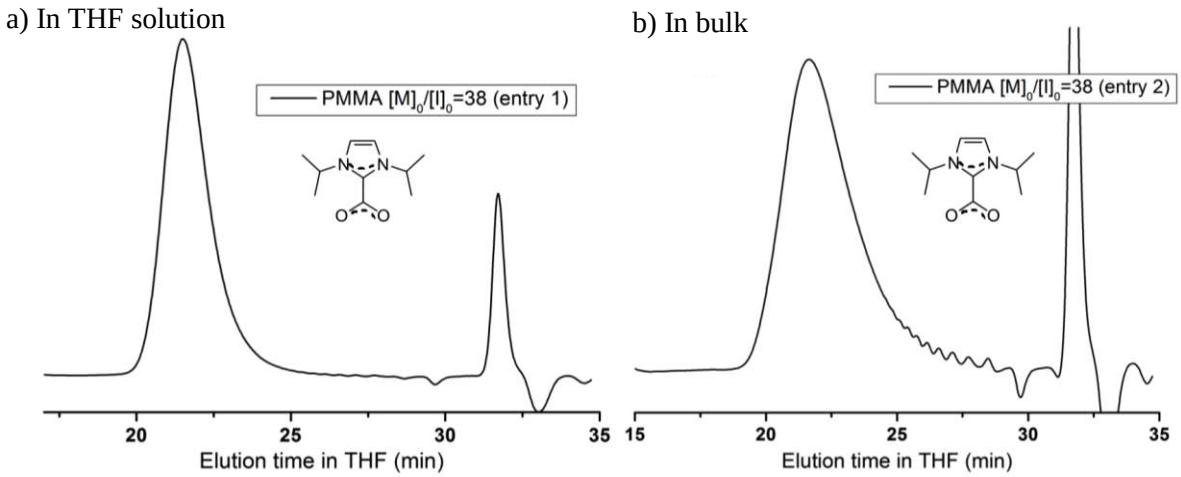

Figure 22. SEC traces (RI detector) of PMMA obtained by GTP of methyl methacrylate at RT using **3a** as pre-catalyst and MTS as initiator: a) in THF (Table 8, entry 1) ; b) in bulk (Table 8, entry 2).

Conclusion

Anion metathesis of azolium chlorides with $KHCO_3$ provides a facile one step synthetic access to air stable azolium hydrogen carbonates ([NHC(H)][HCO_3]). On the basis of experimental NMR results, it can be evidenced that such [NHC(H)][HCO_3] compounds are in equilibrium in solution with their NHC-CO_2 adduct counterparts, depending on the nature and water content of the solvent analysis. Thermogravimetric analysis (TGA) and TGA coupled with mass spectrometry (TGA-MS) of most [NHC(H)][HCO_3] precursors **4** showed a degradation profile in stages, with either a concomitant or a stepwise release of H_2O and CO_2, between 108 and 280 °C, depending on the nature of the azolium and substituents. Formation of the free carbene upon heating a benzimidazolium-type hydrogen carbonate precursor has been evidenced for the first time by NMR spectroscopy.

As supported by DFT calculations, these precursors can serve as a genuine source of NHCs in solution at RT, allowing an easy transfer of the carbene fragment to an organic substrate (e.g. CS_2) and

to catalytically relevant transition metals (e.g. Pd, Au).

These [NHC(H)][HCO_3] salts can also efficiently serve as pre-catalysts both in metal-free molecular and macromolecular syntheses, without any particular precautions of storage. I*n situ* generation of free NHCs can indeed be readily achieved in solution from all types of precursors at room temperature, presumably by a simple solvation effect. Solvents favoring the NHC generation include mainly THF and toluene, presumably owing to a better solvation of both the transition state and the free NHC, relative to the charged NHC-CO_2 adduct and the [NHC(H)][HCO_3] salt precursor.

Transesterification reactions can be triggered from NHC-CO_2 adducts, either in THF or in toluene, while [NHC(H)][HCO_3] precursors exhibits a good catalytic efficiency in THF. Both categories of NHC precursors, including those of benzimidazole-type, proved efficient for the cyanosilylation reaction, giving excellent TOF at RT in THF. They also allow catalyzing the benzoin condensation, preferentially at 80 °C.

In the context of precision polymer synthesis, the principle of an organocatalyzed ROP of D,L-lactide and GTP of MMA triggered by NHC-CO_2 adducts and (benz)midazolium hydrogen carbonates is also established.

Overall, it has to be acknowledge that [NHC(H)][HCO_3] precursors showed a lower catalytic activity in all tested reactions, in comparison to NHC-CO_2 adducts analogues, with the exception of 1,3-dicyclohexylhydrogen carbonate. The catalytic activity of (pre)-catalysts is in the following line: [NHC(H)][HCO_3] < NHC-CO_2 adducts < free NHC.

A major advantage of these [NHC(H)][HCO_3] salts lies in their air-stability in the solid state, combined with an easy one-step access based on anion metathesis.

None of the NHC-CO_2 adducts and [NHC(H)][HCO_3] precursors evaluated in this study, exhibit a latent character, as the ROP of D,L-lactide and GTP of MMA can be performed at RT, generating free NHC *in situ*, presumably by a simple solvation effect.

We believe that the straightforward access to such precursors, which does not involve the generation of a free carbene at any point of their synthesis, coupled with their air and moisture stability both in the solid state and in solution, should provide a competitive alternative to masked NHCs at

large scale. This should open avenues for a practical use of these masked NHCs in organometallic chemistry, and in various NHC-catalyzed molecular and macromolecular reactions. The design of polymer-supported versions of these [NHC(H)][HCO_3] and their use in organocatalysis is also underway.

Experimental and supporting information

Materials. All reagents were purchased from Aldrich with purity ≥99% unless otherwise stated. For the synthesis of azolium hydrogen carbonates as well as for transfer reactions, solvents were used without any purification. All the other experiments were performed under an inert atmosphere using standard Schlenk techniques. Dry, oxygen-free solvents and reagents were employed. THF was distilled over Na/benzophenone, MeOH over Na, toluene and cyclohexane over polystyryllithium prior to use. DMSO was distilled over CaH_2 before use following a minimum of 4 h of reflux. TMSCN was used as received. Vinyl acetate (Aldrich, 95%) was purified by distillation over CaH_2 and stored at 0 °C. Benzaldehyde, benzyl alcohol and ε-caprolactone were purified by fractional distillation. Benzyl alcohol and ε-caprolactone were kept over molecular sieves. Benzophenone was recrystallized twice in dry warm cyclohexane and stored in the glovebox. D,L-lactide (99%, Alfa) was recrystallized three times in warm toluene (freshly distilled from polystyryllithium prior to use), dried under vacuum and kept in the glove box. MMA and MTS (Aldrich, 95%) were purified by distillation over CaH_2 and stored at 0 °C. Carbon disulfide was used as received. $[Pd(allyl)Cl]_2$ (Strem Chemicals) and $Au(Cl)SMe_2$ were used as received. TMC was a gift from Labso and was used as received.

Instrumentation. NMR spectra were recorded on Bruker AC-400 spectrometer (400 MHz) in appropriate deuterated solvents. Molar masses were determined by size exclusion chromatography (SEC) in THF as eluent (1 mL/min) and with trichlorobenzene as a flow marker at 25 °C, using both refractometric (RI) and UV detectors (Varian). Analyses were performed using a three-column set of TSK gel TOSOH (G4000, G3000, G2000 with pore sizes of 20, 75, and 200 Å respectively, connected in series) calibrated with polystyrene standards.

The data for crystal structure of compound **4a** have been collected on a Rigaku MM07 HF rotating anode at the Cu Kα wavelength. The system featured the micromax microfocus x-ray source with the RAPIDII image plate detector combined with the AFC-Kappa goniometer and the osmic mirrors Varimax® HF optics. The system was driven by the CrystalClear© suite which was also used for the unit cell determination, the integration, scaling and absorption correction of the raw data (Reference:

CrystalClear: An Integrated Program for the Collection and Processing of Area Detector Data, Rigaku Corporation, © 1997-2002). The crystal structures of compound **4a** were solved using the charge flipping algorithm implemented in the SUPERFLIP software.[126] All structures were refined using SHELXL-97 (G. M. Sheldrick, Universität Göttingen, 1997). Full-matrix least-squares refinement was performed on F^2 for all unique reflections, minimizing $w(Fo^2- Fc^2)2$, with anisotropic displacement parameters for non-hydrogen atoms. The positions of hydrogen atoms were located on a subsequent differential electron-density map. Hydrogen atoms were mostly spotted in Fourier differences but included in idealized positions and refined with a riding model, with Uiso constrained to 1.2 Ueq value of the parent atom (1.5 Ueq when CH3). The positions and isotropic displacement parameters of the remaining hydrogen atoms were refined freely.

MALDI-ToF spectrometry was performed using a Voyager-DE STR (Applied Biosystems) spectrometer equipped with a nitrogen laser (337 nm), a delay extraction and a reflector. The instrument is equipped with a pulsed N_2 laser (337 nm) and a time-delayed extracted ion source. Spectra were recorded in the positive-ion mode using the reflectron and with an accelerating voltage of 20 kV. Samples were dissolved in THF at 10 mg/mL. The IAA matrix (Indole acrylic acid) solution was prepared by dissolving 10 mg in 1 mL of THF. A MeOH solution of cationization agent (NaI, 10 mg/mL) was also prepared. The solutions were combined in a 10:1:1 volume ratio of matrix to sample to cationization agent. One to two microliters of the obtained solution was deposited onto the sample target and vacuum-dried. Mass spectra (ESI) were performed on a QStar Elite mass spectrometer (Applied Biosystems). The instrument is equipped with an ESI source and spectra were recorded in the positive mode. The electrospray needle was maintained at 4500 V and operated at room temperature. Samples were introduced by injection through a 10 µL sample loop into a 200 µL/min flow of methanol from the LC pump.

SDTQ50 (TA Instrument, USA) with alumina crucibles was used to perform TGA experiments. A constant heating rate of 10 °C/min and gas purging (N_2) at a flow rate of 100mL/min was used for all experiments. The amount of samples used for TGA was between 9 and 10 mg. The resulting T_{onset} and T_{deg} were determined from the step tangent. Thermogravimetric technique coupled with mass spectrometry (TGA–MS) using STA 409C/CD (NETZSCH, Germany) instrument coupled with a

Thermostar (BALZERS, Liechtenstein, max. detected mass: 300) was employed to analyze the thermal decomposition products *in situ*. The TGA–MS experiments were performed from room temperature to 650 °C with a heating rate of 5 °C/min in argon gas purging. The amount of samples was ca. 12 mg. The signal intensity of gaseous products during the heating was measured *in situ* using mass spectrum. Q100 equipped with a refrigerated cooling system (TA Instrument, USA) with aluminum sealed pans was used to perform DSC experiments. A constant heating/cooling rate of 10 °C/min and gas purging (N_2) at a flow rate of 100mL/min was used for all experiments.

Computational Details. All DFT calculations were performed by the group of Karinne Miqueu and Jean-Marc Sotiropoulos at IPREM (Université de Pau & des pays de l'Adour). Calculations were performed with the Gaussian 03 program[127] using the Density Functional Theory method.[128] The various structures were fully optimized at B3LYP level.[129-131] This functional is built with Becke's three parameter exchange functional[130] and the Lee-Yang-Parr correlation functional.[131] The 6-31G(d,p) basis set was used.[132] All atoms were augmented with a single set of polarization functions. The second derivatives were analytically calculated in order to determine if a minimum or a transition state (one negative eigenvalue) existed for the resulting geometry. All total energies and Gibbs free energies have been zero-point energy (ZPE) and temperature corrected using unscaled density functional frequencies. The connection between the transition states and the corresponding minima was confirmed by IRC calculations.[133-134]

Synthesis of 1,3-di-isopropyl-imidazolium hydrogen carbonate [IiPr(H)][HCO_3] 4a. A mixture of 1,3-di-isopropyl-imidazolium chloride (1 g, 5.30 mmol), synthesized using already described procedure,[135] and 1.05 eq. of $KHCO_3$ (550 mg, 5.56 mmol), was dried at 60 °C under vacuum for 12 h. 5 mL of dry MeOH was then added at RT and the resulting suspension was stirred for 48 h at RT. After filtration over celite to remove KCl, MeOH was evaporated under vacuum to yield a sticky solid. Trituration of the solid with acetone and filtration afforded 805 mg of [IiPr(H)][HCO_3] **4a** as a white powder, upon drying under vacuum (yield: 71%). Recrystallization of **4a** in a MeOH/Et_2O mixture at 5 °C, yielded colorless plate-like crystals, suitable for X-Ray diffraction analysis. In MeOD, **4a** was the only compound observed (Figures S1-S2), while in dmso-

d$_6$, **4a** equilibrates with IiPr-CO_2 **3a** in a 1:3 ratio, in favor of 4**a**. ^{1}H NMR (400 MHz, MeOD): δ = 1.62 (d, *J* = 6.8 Hz, 12H, C*H*$_3$*i*Pr), 4.73 (sept, *J* = 6.8 Hz, 2H, C*Hi*Pr), 7.76 (s, 2H, C*H*=C*H*). The N_2C*H* and *H*CO_3^- protons could not be observed due to their rapid exchange with the deuterated solvent on the NMR time scale. ^{13}C NMR (100 MHz, MeOD): δ = 23.0 (*C*H$_3$*i*Pr), 54.6 (*C*H*i*Pr), 121.9 (*C*H=*C*H), 134.4 (br, N_2C*H*), 161.3 (H*C*O_3^-). In DMSO-*d*$_6$, the major compound was **4a**: ^{1}H NMR (400 MHz, DMSO-*d*$_6$): δ = 1.48 (d, *J* = 6.8 Hz, 12H, C*H*$_3$*i*Pr), 4.66 (sept, *J* = 6.8 Hz, 2H, C*Hi*Pr), 7.98 (s, 2H, C*H*=C*H*), 9.71 (s, 1H, N_2C*H*). ^{13}C NMR (100 MHz, DMSO-*d*$_6$): δ = 23.3 (*C*H$_3$*i*Pr), 53.1 (*C*H*i*Pr), 121.5 (*C*H=*C*H), 135.1 (N_2*C*H), 156.8 (H*C*O_3^-). Minor compound **3a**: ^{1}H NMR (400 MHz, DMSO-*d*$_6$): δ = 1.40 (d, *J* = 6.8 Hz, 12H, C*H*$_3$*i*Pr), 5.27 (sept, *J* = 6.8 Hz, 2H, C*Hi*Pr), 7.86 (s, 2H, C*H*=C*H*). ^{13}C NMR (100 MHz, DMSO-*d*$_6$): δ = 23.3 (*C*H$_3$*i*Pr), 51.2 (*C*H*i*Pr), 118.4 (*C*H=*C*H), 143.4 (N_2*C*), 155.4 (CO_2). HRMS (MALDI+): m/z calculated for $C_9H_{17}N_2$ $[M]^+$ 153.1381, found 153.1384.

Crystal data and structure refinement for 4a. Performed by Brice Kaufmann at IECB, Bordeaux (see also Figures S3-S4).

Formula	C10 H18 N2 O3
M	214.26
Crystal system	monoclinic
Space group	P2(1)/c
a/Å	10.3706(17)
b/Å	9.6865(16)
c/Å	11.846(2)
β/o	93.873(13)
U/Å^3	1187.3(3)
T /K	123(2)
Z	4
ρ/g cm^{-1}	1.199
Shape and color	Colorless
size (mm)	0.2x0.1x0.1
λ/ Å	1.54178
μ/mm^{-1}	0.731
Unique data	2206
Absorption correction	None
unique data [*F*o > 4σ*F*o)]	1605
parameters/restraints	140
*R*1, *wR*2	0.0737, 0.1745

Synthesis of 1,3-di-mesityl-imidazolium hydrogen carbonate [IMes(H)][HCO_3] 4b. A similar procedure to that described for the preparation of **[IiPr(H)][HCO3] 4a** was used. **4b** was obtained as a white solid (yield: 76%). In MeOD, **4b** was the only compound observed (Figures S5-S6), while in dry DMSO-d_6, **4b** was only sparingly soluble. ^{1}H NMR (400 MHz, MeOD): δ = 2.20 (s, 12H, o-CH_3Mes), 2.40 (s, 6H, p-CH_3Mes), 7.20 (s, 4H, m-C*H*Mes), 8.06 (s, 2H, C*H*=C*H*). The N_2C*H* and *H*CO_3^- protons could not be observed due to their rapid exchange with the deuterated solvent on the NMR time scale. ^{13}C NMR (100 MHz, MeOD): δ = 17.6, 21.3, 126.5, 131.0, 132.4, 135.8, 139.8, 143.0, 161.5.

Synthesis of 1,3-di-mesityl-imidazolinium hydrogen carbonate [SIMes(H)][HCO_3] 4b'. A similar procedure to that described for the preparation of **[IiPr(H)][HCO3] 4a** was used. **4b'** was obtained as a white solid (yield: 88%). In MeOD, **4b'** was the only compound observed (Figures S7-S8), while in DMSO-d_6, **4b'** equilibrates with **SIMes-CO_2 3b'** in a 1:1.5 ratio, in favor of **4b'**. ^{1}H NMR (400 MHz, MeOD): δ = 2.33 (s, 6H, p-CH_3Mes), 2.41 (s, 12H, o-CH_3Mes), 4.52 (s, 4H, CH_2), 7.10 (s, 4H, m-C*H*Mes). The N2C*H* and *H*CO_3^- protons could not be observed due to their rapid exchange with the deuterated solvent on the NMR time scale. ^{13}C NMR (100 MHz, MeOD): δ = 17.9 (o-*C*H_3Mes), 21.2 (p-*C*H_3Mes), 52.6 (CH_2), 131.1 (m-*C*HMes), 132.1 (p-C_qMes), 136.7 (o-C_qMes), 142.1 (C_{ipso}Mes), 161.5 (N_2*C*H), 162.0 (br, HCO_3^-). In DMSO-d_6, the ^{1}H and ^{13}C NMR data obtained for the major compound **3b'** matched those reported in the literature.[48] Minor compound **4b'**: ^{1}H NMR (400 MHz, DMSO-d_6): δ = 2.27 (s, 6H, p-CH_3Mes), 2.33 (s, 12H, o-CH_3Mes), 4.44 (s, 4H, CH_2), 7.08 (s, 4H, m-C*H*Mes), 9.06 (s, 1H, N_2C*H*). ^{13}C NMR (100 MHz, DMSO-d_6): δ = 17.1 (o-*C*H_3Mes), 20.6 (p-*C*H_3Mes), 51.0 (CH_2), 129.5 (m-*C*HMes), 130.9 (C_qMes), 135.4 (C_qMes), 139.7 (C_qMes), 156.3 (N_2*C*H), 160.3 (HCO_3^-).

Synthesis of 1-methyl,3-ethyl-imidazolinium hydrogen carbonate [MeEt(H)][HCO_3] 4c and 1,3-di-dodecyl-imidazolinium hydrogen carbonate [Dod(H)][HCO_3] 4d. 1,3-di-dodecyl-imidazolium bromide **1d** (500 mg, 1.03 mmol), synthesized using already described procedure,[135] and 1-methyl,3-ethyl-imidazolium chloride **1c** (500 mg, 3.41 mmol), purchased from Alfa Aesar were dried under vacuum for several hours and then dissolved in 5mL MeOH. 1.02 eq. of dry $KHCO_3$ (348

mg, 3.48 mmol with **1c**, 105 mg, 1.05 mmol with **1d**) were added. The solution was stirred under inert atmosphere for 2 days to allow complete precipitation of KBr or KCl. After filtration of the solutions over celite to remove the mentioned salt, MeOH was evaporated under vacuum. The powders were washed with acetone and dried under vacuum (yield: **4c**: 60%, **4d**: 65%).

In MeOD (Figures S9-10), **4c** was the only compound observed, while in DMSO-d_6, **4c** equilibrates with **3c** in a 1:2.5 ratio, in favor of **3c**. ^{1}H NMR (400 MHz, MeOD): δ = 1.62 (t, *J* = 7.2 Hz, 3H, NCH_2CH_3), 3.93 (s, 3H, NCH_3), 4.26 (q, *J* = 7.2 Hz, 2H, NCH_2CH_3), 7.57 (s, 1H, CH=CH), 7.64 (s, 1H, CH=CH). The N_2CH and HCO_3^- protons could not be observed, while integral of CH=CH was lowered both due to their rapid exchange with the deuterated solvent on the NMR time scale. ^{13}C NMR (100 MHz, MeOD): δ = 15.6, 36.4, 46.0, 123.2, 124.8, 137.5, 161.4. HRMS (MALDI+): *m/z* calculated for $C_9H_{17}N_2$ $[M]^+$ 111.0916, found 111.0913.

4d was the only compound observed in MeOD and DMSO-d_6 (Figures S11-12). ^{1}H NMR (400 MHz, DMSO- d_6): δ = 0.85 (t, *J* = 6.6 Hz, 6H, CH_2CH_3), 1.23 (br, 36H, $(CH_2)_9CH3$), 1.78 (quin, *J* = 6.8 Hz, 4H, NCH_2CH_2), 4.16 (t, *J* = 7.2 Hz, 4H, NCH_2CH_2), 7.82 (s, 2H, CH=CH), 9.27 (s, 1H, NCHN). ^{13}C NMR (100 MHz, DMSO- d_6): δ = 13.9, 22.1, 25.4, 28.3, 28.7, 28.8, 28.9, 29.0, 29.0, 29.2, 31.3, 48.8, 122.5, 136.0, 154.0. HRMS (MALDI+): *m/z* calculated for $C_{27}H_{53}N_2$ $[M]^+$ 405.4203, found 405.4200.

Synthesis of benzimidazolium hydrogen carbonates. 1,3-Di-*tert*butyl-benzimidazolium chloride **1e** (500 mg, 1.71 mmol), 1,3-di-cyclohexyl-benzimidazolium bromide **1f** (500 mg, 1.57 mmol), purchased from Strem Chemicals were dried under vacuum for several hours and then dissolved in 5 mL MeOH. 1.02 eq. of dry $KHCO_3$ (174 mg, 1.74 mmol and 160 mg, 1.60 mmol respectively) were added. The solution was stirred under inert atmosphere for 2 days to allow complete precipitation of KBr or KCl. After filtration of the solutions over celite to remove the mentioned salt, MeOH was evaporated under vacuum. The powders were washed with acetone and dried under vacuum (yield 40 and 80% respectively). The obtained products were soluble in MeOD, DMSO and CD_2Cl_2, a single population of signals being observed whatever the analysis solvent.

4e (Figures S13-S14): ^{1}H NMR (400 MHz, CD_2Cl_2): δ = 1.97 (s, 18H, NC(CH_3)$_3$), 7.62 (dd, *J* = 3.2 Hz, 6.4 Hz, 2H, H_{benz}), 8.00 (dd, *J* = 3.2 Hz, 6.8 Hz, 2H, H_{benz}), 9.82 (s, 1H, N_2CH). The HCO_3^- proton could not be observed due to their rapid exchange with the deuterated solvent on the NMR time scale. ^{13}C NMR (100 MHz, CD_2Cl_2): δ = 29.2, 62.3, 116.8, 126.0, 132.0, 140.6, 160.1. HRMS (MALDI+): *m/z* calculated for $C_{15}H_{23}N_2$ $[M]^+$ 251.1859, found 231.1855.

4f (Figures S15-S16): ^{1}H NMR (400 MHz, CD_2Cl_2): δ = 1.27 (m, 2H, $CH_{2cyclohexyl}$), δ = 1.52 (m, 4H, $CH_{2cyclohexyl}$), δ = 1.74 (m, 2H, $CH_{2cyclohexyl}$), δ = 1.92 (m, 8H, $CH_{2cyclohexyl}$), δ = 2.17 (m, 4H, $CH_{2cyclohexyl}$), δ = 4.74 (m, 2H, $NCH_{cyclohexyl}$), 7.68 (dd, *J* = 2.6 Hz, 6.6 Hz, 2H, H_{benz}), 8.19 (dd, *J* = 3.2 Hz, 7.2 Hz, 2H, H_{benz}), 10.00 (s, 1H, N_2CH). The HCO_3^- proton could not be observed due to their rapid exchange with the deuterated solvent on the NMR time scale. ^{13}C NMR (100 MHz, CD_2Cl_2): δ = 24.6, 24.8, 31.8, 48.6, 50.8, 57.0, 114.0, 126.4, 130.6, 139.3, 155.6. HRMS (MALDI+): *m/z* calculated for $C_{19}H_{27}N_2$ $[M]^+$ 283.2168, found 283.2177.

Synthesis of imidazolium-2-carboxylates. 1,3-Di-isopropyl-imidazolium bromide (500 mg, 2.14 mmol), synthesized using already described procedure,[135] 1,3-di-mesityl-imidazolium chloride (50 mg, 0.147 mmol), purchased from Alfa Aesar, were first deprotonated by exposure to 1 eq. of KHMDS or 1 eq. of NaH/cat. *t*BuOK in dry THF. After being stirred overnight, solutions were filtered under inert conditions to remove metallic salts. CO_2 (N-45, Air Liquide) further purified by passing threw a Click-on inline Super Clean Purifier (SGT) before use was then introduced into the flask. White precipitates were observed after few seconds. The solutions were further exposed to CO_2 (1 atm) for 20 minutes before being filtrated in the glovebox. The white powders were washed with dry Et_2O and dried under vacuum affording clean 1,3-di-isopropyl-imidazolium-2-carboxylate **3a** (yield 70%), 1,3-di-mesityl-imidazolium-2-carboxylate **3b** (yield 60%). NMR spectra were in agreement with those already reported in the literature (Figures S19-S22).[39]

Synthesis of IMes-CS_2 5b. CS_2 (10 eq, 2.7 mmol) was added to a THF suspension (1.5 mL) of **4b** (100 mg, 0.27 mmol) at room temperature and the reaction mixture was stirred at 60 °C in a capped vial for 2 h After removing of all the volatiles under vacuum, 98 mg of purple-brownish solid were

isolated (yield 96%). Data from ^{1}H NMR analysis of **5b** in dmso-d_6 were found in good agreement with those reported in the literature.[38]

Synthesis of SIMes-CS_2 5b'. A similar procedure to that described for the synthesis of **4b'** was used, yielding 95 mg of **5b'** as an orange powder (yield 92%), upon removing of the volatiles. ^{1}H NMR data of **5b'** in $CDCl_3$ were found in good agreement with those reported in the literature.[38]

Synthesis of IiPr-Pd(allyl)Cl 6a. 21.3 mg ($5.8\ 10^{-5}$ mol) of $[Pd(allyl)Cl]_2$, 29.4 mg ($1.4\ 10^{-4}$ mol) of compound **4a** and 2 mL of THF were put in a capped vial (air atmosphere). After 1 d of stirring at RT, ^{1}H NMR analysis in $CDCl_3$ attested of the complete disappearance of signals corresponding to $[Pd(allyl)Cl]_2$. The solution was filtered over silica to remove residual compound **4a** and THF was finally removed under vacuum. The resulting pale yellow powder was further washed with Et_2O (yield 87%). ^{1}H NMR (400 MHz, $CDCl_3$): δ = 1.40 (pseudo t, *J* = 7.3 Hz, 12H, C*H*$_3$*i*Pr), 2.35 (d, *J* = 12.1 Hz, 1H, C*H*$_2$), 3.28 (d, *J* = 13.6 Hz, 1H, C*H*$_2$), 3.34 (td, *J* = 2.0, 7.2 Hz, 1H, C*H*$_2$), 4.24 (dd, *J* = 2.0, 7.2 Hz, 1H, C*H*$_2$), 4.98 (br, 2H, C*H*i*Pr*), 5.30 (m, 1H, C*H*$_{allyl}$), 6.94 (s, 2H, C*H*=C*H*). ^{13}C NMR (100 MHz, $CDCl_3$): δ = 23.5 (*C*H$_3$*i*Pr), 23.6 (*C*H$_3$*i*Pr), 47.2 (*C*H$_2$), 52.8 (*C*H*i*Pr), 73.0 (*C*H$_2$), 114.6 (*C*H$_{allyl}$), 116.9 (*C*H=*C*H), 177.2 (C$_{carbene}$).

Synthesis of SIMes-Pd(allyl)Cl 6b. 5 mg ($1.4\ 10^{-5}$ mol) of $[Pd(allyl)Cl]_2$, 12.1 mg ($3.3\ 10^{-5}$ mol) of compound **4b** and 0.5 mL of THF were put in a capped vial (air atmosphere). After 10 min stirring at RT, ^{1}H NMR analysis in $CDCl_3$ attested of the complete disappearance of $[Pd(allyl)Cl]_2$ peaks. The solution was filtered over silica to remove residual compound **2b** and THF was finally removed under vacuum. The resulting pale yellow powder was further washed with Et_2O. NMR spectra in $CDCl_3$ were in agreement with those reported in the literature (yield 95%).[95-96]

Synthesis of IMes-Pd(allyl)Cl 6b'. A similar procedure to compound **6b** was used: 10 min reaction between 5 mg ($1.4\ 10^{-5}$ mol) of $[Pd(allyl)Cl]_2$ and 11.7 mg ($3.3\ 10^{-5}$ mol) of compound **4b'** in THF followed by the aforementioned purification procedures led to compound **6b'** (yield 95%). NMR spectra were in agreement with those reported in the literature.[96]

Synthesis of IiPr-AuCl 7a. 11.4 mg ($3.9\ 10^{-5}$ mol) of $Au(SMe)_2Cl$, 9.8 mg ($4.7\ 10^{-5}$ mol) of compound **4a** and 0.7 mL of THF were put in a capped vial (air atmosphere). After 1 h of stirring at 50

°C, ^{1}H NMR analysis in $CDCl_3$ attested of the consumption of 1 eq. of compound **4a** compared to $Au(SMe)_2Cl$. The solution was filtered over silica to remove residual compound **4a** and THF was finally removed under vacuum (yield 95%). The resulting off-white powder was analyzed by NMR in $CDCl_3$. Spectra were in agreement with those reported in the literature.[97]

Synthesis of SIMes-AuCl 7b. In a similar fashion, 1 h reaction at RT between 11.4 mg ($3.9\ 10^{-5}$ mol) of $Au(SMe)_2Cl$ and 17.2 mg ($4.7\ 10^{-5}$ mol) of compound **4b** in THF followed by the aforementioned purification procedures led to compound **7b** (yield 82%). NMR spectra in $CDCl_3$ were in agreement with those reported in the literature.[98]

Synthesis of IMes-AuCl 7b'. In a similar fashion, 1 h reaction at RT between 11.4 mg ($3.9\ 10^{-5}$ mol) of $Au(SMe)_2Cl$ and 16.7 mg ($4.7\ 10^{-5}$ mol) of compound **4b'** in THF followed by the aforementioned purification procedures led to compound **7b'** (yield 89%). NMR spectra were in agreement with those reported in the literature.[98]

All catalytic tests were carried out under a dry and inert atmosphere using Schlenk equipments. To provide exactly similar conditions for experiments performed at RT and at 80 °C, one reaction medium was first prepared mixing catalyst and reagents. This solution was then equally separated into two different flasks, one being kept at RT and the other being transferred in an 80 °C preset-oil bath. All reactions were stopped by contact with air and small samples were immediately withdrawn for conversion analysis by NMR in $CDCl_3$.

Cyanosilylation (Table 3). In a typical reaction, 0.5 mL (5 mmol) of benzaldehyde and 0.75 mL of TMSCN (6 mmol) were mixed with 5 mL of THF. 23.5 µL (1 µmol) of a 42.5 mM solution (THF:DMSO=5:1) of **3a** was finally added. After few seconds homogenization at RT, the solution was divided as described above. Conversion was calculated by ^{1}H NMR in $CDCl_3$ comparing the integral value of the aldehyde signal of benzaldehyde (δ=10 ppm) to that of the -C*H*- cyanide product (δ=5.5 ppm).

Benzoin condensation (Table 4). In a typical reaction, 31.5 mg (150 µmol) of **4a** and molecular sieves were introduced into a schlenk tube. The powder was submitted to 30 min vacuum and finally three Ar/vacuum cycles. 5 mL of THF and then 0.5 mL (5 mmol) of benzaldehyde were added. After

few seconds at RT, complete solubilization of the catalyst was observed and the solution was divided as described above. Conversion was calculated by ^{1}H NMR in $CDCl_3$ comparing the integral value of the aldehyde signal of benzaldehyde (δ=10 ppm) with that of the -C*H*- benzoin signal (δ=6 ppm).

Transesterification (Table 5). In a typical reaction, 0.5 mL benzyl alcohol (5 mmol) and 0.55 mL (6 mmol) of vinyl acetate were mixed in 5 mL THF. 4.5 mg (25 µmol) of pre-catalyst **3a** was finally added. After few seconds at RT, complete solubilization of the catalyst was observed and the solution was divided as described above. After 10 minutes, conversion was calculated by ^{1}H NMR in $CDCl_3$ comparing the integral value of the -CH_2- benzyl alcohol signal (δ=4.5 ppm) to that of the -CH_2- benzyl acetate signal (δ=5 ppm).

Polymerization of DL-LA. (Table 6). In a typical polymerization, 380 mg (2.64 mmol) of lactide were dissolved in 5 mL of THF, 10 µL (96.8 µmol) of benzyl alcohol were then added. 67 µL (2.9 µmol) of a 42.5 mM solution (THF:DMSO=5:1) of **3a** were finally introduced. After few seconds homogenization at RT, the solution was divided as described above. After 1 h at RT or 80 °C, the conversion was calculated by ^{1}H NMR in $CDCl_3$ comparing integral value of the peak of the polymer (broad peak δ around 5.1 ppm) to that of the monomer signal (quartet δ=5.0 ppm). Molar masses and dispersities were obtained by SEC analysis in THF.

Polymerization of TMC and ε-caprolactone. (see Table 7). In a typical polymerization, 3.4 mg (17.4 µmol) of **4a** and molecular sieves were introduced into a schlenk tube. The powder was submitted to 30 min vacuum and finally three Ar/vacuum cycles. 5 mL of THF and then 500 mg (4.90 mmol) of TMC and 18 µL (174 µmol) of benzyl alcohol were added. After 1 h at RT, the conversion was calculated by ^{1}H NMR in $CDCl_3$ comparing integral value of the peak of the polymer (-OC*H*$_2$-, δ = 4.21 ppm) to that of the monomer signal (OC*H*$_2$-, δ=4.04 ppm). Molar masses and dispersities were obtained by SEC analysis in THF.

GTP of MMA. (see Table 8). In a typical polymerization, 1 mL (9.36 mmol) of MMA was mixed with 5 mL of THF, 50 µL (246 µmol) of MTS were then added. 2.4 mg (12.3 µmol) of **3a** were finally introduced. After few seconds at RT, complete solubilization of the catalyst was observed and the solution was divided as described above. After 1 h at RT or 80 °C, the conversion was calculated by

^{1}H NMR in $CDCl_3$ comparing integral value of the peak of the polymer (-CCH_3 peaks δ=0.8, 1.0 and 1.2 ppm) to that of the monomer signal (CH_2=CH δ=5.5 or 6.0 ppm). Molar masses and dispersities were obtained by SEC analysis in THF.

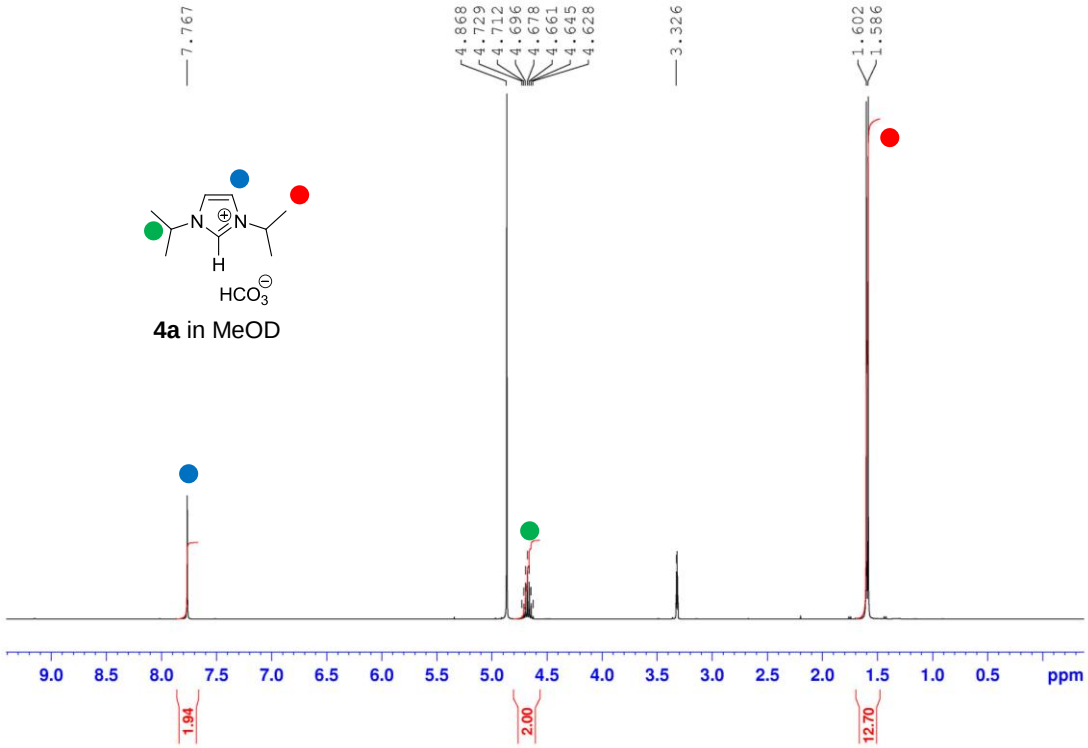

Figure S1. ^{1}H NMR spectrum of compound **4a** in MeOD.

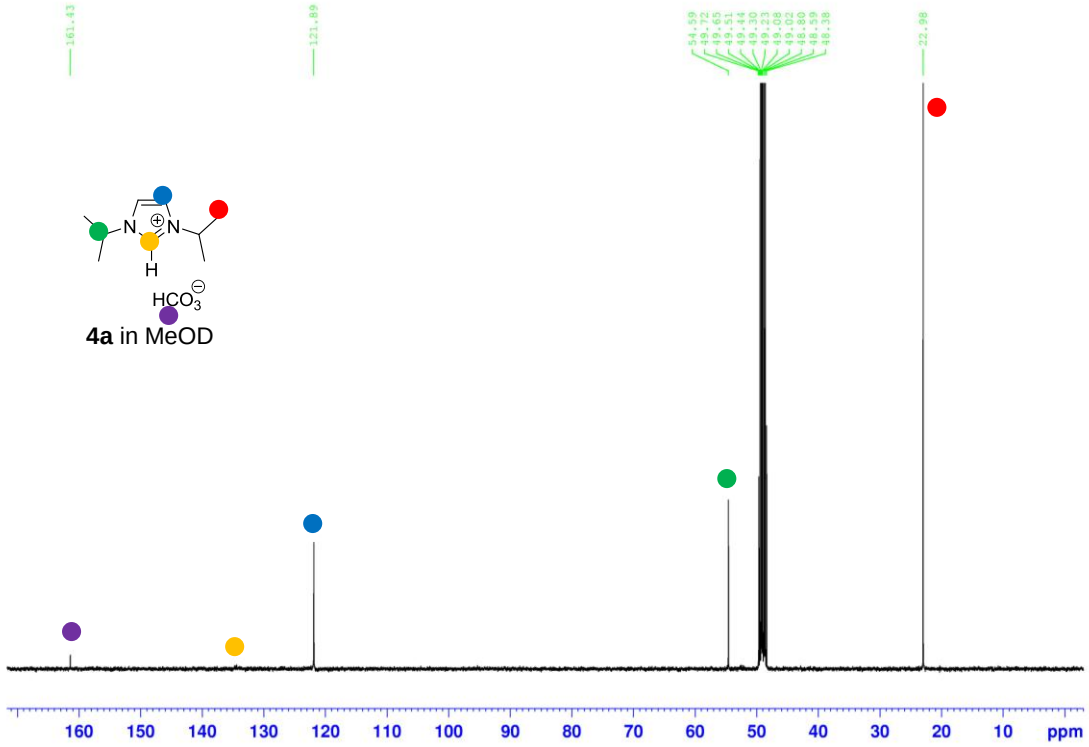

Figure S2. ^{13}C NMR spectrum of compound **4a** in MeOD.

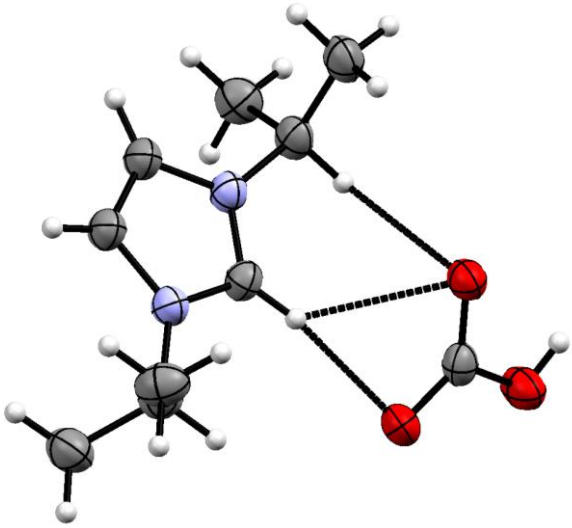

Figure S3. Molecular structure of **4a** (with short contacts in dashed line) with atoms depicted as thermal ellipsoids drawn at the 50% probability level.

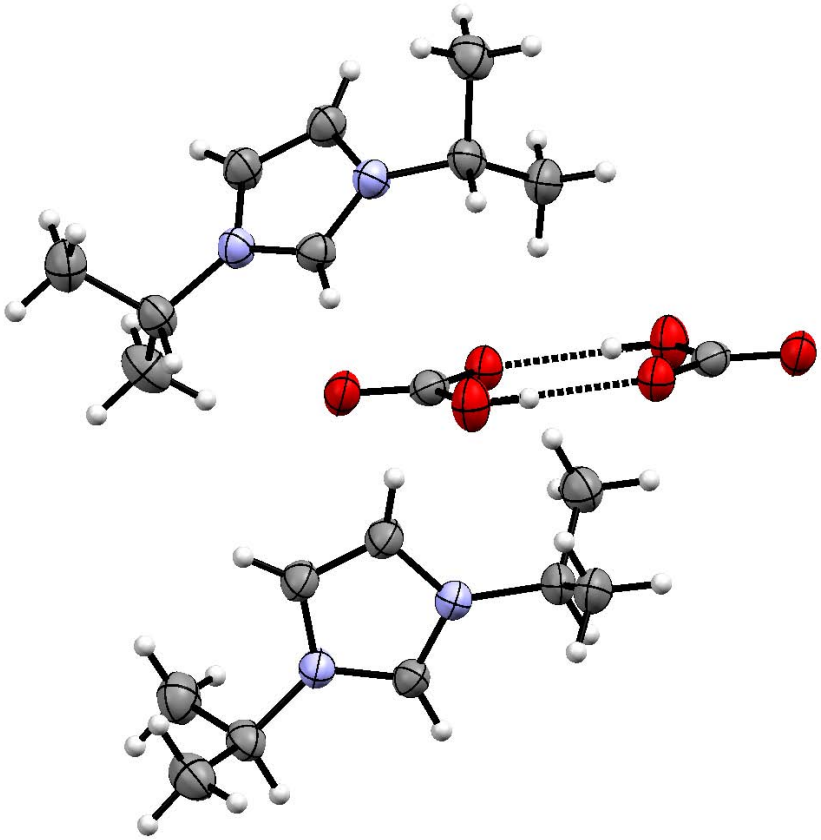

Figure S4. Molecular structure of **4a** (showing a dimer) with atoms depicted as thermal ellipsoids drawn at the 50% probability level.

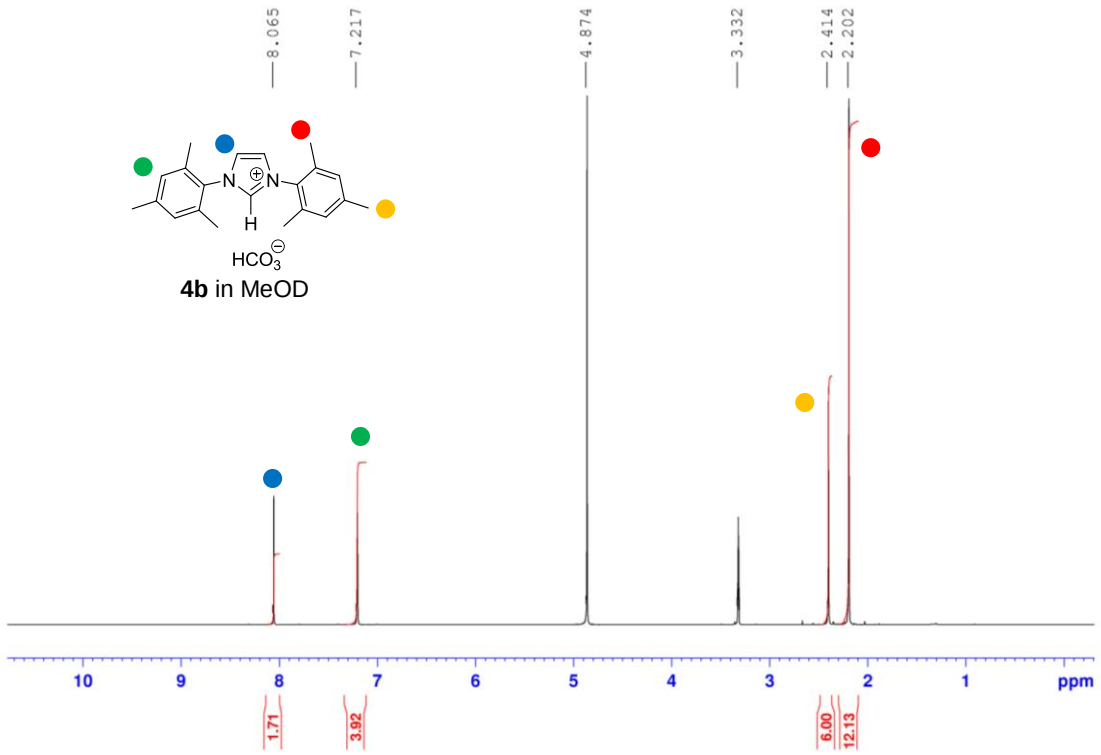

Figure S5. ^{1}H NMR spectrum of compound **4b** in MeOD.

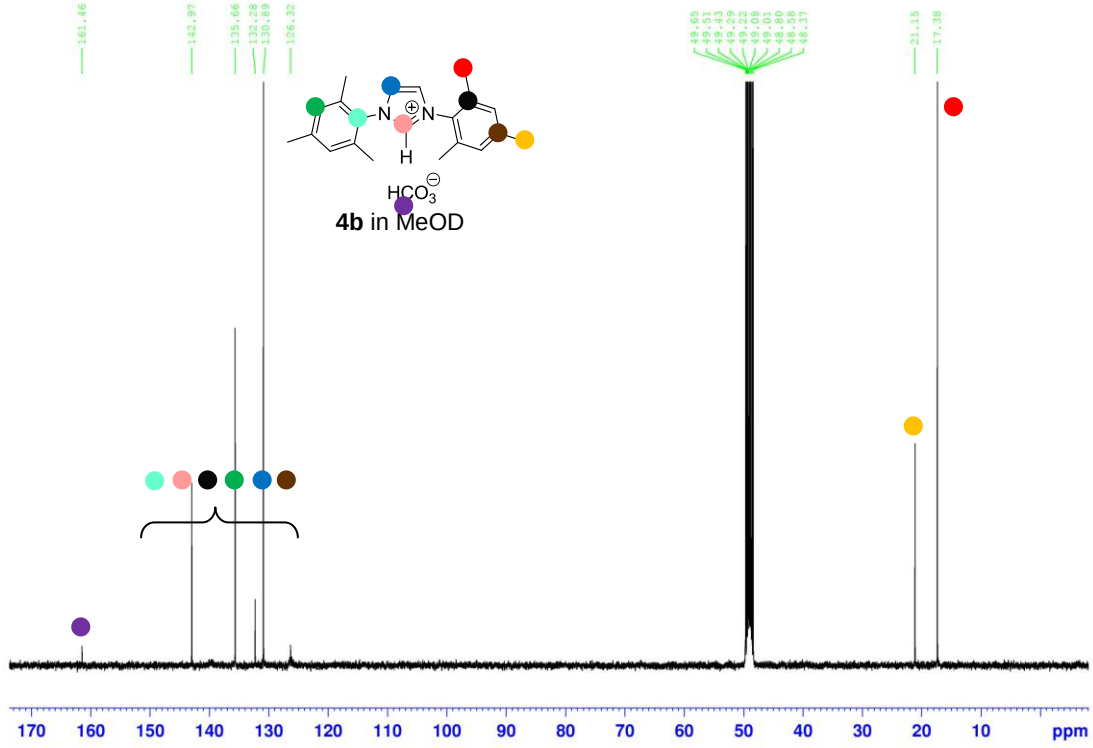

Figure S6. ^{13}C NMR spectrum of compound **4b** in MeOD.

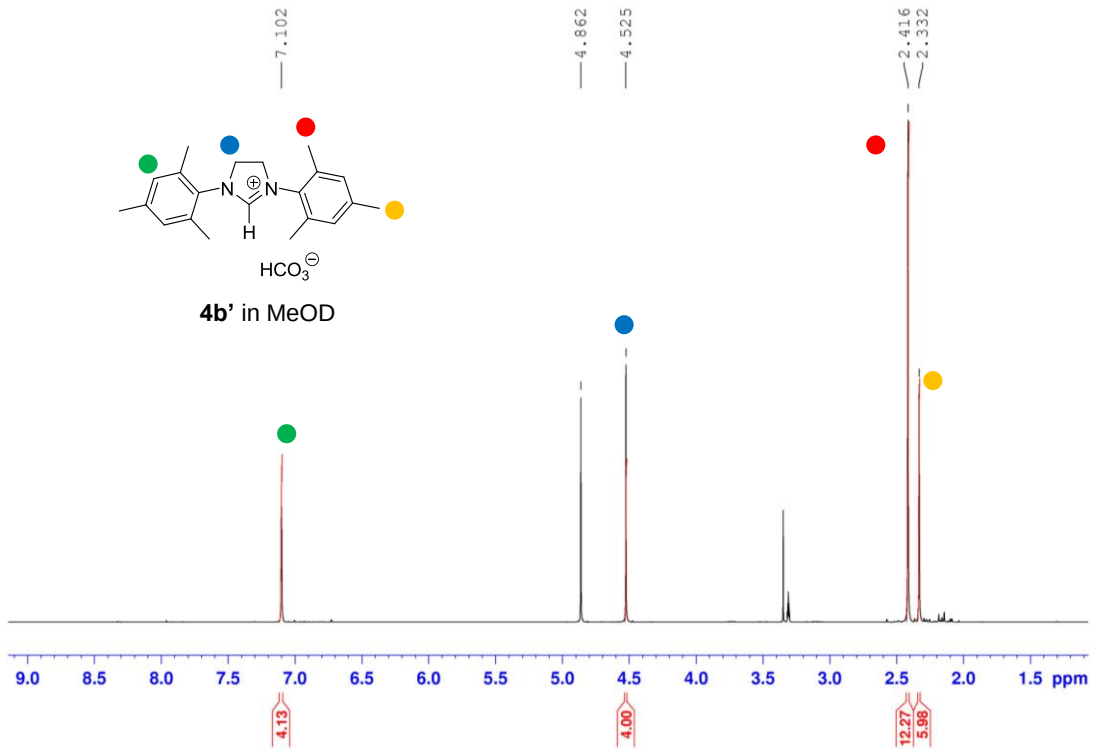

Figure S7. ^{1}H NMR spectrum of compound **4b'** in MeOD.

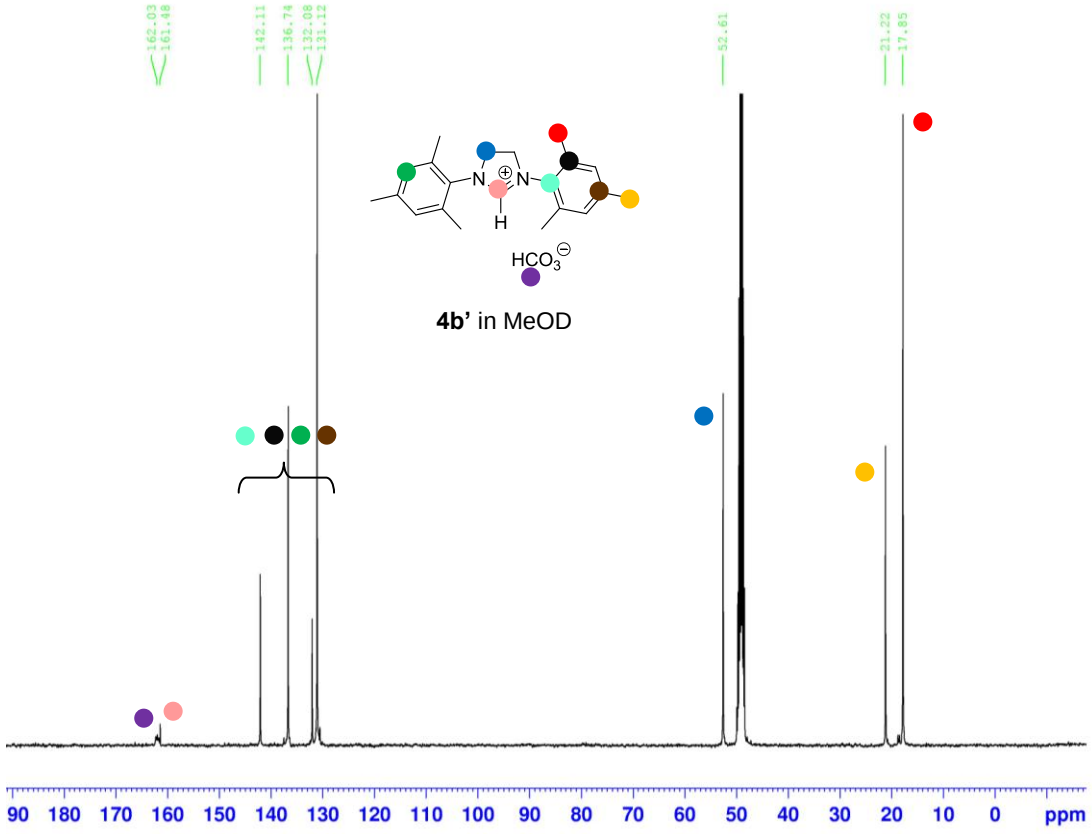

Figure S8. ^{13}C NMR spectrum of compound **4b'** in MeOD.

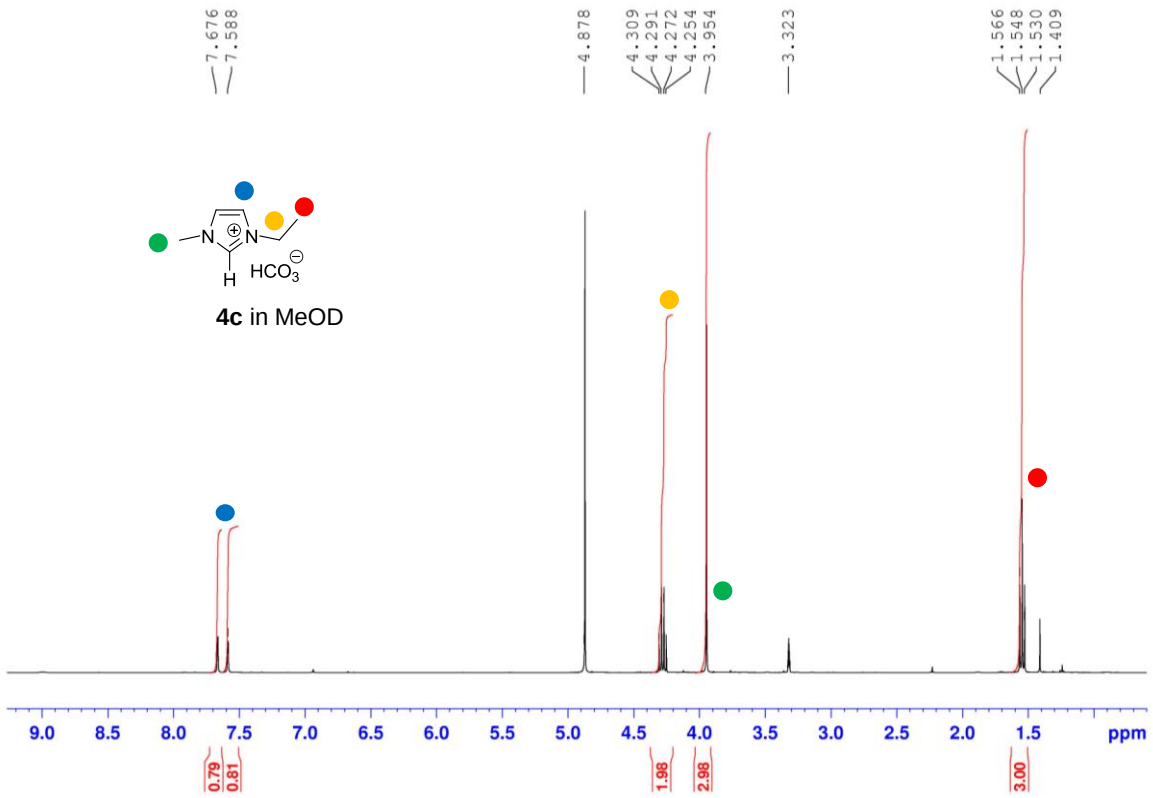

Figure S9. [1]H NMR spectrum of compound **4c** in MeOD.

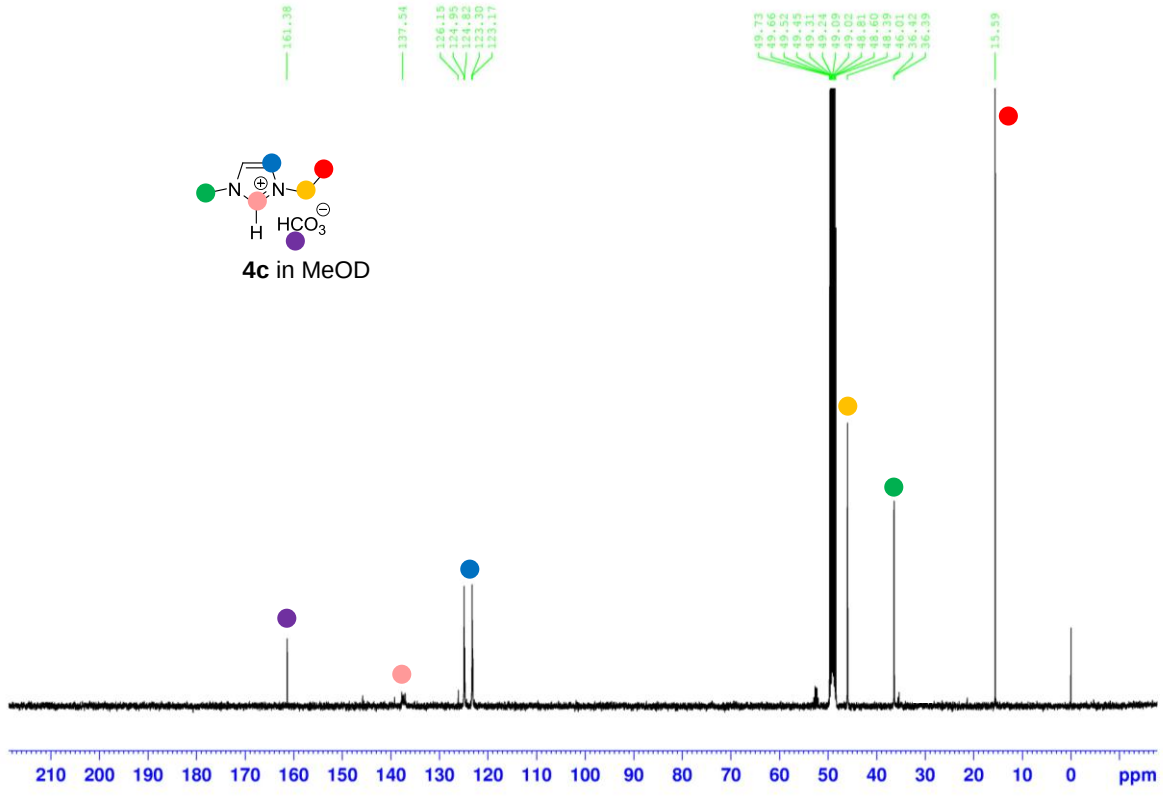

Figure S10. [13]C NMR spectrum of compound **4c** in MeOD.

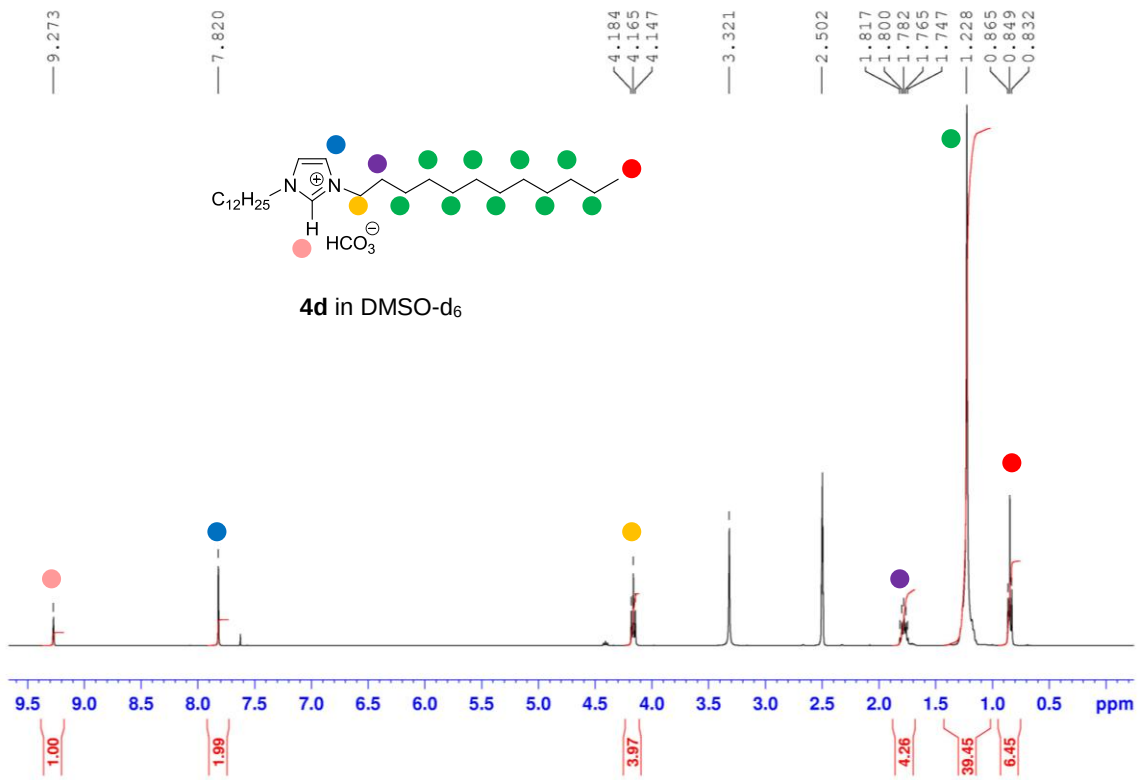

Figure S11. ^{1}H NMR spectrum of compound **4d** DMSO-d_6.

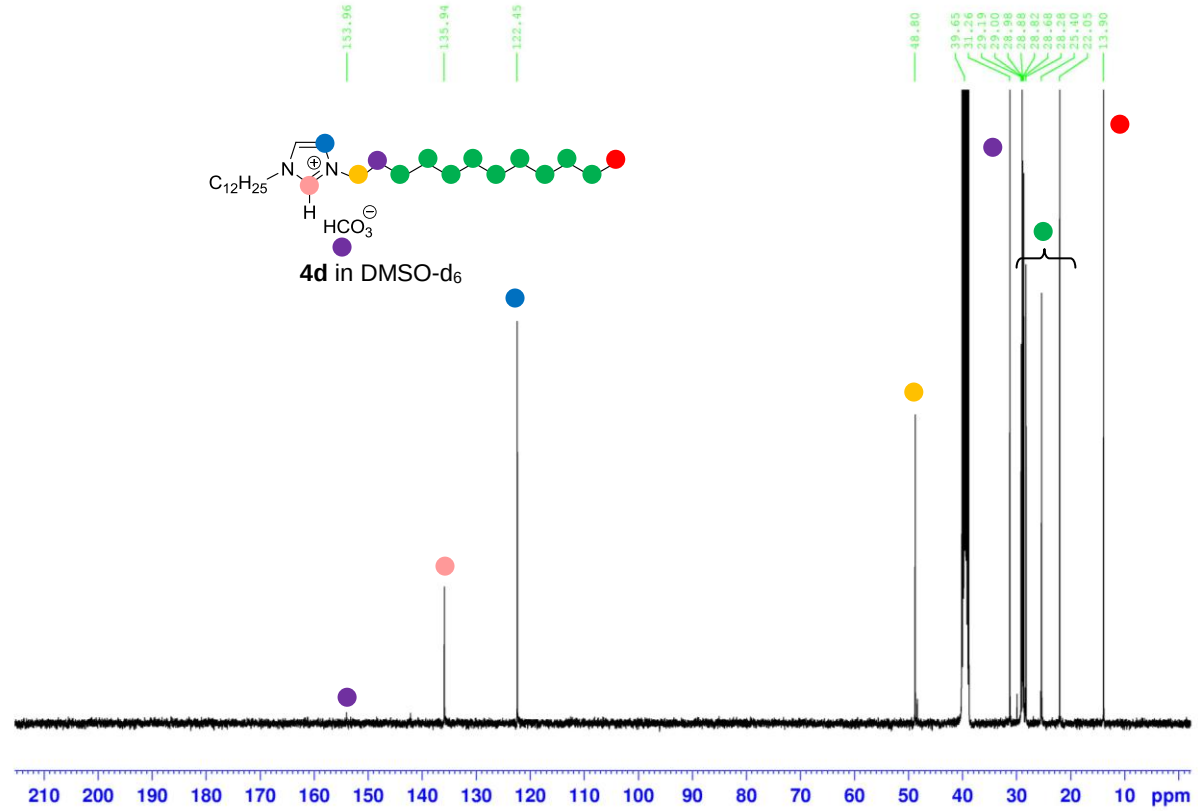

Figure S12. ^{13}C NMR spectrum of compound **4d** in DMSO-d_6.

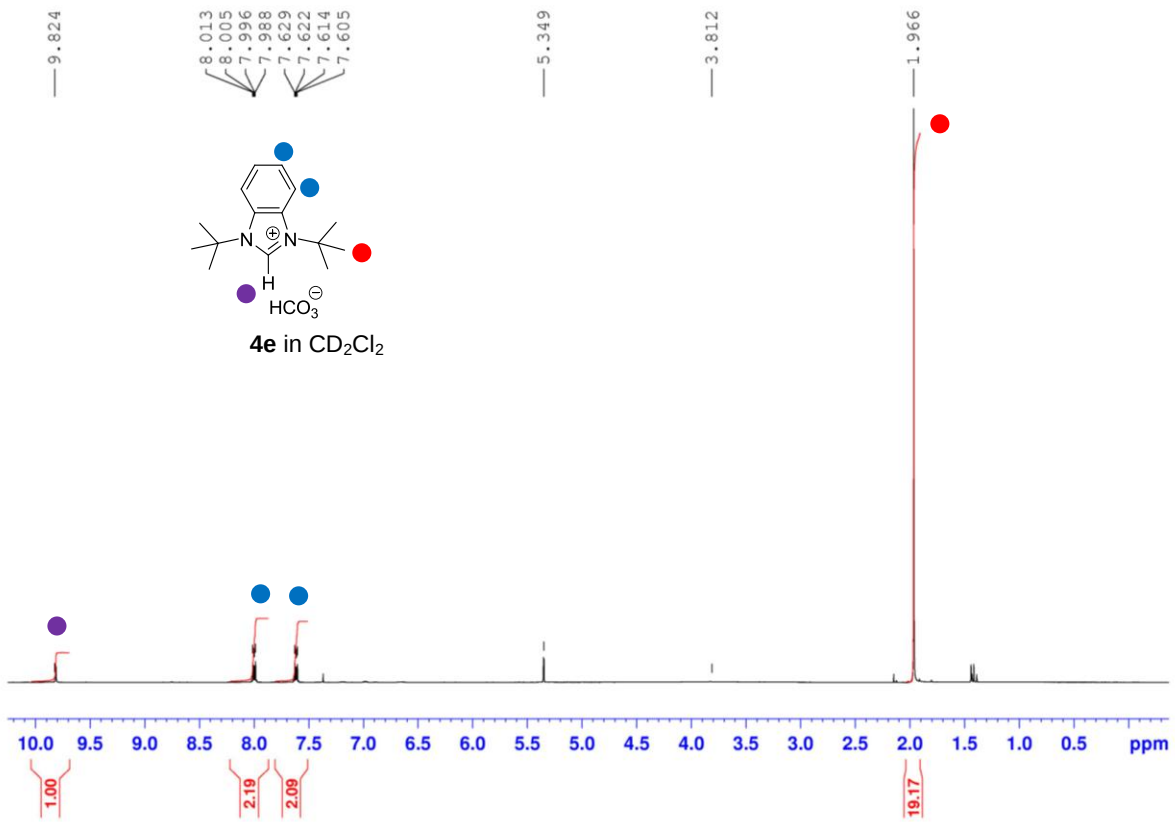

Figure S13. ^{1}H NMR spectrum of compound 4e in CD_2Cl_2.

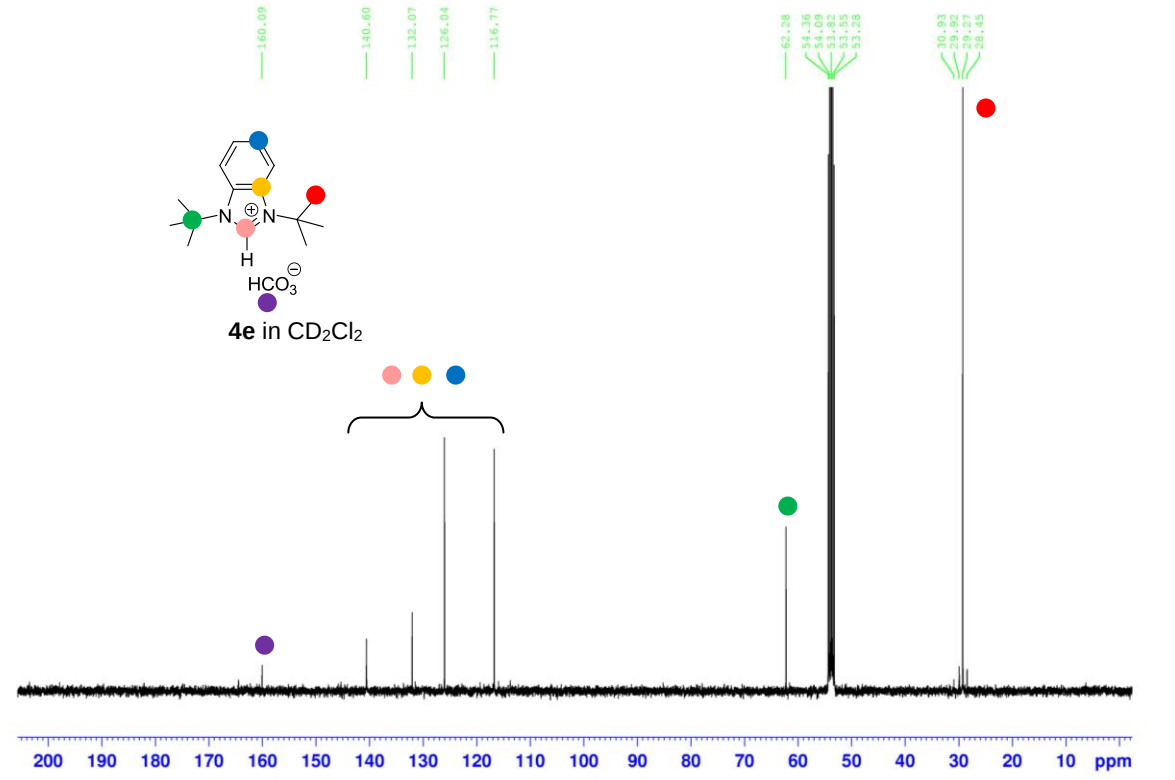

Figure S14. ^{13}C NMR spectrum of compound 4e in CD_2Cl_2.

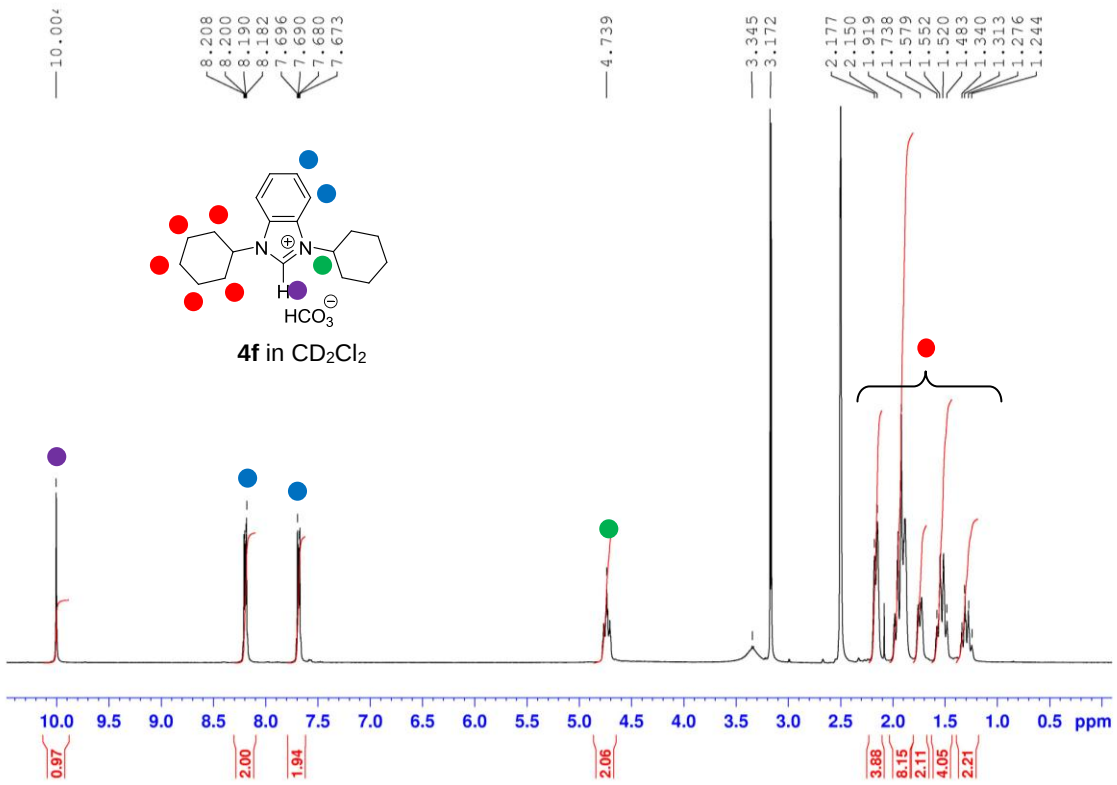

Figure S15. ^{1}H NMR spectrum of compound **4f** in CD_2Cl_2.

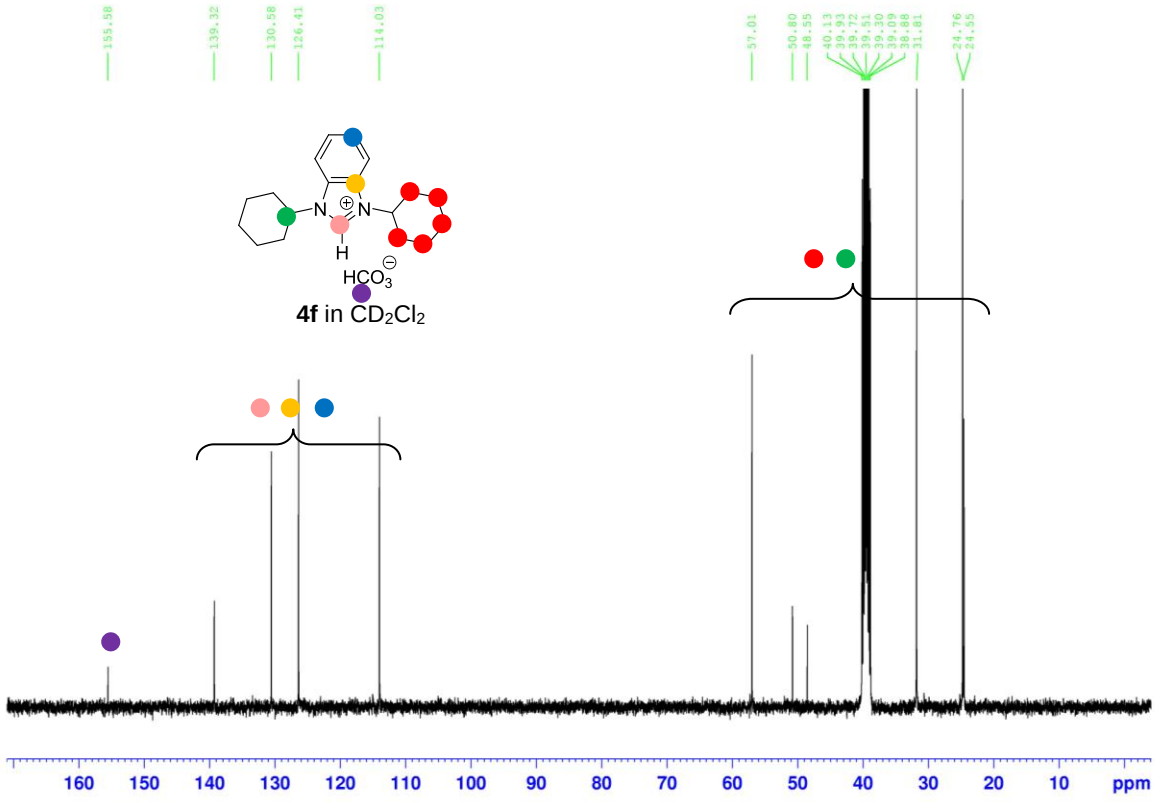

Figure S16. ^{13}C NMR spectrum of compound **4f** in CD_2Cl_2.

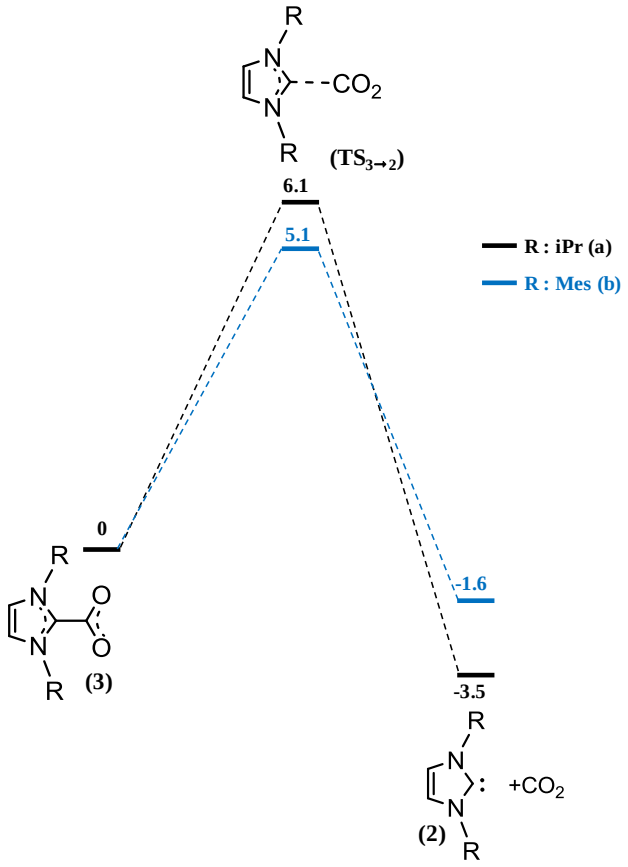

Figure S17. Energy profile computed at the B3LYP/6-31G** level (free energies G at 25 °C including ZPE correction in kcal/mol) for the rearrangement **3**→**2** + CO_2, noted **3**→**2** in the text.

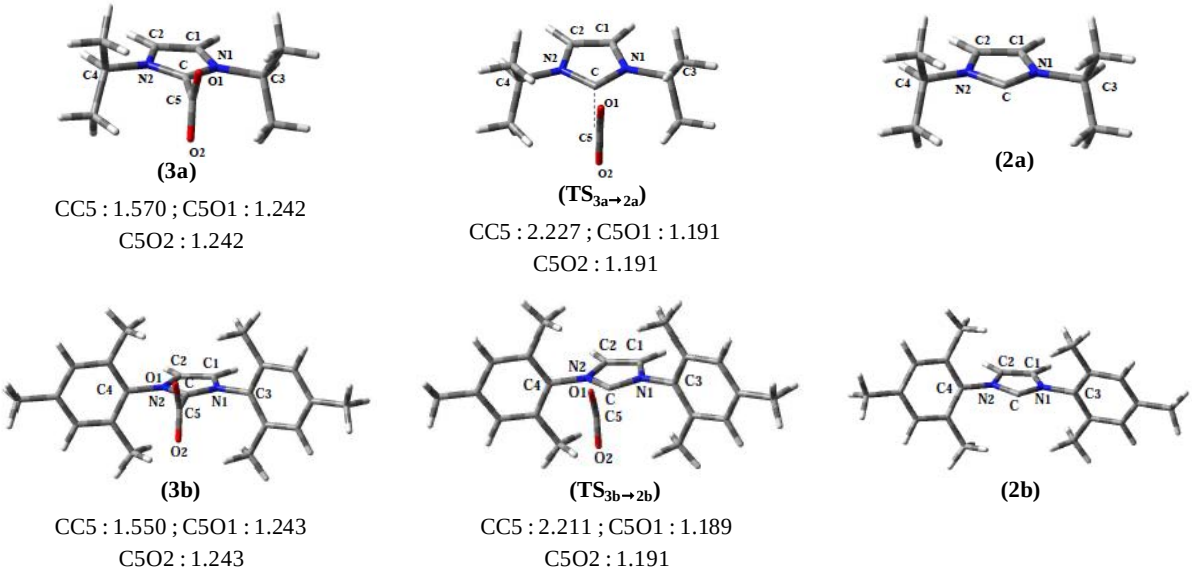

Figure S18. Geometrical structures and main bond lengths for all the compounds involved in the **3**→**2** rearrangement (distances in Å).

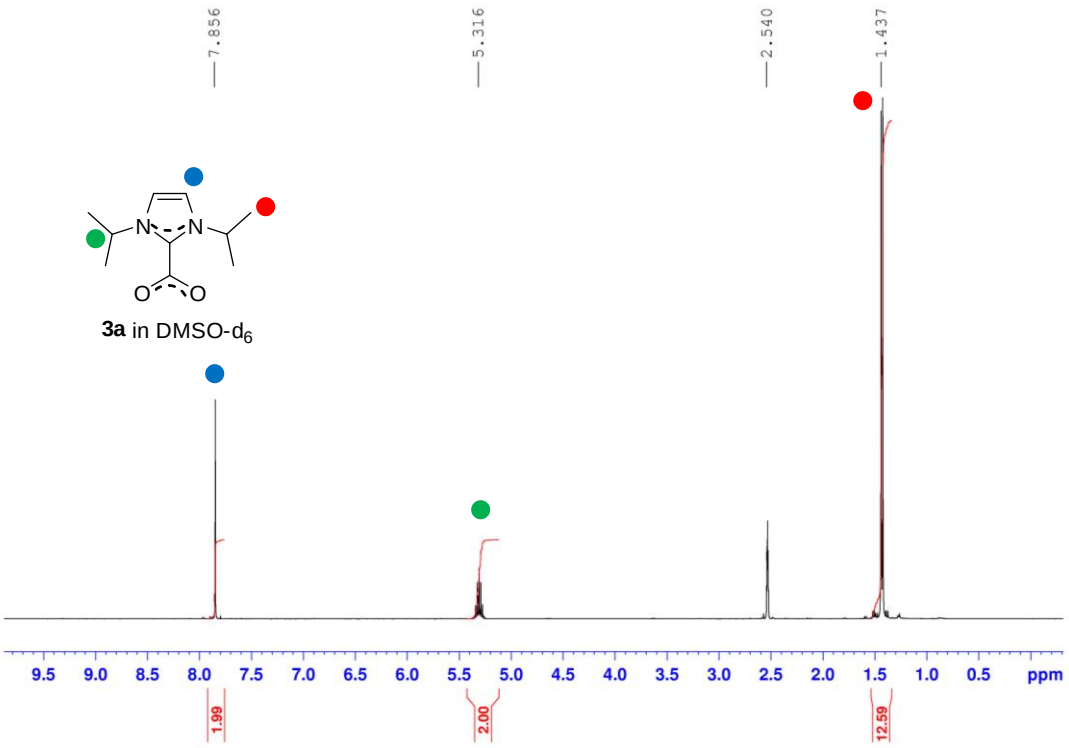

Figure S19. ^{1}H NMR spectrum of compound **3a** in DMSO-d_6.

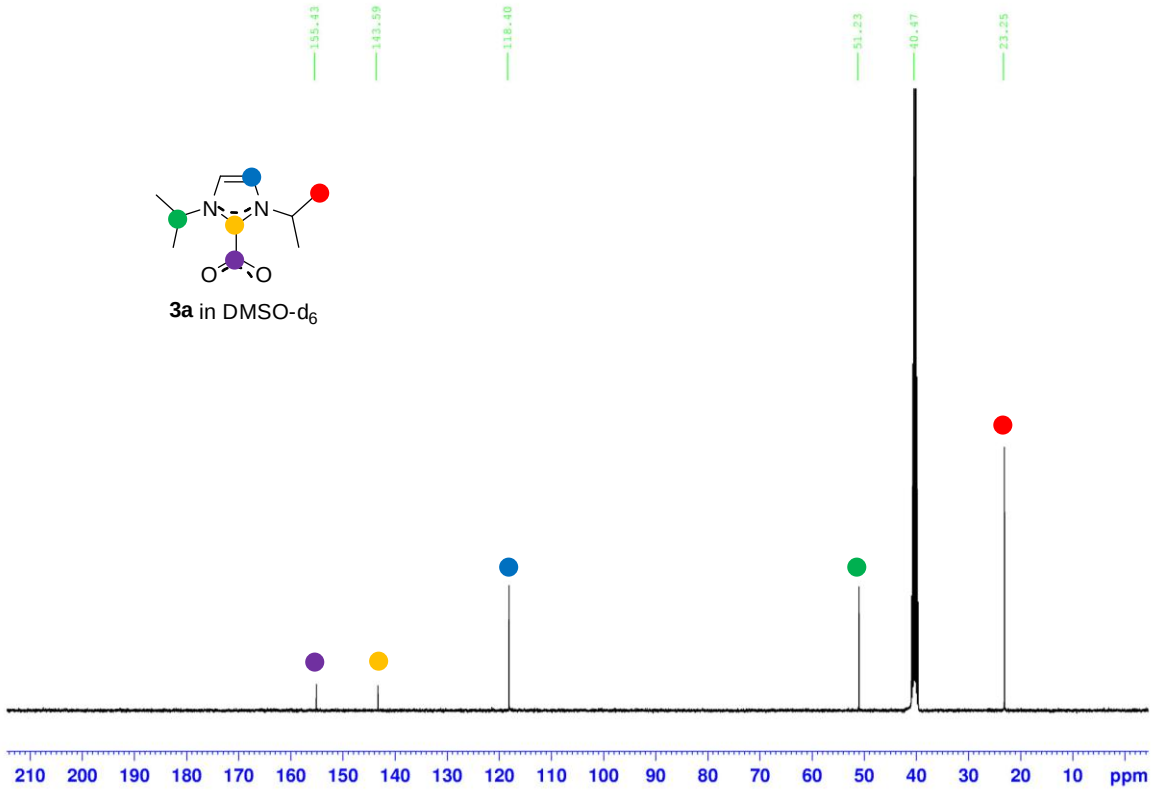

Figure S20. ^{13}C NMR spectrum of compound **3a** in DMSO-d_6.

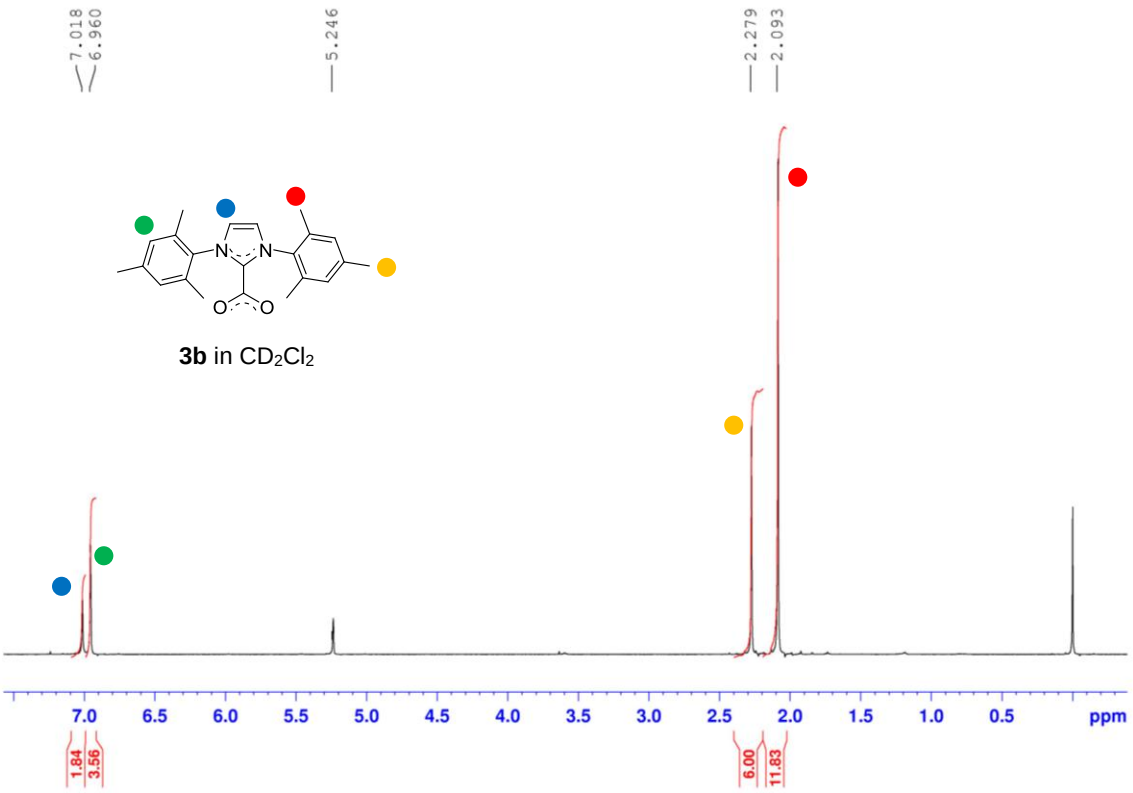

Figure S21. ^{1}H NMR spectrum of compound **3b** in CD_2Cl_2.

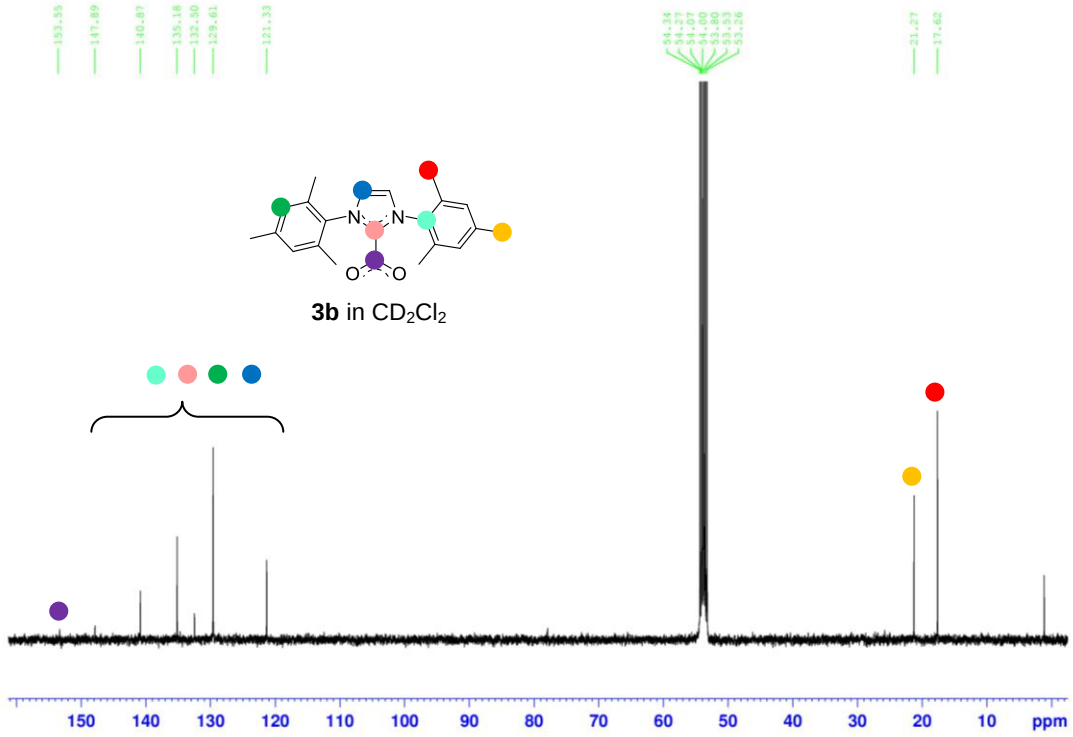

Figure S22. ^{13}C NMR spectrum of compound **3b** in CD_2Cl_2.

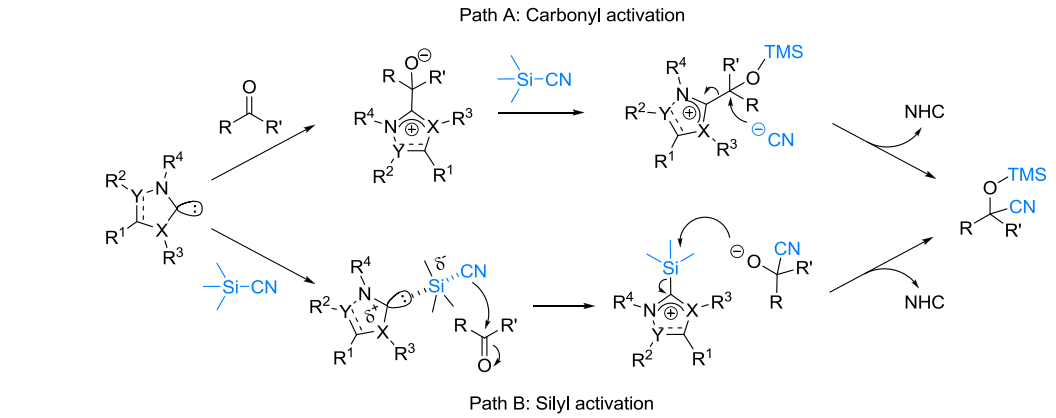

Scheme S1. Mechanism of the NHC-catalyzed cyanosilylation reaction (carbonyl *vs.* silyl activation).

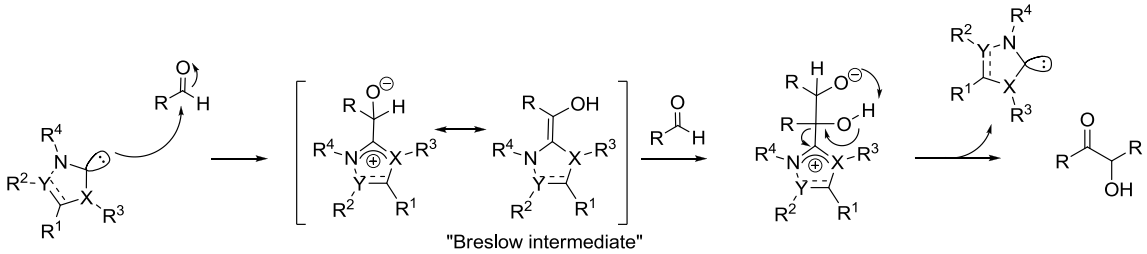

Scheme S2. Mechanism of the NHC-catalyzed benzoin condensation reaction.

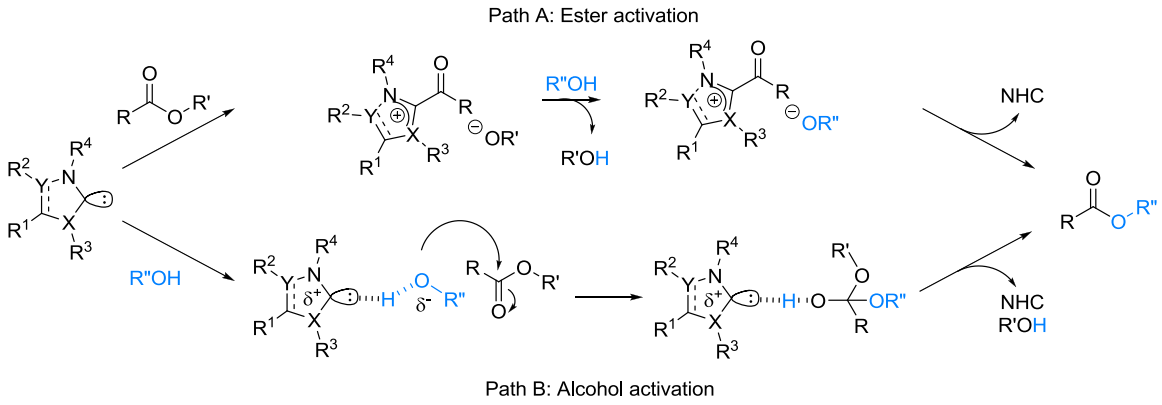

Scheme S3. Mechanism of the NHC-catalyzed tranesterification reaction (ester *vs.* alcohol activation).

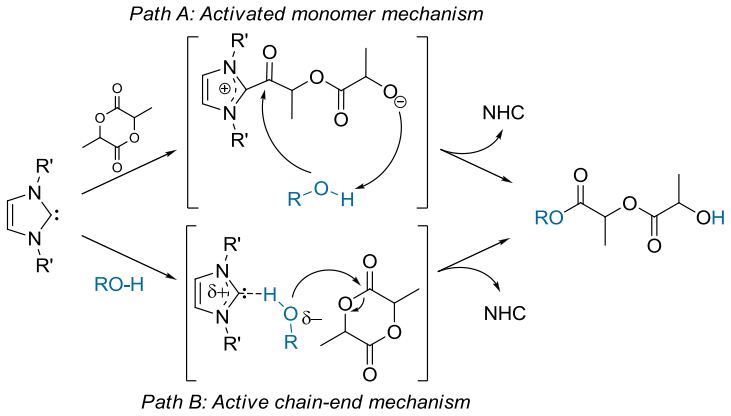

Scheme S4. Initiation of the ROP of LA and subsequent propagation to form PLA (AMM *vs*. ACEM).

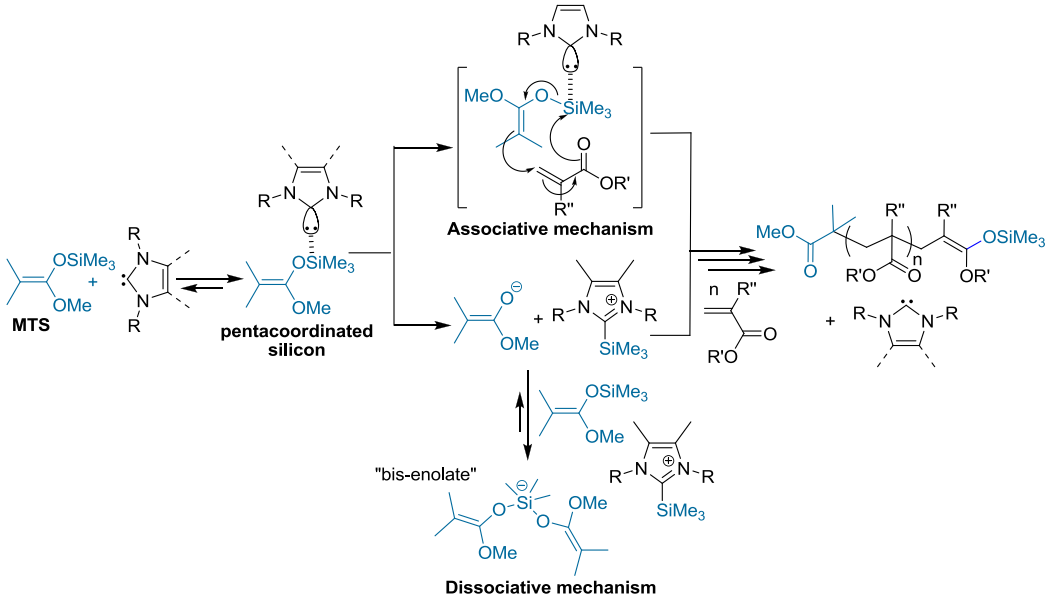

Scheme S5. Associative and dissociative mechanisms for NHC-mediated GTP.

References

1. Fèvre, M.; Pinaud, J.; Leteneur, A.; Gnanou, Y.; Vignolle, J.; Taton, D.; Miqueu, K.; Sotiropoulos, J.-M., *J. Am. Chem. Soc.* **2012,** *134*, 6776.
2. Fèvre, M.; Coupillaud, P.; Miqueu, K.; Sotiropoulos, J.-M.; Vignolle, J.; Taton, D., *submitted to J. Org. Chem.*
3. Bourissou, D.; Guerret, O.; Gabbai, F. P.; Bertrand, G., *Chem. Rev.* **2000,** *100*, 39.
4. Herrmann, W. A., *Angew. Chem. Int. Ed.* **2002,** *41*, 1290.
5. Crabtree, R. H., *Coord. Chem. Rev.* **2007,** *251*, 595.
6. Glorius, F., In *N-Heterocyclic Carbenes in Transition Metal Catalysis*, Springer Berlin / Heidelberg: 2007; Vol. 21, p 1.
7. Díez-González, S.; Marion, N.; Nolan, S. P., *Chem. Rev.* **2009,** *109*, 3612.
8. Dröge, T.; Glorius, F., *Angew. Chem. Int. Ed.* **2010,** *49*, 6940.
9. Enders, D.; Niemeier, O.; Henseler, A., *Chem. Rev.* **2007,** *107*, 5606.
10. Marion, N.; Díez-González, S.; Nolan, S. P., *Angew. Chem. Int. Ed.* **2007,** *46*, 2988.
11. Moore, J.; Rovis, T., In *Asymmetric Organocatalysis*, List, B., Ed. Springer Berlin / Heidelberg: 2009; Vol. 291, p 77.
12. Kamber, N. E.; Jeong, W.; Waymouth, R. M.; Pratt, R. C.; Lohmeijer, B. G. G.; Hedrick, J. L., *Chem. Rev.* **2007,** *107*, 5813.
13. Kiesewetter, M. K.; Shin, E. J.; Hedrick, J. L.; Waymouth, R. M., *Macromolecules* **2010,** *43*, 2093.
14. Raynaud, J.; Absalon, C.; Gnanou, Y.; Taton, D., *Macromolecules* **2010,** *43*, 2814.
15. Raynaud, J.; Ottou, W. N.; Gnanou, Y.; Taton, D., *Chem. Commun.* **2010,** *46*, 3203.
16. Raynaud, J.; Liu, N.; Fevre, M.; Gnanou, Y.; Taton, D., *Polym. Chem.* **2011,** *2*, 1706.
17. Coulembier, O.; Moins, S. b.; Dubois, P., *Macromolecules* **2011,** *44*, 7493.
18. Shin, E. J.; Brown, H. A.; Gonzalez, S.; Jeong, W.; Hedrick, J. L.; Waymouth, R. M., *Angew. Chem. Int. Ed.* **2011,** *50*, 6388.
19. Shin, E. J.; Jeong, W.; Brown, H. A.; Koo, B. J.; Hedrick, J. L.; Waymouth, R. M., *Macromolecules* **2011,** *44*, 2773.
20. de Frémont, P.; Marion, N.; Nolan, S. P., *Coord. Chem. Rev.* **2009,** *253*, 862.
21. Bonnette, F.; Kato, T.; Destarac, M.; Mignani, G.; Cossío, F. P.; Baceiredo, A., *Angew. Chem. Int. Ed.* **2007,** *46*, 8632.
22. Arduengo Iii, A. J.; Calabrese, J. C.; Davidson, F.; Rasika Dias, H. V.; Goerlich, J. R.; Krafczyk, R.; Marshall, W. J.; Tamm, M.; Schmutzler, R., *Helv. Chim. Acta* **1999,** *82*, 2348.
23. Wanzlick, H.-W.; Esser, F.; Kleiner, H.-J., *Chem. Ber.* **1963,** *96*, 1208.
24. Scholl, M.; Ding, S.; Lee, C. W.; Grubbs, R. H., *Org. Lett.* **1999,** *1*, 953.
25. Denk, K.; Sirsch, P.; Herrmann, W. A., *J. Organomet. Chem.* **2002,** *649*, 219.
26. Trnka, T. M.; Morgan, J. P.; Sanford, M. S.; Wilhelm, T. E.; Scholl, M.; Choi, T.-L.; Ding, S.; Day, M. W.; Grubbs, R. H., *J. Am. Chem. Soc.* **2003,** *125*, 2546.
27. Coulembier, O.; Dove, A. P.; Pratt, R. C.; Sentman, A. C.; Culkin, D. A.; Mespouille, L.; Dubois, P.; Waymouth, R. M.; Hedrick, J. L., *Angew. Chem. Int. Ed.* **2005,** *44*, 4964.
28. Csihony, S.; Culkin, D. A.; Sentman, A. C.; Dove, A. P.; Waymouth, R. M.; Hedrick, J. L., *J. Am. Chem. Soc.* **2005,** *127*, 9079.
29. Coulembier, O.; Lohmeijer, B. G. G.; Dove, A. P.; Pratt, R. C.; Mespouille, L.; Culkin, D. A.; Benight, S. J.; Dubois, P.; Waymouth, R. M.; Hedrick, J. L., *Macromolecules* **2006,** *39*, 5617.
30. Nyce, G. W.; Csihony, S.; Waymouth, R. M.; Hedrick, J. L., *Chem. Eur. J.* **2004,** *10*, 4073.
31. Blum, A. P.; Ritter, T.; Grubbs, R. H., *Organometallics* **2007,** *26*, 2122.
32. Enders, D.; Breuer, K.; Raabe, G.; Runsink, J.; Teles, J. H.; Melder, J.-P.; Ebel, K.; Brode, S., *Angew. Chem. Int. Ed.* **1995,** *34*, 1021.
33. Kuhn, N.; Steimann, M.; Weyers, G., *Z. Naturforsch., B: Chem. Sci.* **1999,** *54*, 427.
34. Holbrey, J. D.; Reichert, W. M.; Tkatchenko, I.; Bouajila, E.; Walter, O.; Tommasi, I.; Rogers, R. D., *Chem. Commun.* **2003**, 28.
35. Duong, H. A.; Tekavec, T. N.; Arif, A. M.; Louie, J., *Chem. Commun.* **2004**, 112.
36. Tommasi, I.; Sorrentino, F., *Tetrahedron Lett.* **2006,** *47*, 6453.
37. Voutchkova, A. M.; Feliz, M.; Clot, E.; Eisenstein, O.; Crabtree, R. H., *J. Am. Chem. Soc.* **2007,** *129*, 12834.
38. Delaude, L., *Eur. J. Inorg. Chem.* **2009,** *2009*, 1681.
39. Van Ausdall, B. R.; Glass, J. L.; Wiggins, K. M.; Aarif, A. M.; Louie, J., *J. Org. Chem.* **2009,** *74*, 7935.
40. Smiglak, M.; Hines, C. C.; Rogers, R. D., *Green Chem.* **2010,** *12*, 491.
41. Hans, M.; Wouters, J.; Demonceau, A.; Delaude, L., *Eur. J. Org. Chem.* **2011,** *35*, 7083.

42. Norris, B. C.; Sheppard, D. G.; Henkelman, G.; Bielawski, C. W., *J. Org. Chem.* **2010,** *76*, 301.
43. Wang, H. M. J.; Lin, I. J. B., *Organometallics* **1998,** *17*, 972.
44. Lin, J. C. Y.; Huang, R. T. W.; Lee, C. S.; Bhattacharyya, A.; Hwang, W. S.; Lin, I. J. B., *Chem. Rev.* **2009,** *109*, 3561.
45. Kuhn, N.; Maichle-Mößmer, C.; Weyers, G., *Z. Anorg. Allg. Chem.* **1999,** *625*, 851.
46. Voutchkova, A. M.; Appelhans, L. N.; Chianese, A. R.; Crabtree, R. H., *J. Am. Chem. Soc.* **2005,** *127*, 17624.
47. Tudose, A.; Delaude, L.; André, B.; Demonceau, A., *Tetrahedron Lett.* **2006,** *47*, 8529.
48. Tudose, A.; Demonceau, A.; Delaude, L., *J. Organomet. Chem.* **2006,** *691*, 5356.
49. Delaude, L.; Sauvage, X.; Demonceau, A.; Wouters, J., *Organometallics* **2009,** *28*, 4056.
50. Sauvage, X.; Demonceau, A.; Delaude, L., *Adv. Synth. Catal.* **2009,** *351*, 2031.
51. Sauvage, X.; Demonceau, A.; Delaude, L., *Macromol. Symp.* **2010,** *293*, 28.
52. Zhou, H.; Zhang, W.-Z.; Liu, C.-H.; Qu, J.-P.; Lu, X.-B., *J. Org. Chem.* **2008,** *73*, 8039.
53. Kayaki, Y.; Yamamoto, M.; Ikariya, T., *Angew. Chem. Int. Ed.* **2009,** *48*, 4194.
54. Naik, Prashant U.; Petitjean, L.; Refes, K.; Picquet, M.; Plasseraud, L., *Adv. Synth. Catal.* **2009,** *351*, 1753.
55. Tommasi, I.; Sorrentino, F., *Tetrahedron Lett.* **2009,** *50*, 104.
56. Pawar, G. M.; Buchmeiser, M. R., *Adv. Synth. Catal.* **2010,** *352*, 917.
57. Pinaud, J.; Vignolle, J.; Gnanou, Y.; Taton, D., *Macromolecules* **2011,** *44*, 1900.
58. Van Ausdall, B. R.; Poth, N. F.; Kincaid, V. A.; Arif, A. M.; Louie, J., *J. Org. Chem.* **2011,** *76*, 8413.
59. Zhou, H.; Wang, Y.-M.; Zhang, W.-Z.; Qu, J.-P.; Lu, X.-B., *Green Chem.* **2011,** *13*, 644.
60. Bantu, B.; Pawar, G. M.; Wurst, K.; Decker, U.; Schmidt, A. M.; Buchmeiser, M. R., *Eur. J. Inorg. Chem.* **2009,** *2009*, 1970.
61. Bantu, B.; Pawar, G. M.; Decker, U.; Wurst, K.; Schmidt, A. M.; Buchmeiser, M. R., *Chem. Eur. J.* **2009,** *15*, 3103.
62. Coulembier, O.; Delva, X.; Hedrick, J. L.; Waymouth, R. M.; Dubois, P., *Macromolecules* **2007,** *40*, 8560.
63. Coulembier, O.; Kiesewetter, M.; Mason, A.; Dubois, P.; Hedrick, J.; Waymouth, R., *Angew. Chem. Int. Ed.* **2007,** *46*, 4719.
64. Naik, P. U.; Refes, K.; Sadaka, F.; Brachais, C.-H.; Boni, G.; Couvercelle, J.-P.; Picquet, M.; Plasseraud, L., *Polym. Chem.* **2012,** *3*, 1475.
65. Azouri, M.; Andrieu, J.; Picquet, M.; Richard, P.; Hanquet, B.; Tkatchenko, I., *Eur. J. Inorg. Chem.* **2007,** *2007*, 4877.
66. Zhou, H.; Zhang, W.-Z.; Wang, Y.-M.; Qu, J.-P.; Lu, X.-B., *Macromolecules* **2009,** *42*, 5419.
67. Rauchfuss, T. B., In *Inorg. Synth.*, John Wiley & Sons, Inc.: 2010; p 78.
68. Powell, A. B.; Suzuki, Y.; Ueda, M.; Bielawski, C. W.; Cowley, A. H., *J. Am. Chem. Soc.* **2011,** *133*, 5218.
69. Duong, H. A.; Cross, M. J.; Louie, J., *Org. Lett.* **2004,** *6*, 4679.
70. Bridges, N. J.; Hines, C. C.; Smiglak, M.; Rogers, R. D., *Chem. Eur. J.* **2007,** *13*, 5207.
71. Holloczki, O.; Gerhard, D.; Massone, K.; Szarvas, L.; Nemeth, B.; Veszpremi, T.; Nyulaszi, L., *New J. Chem.* **2010,** *34*, 3004.
72. Gurau, G.; Rodríguez, H.; Kelley, S. P.; Janiczek, P.; Kalb, R. S.; Rogers, R. D., *Angew. Chem. Int. Ed.* **2011,** *50*, 12024.
73. Kelemen, Z.; Holloczki, O.; Nagy, J.; Nyulaszi, L., *Org. Biomol. Chem.* **2011,** *9*, 5362.
74. Rodriguez, H.; Gurau, G.; Holbrey, J. D.; Rogers, R. D., *Chem. Commun.* **2011,** *47*, 3222.
75. [NHC(H)][HCO_3] based IL have been recently employed for the organocatalyzed carbonylation of amines (see Ref 76) and the depolymerization of poly(ethylene terephthalate) (see Ref 77), taking advantage of the basic character of the HCO_3^- counter-anion. The imidazolium cation is thought to remain spectator, the proposed catalyst being the HCO_3^- anion itself.
76. Choi, Y.-S.; Shim, Y. N.; Lee, J.; Yoon, J. H.; Hong, C. S.; Cheong, M.; Kim, H. S.; Jang, H. G.; Lee, J. S., *Appl. Catal., A* **2011,** *404*, 87.
77. Yue, Q. F.; Wang, C. X.; Zhang, L. N.; Ni, Y.; Jin, Y. X., *Polym. Degrad. Stab.* **2011,** *96*, 399.
78. Liu, Y.; Li, M.; Lu, Y.; Gao, G.-H.; Yang, Q.; He, M.-Y., *Catal. Commun.* **2006,** *7*, 985.
79. Smiglak, M.; Holbrey, J. D.; Griffin, S. T.; Reichert, W. M.; Swatloski, R. P.; Katritzky, A. R.; Yang, H.; Zhang, D.; Kirichenko, K.; Rogers, R. D., *Green Chem.* **2007,** *9*, 90.
80. Rijksen, C.; Rogers, R. D., *J. Org. Chem.* **2008,** *73*, 5582.
81. Ratel, M.; Branca, M.; Breault-Turcot, J.; Zhao, S. S.; Chaurand, P.; Schmitzer, A. R.; Masson, J.-F., *Chem. Commun.* **2011,** *47*, 10644.
82. Ye, Y.; Elabd, Y. A., *Macromolecules* **2011,** *44*, 8494.

83. Abu-Rayyan, A.; Abu-Salem, Q.; Kuhn, N.; Maichle-Mößmer, C.; Steimann, M.; Henkel, G., *Z. Anorg. Allg. Chem.* **2008,** *634*, 823.
84. K_2CO_3 was reported to react with [NHC(H)][Cl], leading to [NHC(H)][HCO_3] (see Ref 76).
85. Magill, A. M.; Cavell, K. J.; Yates, B. F., *J. Am. Chem. Soc.* **2004,** *126*, 8717.
86. Ngo, H. L.; LeCompte, K.; Hargens, L.; McEwen, A. B., *Thermochim. Acta* **2000,** *357–358*, 97.
87. Zhang, S.; Sun, N.; He, X.; Lu, X.; Zhang, X., *J. Phys. Chem. Ref. Data* **2006,** *35*, 1475.
88. Ming Lee, K.; Kuan Lee, C.; J. B. Lin, I., *Chem. Commun.* **1997**, 899.
89. D. Holbrey, J.; R. Seddon, K., *J. Chem. Soc., Dalton Trans.* **1999**, 2133.
90. Sobota, M.; Wang, X.; Fekete, M.; Happel, M.; Meyer, K.; Wasserscheid, P.; Laurin, M.; Libuda, J., *ChemPhysChem* **2010,** *11*, 1632.
91. Poater, A.; Ragone, F.; Giudice, S.; Costabile, C.; Dorta, R.; Nolan, S. P.; Cavallo, L., *Organometallics* **2008,** *27*, 2679.
92. Tapu, D.; Dixon, D. A.; Roe, C., *Chem. Rev.* **2009,** *109*, 3385.
93. Hao, Y.; Peng, J.; Hu, S.; Li, J.; Zhai, M., *Thermochim. Acta* **2010,** *501*, 78.
94. Delaude, L.; Demonceau, A.; Wouters, J., *Eur. J. Inorg. Chem.* **2009,** *2009*, 1882.
95. Jensen, D. R.; Sigman, M. S., *Org. Lett.* **2002,** *5*, 63.
96. Viciu, M. S.; Navarro, O.; Germaneau, R. F.; Kelly, R. A.; Sommer, W.; Marion, N.; Stevens, E. D.; Cavallo, L.; Nolan, S. P., *Organometallics* **2004,** *23*, 1629.
97. Baker, M. V.; Barnard, P. J.; Berners-Price, S. J.; Brayshaw, S. K.; Hickey, J. L.; Skelton, B. W.; White, A. H., *J. Organomet. Chem.* **2005,** *690*, 5625.
98. de Frémont, P.; Scott, N. M.; Stevens, E. D.; Nolan, S. P., *Organometallics* **2005,** *24*, 2411.
99. Herrmann, W. A.; Goossen, L. J.; Köcher, C.; Artus, G. R. J., *Angew. Chem. Int. Ed.* **1996,** *35*, 2805.
100. Song, J. J.; Gallou, F.; Reeves, J. T.; Tan, Z.; Yee, N. K.; Senanayake, C. H., *J. Org. Chem.* **2006,** *71*, 1273.
101. Suzuki, Y.; Bakar, M. D. A.; Muramatsu, K.; Sato, M., *Tetrahedron* **2006,** *62*, 4227.
102. Grunewald, G. L.; Brouillette, W. J.; Finney, J. A., *Tetrahedron Lett.* **1980,** *21*, 1219.
103. Utimoto, K.; Wakabayashi, Y.; Horiie, T.; Inoue, M.; Shishiyama, Y.; Obayashi, M.; Nozaki, H., *Tetrahedron* **1983,** *39*, 967.
104. Breslow, R., *J. Am. Chem. Soc.* **1958,** *80*, 3719.
105. Pinaud, J.; Vijayakrishna, K.; Taton, D.; Gnanou, Y., *Macromolecules* **2009,** *42*, 4932.
106. Nyce, G. W.; Lamboy, J. A.; Connor, E. F.; Waymouth, R. M.; Hedrick, J. L., *Org. Lett.* **2002,** *4*, 3587.
107. Grasa, G. A.; Güveli, T.; Singh, R.; Nolan, S. P., *J. Org. Chem.* **2003,** *68*, 2812.
108. Poyatos, M.; Mata, J. A.; Peris, E., *Chem. Rev.* **2009,** *109*, 3677.
109. Nyce, G. W.; Glauser, T.; Connor, E. F.; Mock, A.; Waymouth, R. M.; Hedrick, J. L., *J. Am. Chem. Soc.* **2003,** *125*, 3046.
110. Kamber, N. E.; Jeong, W.; Gonzalez, S.; Hedrick, J. L.; Waymouth, R. M., *Macromolecules* **2009,** *42*, 1634.
111. Nederberg, F.; Lohmeijer, B. G. G.; Leibfarth, F.; Pratt, R. C.; Choi, J.; Dove, A. P.; Waymouth, R. M.; Hedrick, J. L., *Biomacromolecules* **2006,** *8*, 153.
112. Webster, O. W.; Hertler, W. R.; Sogah, D. Y.; Farnham, W. B.; RajanBabu, T. V., *J. Am. Chem. Soc.* **1983,** *105*, 5706.
113. Mukaiyama, T., *Angew. Chem. Int. Ed.* **2004,** *43*, 5590.
114. Webster, O. W., *J. Polym. Sci., Part A: Polym. Chem.* **2000,** *38*, 2855.
115. Raynaud, J.; Liu, N.; Gnanou, Y.; Taton, D., *Macromolecules* **2010,** *43*, 8853.
116. Raynaud, J.; Ciolino, A.; Baceiredo, A.; Destarac, M.; Bonnette, F.; Kato, T.; Gnanou, Y.; Taton, D., *Angew. Chem. Int. Ed.* **2008,** *47*, 5390.
117. Scholten, M. D.; Hedrick, J. L.; Waymouth, R. M., *Macromolecules* **2008,** *41*, 7399.
118. Chen, Y.; Fuchise, K.; Narumi, A.; Kawaguchi, S.; Satoh, T.; Kakuchi, T., *Macromolecules* **2011,** *44*, 9091.
119. Kakuchi, T.; Chen, Y.; Kitakado, J.; Mori, K.; Fuchise, K.; Satoh, T., *Macromolecules* **2011,** *44*, 4641.
120. Hsu, J.-C.; Chen, Y.; Kakuchi, T.; Chen, W.-C., *Macromolecules* **2011,** *44*, 5168.
121. Kakuchi, R.; Chiba, K.; Fuchise, K.; Sakai, R.; Satoh, T.; Kakuchi, T., *Macromolecules* **2009,** *42*, 8747.
122. Fuchise, K.; Sakai, R.; Satoh, T.; Sato, S.; Narumi, A.; Kawaguchi, S.; Kakuchi, T., *Macromolecules* **2010,** *43*, 5589.
123. Zhang, Y.; Lay, F.; García-García, P.; List, B.; Chen, E. Y. X., *Chem. Eur. J.* **2010,** *16*, 10462.
124. Takada, K.; Fuchise, K.; Chen, Y.; Satoh, T.; Kakuchi, T., *J. Polym. Sci., Part A: Polym. Chem.* **2012,** *50*, 3560.
125. Raynaud, J.; Gnanou, Y.; Taton, D., Unpublished results
126. Palatinus, L.; Chapuis, G., *J. Appl. Crystallogr.* **2007,** *40*, 786.

127. M. J. Frisch, G. W. Trucks, H. B. Schlegel, G. E. Scuseria, M. A. Robb, J. R. Cheeseman, J. A. Montgomery, Jr. T. Vreven, K. N. Kudin, J. C. Burant, J. M. Millam, S. S. Iyengar, J. Tomasi, V. Barone, B. Mennucci, M. Cossi, G. Scalmani, N. Rega, G. A. Petersson, H. Nakatsuji, M. Hada, M. Ehara, K. Toyota, R. Fukuda, J. Hasegawa, M. Ishida, T. Nakajima, Y. Honda, O. Kitao, H. Nakai, M. X. Klene, X. Li, J. E. Knox, H. P. Hratchian, J. B. Cross, C. Adamo, J. Jaramillo, R. Gomperts, R. E. Stratmann, O. Yazyev, A. J. Austin, R. Cammi, C. Pomelli, J. W. Ochterski, P. Y. Ayala, K. Morokuma, G. A. Voth, P. Salvador, J. J. Dannenberg, V. G. Zakrzewski, S. Dapprich, A. D. Daniels, M. C. Strain, O. Farkas, D. K. Malick, A. D. Rabuck, K. Raghavachari, J. B. Foresman, J. V. Ortiz, Q. Cui, A. G. Baboul, S. Clifford, J. Cioslowski, B. B. Stefanov, G. Liu, A. Liashenko, P. Piskorz, I. Komaromi, R. L. Martin, D. J. Fox, T. Keith, M. A. Al-Laham, C. Y. Peng, A. Nanayakkara, M. Challacombe, P. M. W. Gill, B. Johnson, W. Chen, M. W. Wong, C. Gonzalez, J. A. Pople, Gaussian 03, Revision D-02, Gaussian, Inc., Pittsburgh PA, **2003**.
128. Parr, R. G.; Yang, W., *Density Functional Theory of Atoms and Molecules*, Breslow, R.; Goodenough, J. B., Eds. Oxford University Press: New York, 1989.
129. Becke, A. D., *J. Chem. Phys.* **1993,** *98*, 5648.
130. Becke, A. D., *Phys. Rev. A: At. Mol. Opt. Phys.* **1988,** *38*, 3098.
131. Lee, C.; Yang, W.; Parr, R. G., *Phys. Rev. B: Condens. Matter* **1988,** *37*, 785.
132. Hariharan, P. C.; Pople, J. A., *Theor. Chem. Acc.* **1973,** *28*, 213.
133. Gonzalez, C.; Schlegel, H. B., *J. Chem. Phys.* **1989,** *90*, 2154.
134. Gonzalez, C.; Schlegel, H. B., *J. Phys. Chem.* **1990,** *94*, 5523.
135. Starikova, O. V.; Dolgushin, G. V.; Larina, L. I.; Ushakov, P. E.; Komarova, T. N.; Lopyrev, V. A., *Russ. J. Org. Chem.* **2003,** *39*, 1467.

Chapitre 3

Vers une Activation Organique Multitâche : Paires de Lewis à Base de Carbènes *N*-Hétérocycliques et de Silanes ou Boranes et leur Utilisation en Polymérisation

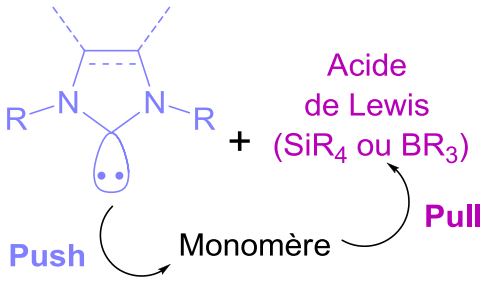

Mots clés: Organocatalyse, Carbènes *N*-hétérocycliques, Acides de Lewis, Silanes, Boranes, Paires de Lewis frustrées, Adduits acide-base, Polymérisation.

Keywords: Organocatalysis, *N*-heterocyclic carbenes, Lewis acids, Silanes, Boranes, Frustrated Lewis pairs, Acid-base adducts, Polymerization.

Résumé: Malgré l'énorme potentiel des carbènes *N*-hétérocycliques (NHCs), tant en chimie moléculaire qu'en synthèse de polymères, leur mode d'activation est souvent limité aux substrats comportant un groupement carbonyle, ou plus rarement aux dérivés silylés. Dans cette partie du travail, nous avons associé des NHCs, utilisés en tant que bases de Lewis, à des co-activateurs non-métalliques de type acide de Lewis (silane ou borane) pour induire des réactions de polymérisation par un effet de double assistance. Dans un premier temps, les avancées récentes concernant les systèmes combinant acide et base de Lewis, en particulier le concept de "paires de Lewis frustrées" ("frustrated Lewis pairs" (FLPs)), sont présentés. Les interactions entre silanes et NHCs ont alors été étudiées. Pour la première fois, nous avons mis en évidence que l'on peut générer une paire de Lewis frustrée ou bien un adduit "classique" en fonction de la structure du NHC avec des silanes. Ces paires de Lewis ont alors été utilisées pour isoler un intermédiaire présumé de la réaction de condensation de la benzoine, appelé "intermédiaire de Breslow". La valorisation de telles paires de Lewis en chimie des polymères nécessite toutefois encore quelques améliorations. En effet, l'utilisation conjointe d'un silane et d'un NHC n'a pas permis d'augmenter significativement l'efficacité de la polymérisation par ouverture de cycle du l'oxyde de propylène. Des paires de Lewis à base de NHC et du tris(pentafluorophenyl)borane ($B(C_6F_5)_3$) ont ensuite été employées pour amorcer/activer la polymérisation zwitterionique du MMA. Les conditions expérimentales ont été optimisées pour induire un processus revêtant un certain caractère "contrôlé". Les masses molaires obtenues ont, par exemple, pu être contrôlées par la quantité initiale de monomère introduite par rapport à celle en NHC, mais la qualité du contrôle de la polymérisation n'est pas encore optimale. Bien que le mécanisme mis en jeu n'ait pu être déterminé avec précision, les investigations cinétiques ont permis d'établir que la polymérisation est caractérisée par une étape d'amorçage lente. Les calculs théoriques et l'étude des interactions entre acide de Lewis, NHC et MMA ont confirmé le rôle clé de l'acide de Lewis en tant qu'activateur du MMA.

This chapter is dedicated to the use of Lewis acid/base pairs to activate several substrates in molecular chemistry but also in polymer synthesis. This chapter is not ready yet for publication as many of the findings are still under consideration. Hypothesis on the mechanisms involved and products formed as well as potential applications are discussed.

Chapter 3

Towards an Organic Multitask Activation: *N*-Heterocyclic Carbenes-Silanes or Boranes Lewis Pairs and their Uses for Polymerization Reactions

TABLE OF CONTENTS

Introduction

As highlighted in previous chapters, challenges still remain to expand the scope of *N*-heterocyclic carbenes (NHCs) in polymer synthesis. For instance, NHCs have shown some limitations during the ring opening polymerization (ROP) of propylene oxide, since relatively low molar masses (<8,000 g/mol) were achieved, due to the occurrence of the transfer reaction to the monomer.[1] On the other hand, NHCs have not been evaluated towards non polar monomer substrates (e.g. styrene or dienes).

To circumvent some of these limitations, we propose here to use a Lewis acid (LA) co-activator in conjunction with the NHC, so as to provide a more versatile organocatalytic platform. In this manner, the Lewis acid and the NHC Lewis base (LB) are expected to increase the monomer reactivity *via* a "push/pull effect" in a dual/cooperative activation mechanism (Figure 1). It is worth pointing out that such a doubly assisted activation of the monomer, through the use of both an electrophilic and a nucleophilic catalyst, is different from that based on the activation by H-bonding of both the monomer and the alcohol initiator, using mono and bi-component catalytic system (e.g. guanidine or thiourea/amino compounds, see Chapter 1 and Figure 1).

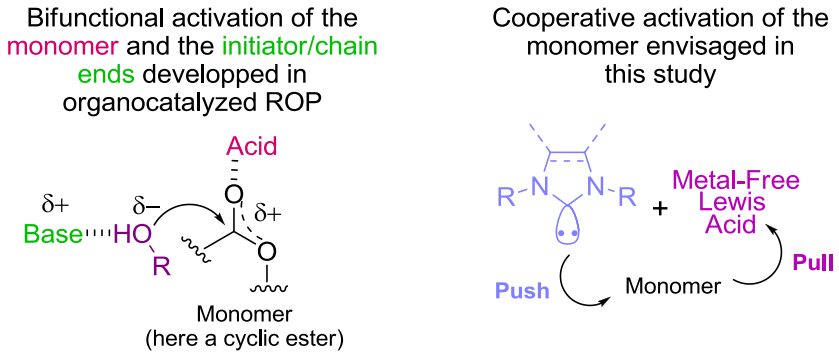

Figure 1. Bifunctional activation by H-bonding developed in the context of organocatalyzed ROP (see Chap. 1) *vs.* cooperative activation of the monomer envisaged in this study.

Several features have to be taken into account, however, to induce the expected "push/pull effect". In a first instance, the LB and the LA should not form a "classical" adduct by quenching each other, that would decrease the activation. It is anticipated that this can be avoided by a proper selection of

both reaction partners and the experimental conditions. In particular, the addition order of the reagents and catalysts should have a strong impact on the quality of control of the polymerizations.

In the context of molecular chemistry, Stephan *et al.* and Erker *et al.* have recently developed the concept of "frustrated Lewis pair" (FLP),[2-3] utilizing both a LB and a LA to activate non-polar substrates. Experimental evidence of such an effect, however, dates back to 1942.[4] A FLP lies on the combination of a LA and a LB that are "*sterically precluded from quenching each other*" (Figure 2).[3]

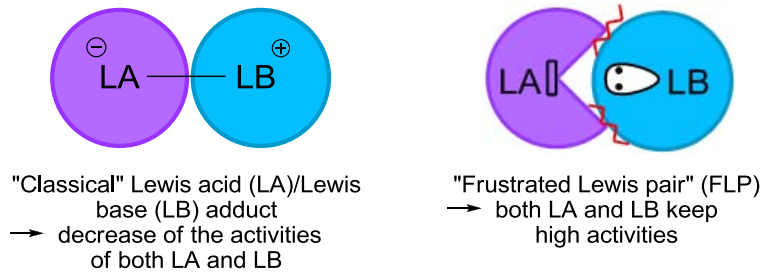

Figure 2. "Classical" Lewis acid/base adduct *vs.* "frustrated Lewis pair".

Typically, non-metallic FLPs use intra- or inter-molecularly bulky NHCs,[5-6] secondary or tertiary amines[7] or trialkyl/triaryl-phosphines,[2,8-11] as Lewis bases, and mainly boron Lewis acids ($B(C_6F_5)_3$ and derivatives, see Figure 3). As these systems were shown to heterolytically cleave dihydrogen,[10,12] they served to catalyze hydrogenation reactions.[13-16] However, they may also react in a 1/1 fashion with a variety of substrates including alkenes,[17] cyclopropanes[18] and THF,[19] just to cite a few (Figure 3).[3,20-22]

The concept of cooperative catalysis was applied to improve the catalytic activity of NHCs. For instance, γ-lactams synthesis[23] or highly stereoselective annulation reactions utilizing homoenolates as substrates[24] were achieved *via* a cooperative catalysis by NHCs and metallic LAs (mainly Mg and Ti-based). Although, the two catalytic species may bind in a reversible manner, the use of both moieties efficiently improve yields and stereoselectivity.

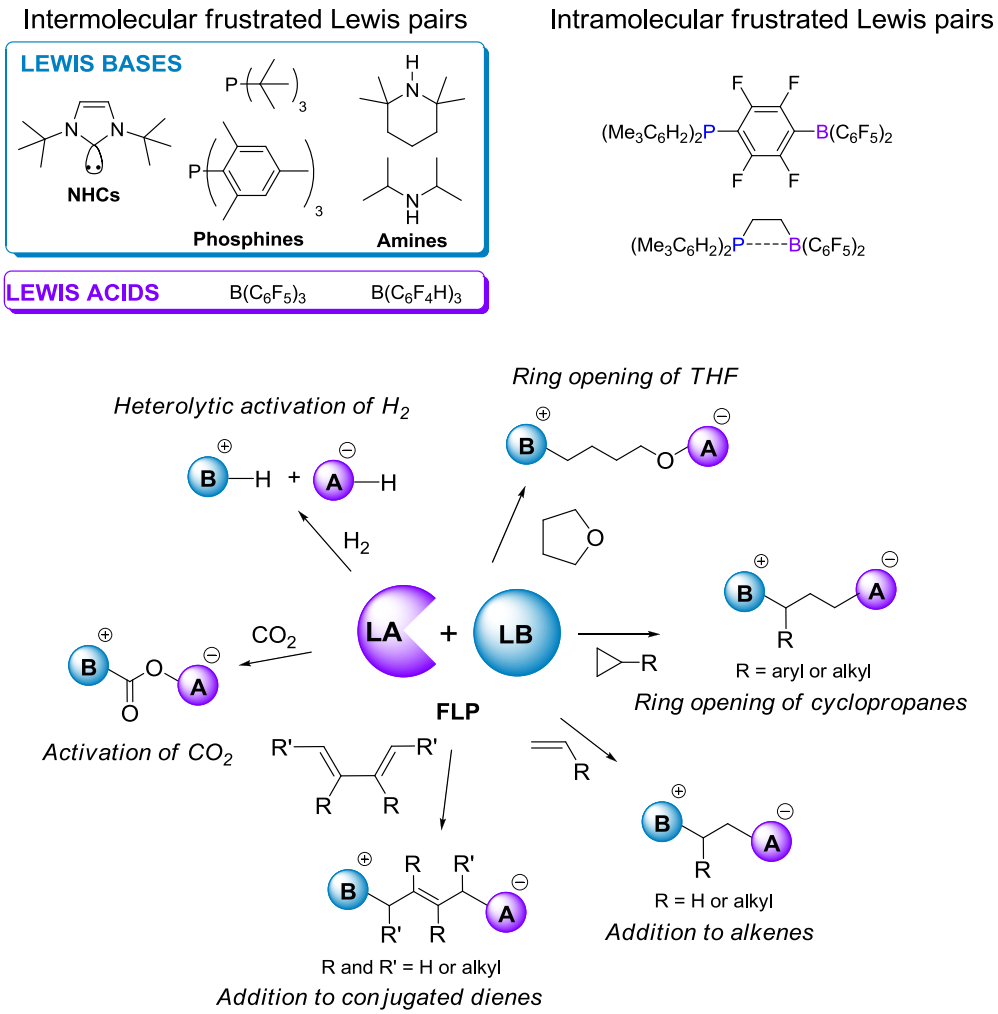

Figure 3. Acids and bases forming FLPs (inter- or intramolecularly) and main FLP-activated substrates.[3]

It has to be mentioned that, during this PhD work, Chen *et al*. (Colorado State Univ.) have reported the "first example of FLPs in polymer synthesis". The authors employed non-organic aluminum-based LA's, such as $Al(C_6F_5)_3$, and NHCs and trialkylphosphines as LB's.[25-26] Different (meth)acrylics were thus polymerized *via* such a dual activation (Scheme 1). Moderate control over molar masses was achieved in this way, with disperties ranging between 1.2 and 2.3.[25-26] Although these systems were claimed as being the first reports on "*FLPs-induced polymerization reactions*", the LA and LB in fact served as initiator and activator/reactivity modulator, respectively, in a zwitterionic polymerization. The authors eventually acknowledge that formation of a FLP was not a prerequisite, as the interactions between LA's and LB's could be prevented by a proper order of addition of the reagents. In practice, the LB was indeed added on a solution of the monomer activated by the LA.

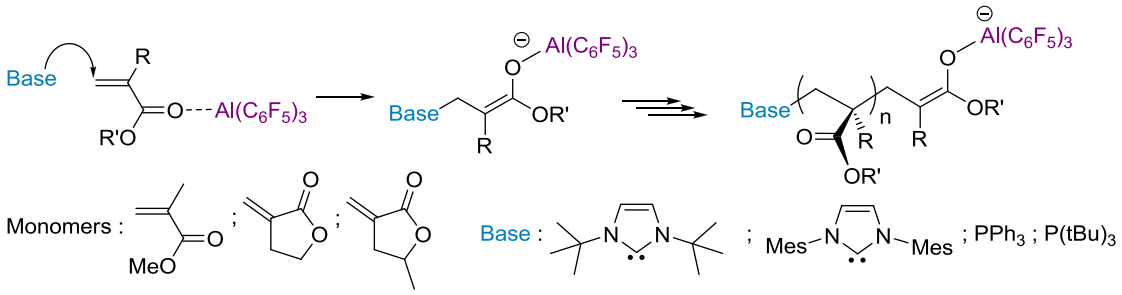

Scheme 1. Zwitterionic polymerization of methacrylics mediated by base/$Al(C_6F_5)_3$ Lewis pairs as reported by Chen *et al.* [25]

In this chapter, several metal-free silicon-based (SiLA) and boron-based (BLA) Lewis acids have been selected at first. Their molecular interactions with various NHCs and other Lewis bases have been studied. The potential of such pairs in elementary reactions of molecular chemistry has next been evaluated. SiLA-containing FLPs have thus been applied to activate molecular substrates while LA/LB combinations' forming "classical" adducts have been employed as co-activators for polymerization of propylene oxide (PO) and methyl methacrylate (MMA).

1. NHC-silane as Lewis pairs

Lewis bases are known to interact with tetravalent silicon derivatives, providing that they are properly substituted. The interaction between LB and Si center can be represented as a donation of the LB lone pair into an accessible σ* orbital of Si-R bond, and results from the ability of Si center for hypercoordination (see Scheme 2 for the interaction between a NHC Lewis base and a SiR_4 forming an adduct featuring an imidazolium and a negatively charged Si center).[27-30] However, due to both the redistribution of the electron density from Si center to R groups and the tendency of silicon to adopt square-planar bipyramidal geometry, Lewis acidity of the silicon atom is in fact increased.[31]

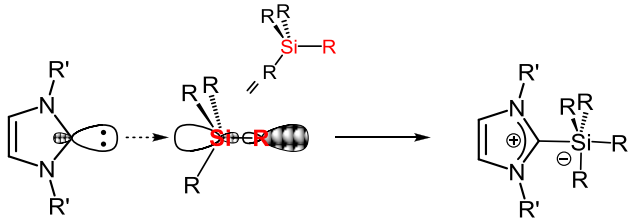

Scheme 2. Interaction of the non-bonding electron pair of a NHC (donor) with the σ* anti-bonding orbital of a silane (acceptor).

To the best of our knowledge, despite their well-established Lewis acidity, silanes have not yet been considered in FLPs. Interactions of NHCs with tetravalent silicon substrates are involved in a variety of (macro)molecular transformations.[32] For instance, NHCs efficiently catalyze cyanosilylation,[33] trifluoromethylation[34] and Mukaiyama-aldol[35] reactions, as well as the group transfer polymerization of (meth)acrylics[36-40] and the ring opening polymerization of Si-containing cyclic monomers (see Chap. 1).[41] In these cases, however, compounds resulting from the interaction of the NHC and the silicon moiety have never been isolated.

Interactions between NHCs and polysiloxanes (~~(~~$Si(R)_2O$~~)~~, R = Me or Ph) were investigated computationally and were shown to be weak ($E_{interaction}$ ≈ 3-5 kcal/mol) and reversible. Thus-encapsulated NHCs were stable in air and further used to mediate several transformations without modification of their reactivity.[42] Stable NHC-silane (SiX_4 or SiX_2R_2, X = F, Br, Cl and R = Me or Ph) adducts have nonetheless been isolated by Kuhn *et al.*,[43] Nyulászi *et al.*[44] and Roesky *et al.*[45]

In this chapter, three imidazol-2-ylidenes (**1a-c**) and two organosilanes (**2**,**3**) were selected to investigate the ability of these compounds to form Lewis pairs, as a function of their substitution pattern (Figure 4).

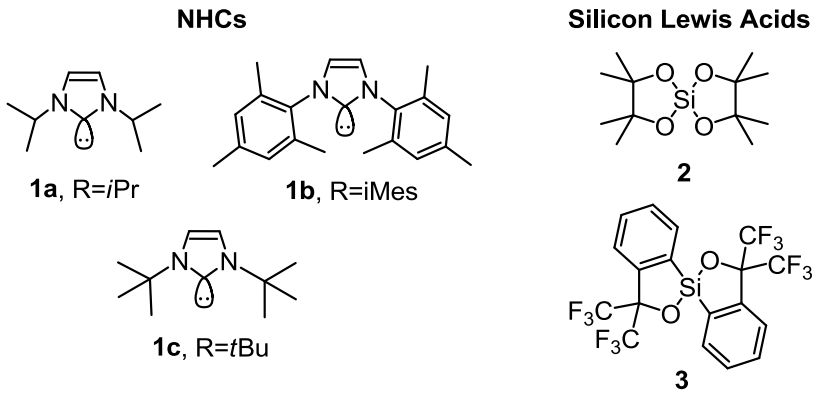

Figure 4. Imidazol-2-ylidenes (**1a-c**) and organosilanes (**2**,**3**) selected for this study.

The two selected spirosilanes can be classified as strain release Lewis acidic silanes.[46] Their acidity relates to the higher tendency of the silicon atom to adopt a hypervalent geometry. The complexation of such Lewis acids with a Lewis base results in the formation of a thermodynamically more favored penta- or hexa-coordinated siliconate, releasing strain around the silicon atom from the tetrahedral

geometry.[27] The ability of these organosilanes to generate pentacoordinate species has already been reported. For instance, the pinacol spirosilane **2** reacts with MeOH in the presence of amines to generate a silicate,[47] while stable pentacoordinate adducts formed from so-called Martin spirosilane **3** with cyanide[48] or fluoride[49-50] anions and amines[51] have been isolated (Scheme 3).[46]

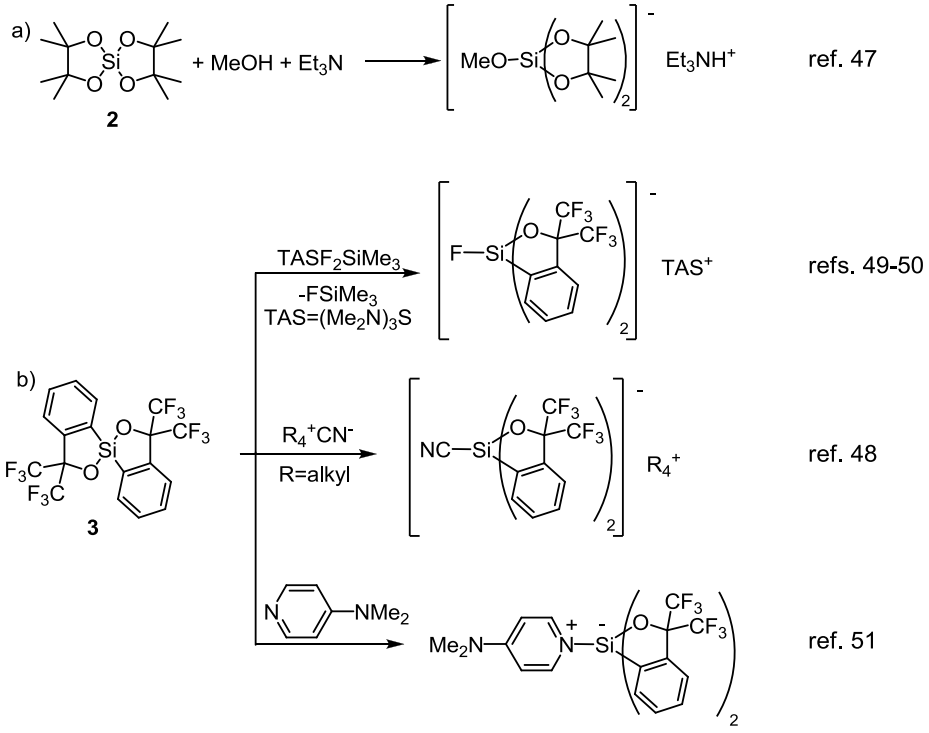

Scheme 3. Reported reactivities of spirosilanes **2** (a) and **3** (b).

1.1. NHCs and silanes in 1 to 1 experiments

Model experiments, employing the NHC and the silane in 1/1 molar ratio, were implemented as a means to investigate the interactions between the two partners. This was monitored by ^{1}H, ^{13}C and ^{29}Si NMR spectroscopy. Typically, equimolar mixtures of **1a-c** and **2** or **3** were analyzed in dry THF-d_8 in Young tubes.

As highlighted in Figure 5, reacting **1a** with **2**, at room temperature, led to a white powder that was sparingly soluble in THF. The ^{1}H NMR spectrum of the resulting solid revealed the presence of only one product, noted **2'a**, attributed to a zwitterionic imidazolium siliconate "classical" Lewis acid/base adduct of **1a** with **2**. By comparing the ^{1}H NMR spectra of the obtained compound with those of the two starting reagents (Figure 6), one can note that both the singlet and the septet

corresponding to the C*H*=C*H* and N-C*H*(CH_3)$_2$ of the imidazole backbone, respectively, are shifted downfield. Moreover, the characteristic signal due to the protons of the silane now appears as two broad singlets. Finally, the ^{29}Si NMR spectrum of **2'a** shows a single signal at δ = -108.6 ppm, attributed to the formation of a pentacoordinate silicon atom, consistently with the other adducts derived from **2** reported in the literature.[52]

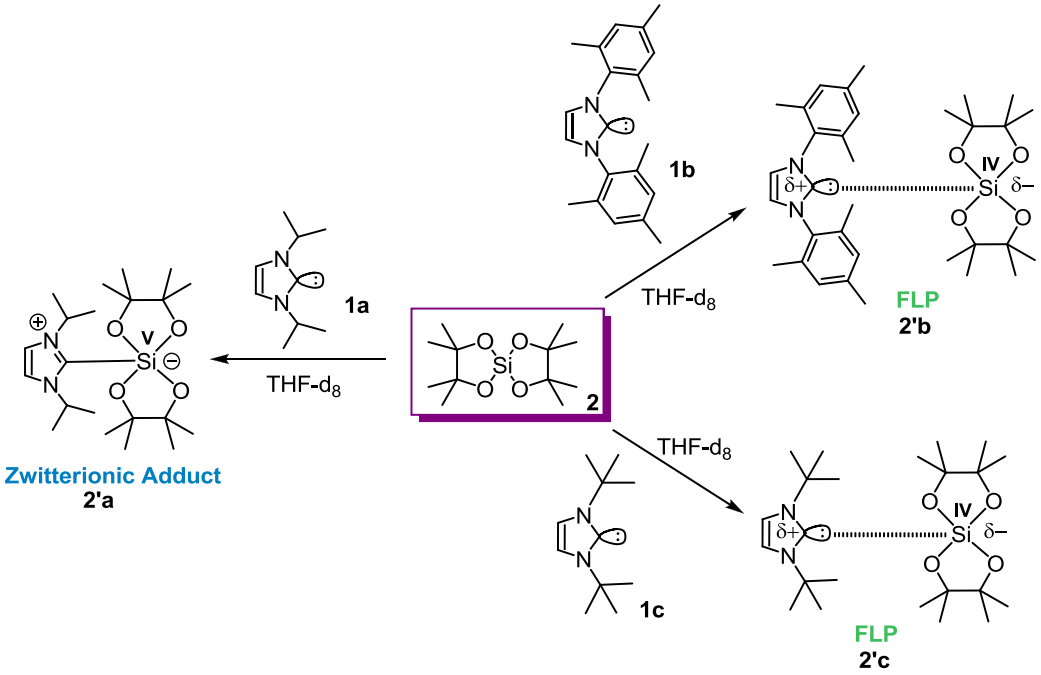

Figure 5. Lewis acid/base pairs formed when reacting NHCs **1a-c** with silane **2**.

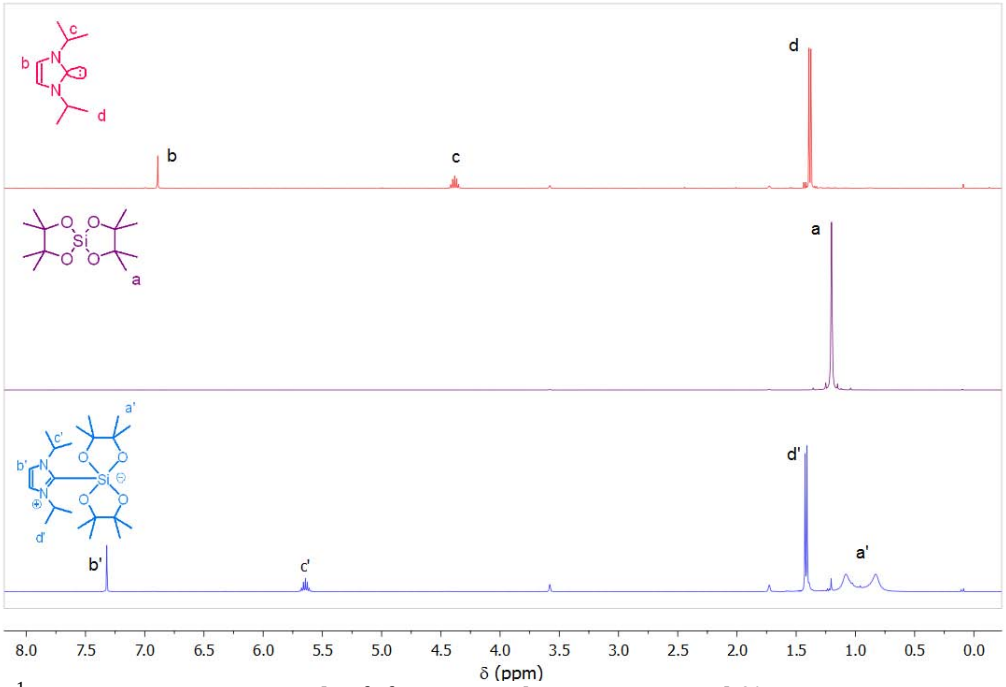

Figure 6. ^{1}H NMR spectra in THF-d$_8$ of, from top to bottom: **1a**, **2** and **2'a**.

Of particular interest, reacting **2'a** with CO_2 (1.5 atm) gave the corresponding NHC-CO_2 adduct (Scheme 4), attesting to the fact that adduct **2'a** can release the NHC.

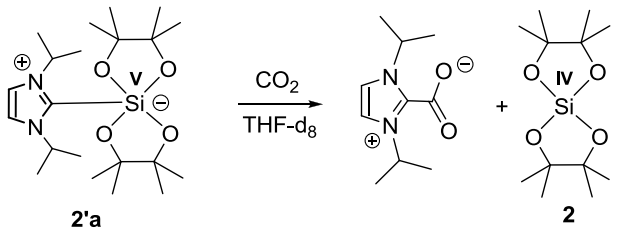

Scheme 4. Formation NHC-CO_2 adduct and release of **2** when reacting **2'a** with CO_2.

Crystals of **2'a**, obtained by slow evaporation of THF from a concentrated solution of **2'a**, were analyzed by X-ray diffraction. Figure 7 shows that **2'a** adopts a distorted trigonal-bipyramidal geometry, owing to the ring strain of the pinacol moieties on the silicon spirocenter (angles: C3-Si-O2: 111.51°, C3-Si-O3: 113.58°, C3-Si-O4: 91.44°, O1-Si-O2: 89.95°, O1-Si-O3: 87.35°). The NHC moiety occupies an equatorial position in this structure, with a Si-C3 distance of 1.950 Å. The C-*H* hydrogen atoms of the isopropyl substituents of the imidazole backbone are pointed to the silicon side (Figure 7a), which allows minimizing the steric hindrance between **2** and **1a**.

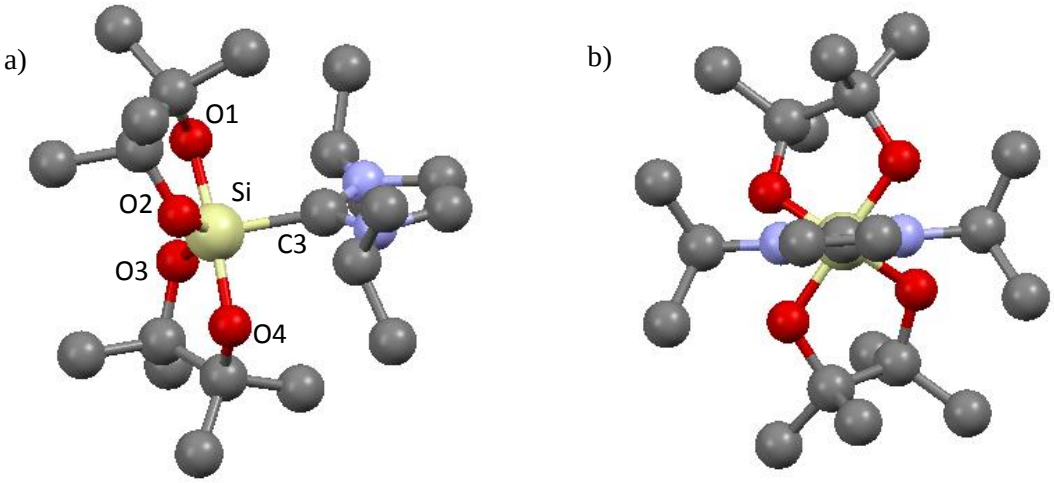

Figure 7. Molecular structure of **2'a** (C: grey, N: blue, O: red, Si: yellow). Hydrogen atoms are omitted for clarity.

These data are consistent with the formation of a stable 1/1 adduct between **1a** with **2**. Adducts between NHCs and SiR_4 acceptors indeed usually feature a trigonal-bipyramidal-type geometry with

NHC moiety adopting either an axial (*i.e.* complexes with SiF_4, Si-C=2.004 Å)[45,53] or an equatorial position (*i.e.* complexes with $SiCl_4$ or $SiBr_4$, C-Si=1.911-1.935 Å).[32,43-45]

In contrast, such adduct could not be formed upon reaction between **1b** and **2** and between **1c** and **2**. Indeed, the same chemical shifts were observed for the protons of the NHC and the silane before and after reaction (see Figure 8 for the case of **2'b**). Moreover, the characteristic signal of the carbenic carbon was detected at 216.8 and 210.4 ppm respectively,[54] in the ^{13}C spectra of compounds **2'b** and **2'c**, while ^{29}Si spectra exhibited only one signal at -43.8 ppm, which is consistent with the presence of tetracoordinate silane moiety.[52] All these observations suggest that combination of more bulky NHCs such as **1b**,**c** with the LA **2** can generate FLPs.[†]

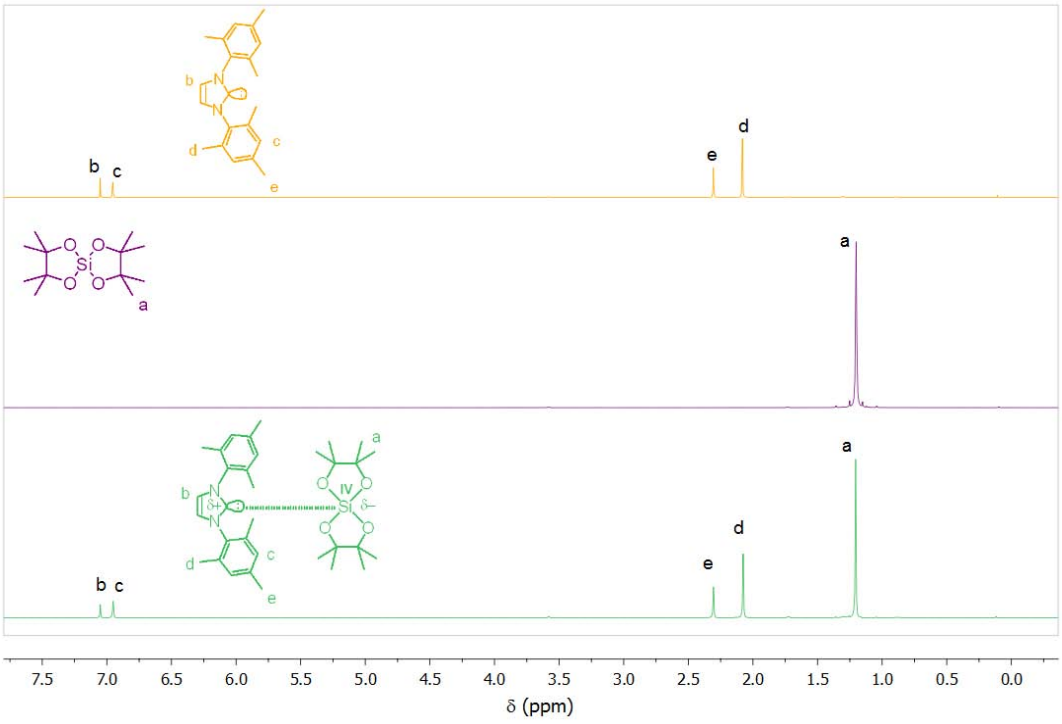

Figure 8. ^1H NMR spectra in THF-d_8 of, from top to bottom: **1b**, **2** and **2'b**.

[†] As already mentioned,[5] NMR spectra of a FLP indicate no interaction between the involved Lewis acid and base. However, it is very unlikely that mixing a Lewis acid with a Lewis base results, in solution, in no interaction at all. Moreover, the term FLP is often closely associated with the reactivity of such a Lewis pair with small molecules (Figure 3).[3] In this chapter, we chose to refer to frustrated Lewis pair when no detectable interaction was evidenced by NMR. Nevertheless, the reactivity of such pairs towards small molecules has not been demonstrated yet; in particular, **2'b** and **2'c** did not prove to trigger the ring-opening reaction of THF.

The geometry observed in **2'a** may explain why FLPs can form upon using more sterically hindered NHCs such as **1b** or **1c** instead of **1a**. Indeed, the presence of a third methyl group, on the N-*C* in the case of the *tert*-butyl substituents of **1c**, as well as the bulkiness of the mesityl groups of **1b**, may preclude the formation of stable adducts. To the best of our knowledge, this represents the first example of a FLP generated from NHCs and silanes.

In contrast, the Martin spirosilane LA **3** formed stable zwitterionic adducts with all tested NHCs (**1a-c**). This was evidenced by ^{29}Si NMR spectroscopy showing characteristic signals at δ = -84.6 to -81.0 ppm, consistent with the existence of pentavalent siliconates of **3**.[49] Thus, in the case of **3**, none of the NHCs formed FLPs but gave stable 1/1 imidazolium siliconate adducts, most probably owing to the higher Lewis acidity of **3** compared to that of **2**.

1.2. Use of NHC-silane pairs

1.2.1. In molecular chemistry

The reactivity of Lewis pairs **2'a-c** was tested toward different substrates. Since FLPs were established to cleave H_2,[10,12] the potential of **2'c** to activate this non-polar molecule was first evaluated (Scheme 5). After 12 h of exposure of FLP **2'c** to H_2 (1 atm) in THF, a white powder precipitated out, the ^{1}H NMR spectrum of which, in DMSO-d_6, showed a singlet at δ=9.03 ppm attributable to an imidazolium proton. A new side set of signals, from δ=1.00 to 1.11 ppm, was also observed. The silicon center was found to be involved in a pentacoordinate derivative (^{29}Si NMR). However, the signal corresponding to Si-*H* of expected compound **4c** could not be detected by ^{1}H NMR spectroscopy. This might be due to the presence of minute amounts of H_2O/air in the reaction vessel. If this was the case, hydrolysis of **2'c** should be considered as a possible side reaction, as illustrated in Scheme 5. Although NHCs hydrolysis was shown to form imidazolium moieties only with an excess of H_2O,[55] FLP **2'c** may favor such a hydrolysis by increasing the acidity of the water molecule. However, the signal corresponding to Si-O*H* could not be detected either on the ^{1}H NMR spectrum.

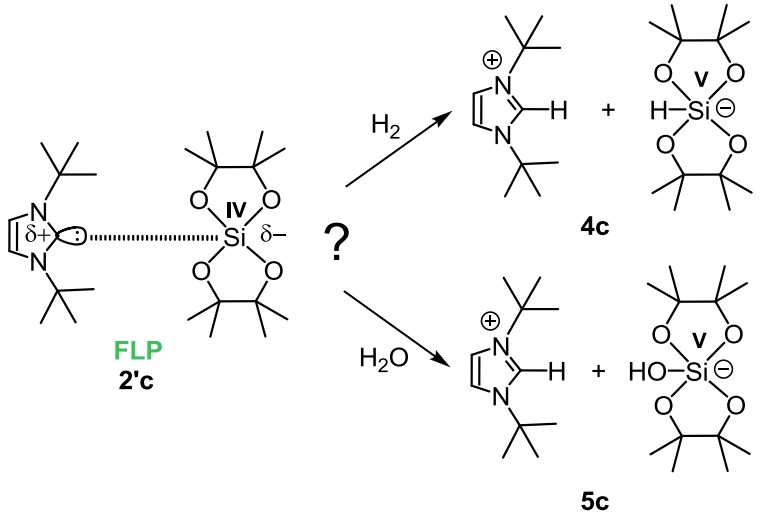

Scheme 5. Cleavage of H_2 with FLP **2'c** resulting in the formation of **4c** or hydrolysis of **2'c** leading to **5c**.

Finally, a ^{29}Si-proton coupled NMR experiment was attempted, as different coupling should be observed for **4c** and **5c**. For instance, the spectrum of Et_3SiH shows a doublet due to $^{1}J_{Si\text{-}H}$ coupling, while Et_3SiOH exhibits only a singlet (Figure 9), the multiplicity of both signals being due to $^{2}J_{Si\text{-}H}$ coupling. In our case, no such $^{1}J_{Si\text{-}H}$ coupling could be detected, ruling out the existence of a SiH (**4c**) in solution. This result would support the hypothesis of Si-OH formation (**5c**). However, the influence of the four oxygen atoms around the Si center of **2** on the $^{1}J_{Si\text{-}H}$ coupling is not known. Thus, more evidence is needed to unambiguously conclude about the generation of **4c** or **5c** from the organic NHC-silane FLP **2'c**.

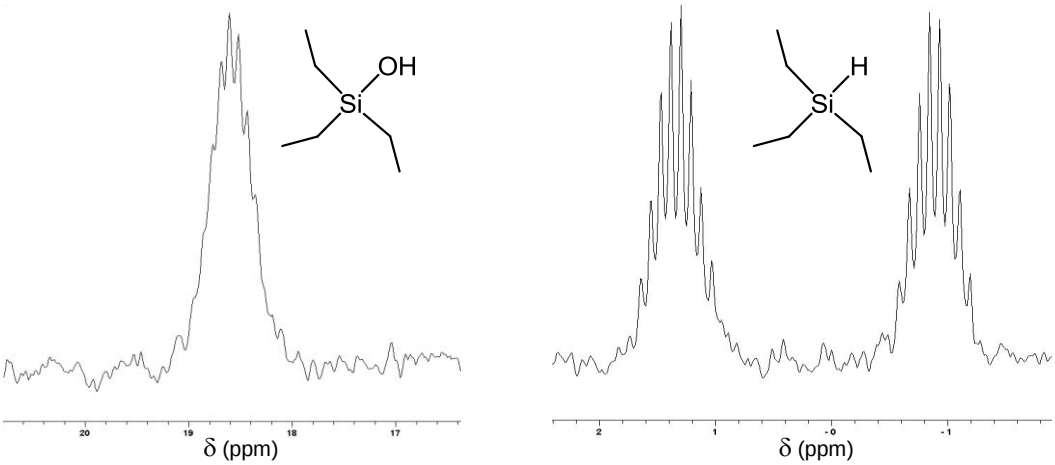

Figure 9. ^{29}Si proton coupled NMR spectra of Et_3SiH and Et_3SiOH.

Experiments are in progress to better analyze the products obtained after exposure of FLP **2'c** to air and/or moisture. The ability of both **2'b** and **2'a** to cleave H_2 is also under investigation.

FLP **2'b** was next used in the benzoin condensation. The mechanism of this reaction has been proposed in 1958 by Breslow for the thiazol-catalyzed benzoin condensation (Scheme 6, see also section 3.2.1., Chap. 1).[56] Reaction intermediates have already been isolated and characterized both by NMR spectroscopy and mass spectrometry, from thiazol- and triazol-type catalysts. For instance, Jordan *et al.*[57] and Lepper *et al.*[58] have evidenced the presence of a protonated form of **6d** (Scheme 6), namely 2-(α-hydroxybenzy1)thiazolium salt (HBT, **6'd**, Scheme 6). Glorius *et al.* have studied intermediates involved in the **1b**-catalyzed conjugate *umpolung* reaction, by electron spray ionization mass spectrometry (ESI-MS).[59] Low intensity signals corresponding to **6** and to the "Breslow intermediate" exhibiting the same *m/z* were detected. More recently, Berkessel *et al.* have isolated a keto form of the "Breslow intermediate", involving a triazole-type NHC.[60]

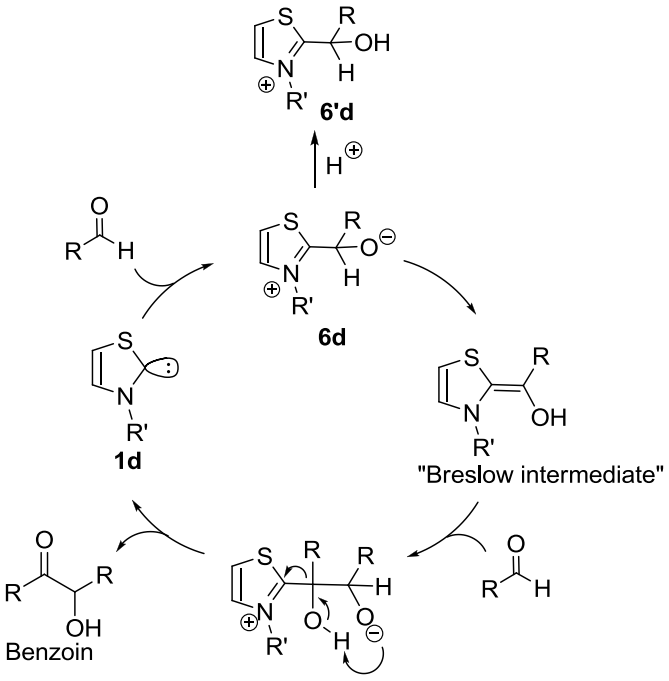

Scheme 6. Benzoin condensation catalyzed by a thiazole-type NHC.[56]

In an attempt to increase yields of the Stetter reaction (see section 3.2.1, Chap. 1), Scheidt *et al.* have used less reactive (more bulky) acylsilanes instead of aldehydes, in order to decrease the formation of benzoin side-products.[61] In the course of their investigations on the mechanism of this so-

called "sila-Stetter" reaction, they have synthesized a thiazolium carbinol (Scheme 7b), that is, a silylated equivalent of **6'd** thought to be involved in the first steps of the mechanism (**7'd**, Scheme 7a).[62] The latter compound can indeed serve as precursor for the generation of 1,4-diketones, after reaction with a chalcone, evidencing the key role of this intermediate. However, efforts to isolate other intermediates by deprotonation of the thiazolium carbinol failed. It is worth mentioning that NHC **1b** was not efficient for the sila-Stetter reaction, the only product observed after 24 h of reaction being benzaldehyde.[61-62]

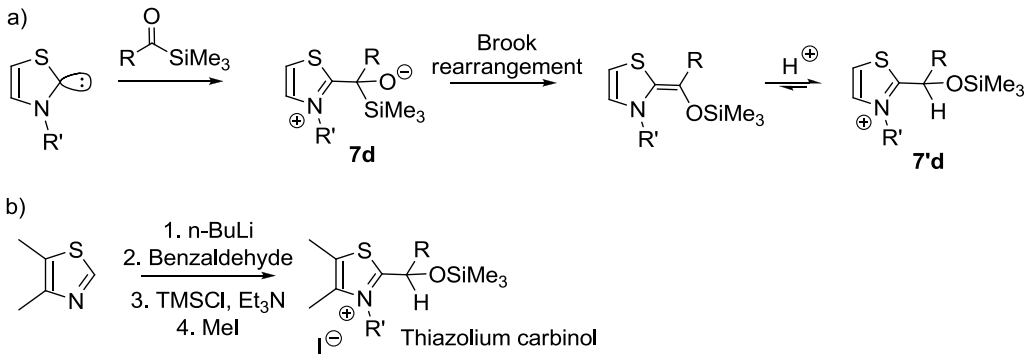

Scheme 7. a) First steps proposed of the sila-Stetter reaction and, b) Synthesis of a putative intermediate of the sila-Stetter reaction.[62]

We hypothesized that the spirosilane LA **2** could be able to quench the zwitterionic intermediate resulting from the attack of the NHC onto a benzaldehyde molecule. Thus, reacting the NHC-silane Lewis pair **2'b** with one equivalent of benzaldehyde, in toluene, led to the precipitation of a white powder.

After work-up, ^{1}H, ^{13}C and ^{29}Si NMR analyses in THF-d_8 of the obtained compound revealed the formation of a new product, and the presence of approximately 10 %mol of the free silane **2**. The ^{1}H NMR spectrum of the new compound exhibited four singlets, from 0.38 to 0.96 ppm, attributable to the eight methyl groups of the silane. In contrast, these methyl protons appeared as a broad set of three singlets in MeOD. The singlet at 6.66 ppm, in THF-d_8, was assigned to the proton at the α-position of the phenyl group, while the proton of the benzaldehyde moiety could not be detected anymore. Moreover, the ^{29}Si NMR spectrum showed a single signal at -113.8 ppm, attesting to the presence of a pentacoordinate silicon center. All these data are consistent with the formation of a 1/1 adduct between

FLP **2'b** and benzaldehyde, noted **8b** in Scheme 8. The latter compound could not be analyzed by ESI-MS, most probably owing to its air sensitivity and to the weakness of the $C_{carbonyl}$-$C_{carbene}$ and O-Si bonds upon ionization. Other characterization by XRay diffraction to isolate **8b** is currently in progress.

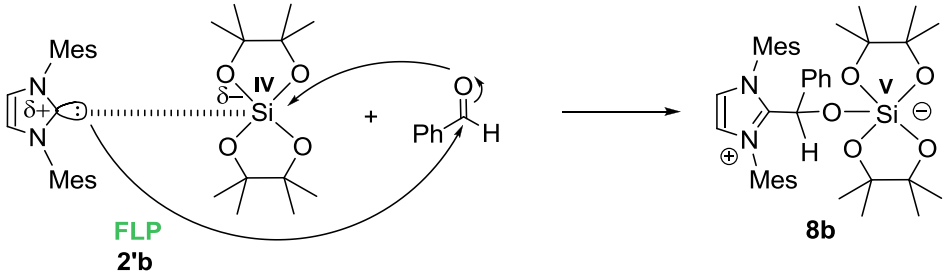

Scheme 8. Synthesis of **8b** from an equimolar mixture of **2'b** and benzaldehyde.

Interestingly, formation of **8b** was found reversible. Indeed, after one day in dry MeOD at RT, the singlet at δ = 1.20 ppm corresponding to the methyl protons of the spirosilane **2** could be detetcted (90%), indicating the presence of the free silane in solution. However, benzaldehyde molecules regenerated from **8b** partly converted into benzoin (40%).

As benzoin is sparingly soluble in MeOH, the ability of **8b** to release benzaldehyde and subsequently produce benzoin was then evaluated in THF. This experiment was conducted at 50 °C, owing to the poor solubility of **8b** in this solvent. Results are summarized in Figure 10.

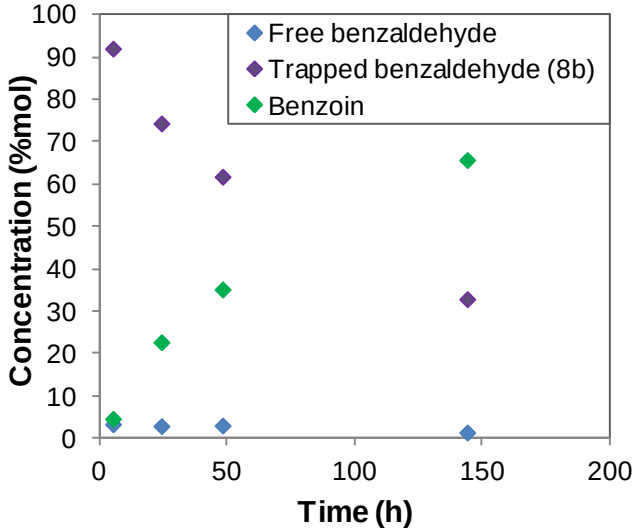

Figure 10. Evolution of the molar concentration of: free benzaldehyde (blue), "trapped" benzaldehyde in the form of **8b** (purple) and benzoin (green) *vs.* time when **8b** was heated in THF-d_8 at 50 °C.

After 6 days at 50 °C, 33% of **8b** were still present, as observed on the ^{1}H NMR spectrum. However, 90% of benzaldehyde released from **8b** was transformed into benzoin. Though the yield in benzoin was lower than that generally obtained upon using a free NHC as catalyst (50-100% after 24 h with 10 %mol NHC, see Chapter 2), these results confirmed that the formation of **8b** is reversible, both in MeOH and in THF as solvents.

The potential of **8b** to trigger the Stetter reaction was also investigated. In this reaction forming 1,4-diketones from an aldehyde and an α,β-insaturated ketone, one challenge is to prevent the aldehyde "self-condensation" generating a benzoin-type compound. As already mentioned, Scheidt *et al.* have proposed to use acylsilanes (instead of aldehydes) to avoid benzoin formation.[61-62] In our case, adduct **8b** was employed as a "benzaldehyde reservoir" that was expected to react with a ketone. An equimolar mixture of **8b** and trans-chalcone was thus heated for 24 h in THF-d_8 at 40 °C (Scheme 9). However, the only detected product on the ^{1}H NMR spectrum was again benzoin (free benzaldehyde/benzaldehyde in **8b**/benzoin = 0.5/1/2.8).

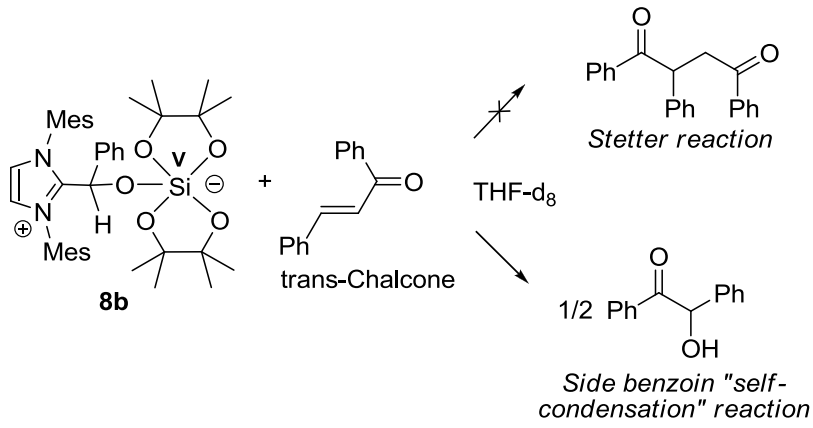

Scheme 9. Attempt to react **8b** with trans-chalcone in a Stetter reaction.

As the polarity of the benzaldehyde moiety in **8b** is virtually inverted, the ability of **8b** to incorporate CO_2 was also assessed (Scheme 10). However, release of the free silane **2** and benzaldehyde along with the precipitation of a white powder were noted in THF-d_8, instead of the isolation of the expected compound with a pentacoordinate silicon moiety and a carbonate bond (Scheme 10). The obtained powder was eventually identified as being the CO_2 adduct of **1b**, namely

1,3-dimesityl-imidazolium-2-carboxylate (**1'b**, Scheme 10). It thus turns out that the reactivity of the NHC prevails over the reactivity of the "aldehyde" moiety, during the manipulation of adduct **8b**.

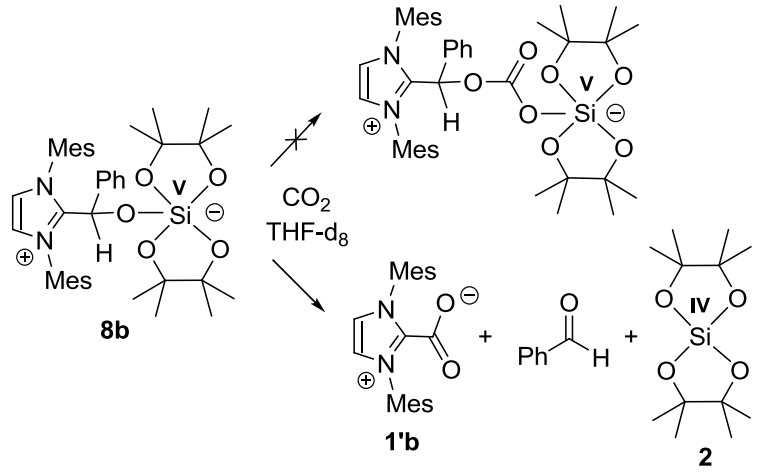

Scheme 10. Reaction of **8b** with CO_2: release of **2** and benzaldehyde and formation of **1'b** was observed by NMR.

In conclusion, novel Lewis pairs utilizing NHCs as bases and tetravalent silanes (SiR_4) as Lewis acids were investigated. Formation of frustrated Lewis pairs NHC-SiR_4, using sterically hindered NHCs, was evidenced for the first time. FLP made of NHC **1c** and silane **2** was shown to react with H_2, forming an imidazolium salt and a pentacoordinate silicon center. However, the accurate structure of the resulting product is still to be established.

The FLP **2'b** was shown to form a 1/1/1 adduct with benzaldehyde, corresponding to the quenched intermediate involved in the benzoin condensation reaction. The generation of this adduct proved reversible in MeOH at RT, and in THF upon heating. This was verified through the synthesis of benzoin. Attempts to employ such an adduct as a "benzaldehyde reservoir" failed, however. For instance, the Stetter reaction could not be performed, the competitive self-condensation of benzaldehyde being the dominant process in this case.

Thus, more experiments are needed to unambiguously state about the reactivity of NHC-silane FLP's. In molecular chemistry, for instance, FLP **2'b** could be employed to quench 1/1 adducts between NHC **1b** and α,β-unsaturated aldehydes. As such reactions of a NHC on an α,β-unsaturated aldehyde are thought to proceed *via* a 1,2-addition,[63-65] the appropriate choice of the α,β-unsaturated

aldehyde may favor quenching of the less thermodynamically stable product from the 1,4-addition (Scheme 11).

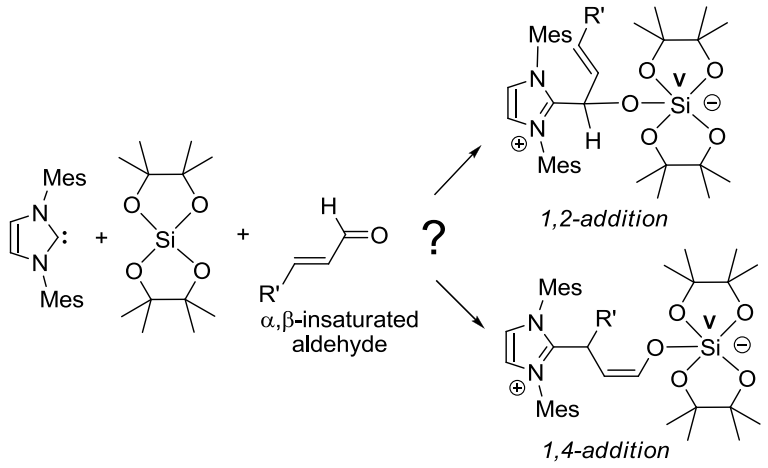

Scheme 11. Possible reaction pathway between FLP **2'b** and α,β-unsaturated aldehyde: 1,2 or 1,4-addition?

1.2.2. For the ROP of propylene oxide

The activation capability of NHC-silane Lewis pairs, involving silanes **2** and **3**, in polymerization reaction experiments were evaluated for the ring opening polymerization (ROP) of propylene oxide (PO). Use of aluminum-based Lewis acids as activators of the ROP of epoxides is well-documented.[66-71] For instance, triisobutyl aluminum serves both to activate the monomer substrate and to decrease the basicity of the alkoxide active centers, by forming so-called "ate" complexes, allowing for both enhanced polymerization rates and minimized occurrence of transfer reactions.

Spirosilanes **2** and **3** were tested here as organic activators of PO, in conjunction with NHCs as Lewis bases. Scheme 12 shows the expected reaction pathway of such a doubly assisted ROP of PO.

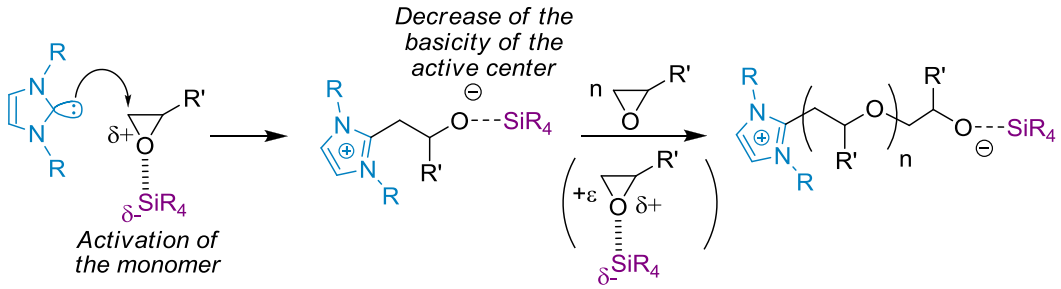

Scheme 12. Activation mode using silanes and NHCs as Lewis pairs for the ROP of propylene oxide.

As **2'b** and **2'c** were shown to behave as FLPs, they were employed as such in the reaction vessel to trigger the ROP of PO. In contrast, as **2'a** and **3'a-c** displayed a low activity, due to their quenching, the NHC was added on a solution of the silane-activated PO to prevent adduct formation. In both cases, the molar mass of the final polymer was expected to be controlled by the amount of NHC ($DP_{n,theo}$ = ([PO]/[NHC]) × conversion).

However, the use of silane **2** as LA did not improve the results obtained with free NHCs used alone.[1] Indeed, poor yields were noted in THF and in bulk as well at 50 °C (<10%), whatever the NHC initiator. Such a low efficiency of the NHC-silane pairs might be explained by a lack of interaction between the silane **2** and PO. This was also suggested by ^{1}H and ^{29}Si NMR spectra, performed at RT from an equimolar mixture of PO and **2**, which did not show any signal that could be attributable to an activation of the epoxide moiety by the Lewis acid **2**.

In contrast, LA **3** was able to polymerize PO by itself, that is in total absence of the NHC (Table 1, entry 3). This may be due to the higher Lewis acidity of **3** compared to **2** (as already mentioned). The polymerization likely proceeded *via* a cationic mechanism (Scheme 13a, dry conditions). Previous works by Penczek *et al.*,[72-73] regarding the Lewis acid (mainly boron and aluminum)-mediated cationic polymerization of epoxides, have shown that initiation involves the monomer substrate which is activated by a Bronsted acid moiety, due to H_2O traces or deliberate addition of an alcohol (Scheme 13b).

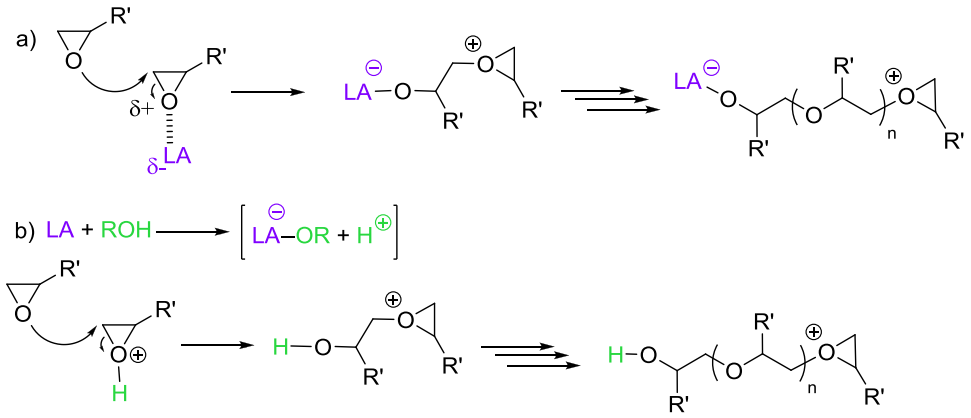

Scheme 13. Cationic polymerization of epoxides by the ACEM using: a) a Lewis acid in dry conditions; b) a Lewis acid with H_2O traces or an alcohol.

Generally speaking, the propagation may occur both *via* active chain end mechanism (ACEM) and activated monomer mechanism (AMM), as depicted in Scheme 14. Cyclic oligomers can form by back-biting reactions in the ACEM (Scheme 15). Control over the polymerization is thus generally improved by favoring the occurrence of the AMM, though relatively limited molar mass values are achieved. The occurrence of the AMM is usually favored by maintaining a low PO concentration in the medium by slow addition of the monomer and/or by addition of an alcohol molecule.

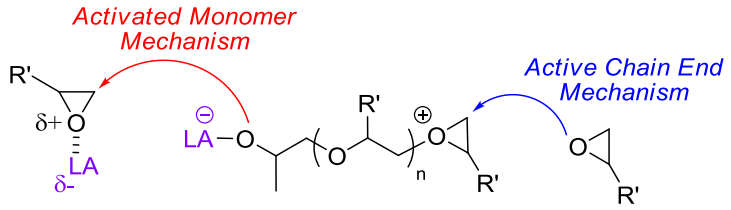

Scheme 14. Cationic ROP of epoxides (counterions omitted): activated monomer mechanism (AMM) *vs.* active chain end mechanism (ACEM).

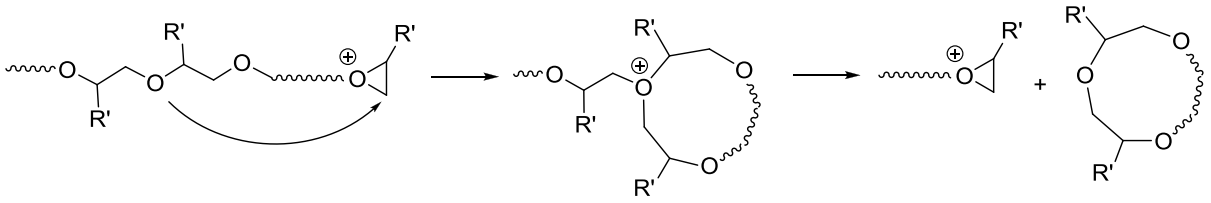

Scheme 15. Formation of cyclic oligomers by back-biting reactions during the cationic polymerization of epoxides by active chain end mechanism (counterions omitted).

The amount of cyclic oligomers can indeed be reduced thanks to the presence of the alcohol, playing the role of a reversible chain transfer agent/initiator, which controls the polymer chain length (Scheme 16). In this case, the polymer chain exists in a (neutral) dormant form with a terminal OH-functionality. Under such conditions, back-biting is minimized, allowing for the synthesis of well-defined polyethers.

To favor AMM over ACEM, a slow monomer addition process is also beneficial as the instantaneous concentration of monomer is kept low. In the ideal case where the ACEM is totally suppressed, the molar mass of the final polymer is controlled by the initial [ROH]/[monomer] ratio and a linear relationship is observed between M_n and [ROH]/[monomer]. However, exclusive AMM is

rarely observed. Monomer starved conditions have also been used, for instance, to better control the anionic polymerization of epoxides.[74]

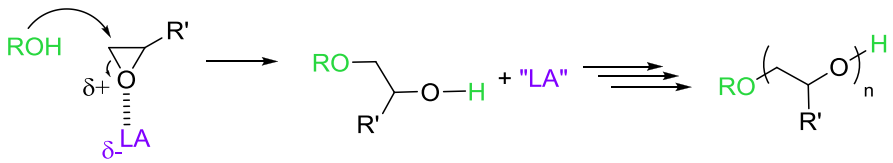

Scheme 16. Nucleophilic attack of an alcohol (water) molecule on a LA-activated epoxide and propagation by the AMM.

A series of experiments was carried out to achieve PPO's in a controlled manner from **3** as activator (Table 1). For instance, the sequential addition of the NHC on **3**-activated PO was performed at low temperature (-30 °C, entry 4), in order to limit the occurrence of the cationic mechanism (Scheme 13a). Next, an alcohol initiator (benzyl alcohol) was introduced, the PO monomer being slowly added (continuous addition) on a **3**/alcohol 0.1/1 mixture. However, only poor yields (<30%) and low molar masses (<2,000 g/mol) could be achieved in all cases.

Table 1. ROP of PO in bulk mediated by **1a**, **2**, **3** or benzyl alcohol.

Entry	Lewis Acid	Lewis Base	[PO]/[LA]/[LB]	*T* (°C)	*t* (days)	Yield[a] (%)	$M_{n,theo}$[b] (g/mol)	$M_{n,SEC}$[c] (g/mol)	*Đ*[c]
1	**2**	-	250/1/-	50	5	0	-	-	-
2	-	**1a**	250/-/1	50	5	27	3,900	4,500[d]	1.24
3	**3**	-	250/1/-	25	1	10	-	2,400	1.30
4	**3**	**1a**	380/1/1	-30/50[e]	5	11	2,400	1,600	1.15
5[f]	**3**	ROH	104/1/0.1	25	1	30	1,800	2,900	1.13
6[g]	**3**	ROH	104/1/0.1	25	1	20	1,200	2,100	1.10

[a] Yield was determined by gravimetry. [b] Theoretical molar masses: $M_{n,theo}$ = ([PO]/[LB]) × yield × M_{PO} [c] SEC in THF calibrated with polystyrene standards was used for characterization. [d] Second population in the low molar mass region (≈ 10% of the total distribution). [e] Addition of **1a** on the **3**-activated PO was realized at -30 °C and the reaction was then conducted for 5 days at 50 °C. [f] Benzyl alcohol (ROH) was used as initiator, the addition of PO was sequential (0.5 mL every 30 min for 3 h). [g] Benzyl alcohol (ROH) was used as initiator, the addition of PO was continuous (3 mL/h for 1 h).

Hence, none of the LA's **2** and **3** was able to induce a controlled/living ROP of PO when used alone or in conjunction with NHCs **1a-c**. It can be speculated that a more appropriate design of the silane Lewis acid partner is needed to trigger ROP by a "push/pull" activation mechanism. One condition to fulfill is that the latter activator compound should not directly polymerize PO by a cationic mechanism. It is worth mentioning that, although **3** showed a higher Lewis acidity compared

to **2**, none of the other monomer substrates tested ((meth)acrylics, dienes, …) could be activated. It thus appears that stronger Lewis acids are required. In the next section, we discuss the utilization of a boron Lewis acid, namely tris(pentafluorophenyl)borane ($B(C_6F_5)_3$), as an alternative to the SiLA's.

2. NHC-borane as Lewis pairs

As already mentioned, methyl methacrylate (MMA) was here selected as a vinyl monomer to get an insight into the ability of Lewis pairs to trigger a polymerization reaction *via* a cooperative activation. Boron (III) derivatives exhibit a high Lewis acid character,[75-76] which can compete with metal-based species, depending on substituents on the boron center. Tris(pentafluorophenyl)borane ($B(C_6F_5)_3$), a commercially available reagent, was chosen as the boron-based Lewis acid to activate MMA. $B(C_6F_5)_3$ proved efficient in a variety of organic transformations,[77-78] including when involved in FLPs with phosphines and NHCs as Lewis bases.[79-80] In polymer synthesis, $B(C_6F_5)_3$ also served to catalyze the synthesis of silicones[81] and as (co)-catalyst for the cationic polymerization of dienes,[82-83] styrenics[84-86] and propylene oxide.[87]

Not only NHCs were selected as Lewis bases,[88] but, two phosphines, namely tributylphosphine and tri-*tert*-butylphosphine for a comparison purpose. The principle of such a $B(C_6F_5)_3$/NHC doubly activated zwitterionic polymerization of MMA is presented in Scheme 17. In some cases, addition of a NuE type functionalizing agent at the completion of the polymerization was attempted. As depicted in Scheme 18, it is expected that both the imidazolium and borane moieties can be displaced, so as to introduce chain ends (in both α- and ω-positions). The leaving capability of the imidazolium moiety has already been evidenced in the context of NHC-initiated polymerizations of ethylene and propylene oxides giving access to α-Nu, ω-E PPO's and PEO's.[1,89]

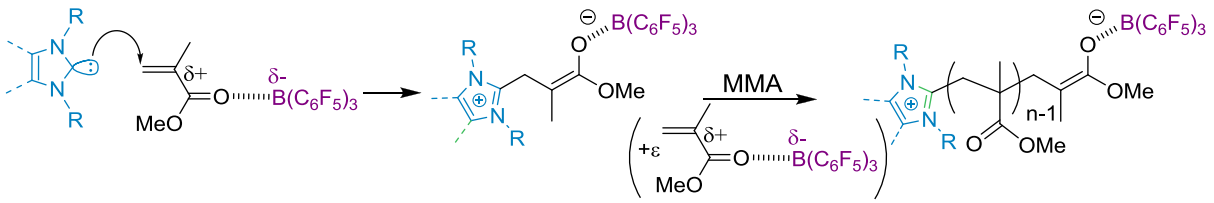

Scheme 17. Dual activation of MMA polymerization using a NHC and $B(C_6F_5)_3$ Lewis pair.

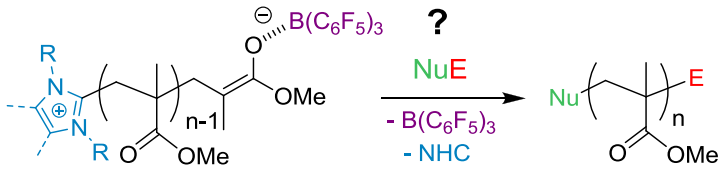

Scheme 18. Addition of a NuE-type functionalizing agent on a PMMA chain grown by zwitterionic polymerization using a NHC and $B(C_6F_5)_3$ Lewis pair.

It is worth pointing out that, in the course of this PhD work, Chen *et al.* have reported the polymerization of several (meth)acrylates by Lewis pairs as activating systems.[25-26] Lewis bases used by the authors included NHCs, while Lewis acids consisted of an alane, i.e. an aluminum LA (Scheme 1). Such a dual activation (alane is thought to activate the monomer substrate while LB initiates the polymerization) led to PMMA's within 1 to 60 min quantitatively, polymers obtained exhibiting molar masses from 26,600 to 600,000 g/mol (targeted molar mass = 80,000 g/mol) with disperties ranging from 1.17 to 1.77. However, the influence of the nature of the Lewis pair (i.e. FLP *vs.* 1/1 adduct) on the polymerization was not assessed, since the LB initiator was added on the LA-activated monomer solution, precluding any interaction between LA and LB. Although the structure of the resulting polymers remained unclear, several features of these polymerizations were unlighted. For instance, *i)* 1/1/1 adducts between Lewis base/monomer substrate/alane were isolated, *ii)* the reaction was shown to proceed *via* a bimetallic pathway (i.e. through the addition of such 1/1/1 adduct on an activated monomer moiety).

It is important to note that attempts by Chen *et al.* to use metal-free Lewis acids, such as $B(C_6F_5)_3$ instead of alanes, were unsuccessful.

In another contribution, Chen *et al.* evidenced that NHCs were able to directly initiate the polymerization of the same (meth)acrylic monomers mentioned above, in total absence of a Lewis acid.[90] Such "organopolymerization" reactions could only be triggered in DMF as solvent, likely *via* a zwitterionic mechanism (see Chapter 1 of this manuscript, section 3.3.3.).

In this section, the interaction of NHC Lewis bases with $B(C_6F_5)$ as Lewis acid was (re)investigated. The ability of such pairs to trigger the polymerization of MMA was next evaluated.

Some kinetics and mechanism considerations are also discussed, in light of the structures of the obtained PMMA's, and on the basis of the results obtained by DFT calculations.

2.1. Investigations on the LB/B(C_6F_5)$_3$ interactions and selection of the Lewis pairs

Three "bare" NHCs (**1a**,**b**,**e**, Figure 11) were selected as Lewis bases. NHC **1a** proved efficient for a variety of (macro)molecular reactions.[1,37-38,89] NHC **1b**, bearing bulky mesityl groups, was also chosen. Finally, NHC **1e**, where methyl groups were substituted for the hydrogen atoms located at the 4,5 positions as in **1a**, was also tested.

The latter choice can be justified as follows. A "side reaction" that can occur while reacting NHCs with B(C_6F_5)$_3$ is the formation of a NHC-borane adduct at the 4-position of the NHC (instead of 2-). For instance, equimolar mixture of 1,3-di-*tert*butylimidazol-2-ylidene (**1c**) and B(C_6F_5)$_3$ were shown to generate a FLP at low temperature (-60 °C).[5-6] In contrast, stirring the same equimolar mixture at RT for few hours, resulted in the isolation of a 1/1 adduct, the borane moiety being attached to the 4-position of the NHC backbone (Scheme 19).[6] The formation of this "abnormal"[91-92] carbene ligand involves the migration of a proton from the 4 to the 2-position. Methyl groups in position 4 and 5 also increase the Lewis basicity of **1e**, in comparison to **1a**.

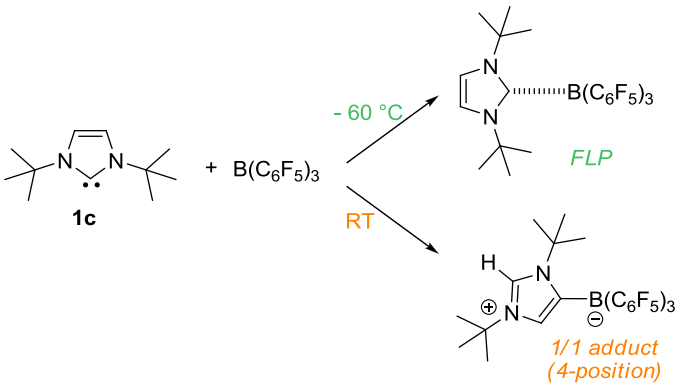

Scheme 19. Products formed while mixing NHC **1c** and B(C_6F_5)$_3$ at -60 °C or at RT.

Two phosphines, namely tributylphosphine (**9a**) and tri-*tert*-butylphosphine (**9b**) were also selected (Figure 11). The sterically hindered phosphine **9b** was reported to generate a FLP with B(C_6F_5)$_3$.[3] In contrast, phosphine **9a** is less bulky and less nucleophilic and can form a "classical"

LA/LB adduct with $B(C_6F_5)_3$.[93] Such adduct was thought to liberate both the free LA and LB upon heating, which further rearrange into the zwitterionic species $[Bu_3P(C_6F_4)BF(C_6F_5)_2]$.[93]

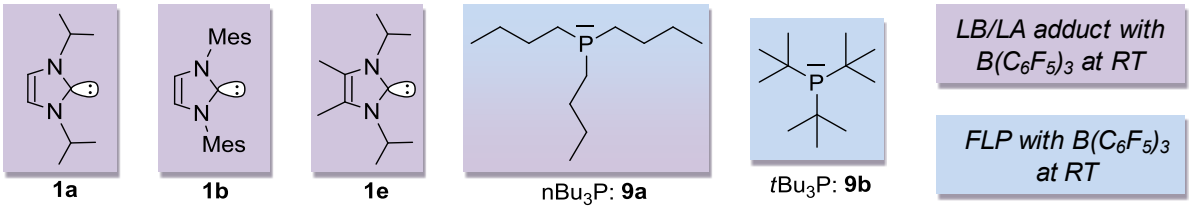

Figure 11. NHCs and phosphines used in this study and summary of their interactions with $B(C_6F_5)_3$ (in purple: formation of a 1/1 adduct, in blue: formation of a FLP).

Molecular interactions between the three NHCs and $B(C_6F_5)_3$ were first studied by NMR analysis of equimolar mixtures in toluene-d_8.[‡] Results of these studies are summarized in Figure 11. Analysis by ^{11}B NMR spectroscopy is of particular interest as it allows studying the environment of the boron atom of the LA partner.

For instance, ^{11}B NMR spectrum of the "free"[§] $B(C_6F_5)_3$ showed a broad signal at $\delta \approx 53$ ppm. In contrast, all spectra obtained from mixtures of this LA with the NHCs **1a**,**b**,**e** exhibited a sharp signal at $\delta \approx$ -22 ppm, attributable to the tetracoordinate boron center due to the formation of a NHC/$B(C_6F_5)_3$ adduct. A similar chemical shift (δ = -15.6 ppm) has already been reported for a 1,3-bis(2,6-diisopropylphenyl)-1,3-imidazol-2-ylidene/$B(C_6F_5)_3$ adduct.[5]

In the case of **1a**,**b**, formation of an adduct at the 2-position of the NHC was also supported by ^1H NMR spectroscopy, by evaluating the integrals corresponding to the C*H*=C*H* protons. Thus, the three chosen NHC Lewis bases generated 1/1 adducts with $B(C_6F_5)_3$; as shown in purple color in Figure 11.

The ability of such Lewis pairs to trigger the polymerization of MMA was next investigated. In order to avoid quenching between the LA and the LB moieties, and formation of the aforementioned 1/1 adduct, addition of a solution of LB onto a solution of LA and the monomer was implemented.

[‡] THF or other coordinating solvents cannot be used due to interactions with $B(C_6F_5)_3$.

[§] The purification of $B(C_6F_5)_3$ is quite a tedious process.[94] Indeed, it was reported to form several adducts with water ($[(C_6F_5)_3B(OH_2)]$, $[(C_6F_5)_3B(OH_2)]\bullet H_2O$ and $[(C_6F_5)_3B(OH_2)]\bullet 2H_2O$).[95-96] The purity of $B(C_6F_5)_3$ may be evaluated by ^1H and ^{19}F NMR analyses,[96] though this technique is not precise enough to guarantee the absence low amounts of water.

Lewis bases **1a**,**b**,**e** and **9a**,**b** were then added onto a toluene solution of 2 equivalents of MMA•$B(C_6F_5)_3$. Main results are presented in Table 2.

Table 2. Polymerization of MMA induced by **1a**,**b**,**e** and **9a**,**b** as Lewis bases and $B(C_6F_5)_3$ as Lewis acid (T = 20 °C, [MMA] = 0.94 M in toluene, quenching = 5% HCl in MeOH).

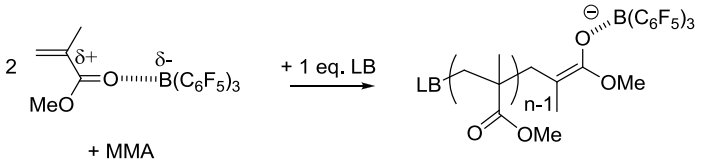

Entry	LB	$[LB]_0/[LA]_0/[MMA]_0$	t (h)	Conv (%)[a]	$M_{n,SEC}$ (g/mol)[b]	D[b]
1	**1a**	1/2/165	96	0	-	-
2	**1b**	1/2/165	1.5	100	7,200	2.14
3	**1e**	1/2/165	1.3	90	11,000	1.53
4	**1e**	1/-/165	96	1	-	-
5	**9a**	1/2/165	96	100	8,700	2.40
6	**9b**	1/2/165	96	4	-	-
7	-	-/2/165	96	0	-	-

[a] Conversion was calculated by ^{1}H NMR in $CDCl_3$ (Figure S3) comparing the integral value of the peak of the polymer (-CCH_3 peaks δ=0.8, 1.0 and 1.2 ppm) to that of the monomer signal (CH_2=C δ=5.5 or 6.0 ppm). [b] SEC in THF calibrated with polystyrene standards was used for characterization.

It can be observed that, neither NHC **1a** nor phosphine **9b** was able to trigger the polymerization of MMA (entries 1 and 4). In contrast, **1b**,**e** and **9a** afforded PMMA's, after 1.5 h with the NHCs (entries 2-3), and after 4 days with phosphine **9a** (entry 5). Hence, the nature of the Lewis pair (FLP *vs.* adduct) does not allow predicting the efficiency of the system. For instance, **1a** and **1e** both generate a 1/1 adduct with $B(C_6F_5)_3$, but only **1e** can mediate MMA polymerization. Although phosphine **9b** and $B(C_6F_5)_3$ form a FLP, they do not allow polymerizing MMA. In contrast, as observed by Chen *et al.*,[25-26] while **9b** forms an FLP with $Al(C_6F_5)_3$, adding 1 eq. of **9b** on a $Al(C_6F_5)_3$-MMA solution allowed triggering the polymerization of MMA (100% conversion with less than an hour), likely because of the higher Lewis acidity of the alane compared to the borane with the same substituents. These data can be explained by the fact that Lewis pairs were not employed as such, since the formation of the pair is avoided by a specific order of addition of the activators.

PMMA's obtained from **1b** and **9a** showed multimodal molar masses, as can be seen on the SEC traces (RI detector, Figure 12a for the chromatogram corresponding to entry 2).

Some populations could be ascribed to back-biting reactions, as detected by the UV signal at λ = 305 nm, which is reminiscent to propagating enolate generated by anionic polymerization of MMA.[97-98]

In the case of **1e**, a shoulder in the low molar mass region of the main RI signal was also observed (Figure 12b). Amongst all tested NHCs, **1e** allowed us to relatively well control the polymerization of MMA: $M_{n,SEC}$ = 11,000 g/mol *vs.* $M_{n,theo}$ = 14,800 g/mol. The resulting PMMA was predominantly syndiotactic (*mm/mr/rr* = 0.01/0.20/0.79 with **1e** and $B(C_6F_5)_3$), consistently with observations made with polymerization of MMA induced by $Al(C_6F_5)_3$ and NHC (*mm/mr/rr* = 0.02/0.23/0.75 with **1c** and $Al(C_6F_5)_3$).[25] Control experiments using NHC **1e** or $B(C_6F_5)_3$ alone did not yield any PMMA (entries 4 and 7), evidencing that both activators were needed to polymerize MMA.

As NHC **1e** allowed for a better control of the polymerization, it was chosen as the Lewis base in the following parts of this work. The next section focuses on parameters influencing the zwitterionic polymerization of MMA mediated by $B(C_6F_5)_3$ and NHC **1e**. Experiments will be compared to that reported in entry 3 of Table 2.

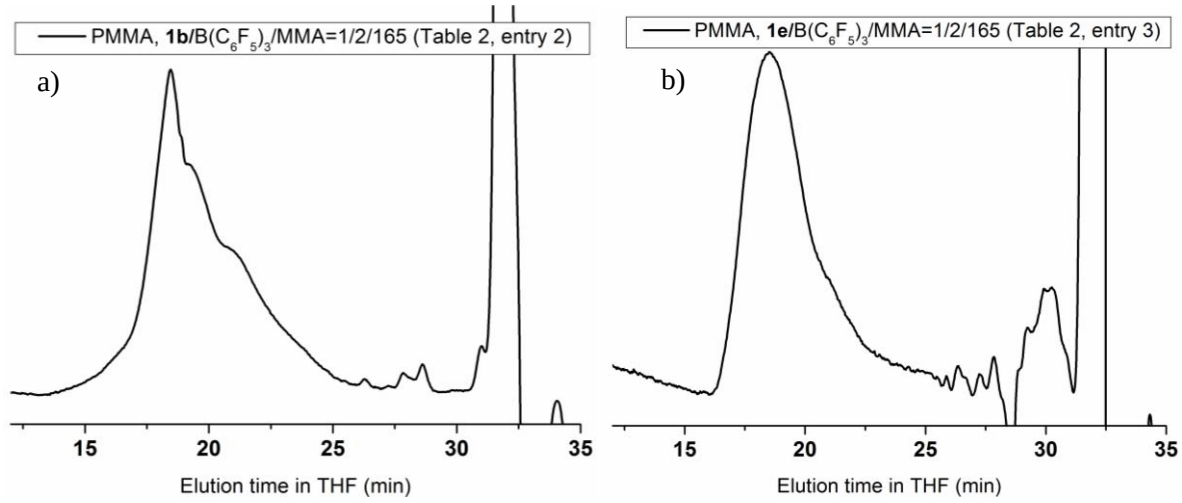

Figure 12. SEC traces (RI detector) of: a) PMMA obtained with NHC **1b** and $B(C_6F_5)_3$ (Table 1, entry 2); b) PMMA obtained with NHC **1b** and $B(C_6F_5)_3$ (Table 1, entry 3).

2.2. Factors influencing the polymerization of MMA with 1e/B(C_6F_5)$_3$

2.2.1. *Lewis acid/Lewis base ratio*

The LA/LB ratio was varied, from 1 to 2.4, to study the effect of B(C_6F_5)$_3$ on the quality of control over the polymerization (see Table 3 and Figure 13 for related SEC traces). For instance, 1 equivalent of B(C_6F_5)$_3$ compared to NHC **1e** did not yield any PMMA, even after prolonged reaction time (4 days, entry 1). In contrast, a LA/LB ratio higher than 1 allowed the polymerization to take place (entries 2-5). An excess of B(C_6F_5)$_3$ relative to the NHC is thus needed to efficiently activate MMA.

Table 3. Polymerization of MMA in the presence of NHC **1e** and B(C_6F_5)$_3$, T = 20 °C, [MMA] = 0.94 M in toluene, quenching = 5% HCl in MeOH.

Entry	$[\mathbf{1e}]_0/[B(C_6F_5)_3]_0/[MMA]_0$	t (h)	Conv (%)[a]	$M_{n,SEC}$ (g/mol)[b]	$Đ$[b]
1	1/1/165	96	0	-	-
2	1/1.2/165	96	50	multimodal	
3	1/1.6/165	3	87	5,400	1.97
4	1/2/165	1.3	90	11,000	1.53
5	1/2.4/165	1	100	multimodal	

[a] Conversion was calculated by ^{1}H NMR in $CDCl_3$ (Figure S3). [b] SEC in THF calibrated with PS standards was used for characterization.

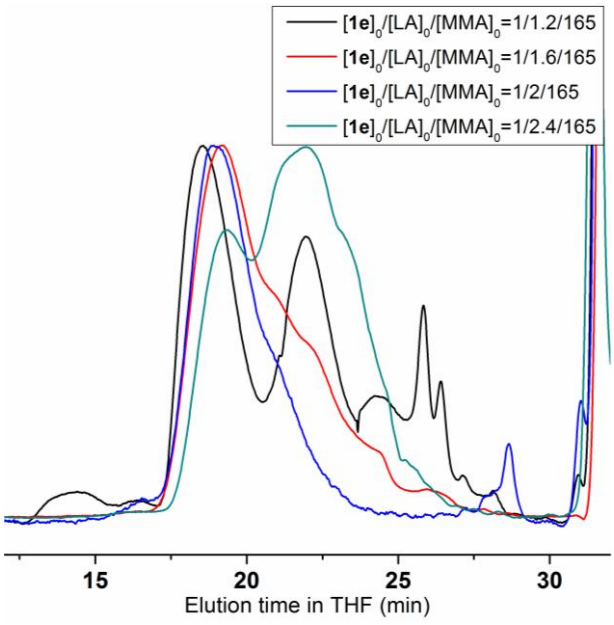

Figure 13. SEC traces (RI detector) of PMMA's obtained with NHC **1e** and B(C_6F_5)$_3$ using different initial ratios $[\mathbf{1e}]_0/[B(C_6F_5)_3]_0$ (Table 3, entries 2-5).

As expected, a higher amount of $B(C_6F_5)_3$ increased the polymerization rate: from 50% conversion after 4 days with a ratio of LA/LB = 1.2, to 100% within 1 h with a ratio of LA/LB = 2.4. A PMMA having a $M_{n,SEC}$ rather close to $M_{n,theo}$, and featuring a monomodal SEC profile was obtained only with a LA/LB ratio equal to 2 (entry 4, Figure 13). The SEC trace (RI and UV detectors) of the PMMA formed from a LA/LB of 1.6 (entry 3) showed several populations, similarly to that of the PMMA obtained from NHC (Table 2, entry 2). Thus, the LA/LB ratio was kept equal to 2 in the following part of this work.

2.2.2. *Temperature*

One strategy to favor propagation over side reactions (transfer and/or termination) in "living" anionic polymerization of MMA is to lower the temperature.[97-98] Increasing the temperature, from -60 °C to 20 °C, allowed enhancing the reaction rate in our conditions (Table 4). For instance, at T = -60 °C, no polymer was obtained after 3 h (entry 1), while 90% conversion were reached after 1.3 h at 20 °C (entry 3). Although the kinetics was slower at 0 °C than at 20 °C (entry 2 *vs.* entry 3), the corresponding SEC trace showed three different signals (RI detector), witnessing poor control at 0 °C.

It is also worth mentioning that, upon conducting the reaction at 50 °C (entry 4), we observed that the conversion was somehow limited to 40%, even after prolonged period of reaction. Though, in this case the dispersity was lower (1.3), the M_n value obtained by SEC was about twice smaller than the targeted value (based on an initial ratio between MMA and NHC **1e**, assuming that the NHC plays the role of initiator). It thus appeared that the probability of side reactions could be minimized at 20 °C.

Table 4. Polymerization of MMA in the presence of NHC **1e** and $B(C_6F_5)_3$, at different temperatures, [MMA] = 0.94 M in toluene, quenching = 5% HCl in MeOH.

Entry	$[\mathbf{1e}]_0/[B(C_6F_5)_3]_0/[MMA]_0$	T (°C)	t (h)	Conv (%)[a]	$M_{n,theo}$ (g/mol)[b]	$M_{n,SEC}$ (g/mol)[c]	D[c]
1	1/2/165	-60	3	0	-	-	-
2	1/2/165	0	2	72	11,900	multimodal	
3	1/2/165	20	1.3	90	14,800	11,000	1.53
4	1/2/165	50	0.5	40[d]	6,600	3,600	1.33

[a] Conversion was calculated by ^{1}H NMR in $CDCl_3$ (Figure S3). [b] Calculated as follows: $M_{n,theo} = ([MMA]_0/[\mathbf{1e}]_0) \times conv \times M_{MMA}$, assuming that NHC **1e** plays the role of initiator. [c] SEC in THF calibrated with PS standards was used for characterization. [d] The conversion was still 40% even after 1 h of reaction.

2.2.3. *Concentration*

It was expected here that molar masses could be varied by changing the initial ratio of MMA to NHC **1e**. Results are summarized in Table 5. The initial concentration in NHC **1e**, $[\mathbf{1e}]_0$, was kept constant and MMA was progressively added (entries 1 to 4, see Figure 14a for related SEC traces). Targeted M_n values thus increased, from 2,000 to 33,000 g/mol, in theory. Almost quantitative conversions were reached within 1.5 h, and M_n values obtained by SEC were relatively close to expected ones (e.g. 2,400 *vs.* 1,900 g/mol for a targeted DP of 20, entry 1).

However, most of SEC traces showed two distinct populations, indicative of the growth of PMMA chains by at least two different types of active species. Interestingly, PMMA obtained with an initial ratio of $[MMA]_0/[\mathbf{1e}]_0$ =165/1 exhibited a monomodal SEC trace (entry 3).

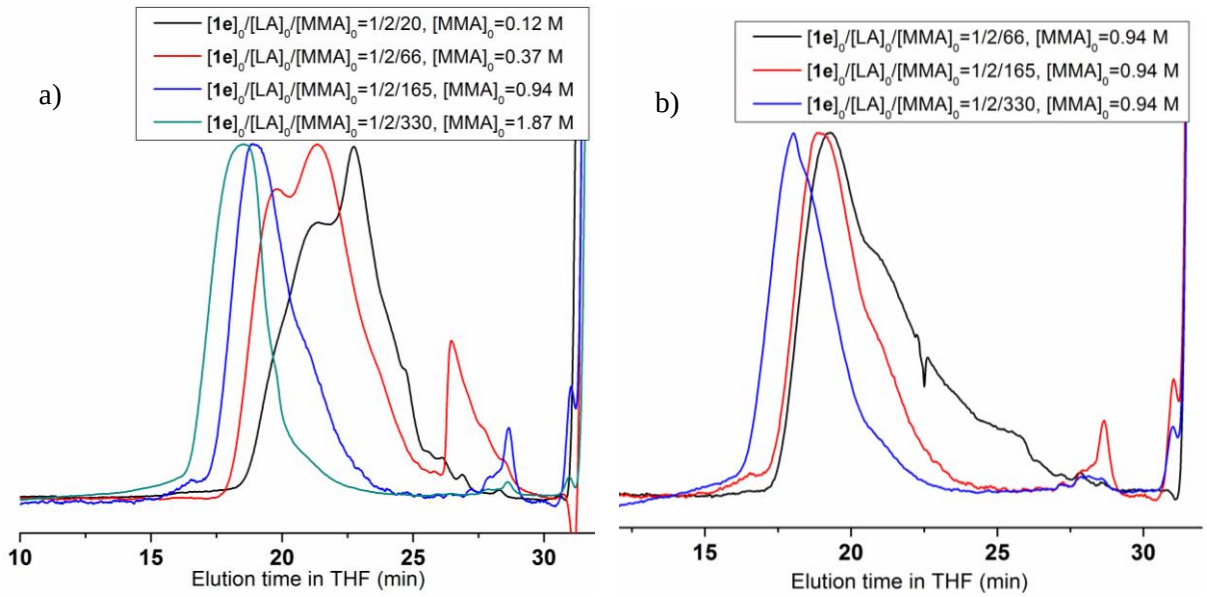

Figure 14. SEC traces (RI detector) of PMMA's obtained with NHC **1e** and $B(C_6F_5)_3$: a) keeping the initial $[\mathbf{1e}]_0$ constant and adding progressively MMA (Table 5, entries 1-4); b) keeping the initial $[MMA]_0$ constant (Table 5, entries 5,3,6).

The targeted molar mass was then varied by changing $[\mathbf{1e}]_0$, while the initial concentration of MMA was kept constant and equal to 0.94 M (entries 3, 5-6). Here again, targeting low molar masses (entry 5) resulted in PMMA's whose SEC profile showed a tail in the low molar mass region (Figure 14b). In contrast, an initial $[\mathbf{1e}]_0/[MMA]_0$ ratio of 330 (entry 6) led to a PMMA with M_n = 21,800

g/mol (SEC in THF, PS standards), in good agreement with the expected value, but at the expense of the polymerization rate. Although dispersity remained relatively low (1.38), the shape of the SEC trace revealed a progressive loss of control.

It turns out that, [MMA] has a strong effect on the quality of control of the polymerization, in particular when the targeted molar mass is higher than 16,500 g/mol. Indeed, decreasing the concentration in active species gives access to PMMA's exhibiting M_ns up to 21,800 g/mol, with a rather good control. In contrast, low M_n PMMAs with monomodal SEC profiles are difficult to achieve with this method, irrespective of the initial concentration in MMA.

Table 5. Polymerization of MMA in the presence of NHC **1e** and $B(C_6F_5)_3$, T = 20 °C, quenching = 5% HCl in MeOH).

Entry	$[1e]_0/[LA]_0/[MMA]_0$	$[MMA]_0$ (M)	t (h)	Conv (%)[a]	$M_{n,theo}$ (g/mol)[b]	$M_{p,SEC}$ (g/mol)[c]	$M_{n,SEC}$ (g/mol)[c]	D[c]
1	1/2/20	0.12	1	94	1,900	2,000-3,700	2,400	1.41
2	1/2/66	0.37	1.5	95	6,300	4000-10,000	3,800	1.60
3	1/2/165	0.94	1.3	90	14,800	15,000	11,000	1.53
4	1/2/330	1.87	1.5	70	23,100	20,200	19,600	1.42
5	1/2/66	0.94	1	97	6,400	12,800	8,400	1.80
6	1/2/330	0.94	16	70	23,100	29,000	21,800	1.38

[a] Conversion was calculated by ^{1}H NMR in $CDCl_3$ (Figure S3). [b] Calculated as follows: $M_{n,theo} = ([MMA]_0/[\mathbf{1e}]_0) \times conv \times M_{MMA}$, assuming that NHC **1e** plays the role of initiator. [c] SEC in THF calibrated with PS standards was used for characterization.

To conclude, we observed at least two populations of PMMA chains by SEC, though under appropriate conditions of temperature and initial concentrations, monomodal SEC traces could be obtained. The final M_n of the obtained PMMAs were controlled by the initial $[NHC]_0/[MMA]_0$ ratio. However, the synthesis PMMA's of low molar masses and narrow molar mass distributions could not be achieved from this $B(C_6F_5)_3$ /NHC **1e** Lewis pair polymerization. An initial $[\mathbf{1e}]_0/[MMA]_0$ ratio of 165, with $[MMA]_0$ = 0.94 M, gives the better results.

2.3. Analysis of PMMA chains derived from NHC 1e and $B(C_6F_5)_3$

As described above, the synthesis of low molar mass PMMA's utilizing both $B(C_6F_5)_3$ and NHC **1e** in a doubly activated zwitterionic polymerization proved poorly controlled. Polymers obtained

when targeting small DP_n value ([**1e**]$_0$/[LA]$_0$/[MMA]$_0$ = 1/2/20, Table 5, entry 1) at RT, or while performing the reaction at 50 °C ([**1e**]$_0$/[LA]$_0$/[MMA]$_0$ = 1/2/165, Table 4, entry 4) were nonetheless analyzed by MALDI-ToF mass spectrometry. In both cases, obtained mass spectra were similar. The one observed in the first case, and some simulations of isotopic profiles, are presented in Figure 15 (Table 5, entry 1). Several populations of peaks can be observed, with individual peaks being separated by *m/z* equal to 100.12 mass units, corresponding to the molar mass of one MMA unit.

The isotopic profile of brown populations can be attributed to two distinct types of polymer chains (A and B) separated by a *m/z* = 2 (A → *m/z* and B → *m/z* + 2, Figure 15b). Population A is predominant at low *m/z* and population B at high *m/z*.

As illustrated in Figure 15d, two structures exhibiting the same *m/z* can be hypothesized to account for the presence of population B. As the chain growth is thought to follow a zwitterionic mechanism (Scheme 20a), quenching the reaction by a 5% HCl/MeOH solution is expected to protonate the enolate chain end, forming a $(CH_3)CH(CO_2Me)$ after rearrangement, at the ω-position (Scheme 20b). The imidazolium moiety introduced in α-position might be stabilized by a Cl^- or MeO^- counter-anion. Such small counter-anions are usually not observed by MALDI-ToF MS analysis.

On the other hand, spirocyclic species can be generated upon quenching the polymerization (Scheme 20b). Related cyclic compounds would be cationized by a proton during the MALDI-ToF experiment. Similar structures have already been reported for the NHC-initiated zwitterionic ring opening polymerization of *N*-carboxyanhydrides[99] or β-lactones.[100]

Unfortunately, population A (Figure 15b) could not be identified. Molecular structures that would have resulted from backbiting and/or branching reactions were not detected in our MS spectra (Scheme 20c,d). Hence, the occurrence of such side reactions under the implemented polymerization conditions may be ruled out.

The population C (shown in green) was ascribed to cyclic PMMA's featuring a sodium cation generated during the MALDI-ToF analysis (Figure 15c). However, the ratio between populations A, B and C cannot be evaluated by MALDI-ToF, especially due to their different nature (C is neutral and only observed while adding NaI to the IAA matrix).

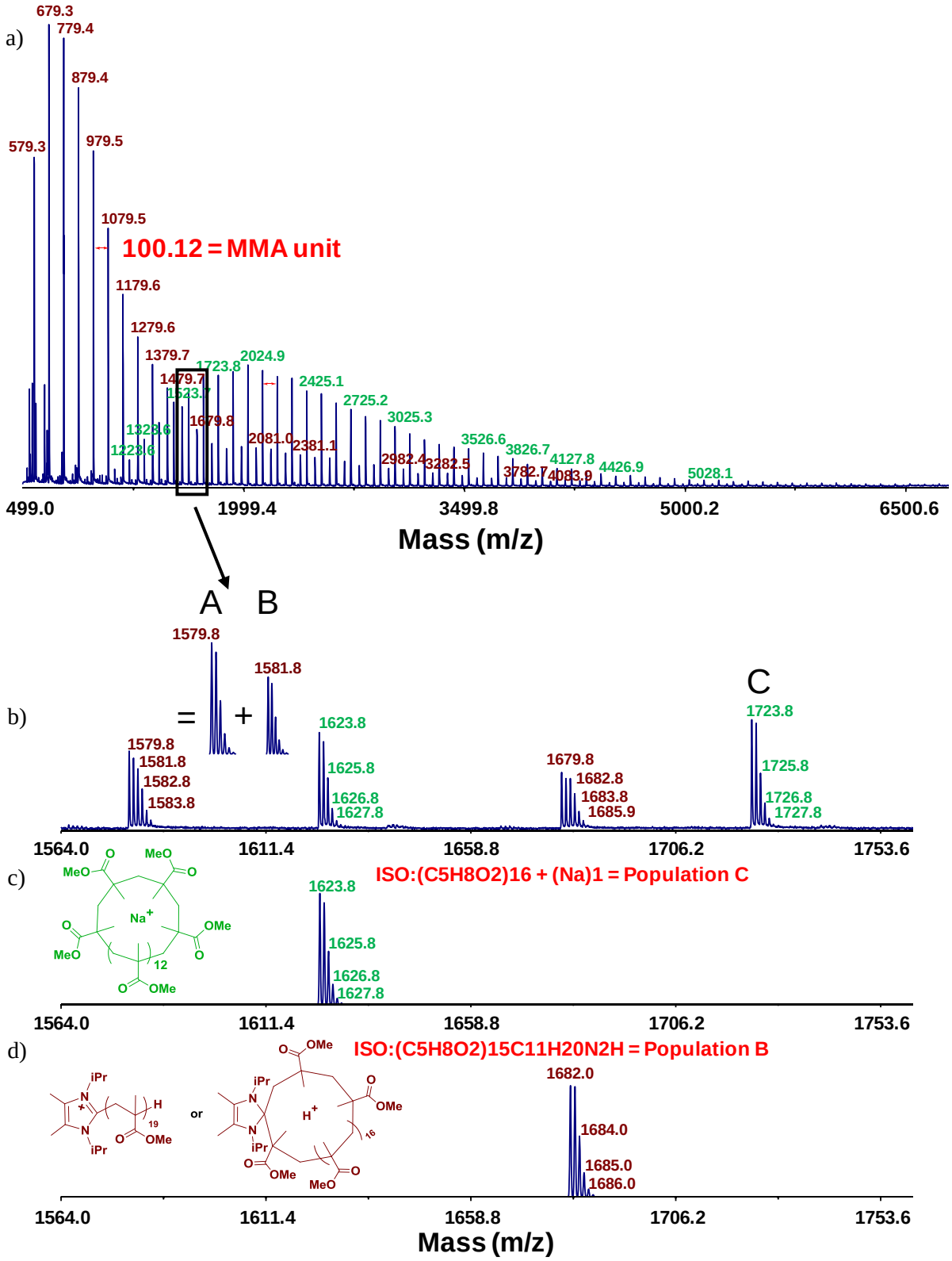

Figure 15. MALDI-ToF mass spectrum in reflector mode of a PMMA prepared at T = 20 °C with an initial [**1e**]$_0$/[B(C$_6$F$_5$)$_3$]$_0$/[MMA]$_0$ = 1/2/20 (Table 5, entry 1) and simulation of the obtained isotopic profiles (ISO).

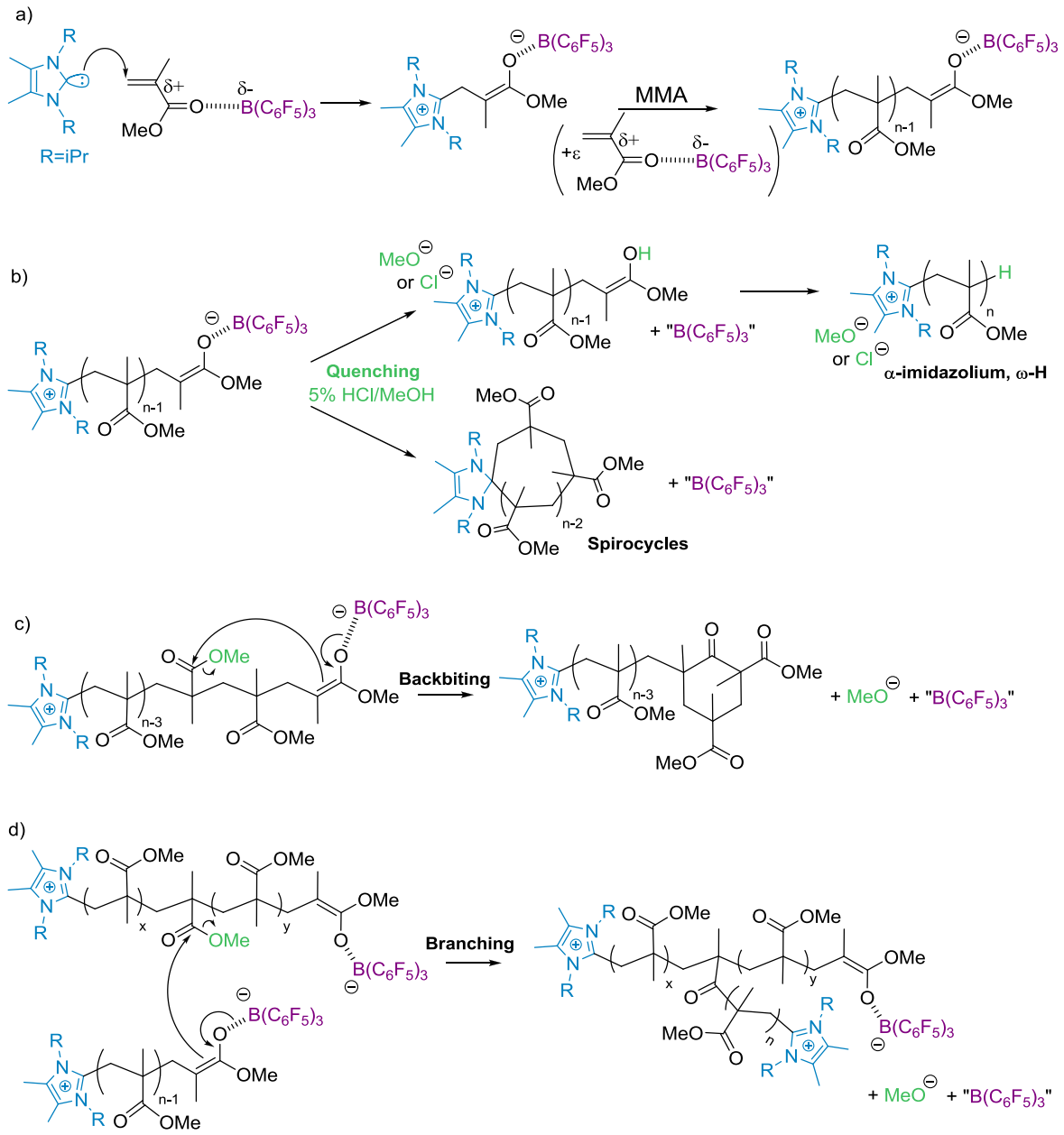

Scheme 20. a) Dual activation of MMA polymerization using NHC **1e** (R=iPr) and $B(C_6F_5)_3$; b) quenching of the polymerization with 5% HCl/MeOH forming α-imidazolium,ω-H PMMA chains or spirocycles; c) backbiting reaction; d) branching reaction.

2.4. Kinetics of the polymerization of MMA mediated by NHC 1e and $B(C_6F_5)_3$

To study the kinetics of the $B(C_6F_5)_3$/NHC **1e** doubly activated polymerization of MMA, we assumed a first-order in MMA concentration. An initial [NHC **1e**]$_0$/[$B(C_6F_5)_3$]$_0$/[MMA]$_0$ = 1/2/165 was selected so as to obtain a PMMA with a distribution of molar masses as narrow as possible. Aliquots were taken out periodically and analyzed by ^{1}H NMR so as to determine the monomer conversion.

SEC analyses were performed in THF. Due to low amounts of polymer formed for the two first aliquots (conversion < 30%), corresponding SEC analyses were of limited accuracy. For instance, the SEC trace of the polymer obtained after 35 min exhibited a noisy baseline and a side signal of $M_n \approx$ 700 g/mol (elution time ≈ 27 min), attributed to the Lewis acid and/or NHC **1e** that could not be washed out from the polymer sample.

As depicted in Figure 16a and 16b, molar masses do not increase linearly with monomer conversion. From low conversions to approximately 60%, M_n values are nearly constant and are approximately equal to 15,000 g/mol. A decrease of M_n values is then observed, along with an increase in the dispersity values. In contrast, after a short induction period of about 20 min, the first order kinetic plot shows a linear evolution (Figure 16c).

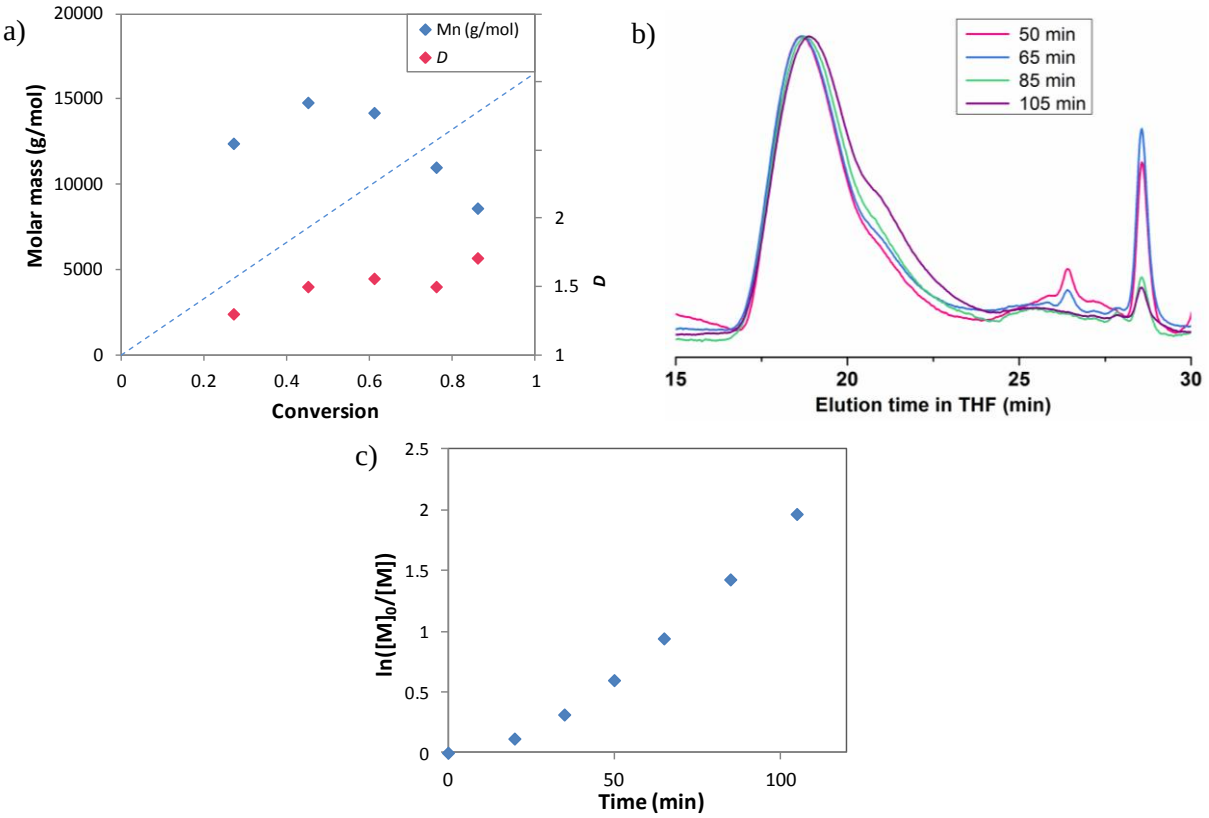

Figure 16. Kinetic study of the polymerization of MMA triggered by $B(C_6F_5)_3$ and NHC **1e** in toluene ([NHC **1e**]$_0$/[$B(C_6F_5)_3$]$_0$/[MMA]$_0$= 1/2/165, [MMA]$_0$ = 0.94 M); a) average molar masses (M_n, in blue) and dispersities ($D = M_w/M_n$, in pink) (determined by SEC in THF, PS standards) *versus* conversion (determined by ^{1}H NMR in $CDCl_3$); dotted line represents theoretical M_n based on [MMA]$_0$/[**1e**]$_0$ ratio; b) corresponding SEC traces (RI detector); c) corresponding first order kinetic plot.

These results can be summarized as follows:

- At low conversions, experimental $M_{n,SEC}$ values have already reached the final theoretical M_n values ($M_{n,theo}$ = 16,500 g/mol based on the initial [NHC **1e**]$_0$/[MMA]$_0$ at 100% conversion). In other words, the conversion increases, producing a higher amount of PMMA while $M_{n,SEC}$ values of the produced PMMA remains constant.
- At higher conversions (> 60%), experimental $M_{n,SEC}$ values decrease slightly while the dispersity increases.

Side reactions due to aggregation of the zwitterionic polymer chain ends in toluene should be considered (Scheme 21). As already indicated, experiments had to be conducted in this solvent to minimize side reactions with LA or LB.

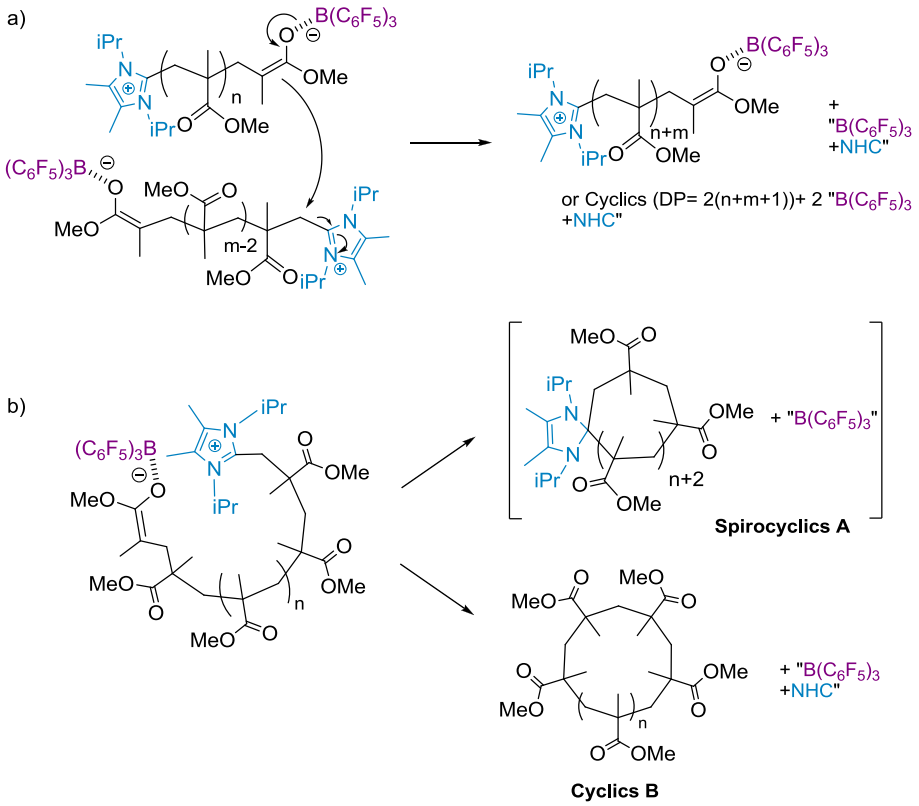

Scheme 21. Possible inter (a) and intramolecular (b) reactions due to the aggregation of the polymer chain ends in toluene during the zwitterionic polymerization of MMA induced by $B(C_6F_5)_3$ and NHC **1e**.

Intermolecular "coupling reactions" would duplicate the molar mass, while releasing NHC moieties that could initiate new chains (Scheme 21a). As the $M_{n,SEC}$ value of final PMMA's seemed to be relatively well-controlled by the initial [NHC **1e**]$_0$/[MMA]$_0$ ratio, the occurrence of such side reactions can be ruled out.

In contrast, intramolecular "coupling reactions" can create different types of cyclic PMMA's (Scheme 21b). For instance, cyclic species, denoted as A, bear an imidazolium moiety in α-position, while cyclic species B are exclusively made of MMA units. The former cyclics A can actually be viewed as dormant polymer species, whereas formation of cyclics B would result from a transfer reaction, releasing an imidazolium moiety during cyclization. Observation of cyclic polylactides, polylactones and poly(^{N}-carboxyanhydrides) has already been reported during the NHC-induced ZROP of related cyclic monomers.[99-106]

The loss of control at high conversions observed in our case may also be explained by the occurrence of side reactions, typically by back-biting reaction forming a β-keto-ester chain end (Scheme 20c).[97] As already mentioned, the latter function is characterized by an absorbance at λ = 305 nm. Such a signal was not yet observed on the UV response of the SEC trace at this wavelength, attesting that the polymerization of MMA induced by $B(C_6F_5)_3$ and NHC **1e** occurred with negligible extent –if any– of this back-biting reaction.

The generation of cyclic PMMA structures is in fact hard to establish in our case. Indeed, polymers exhibit quite high molar mass, precluding their analysis by MALDI-ToF MS. Moreover, the dispersities ($D \approx$ 1.4-1.6) do not allow us to conclude unambiguously about the presence of linear *vs.* cyclic polymers by viscosity studies. However, a reasonable hypothesis to account for the nearly constant evolution of molar masses *vs.* conversion (conversion < 60%) is as follows. A few active species can form and propagate very fast before undergoing cyclization, when PMMA chains have reached a certain molar mass due to the low polarity of toluene.

It is also likely that, due to the higher polarity of MMA (ε_r = 6.32 at 30 °C) compared to toluene (ε_r = 2.38 at 23 °C),[107] a progressive decrease in [MMA] can limit the ability of the reaction medium to

solvate the polymeric zwitterionic charges. Cyclization may then occur at lower molar mass, i.e. when [MMA] is low. This could explain the observed drop of M_n along with the increase in dispersity at high monomer conversions.

A series of experiments was attempted to introduce functional groups in α- and ω- positions of PMMA ends, using appropriate quenching agents (NuE, see Scheme 22a). However, the final M_n of the PMMA being too high to allow for a through characterization by MALDI-ToF MS, the as-generated PMMA's could be only discussed on the basis of SEC analyses. All samples exhibited the same SEC profile (Figure 17), whatever the quencher selected. Moreover, using a bifunctional quenching agent, namely 1,4-bis(bromomethyl)benzene (Scheme 22b), did not allow doubling the molar mass. Hence, the functionalization efficiency could not be evaluated.

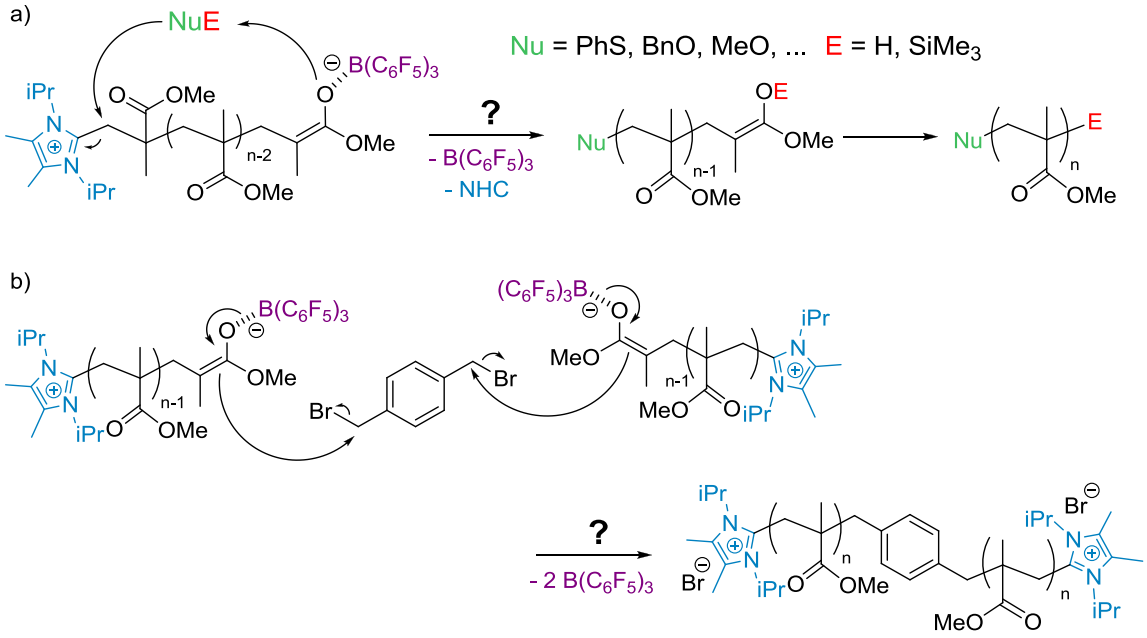

Scheme 22. Addition of a functionalizing agent on a PMMA chain grown by zwitterionic polymerization using NHC **1e** and $B(C_6F_5)_3$ Lewis pair: a) NuE-type functionalizing agent; b) bifunctional quenching agent (1,4-bis(bromomethyl)benzene).

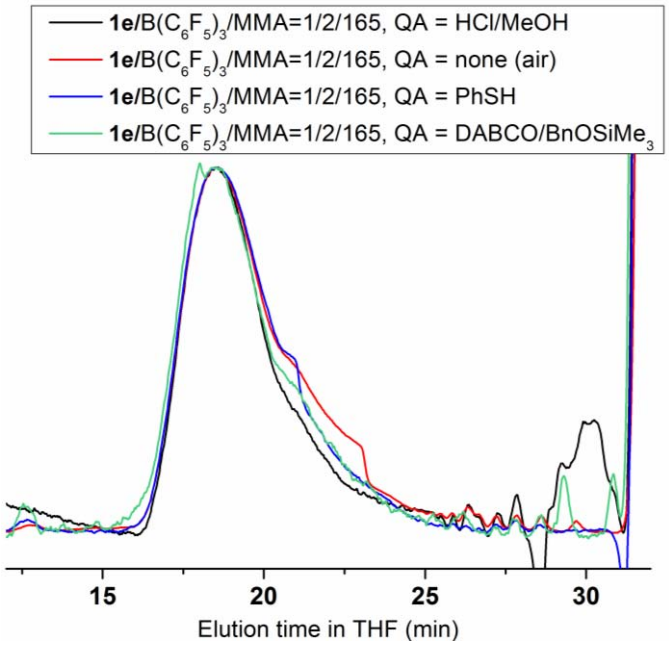

Figure 17. SEC traces (RI detector) of PMMA's obtained with NHC **1e** and $B(C_6F_5)_3$ using different quenching agents (QA, $[\mathbf{1e}]_0/[B(C_6F_5)_3]_0/[MMA]_0=1/2/165$).

2.5. Investigation of initiation step of the polymerization of MMA induced by NHC 1e and $B(C_6F_5)_3$

The extent of interaction between NHC **1e**, MMA and $B(C_6F_5)_3$ was studied by NMR analysis. On the other hand, computations by DFT were also undertaken on the basis of an initial 1,4-addition of MMA by the NHC, forming a zwitterionic transient species.

All DFT calculations were performed by the group of Karinne Miqueu and Jean-Marc Sotiropoulos from IPREM (Université de Pau et des pays de l'Adour). Some of their results will be mentioned in this section as they are of particular interest to explain some of the experimental features.

Combinations of NHC **1e**, MMA and $B(C_6F_5)_3$ at different ratios were analyzed by ^{1}H and ^{11}B NMR spectroscopy. Interactions between MMA and $B(C_6F_5)_3$ were studied first. The ^{11}B and ^{1}H NMR spectra of equimolar mixtures of the two compounds are reported in Figures 18 and 19. Adding one equivalent of MMA to a solution of $B(C_6F_5)_3$ in toluene resulted in an upfield shift of the signal ($\Delta\delta \approx$ -24 ppm) on the ^{11}B NMR spectrum (Figure 18). However, the shape of the signal remained broad. In

contrast, the ^{11}B NMR spectrum of the NHC/$B(C_6F_5)_3$ adduct, **11**, exhibited a sharp signal ($\Delta\delta \approx$ -74 ppm, as compared to "free" $B(C_6F_5)_3$). This suggests that the interaction between $B(C_6F_5)_3$ and MMA is weak. The ^1H NMR spectrum of the same mixture showed the same signals as those of free MMA, the chemical shifts being slightly shifted upfield (Figure 19).

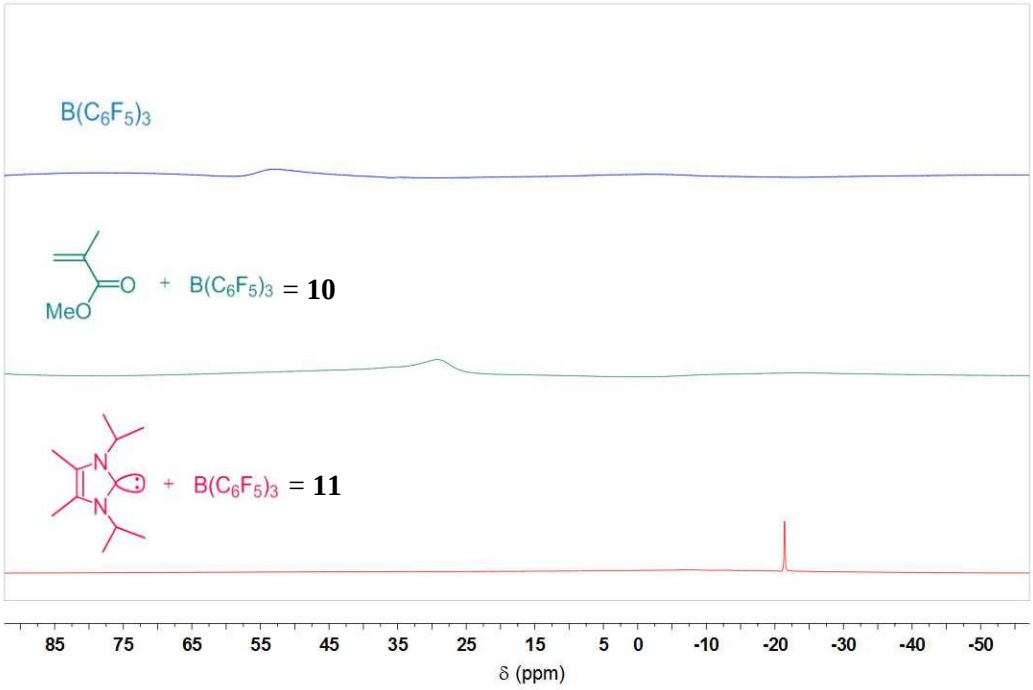

Figure 18. ^{11}B NMR spectra in toluene-d_8 from top to bottom of: $B(C_6F_5)_3$, $B(C_6F_5)_3$ + MMA (1/1) = **10** and $B(C_6F_5)_3$ + **1e** (1/1) = **11**.

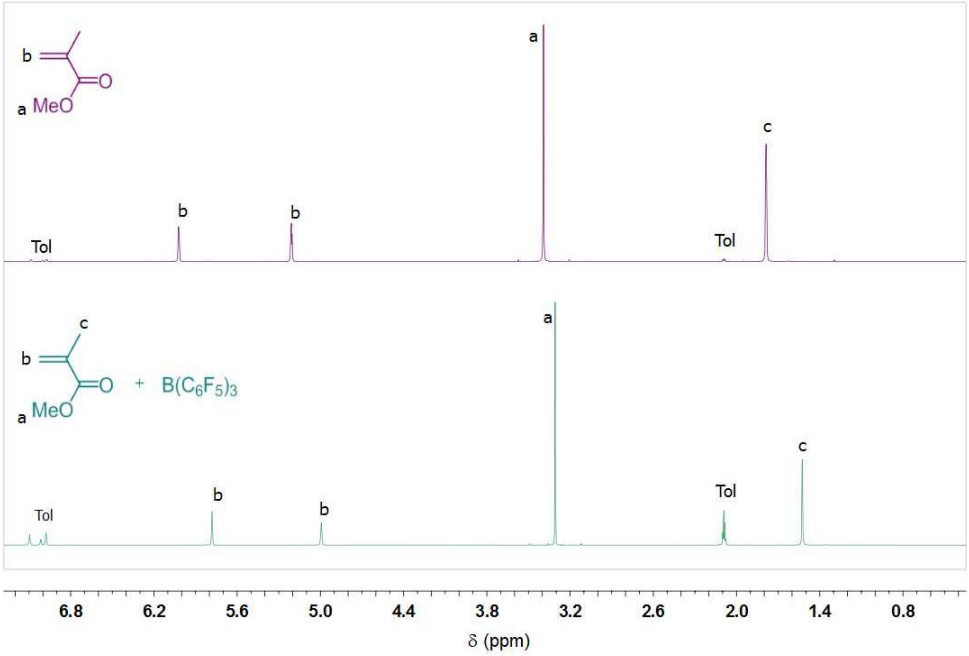

Figure 19. ^1H NMR spectra in toluene-d_8 from top to bottom of: MMA, $B(C_6F_5)_3$ + MMA (1/1).

Next, the initiation step was studied by NMR spectroscopy. In order to isolate a NHC/MMA/$B(C_6F_5)_3$ = 1/1/1 adduct, one equivalent of $B(C_6F_5)_3$-activated MMA (**10**, $B(C_6F_5)_3$/MMA = 1/1) was added onto a solution of **1e** (addition order A). However, as shown in Figure 20a-d, the ^1H NMR spectra of the obtained mixtures were similar to an overlap of spectra corresponding to free MMA and **1e**/$B(C_6F_5)_3$ adduct **11**. The ^{11}B NMR spectrum of the mixture exhibited a sharp signal around δ = -21 ppm, analogous to that observed for **11**. It is worth mentioning that addition of an equivalent of $B(C_6F_5)_3$-activated MMA on this mixture allowed us to observe PMMA signals (Figure 20e), while no appearance/disappearance of other products could be detected. Signals due to the **1e**/$B(C_6F_5)_3$ adduct were still observed.

In contrast, adding an "activated MMA", that was $B(C_6F_5)_3$/MMA = 1/1, onto a **1e**/$B(C_6F_5)_3$ adduct **11** solution (addition order B) did not permit the polymerization of MMA. It is thus very likely that, while using the addition order A, the concentration in active species was too low to be detected by NMR (Figure 20d). The main amount of NHC likely remained "trapped" in compound **11**.

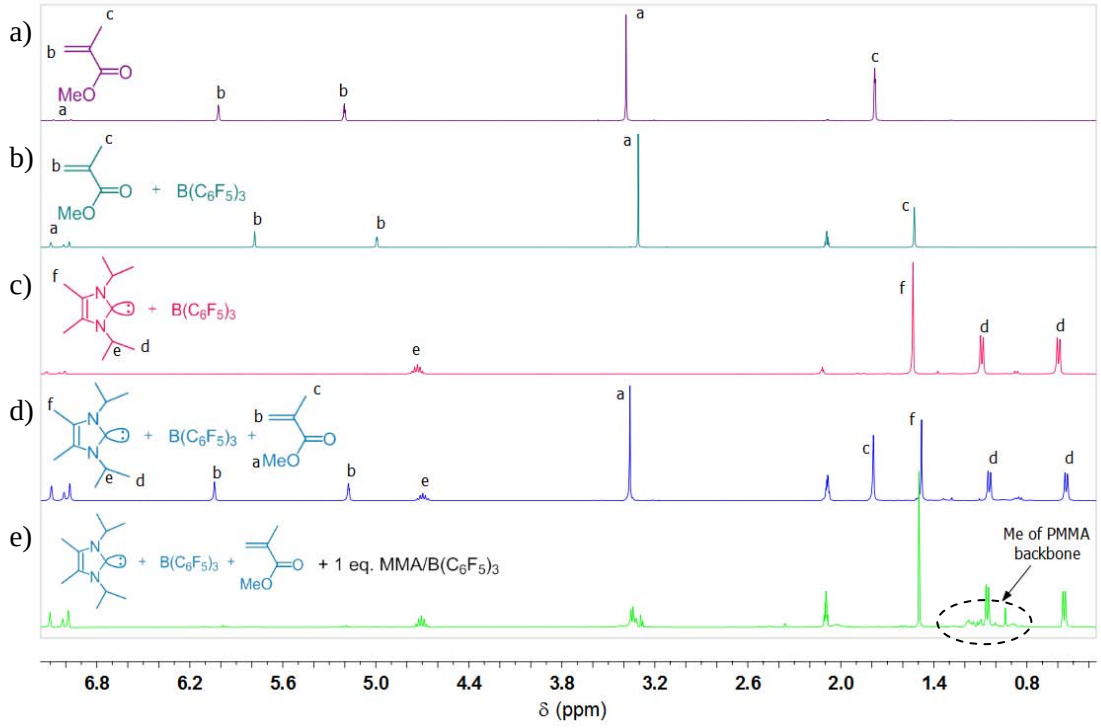

Figure 20. ^1H NMR spectra in toluene-d_8 from top to bottom of: a) MMA, b) $B(C_6F_5)_3$ + MMA (1/1), c) $B(C_6F_5)_3$ + **1e** (1/1), d) mixture obtained after addition of (b) on 1 eq. of **1e**, e) mixture obtained after addition of $B(C_6F_5)_3$ + MMA (1/1) on (d).

As the final M_n seemed to be quite controlled by the initial $[\mathbf{1e}]_0/[MMA]_0$ ratio, it can be hypothesized that either some NHC moieties are released from adduct **11**, or that transfer reactions releasing the NHC takes place. As the extent of such transfer reactions could not be monitored, the initiation efficiency could not be precisely evaluated. However, MALDI-ToF analysis of low molar masses polymers have shown that the amount of polymer chains featuring a NHC moiety, even after quenching, is not negligible (see section 2.3.). Thus, some NHC initiator molecules may have been released from **11**. If this happens, this is also consistent with a slow-initiated polymerization process, as we observed from our kinetic data (section 2.4.).

Although the addition order method A should favor the occurrence of a slow release of NHC from **11**, no polymerization could be observed using the addition order method B. These contradictory results are still under consideration. Finally, the equilibrium between the zwitterion and "trapped" NHC in adduct **11** could not be evidenced, even performing the NMR analysis at low or high temperatures (-50/50 °C).

The extent of interaction between, MMA and $B(C_6F_5)_3$ on one hand, and between NHC **1e** and $B(C_6F_5)_3$ on the other hand, were next investigated by DFT. These calculations were performed at the B3LYP/6-31G** level of theory at IPREM. DFT calculations at the M06-2X/6-31G** level of theory are currently under progress. Indeed, this latter technique is thought to be more suitable to evaluate long range interactions.[108] The binding energies obtained with the B3LYP are thus often thought to be underestimated.[26]

As depicted in Figure 21, the reaction MMA + $B(C_6F_5)_3$ → **10** was found kinetically favorable ($\Delta G_{MMA+LA \rightarrow TS}$ = 13.6 kcal/mol), but thermodynamically unfavorable ($\Delta G_{MMA+LA \rightarrow \mathbf{10}}$ = 10.1 kcal/mol). In contrast, the generation of the **1e**-$B(C_6F_5)_3$ adduct **11** from the corresponding free components proved an exothermic process ($\Delta G_{NHC+LA \rightarrow \mathbf{11}}$ = -14 kcal/mol). These results are in good agreement with the aforementioned ^{11}B NMR analysis. Indeed, the rather low energy barrier for the transformation MMA + $B(C_6F_5)_3$ → **10**, as well as its endothermic character, indicate that interaction between MMA and $B(C_6F_5)_3$ is weak. In contrast, $Al(C_6F_5)_3$ was reported to form a stable adduct with MMA ($\Delta G_{MMA+LA \rightarrow adduct}$ = -25.7 kcal/mol with BP86 functional).[26] Hence, $B(C_6F_5)_3$ is probably a too weak

LA to activate MMA in the context of a zwitterionic polymerization induced by NHC and a LA. Moreover, DFT calculations revealed that formation of a NHC-$B(C_6F_5)_3$ adduct, **11**, was favorable, also in agreement with the observed generation of this adduct while mixing NHC with **10**.

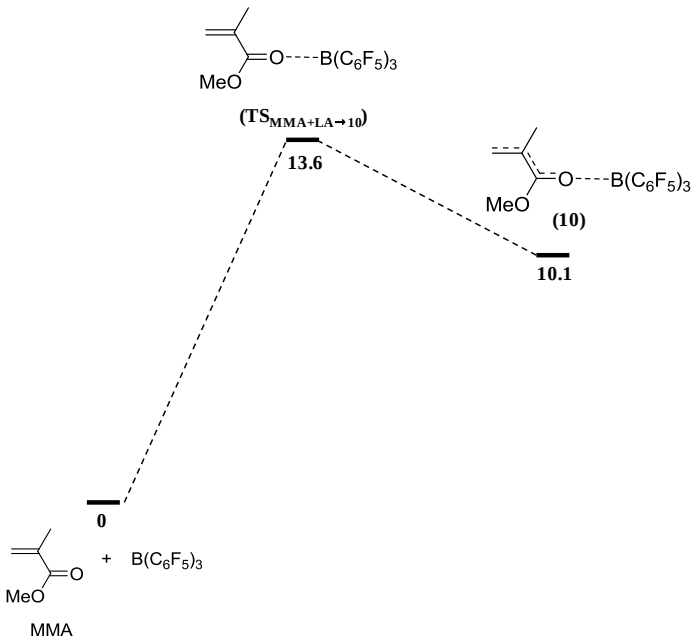

Figure 21. Energy profile computed at the B3LYP/6-31G** level (free energies G at 25°C including ZPE correction in kcal/mol) for the reaction MMA + $B(C_6F_5)_3$ → **10**.

DFT calculations also confirmed the key role of the Lewis acid in the polymerization process. The reaction NHC + MMA → **12** was not found favorable (Figure 22a). Indeed, the transition state structure associated with attack of the NHC onto MMA laid 33.3 kcal/mol above the separated NHC and MMA. The overall transformation was endothermic by + 23.2 kcal/mol. In contrast, the 1/1/1 zwitterionic adduct between 1e/MMA/$B(C_6F_5)_3$, **13**, was 8.8 kcal/mol more stable than NHC and **10** in their isolated form (Figure 22b), indicating that NHC + **10** → **13** was an exothermic reaction. Moreover, the $\Delta G^{\#}$ was decreased, from 33.3 without $B(C_6F_5)_3$ to 19.7 kcal/mol, with $B(C_6F_5)_3$.

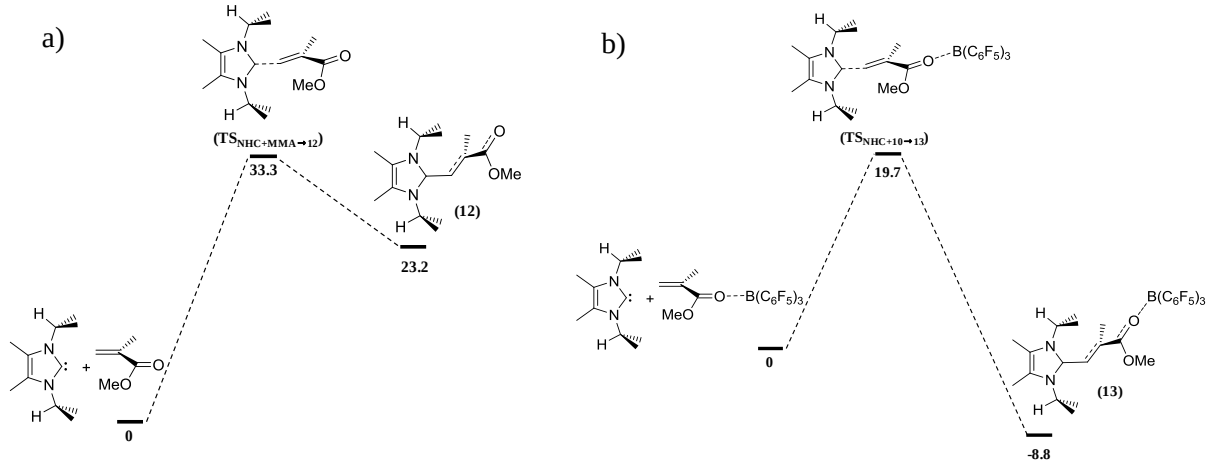

Figure 22. Energy profile computed at the B3LYP/6-31G** level (free energies G at 25°C including ZPE correction in kcal/mol) for the reactions: a) NHC + MMA → **12**; b) NHC + MMA/$B(C_6F_5)_3$ → **13**.

Hence, though the mechanism of the NHC **1e**/ $B(C_6F_5)_3$ activated polymerization of MMA could not be established accurately, several features have been evidenced in this study:

- Some of the PMMA chains obtained by targeting low molar masses and polymerizing MMA at RT carry a NHC/imidazolium moiety, as shown by MALDI-ToF MS. As experimental and theoretical M_n values are in relative close agreement, it is likely that the initiation efficiency by $B(C_6F_5)_3$ and NHC **1e** is quite high.
- The first order kinetic plot exhibits an induction period. Molar mass are almost constant at low conversion (< 60%), and slightly decrease at higher conversion (> 60%) while the dispersity increases. These results suggest that the initiation step is slow. However, attempts to fit these results with theoretical models based on a slow-initiated polymerization process failed.
- Corroborating these hypotheses, both NMR analyses and DFT calculations support that the formation of the NHC/$B(C_6F_5)_3$ adduct is more favorable than that of NHC/MMA/$B(C_6F_5)_3$ adduct. Hence, in contrast to $Al(C_6F_5)_3$, the use of $B(C_6F_5)_3$ does not allow the isolation of such 1/1/1 adducts. The key role of the $B(C_6F_5)_3$ activator has nonetheless been confirmed.

2.6. Continuous addition of the monomer: is the polymerization living?

Two strategies were implemented in order to keep the conversion lower than 50% in order to maintain a certain quality of control of the polymerization as discussed above. The first method consisted in sequential additions of MMA (+65 eq. as compared to **1e**) every 30 min, over a period of 2.5 h. Aliquots were taken before each new MMA loading. Results are summarized in Table 6, and SEC traces obtained after 2 h and 3 h are reported in Figure 23a.

In the second method, the monomer was continuously added (*via* syringe pump in the glovebox) for 3.5 h (130 eq. compared to **1e**/h with a rate of 0.4 mL/h). The characteristic of the obtained PMMA's are presented in Table 7, and SEC traces of polymers obtained are shown in Figure 23b.

Table 6. Sequential monomer addition during polymerization of MMA using **1e** as initiator and $B(C_6F_5)_3$ as MMA activator: +65 eq. of MMA every 30 min (red lines) from 0.5 to 2.5 h reaction ($[\mathbf{1e}]_0/[LA]_0/[MMA]_0 = 1/2/165$, T = 20 °C, quenching = 5% HCl in MeOH).

Entry	t (h)[a]	Conv (%)[b]	$M_{n,theo}$ (g/mol)[c]	$M_{p,SEC}$ (g/mol)[d]	$M_{n,SEC}$ (g/mol)[d]	D[d]
1	0.5	16	2,600	-	-	-
2	1	34	7,800	-	-	-
3	1.5	35	10,300	-	-	-
4	2	39	14,000	32,800	16,500	1.78
5	2.5	40	17,000	35,400	24,000	1.46
6	3	39	19,100	39,000	26,400	1.44

[a] Accumulated time. [b] Conversion was calculated by ^{1}H NMR in $CDCl_3$ (Figure S3). [b] Calculated as follows: $M_{n,theo}$ = ("$[MMA]_0$"/$[\mathbf{1e}]_0$) × conv × M_{MMA}. [c] SEC in THF calibrated with polystyrene standards was used for characterization.

Table 7. Continuous addition (CA) process during the polymerization of MMA using 1e as initiator and $B(C_6F_5)_3$ as MMA activator ($[\mathbf{1e}]_0/[LA]_0/[MMA]_0 = 1/2/165$, T = 20 °C, quenching = 5% HCl in MeOH, red lines = beginning and end of the continuous addition, rate = +130 eq. MMA/h).

Entry	t (h)[a]	Conv (%)[b]	$M_{n,theo}$ (g/mol)[c]	$M_{p,SEC}$ (g/mol)[d]	$M_{n,SEC}$ (g/mol)[d]	D[d]
1	1	35	5,800	20,700	16,600	1.38
2	3.5	48	23,800	36,300	25,800	1.43
3	4.5	46	28,800	38,600	27,400	1.49
4	8.5	70	43,900	46,000	33,700	1.46

[a] Accumulated time. [b] Conversion was calculated by ^{1}H NMR in $CDCl_3$ (Figure S3). [c] Calculated as follows: $M_{n,theo}$ = ("$[MMA]_0$"/$[\mathbf{1e}]_0$) × conv × M_{MMA}. [d] SEC in THF calibrated with polystyrene standards was used for characterization.

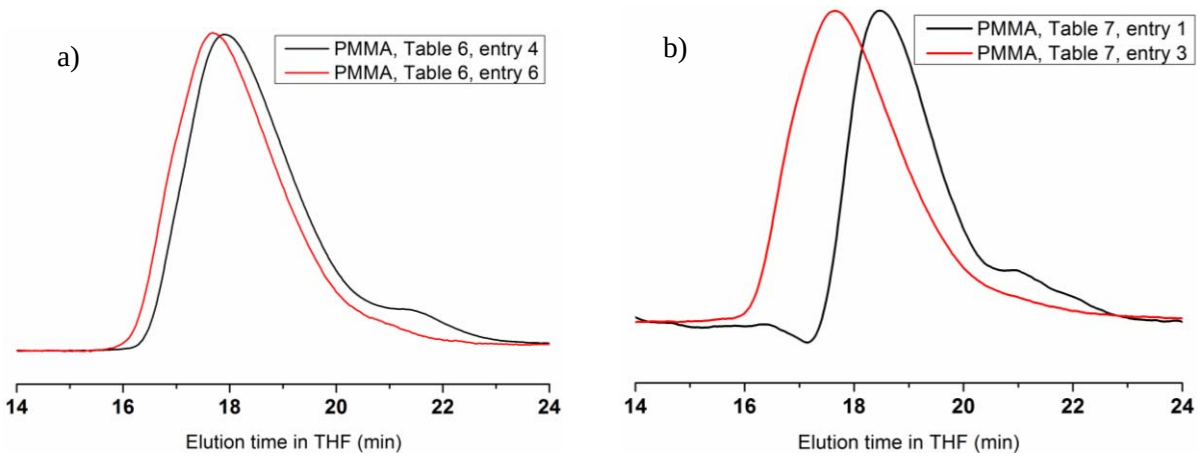

Figure 23. SEC traces (RI detector) of: a) PMMA's obtained by sequential MMA additions (Table 6, entries 4 *vs.* 6); b) PMMA's obtained by continuous MMA addition (Table 7, entries 1 = before CA *vs.* 3 = just after CA was stopped).

Both techniques allowed us to achieve PMMA's with M_n up to 27,000 g/mol with monomodal distributions of molar masses (D < 1.5). In both cases, PMMA's obtained at the beginning of the polymerization exhibited a value of M_n around 15,000 g/mol, whatever the conversion. SEC traces show a major peak with a small tail in the low molar masses region. When the amount of consumed MMA corresponded to a theoretical $M_n \approx$ 15,000 g/mol, the M_p increased and the tail at the low molar mass region progressively disappeared. Polymers obtained by the sequential addition technique eventually exhibited higher molar masses than expected (Table 6). In contrast, with the continuous addition process, $M_{n,SEC}$ values were in good agreement with theoretical values (Table 7).

Thus, both continuous addition techniques of MMA allowed us to broaden the scope of the $B(C_6F_5)_3$/NHC**1e** doubly activated polymerization of MMA, higher molar masses being achieved with a relatively good control.

Conclusion

In this chapter, the cooperative activation of various substrates using NHCs, as Lewis bases, and silanes (SiLA's) and boranes (BLA's), as Lewis acids, was proposed as a strategy to improve the activation potential of NHCs. Innovations in molecular chemistry were demonstrated using silanes in conjugation with NHCs, while boranes were found more relevant for a use in polymer chemistry.

Formation of FLPs from pinacol spirosilane **2** and sterically hindered NHCs was demonstrated for the first time. A more acidic silane, the so-called Martin spirosilane **3** yielded "classical" Lewis adducts with all NHCs tested in this study. Formation of a 1/1/1 adduct between NHC, benzaldehyde and **2** was hypothesized upon using the FLP based on **2** in the presence of an equimolar amount of benzaldehyde. The same adduct was evaluated in the NHC-catalyzed Stetter and cross-benzoin reactions. However, these attempts met so far with limited success mainly due to the occurrence of the self-condensation of benzaldehyde forming benzoin. This nonetheless evidenced that the NHC moiety can be released from the aforementioned 1/1/1 adduct.

A commercial borane, namely tris(pentafluorophenyl)borane ($B(C_6F_5)_3$), was used in conjunction with NHCs in order to mediate the doubly activated zwitterionic polymerization of MMA. Under very specific conditions, these polymerizations exhibit a certain degree of control. For instance, the $B(C_6F_5)_3$-activated toluene solution of MMA was added on the 1,3-diisopropyl-4,5-dimethyl-imidazol-2-ylidene solution ($B(C_6F_5)_3$/NHC = 2/1).

In general terms, a slow-initiation step may characterize the polymerization. Transfer side reactions seemed to be minimized except when polymerization was performed at 50 °C. Attempts to functionalize the obtained PMMA by quenching the polymerization with different agents failed so far, most probably owing to the lack of lability of the imidazolium moiety.

It can be speculated that a more appropriate design of both the LA and LB partners, in light of the targeted (macro)molecular reaction, is needed to better improve the activation potential of organic Lewis pairs. For instance, the use of stronger organic Lewis acids may be beneficial to trigger efficiently the zwitterionic polymerization of MMA and, in a broader perspective, of other less polar monomers.

Annexe: Supporting Information

Materials. All reagents were purchased from Aldrich with purity ≥99% unless otherwise stated. All the other experiments were performed under an inert atmosphere using standard Schlenk techniques. Dry, oxygen-free solvents and reagents were employed. THF was distilled over Na/benzophenone, toluene over polystyryllithium prior to use. THF-d_8 was distilled over Na, toluene-d_8 over CaH_2 and kept in a glovebox. Benzaldehyde was purified by fractional distillation. PO was distilled over Na. MMA was purified by distillation over CaH_2 and stored at 0 °C. $B(C_6F_5)_3$ was purchase from TCI and sublimed twice prior to use.

Instrumentation. ^{1}H NMR (400 MHz) spectra were recorded on Bruker AC-400 spectrometer in appropriate deuterated solvents. One to one experiments were conducted in NMR Young tubes to ensure inert atmosphere along the whole measurement. The NMR Young tubes were filled inside the argon atmosphere of the glove-box. All mixtures were prepared and introduced in the tube in the glovebox. Molar masses were determined by size exclusion chromatography (SEC) in THF as eluent (1 mL/min) and with trichlorobenzene as a flow marker at 25 °C, using both refractometric (RI) and UV detectors (Varian). Analyses were performed using a three-column set of TSK gel TOSOH (G4000, G3000, G2000 with pore sizes of 20, 75, and 200 Å respectively, connected in series) calibrated with polystyrene standards. The data for crystal structure of compound **2'a** have been collected on a Rigaku MM07 HF rotating anode at the Cu Kα wavelength. The system featured the micromax microfocus x-ray source with the RAPIDII image plate detector combined with the AFC-Kappa goniometer and the osmic mirrors Varimax® HF optics. The system was driven by the CrystalClear© suite which was also used for the unit cell determination, the integration, scaling and absorption correction of the raw data (Reference: CrystalClear: An Integrated Program for the Collection and Processing of Area Detector Data, Rigaku Corporation, © 1997-2002). MALDI-ToF spectrometry was performed using a Voyager-DE STR (Applied Biosystems) spectrometer equipped with a nitrogen laser (337 nm), a delay extraction and a reflector. The instrument is equipped with a pulsed N_2 laser (337 nm) and a time-delayed extracted ion source. Spectra were recorded in the

positive-ion mode using the reflectron and with an accelerating voltage of 20 kV. Samples were dissolved in THF at 10 mg/mL. The IAA matrix (Indole acrylic acid) solution was prepared by dissolving 10 mg in 1 mL of THF. A MeOH solution of cationization agent (NaI, 10 mg/mL) was also prepared. The solutions were combined in a 10:1:1 or 10:1:0 volume ratio of matrix to sample to cationization agent. One to two microliters of the obtained solution was deposited onto the sample target and vacuum-dried.

Computational Details. All DFT calculations were performed by the group of Karinne Miqueu and Jean-Marc Sotiropoulos at IPREM (Université de Pau & des pays de l'Adour). Calculations were performed with the Gaussian 03 program[109] using the Density Functional Theory method.[110] The various structures were fully optimized at B3LYP level.[111-113] This functional is built with Becke's three parameter exchange functional[112] and the Lee-Yang-Parr correlation functional.[113] The 6-31G(d,p) basis set was used.[114] All atoms were augmented with a single set of polarization functions. The second derivatives were analytically calculated in order to determine if a minimum or a transition state (one negative eigenvalue) existed for the resulting geometry. All total energies and Gibbs free energies have been zero-point energy (ZPE) and temperature corrected using unscaled density functional frequencies. The connection between the transition states and the corresponding minima was confirmed by IRC calculations.[115-116]

Synthesis of NHCs 1a-1e and Lewis acids 2,3. NHCs were synthesized according to the literature procedure: **1a-1c**,[117] **1e**.[118] **2** and **3** were synthesized using already described procedures.[119-120] NHCs were stored in the glovebox.

Synthesis of Lewis pairs NHC/SiLA 3 (2a-c, 3a-c). In a typical procedure, 43 mg (2.8×10^{-4} mol) of **1a** was mixed with 73 mg (2.8×10^{-4} mol) of **2** in 0.5 mL of THF-d_8, in the glovebox. The clear solution was transferred in a Young tube and analyzed by RNM spectroscopy. Slow evaporation of a concentrated THF solution of **2a** yielded colorless plate-like crystals, suitable for X-Ray diffraction analysis.

2a: ^{1}H NMR (400 MHz, THF-d_8): δ = 0.96 (br. d, C*H*$_3$ **2**, 24 H), 1.42 (d, *J* = 6.4 Hz, C*H*$_3$*i*Pr, 12H), 5.64 (sept, *J* = 6.4 Hz, C*Hi*Pr, 2H), 7.42 (s, C*H*=C*H*, 2H); ^{13}C NMR (100 MHz, THF-d_8): δ = 21.1 (*C*H$_3$*i*Pr), 25.5 (*C*H$_3$ **2**), 50.1 (*C*H*i*Pr), 74.0 (*C*(CH$_3$)$_2$ **2**), 115.5 (*C*H=*C*H), 161.6 (N$_2$*C*); ^{29}Si NMR (79.6 MHz, THF-d_8): δ = 108.4.

2b: ^{1}H NMR (400 MHz, THF-d_8): δ = 1.19 (s, C*H*$_3$ **2**, 24 H), 2.06 (s, *o*-C*H*$_3$Mes, 12H), 2.29 (s, *p*-C*H*$_3$Mes, 6H), 6.94 (s, *m*-C*H*Mes, 4H), 7.04 (s, C*H*=C*H*, 2H); ^{13}C NMR (100 MHz, THF-d_8): δ = 15.3 (*o*-*C*H$_3$Mes), 18.3 (*p*-*C*H$_3$Mes), 22.5 (*C*H$_3$ **2**), 63.5 (*C*(CH$_3$)$_2$ **2**), 118.55 (*C*H=*C*H), 126.5 (*m*-*C*Mes), 133.0 (*o*-*C*Mes), 134.8 (*p*-*C*Mes), 137.0 (*C*Mes), 216.9 (N$_2$*C*); ^{29}Si NMR (79.6 MHz, THF-d_8): δ = 45.9.

2c: ^{1}H NMR (400 MHz, THF-d_8): δ = 1.19 (s, C*H*$_3$ **2**, 24 H), 1.60 (s, C*H*$_3$*t*Bu, 18H), 7.15 (s, C*H*=C*H*, 2H); ^{13}C NMR (100 MHz, THF-d_8): δ = 22.5 (*C*H$_3$ **2**), 28.8 (*C*H$_3$*t*Bu), 53.2 (*C*(CH$_3$)$_3$ *t*Bu), 63.5 (*C*(CH$_3$)$_2$ **2**), 112.6 (*C*H=*C*H), 210.4 (N$_2$*C*); ^{29}Si NMR (79.6 MHz, THF-d_8): δ = 45.9.

3a: ^{1}H NMR (400 MHz, THF-d_8): δ = 0.63 (d, *J* = 6.7 Hz, C*H*$_3$*i*Pr, 6H), 1.45 (d, *J* = 6.7 Hz, C*H*$_3$*i*Pr, 6H), 5.45 (sept, *J* = 6.7 Hz, C*Hi*Pr, 2H), 7.38 (s, C*H*=C*H*, 2H), 7.5 (m, C*H*$_{benz}$**3**, 6H), 8.26 (d, C*H*$_{benz}$**3**, 2H); ^{29}Si NMR (79.6 MHz, THF-d_8): δ = 84.4.

3b: ^{1}H NMR (400 MHz, THF-d_8): δ = 1.40 (s, *o*-C*H*$_3$Mes, 12H), 1.50 (s, *p*-C*H*$_3$Mes, 6H), 7.01 (s, C*H*=C*H*, 2H), 7.35 and 8.30 (m, *m*-C*H*Mes, 4H and C*H*$_{benz}$**3**, 8H); ^{29}Si NMR (79.6 MHz, THF-d_8): δ = 84.4.

3c: ^{1}H NMR (400 MHz, THF-d_8): δ = 1.18 (s,C*H*$_3$*t*Bu, 6H), 2.19 (s,C*H*$_3$*t*Bu, 6H), 3.36 (s,C*H*$_3$*t*Bu, 6H), 6.43 (s, C*H*=C*H*, 1H), 7.0 (m, C*H*$_{benz}$**3**, 8H); ^{29}Si NMR (79.6 MHz, THF-d_8): δ = 84.4.

Synthesis of 1b/Benzaldehyde/2 1/1/1 adduct (8b). In the glovebox, 48.4 mg (1.6×10^{-4} mol) of **1b** was first mixed with 41.6 mg (1.6×10^{-4} mol) of **2** in 1 mL toluene affording a clear solution. 16.2 µL (1.6×10^{-4} mol) of benzaldehyde was next added *via* a precision syringe. A white powder precipitated immediately. After filtration of the medium, the powder was washed several times with dry Et_2O. The volatiles were removed under vacuum affording **8b** as a white powder (yield: 81 mg, 76%). ^{1}H NMR (400 MHz, THF-d_8): δ = 0.39 (s, C*H*$_3$ **2**, 6 H), 0.64 (s, C*H*$_3$ **2**, 6 H), 0.83 (s, C*H*$_3$ **2**, 6 H), 0.96 (s, C*H*$_3$ **2**,

6 H), 1.81 (s, C*H*$_3$ **1b**Mes, 6 H), 2.34 (s, C*H*$_3$ **1b**Mes, 6 H), 2.42 (s, C*H*$_3$ **1b**Mes, 6 H), 6.66 (s, CO*H*, 1 H) 6.84 (m, Ar*H* benzal, 5 H) 6.92 (m, Ar*H* **1b**, 1 H), 7.00 (m, Ar*H* **1b**, 1 H), 7.07 (s, Ar*H* **1b**, 2 H), 7.68 (s, NC*H*, 2 H); ^{29}Si NMR (79.6 MHz, THF-d_8): δ = 113.78. See Figures S1-S2.

Polymerization of PO using NHC and SiLA 2 or 3. In a typical procedure, 58.4 mg (1.14×10^{-4} mol) of **3** was first dissolved in 3 mL of PO (4.29×10^{-2} mol) at -30 °C. A 0.5 mL toluene solution of 17.4 mg (1.14×10^{-4} mol) of **1a** was added. After 30 min at -30 °C, the mixture was warmed up to room temperature. After stirring for an additional 30 min, the schlenk was then transferred into a preset oil bath (50 °C). After 5 days stirring, the polymerization was quenched by contact with air. The unreacted PO was removed by vacuum distillation and the conversion was determined by gravimetry (11%). Molecular characteristics were determined by SEC in THF (Table 1): M_n=1,600 g/mol, D=1.15 (RI detection).

Zwitterionic polymerization of MMA triggered by $B(C_6F_5)_3$/NHC. In a typical procedure, 5 mg (2.84×10^{-5} mol) of **1e** was first dissolved in 2.5 mL of toluene overnight. A 2.5 mL toluene solution of 29.4 mg (5.68×10^{-5} mol) of $B(C_6F_5)_3$ and 0.5 mL MMA (4.67×10^{-3} mol) was added drop by drop over 5 min on the **1e** solution at 20 °C. After 1 h 20 at RT, the polymerization was quenched with about 0.5 mL of degassed HCl(5%)/MeOH. An aliquot of the polymerization mixture was taken to determine the conversion by ^{1}H NMR in $CDCl_3$ (90%, Figure S3). The polymer was isolated by several precipitations in pentane. Molecular characteristics were determined by SEC in THF (Table 2): M_n=11,000 g/mol, D=1.53 (RI detection).

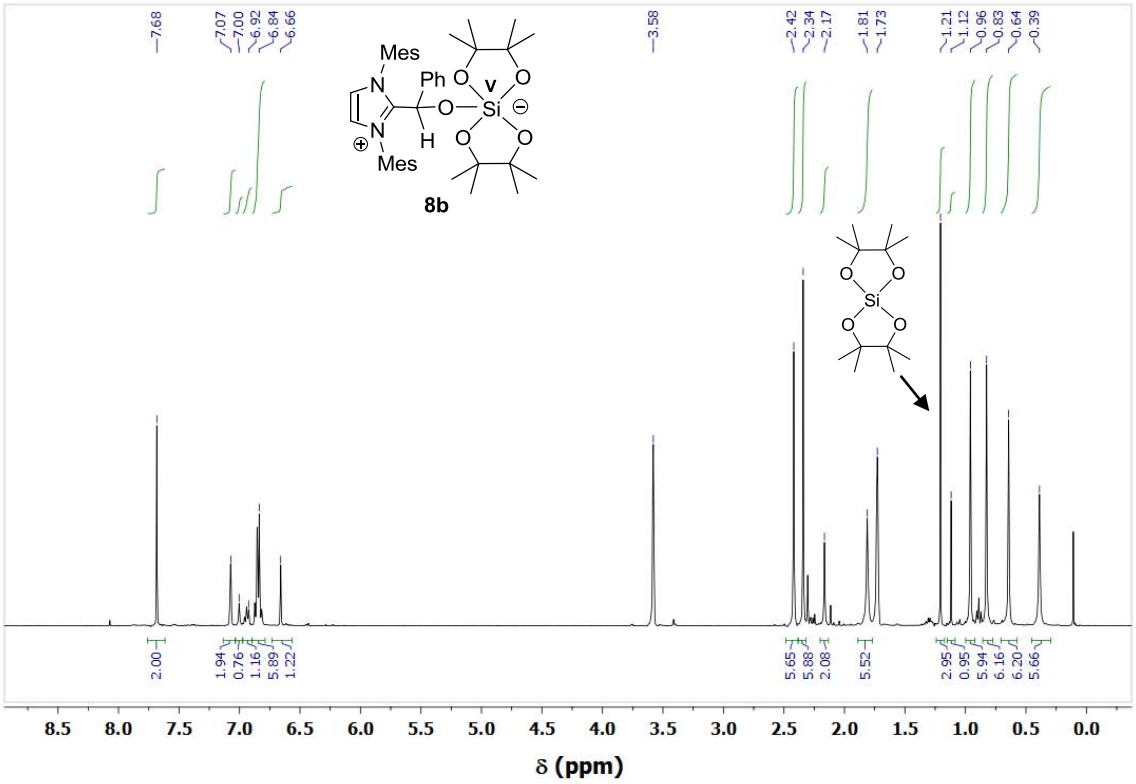

Figure S1. ^{1}H NMR of **8b** in THF-d_8.

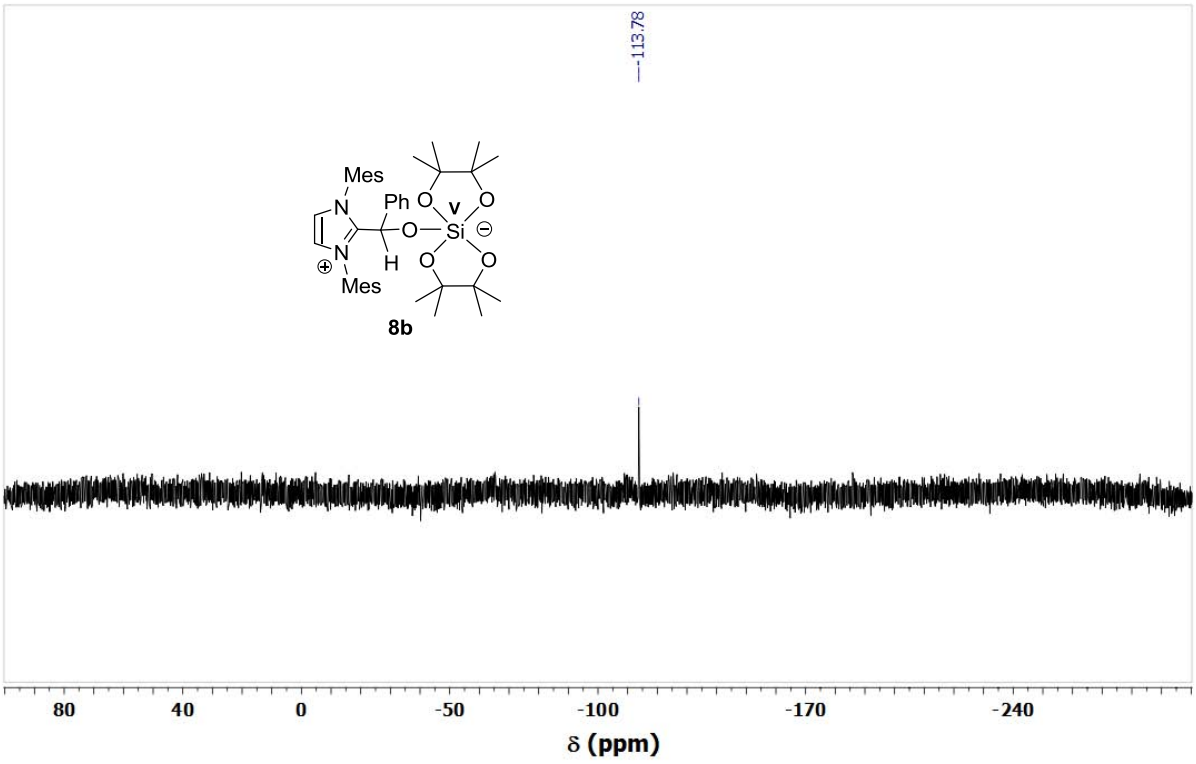

Figure S2. ^{29}Si NMR of **8b** in THF-d_8.

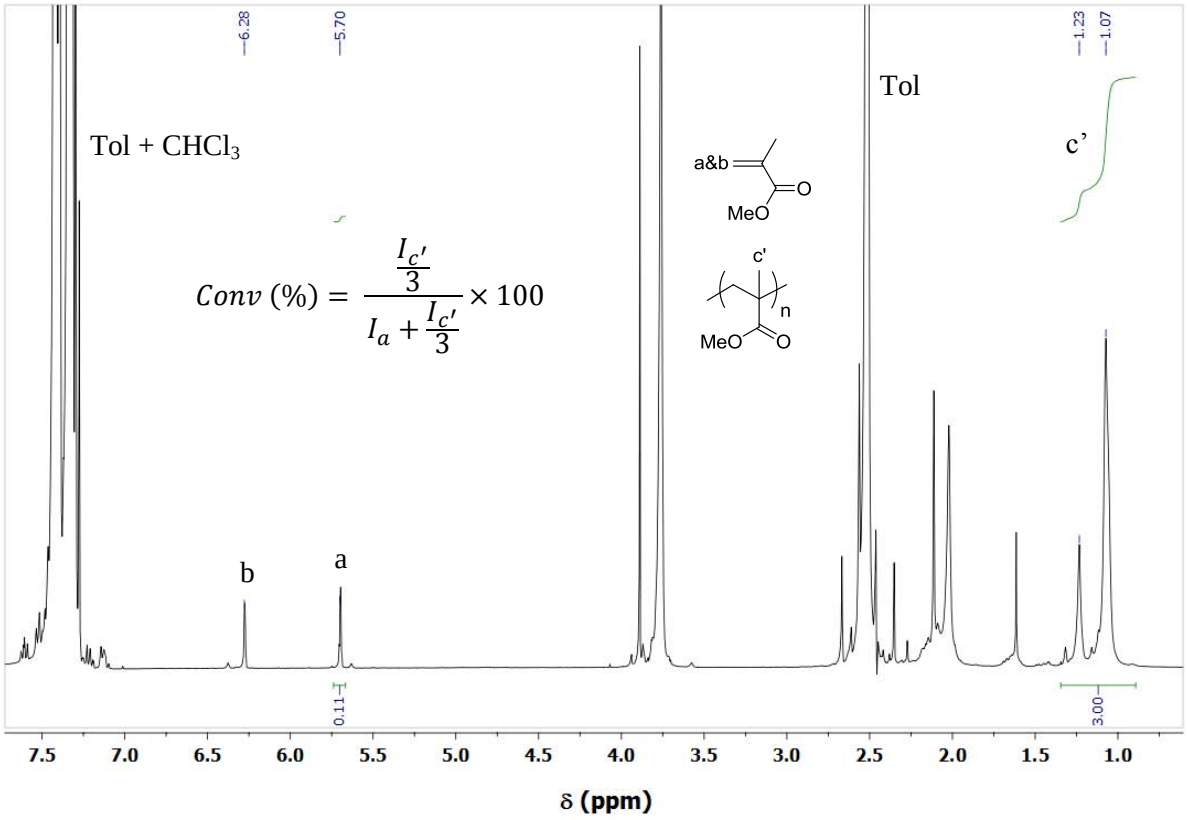

Figure S3. ^{1}H NMR spectrum in $CDCl_3$ to determine the conversion during $B(C_6F_5)_3$-activated and NHC-initiated polymerization of MMA in toluene.

References

1. Raynaud, J.; Ottou, W. N.; Gnanou, Y.; Taton, D., *Chem. Commun.* **2010,** *46*, 3203.
2. Welch, G. C.; Juan, R. R. S.; Masuda, J. D.; Stephan, D. W., *Science* **2006,** *314*, 1124.
3. Stephan, D. W.; Erker, G., *Angew. Chem. Int. Ed.* **2010,** *49*, 46.
4. Brown, H. C.; Schlesinger, H. I.; Cardon, S. Z., *J. Am. Chem. Soc.* **1942,** *64*, 325.
5. Chase, Preston A.; Stephan, Douglas W., *Angew. Chem. Int. Ed.* **2008,** *47*, 7433.
6. Holschumacher, D.; Bannenberg, T.; Hrib, Cristian G.; Jones, Peter G.; Tamm, M., *Angew. Chem. Int. Ed.* **2008,** *47*, 7428.
7. Voss, T.; Mahdi, T.; Otten, E.; Fröhlich, R.; Kehr, G.; Stephan, D. W.; Erker, G., *Organometallics* **2012,** *31*, 2367.
8. Momming, C. M.; Kehr, G.; Wibbeling, B.; Frohlich, R.; Erker, G., *Dalton Trans.* **2010,** *39*, 7556.
9. Wiegand, T.; Eckert, H.; Ekkert, O.; Fröhlich, R.; Kehr, G.; Erker, G.; Grimme, S., *J. Am. Chem. Soc.* **2012,** *134*, 4236.
10. Ullrich, M.; Lough, A. J.; Stephan, D. W., *Organometallics* **2010,** *29*, 3647.
11. Bouhadir, G.; Amgoune, A.; Bourissou, D., In *Adv. Organomet. Chem.*, Anthony, F. H.; Mark, J. F., Eds. Academic Press: 2010; Vol. 58, p 1.
12. Stephan, D. W., *Chem. Commun.* **2010,** *46*, 8526.
13. Erős, G.; Mehdi, H.; Pápai, I.; Rokob, T. A.; Király, P.; Tárkányi, G.; Soós, T., *Angew. Chem. Int. Ed.* **2010,** *49*, 6559.
14. Spies, P.; Schwendemann, S.; Lange, S.; Kehr, G.; Fröhlich, R.; Erker, G., *Angew. Chem. Int. Ed.* **2008,** *47*, 7543.
15. Erős, G.; Nagy, K.; Mehdi, H.; Pápai, I.; Nagy, P.; Király, P.; Tárkányi, G.; Soós, T., *Chem. Eur. J.* **2012,** *18*, 574.
16. Farrell, J. M.; Heiden, Z. M.; Stephan, D. W., *Organometallics* **2011,** *30*, 4497.
17. Dureen, M. A.; Brown, C. C.; Stephan, D. W., *Organometallics* **2010,** *29*, 6594.
18. Morton, J. G. M.; Dureen, M. A.; Stephan, D. W., *Chem. Commun.* **2010,** *46*, 8947.
19. Birkmann, B.; Voss, T.; Geier, S. J.; Ullrich, M.; Kehr, G.; Erker, G.; Stephan, D. W., *Organometallics* **2010,** *29*, 5310.
20. Basle, O.; Porcel, S.; Ladeira, S.; Bouhadir, G.; Bourissou, D., *Chem. Commun.* **2012,** *48*, 4495.
21. Feldhaus, P.; Schirmer, B.; Wibbeling, B.; Daniliuc, C. G.; Frohlich, R.; Grimme, S.; Kehr, G.; Erker, G., *Dalton Trans.* **2012,** *41*, 9135.
22. Theuergarten, E.; Schlosser, J.; Schluns, D.; Freytag, M.; Daniliuc, C. G.; Jones, P. G.; Tamm, M., *Dalton Trans.* **2012,** *41*, 9101.
23. Raup, D. E. A.; Cardinal-David, B.; Holte, D.; Scheidt, K. A., *Nat Chem* **2010,** *2*, 766.
24. Cardinal-David, B.; Raup, D. E. A.; Scheidt, K. A., *J. Am. Chem. Soc.* **2010,** *132*, 5345.
25. Zhang, Y.; Miyake, G. M.; Chen, E. Y. X., *Angew. Chem. Int. Ed.* **2010,** *49*, 10158.
26. Zhang, Y.; Miyake, G. M.; John, M. G.; Falivene, L.; Caporaso, L.; Cavallo, L.; Chen, E. Y. X., *Dalton Trans.* **2012,** *41*, 9119.
27. Chuit, C.; Corriu, R. J. P.; Reye, C.; Young, J. C., *Chem. Rev.* **1993,** *93*, 1371.
28. Holmes, R. R., *Chem. Rev.* **1996,** *96*, 927.
29. Sereda, O.; Tabassum, S.; Wilhelm, R., In *Asymmetric Organocatalysis*, List, B., Ed. Springer Berlin / Heidelberg: 2009; Vol. 291, p 349.
30. Dilman, A. D.; Ioffe, S. L., *Chem. Rev.* **2003,** *103*, 733.
31. Sereda, O.; Tabassum, S.; Wilhelm, R., In *Top. Curr. Chem.*, List, B., Ed. Springer Berlin / Heidelberg: 2009; Vol. 291, p 349.
32. Fuchter, M. J., *Chem. Eur. J.* **2010,** *16*, 12286.
33. Song, J. J.; Gallou, F.; Reeves, J. T.; Tan, Z.; Yee, N. K.; Senanayake, C. H., *J. Org. Chem.* **2006,** *71*, 1273.
34. Song, J. J.; Tan, Z.; Reeves, J. T.; Gallou, F.; Yee, N. K.; Senanayake, C. H., *Org. Lett.* **2005,** *7*, 2193.
35. Song, J. J.; Tan, Z.; Reeves, J. T.; Yee, N. K.; Senanayake, C. H., *Org. Lett.* **2007,** *9*, 1013.
36. Scholten, M. D.; Hedrick, J. L.; Waymouth, R. M., *Macromolecules* **2008,** *41*, 7399.
37. Raynaud, J.; Ciolino, A.; Baceiredo, A.; Destarac, M.; Bonnette, F.; Kato, T.; Gnanou, Y.; Taton, D., *Angew. Chem. Int. Ed.* **2008,** *47*, 5390.
38. Raynaud, J.; Liu, N.; Fevre, M.; Gnanou, Y.; Taton, D., *Polym. Chem.* **2011,** *2*, 1706.
39. Raynaud, J.; Liu, N.; Gnanou, Y.; Taton, D., *Macromolecules* **2010,** *43*, 8853.
40. Raynaud, J.; Gnanou, Y.; Taton, D., *Macromolecules* **2009,** *42*, 5996.

41. Rodriguez, M.; Marrot, S.; Kato, T.; Stérin, S.; Fleury, E.; Baceiredo, A., *J. Organomet. Chem.* **2007,** *692*, 705.
42. Bonnette, F.; Kato, T.; Destarac, M.; Mignani, G.; Cossío, F. P.; Baceiredo, A., *Angew. Chem. Int. Ed.* **2007,** *46*, 8632.
43. Kuhn, N.; Kratz, T.; Bläser, D.; Boese, R., *Chem. Ber.* **1995,** *128*, 245.
44. Hollóczki, O.; Nyulászi, L., *Organometallics* **2009,** *28*, 4159.
45. Ghadwal, R. S.; Sen, S. S.; Roesky, H. W.; Tavcar, G.; Merkel, S.; Stalke, D., *Organometallics* **2009,** *28*, 6374.
46. Stevenson, W. H.; Wilson, S.; Martin, J. C.; Farnham, W. B., *J. Am. Chem. Soc.* **1985,** *107*, 6340.
47. Frye, C. L., *J. Am. Chem. Soc.* **1970,** *92*, 1205.
48. Dixon, D. A.; Hertler, W. R.; Chase, D. B.; Farnham, W. B.; Davidson, F., *Inorg. Chem.* **1988,** *27*, 4012.
49. Stevenson, W. H.; Martin, J. C., *J. Am. Chem. Soc.* **1982,** *104*, 309.
50. Farnham, W. B.; Harlow, R. L., *J. Am. Chem. Soc.* **1981,** *103*, 4608.
51. Perozzi, E. F.; Martin, J. C., *J. Am. Chem. Soc.* **1979,** *101*, 1591.
52. Kemmitt, T. M., NB, *Aust. J. Chem.* **1995,** *48*, 93.
53. Wang, Y.; Xie, Y.; Wei, P.; King, R. B.; Schaefer, H. F.; von R. Schleyer, P.; Robinson, G. H., *Science* **2008,** *321*, 1069.
54. Tapu, D.; Dixon, D. A.; Roe, C., *Chem. Rev.* **2009,** *109*, 3385.
55. Hollóczki, O.; Terleczky, P.; Szieberth, D.; Mourgas, G.; Gudat, D.; Nyulászi, L., *J. Am. Chem. Soc.* **2010,** *133*, 780.
56. Breslow, R., *J. Am. Chem. Soc.* **1958,** *80*, 3719.
57. Chen, Y.-T.; Barletta, G. L.; Haghjoo, K.; Cheng, J. T.; Jordan, F., *J. Org. Chem.* **1994,** *59*, 7714.
58. White, M. J.; Leeper, F. J., *J. Org. Chem.* **2001,** *66*, 5124.
59. Schrader, W.; Handayani, P. P.; Burstein, C.; Glorius, F., *Chem. Commun.* **2007**, 716.
60. Berkessel, A.; Elfert, S.; Etzenbach-Effers, K.; Teles, J. H., *Angew. Chem. Int. Ed.* **2010,** *49*, 7120.
61. Mattson, A. E.; Scheidt, K. A., *Org. Lett.* **2004,** *6*, 4363.
62. Mattson, A. E.; Bharadwaj, A. R.; Zuhl, A. M.; Scheidt, K. A., *J. Org. Chem.* **2006,** *71*, 5715.
63. Burstein, C.; Glorius, F., *Angew. Chem. Int. Ed.* **2004,** *43*, 6205.
64. Grossmann, A.; Enders, D., *Angew. Chem. Int. Ed.* **2012,** *51*, 314.
65. Nair, V.; Babu, B. P.; Vellalath, S.; Varghese, V.; Raveendran, A. E.; Suresh, E., *Org. Lett.* **2009,** *11*, 2507.
66. Sugimoto, H.; Kawamura, C.; Kuroki, M.; Aida, T.; Inoue, S., *Macromolecules* **1994,** *27*, 2013.
67. Braune, W.; Okuda, J., *Angew. Chem. Int. Ed.* **2003,** *42*, 64.
68. Billouard, C.; Carlotti, S.; Desbois, P.; Deffieux, A., *Macromolecules* **2004,** *37*, 4038.
69. Labbe, A.; Carlotti, S.; Billouard, C.; Desbois, P.; Deffieux, A., *Macromolecules* **2007,** *40*, 7842.
70. Rejsek, V.; Sauvanier, D.; Billouard, C.; Desbois, P.; Deffieux, A.; Carlotti, S., *Macromolecules* **2007,** *40*, 6510.
71. Gervais, M.; Labbé, A.; Carlotti, S.; Deffieux, A., *Macromolecules* **2009,** *42*, 2395.
72. Kubisa, P.; Penczek, S., *Prog. Polym. Sci.* **1999,** *24*, 1409.
73. Penczek, S.; Cypryk, M.; Duda, A.; Kubisa, P.; Slomkowski, S., *Prog. Polym. Sci.* **2007,** *32*, 247.
74. Sunder, A.; Hanselmann, R.; Frey, H.; Mülhaupt, R., *Macromolecules* **1999,** *32*, 4240.
75. Laszlo, P.; Teston, M., *J. Am. Chem. Soc.* **1990,** *112*, 8750.
76. James, T.; Shinkai, S., In *Top. Curr. Chem.*, Penadés, S., Ed. Springer Berlin / Heidelberg: 2002; Vol. 218, p 159.
77. Erker, G., *Dalton Trans.* **2005**, 1883.
78. Thirupathi, P.; Neupane, L. N.; Lee, K.-H., *Tetrahedron* **2011,** *67*, 7301.
79. Farrell, J. M.; Heiden, Z. M.; Stephan, D. W., *Organometallics* **2011,** *30*, 4497.
80. Kronig, S.; Theuergarten, E.; Holschumacher, D.; Bannenberg, T.; Daniliuc, C. G.; Jones, P. G.; Tamm, M., *Inorg. Chem.* **2011,** *50*, 7344.
81. Brook, M. A.; Grande, J. B.; Ganachaud, F., In *Silicon Polymers*, Muzafarov, A. M., Ed. 2011; Vol. 235, p 161.
82. Kostjuk, S. V.; Radchenko, A. V.; Ganachaud, F., *J. Polym. Sci., Part A: Polym. Chem.* **2008,** *46*, 4734.
83. Ouardad, S.; Kostjuk, S. V.; Ganachaud, F.; Puskas, J. E.; Deffieux, A.; Peruch, F., *J. Polym. Sci., Part A: Polym. Chem.* **2011,** *49*, 4948.
84. Kostjuk, S. V.; Ganachaud, F., *Macromolecules* **2006,** *39*, 3110.
85. Radchenko, A. V.; Kostjuk, S. V.; Vasilenko, I. V.; Ganachaud, F.; Kaputsky, F. N.; Guillaneuf, Y., *J. Polym. Sci., Part A: Polym. Chem.* **2008,** *46*, 6928.
86. Vergnaud, J.; Sarazin, Y.; Strub, H.; Carpentier, J. F., *Eur. Polym. J.* **2010,** *46*, 1093.
87. Chakraborty, D.; Rodriguez, A.; Chen, E. Y. X., *Macromolecules* **2003,** *36*, 5470.

88. Maji, B.; Breugst, M.; Mayr, H., *Angew. Chem. Int. Ed.* **2011,** *50*, 6915.
89. Raynaud, J.; Absalon, C.; Gnanou, Y.; Taton, D., *J. Am. Chem. Soc.* **2009,** *131*, 3201.
90. Zhang, Y.; Chen, E. Y. X., *Angew. Chem. Int. Ed.* **2012,** *51*, 2465.
91. Arnold, P. L.; Pearson, S., *Coord. Chem. Rev.* **2007,** *251*, 596.
92. Krüger, A.; Albrecht, M., *Aust. J. Chem.* **2011,** *64*, 1113.
93. Welch, G. C.; Holtrichter-Roessmann, T.; Stephan, D. W., *Inorg. Chem.* **2008,** *47*, 1904.
94. Lee, J. Y.; Diefenbach, S. P.; Power, J. M.; Lin, R. W. US Patent 5959151, 1999.
95. Danopoulos, A.; Galsworthy, J.; Green, M.; Doerrer, L.; Cafferkey, S.; Hursthouse, M., *Chem. Commun.* **1998**, 2529.
96. Beringhelli, T.; Maggioni, D.; D'Alfonso, G., *Organometallics* **2001,** *20*, 4927.
97. Baskaran, D., *Prog. Polym. Sci.* **2003,** *28*, 521.
98. Baskaran, D.; Müller, A. H. E., *Prog. Polym. Sci.* **2007,** *32*, 173.
99. Guo, L.; Zhang, D., *J. Am. Chem. Soc.* **2009,** *131*, 18072.
100. Jeong, W.; Hedrick, J. L.; Waymouth, R. M., *J. Am. Chem. Soc.* **2007,** *129*, 8414.
101. Culkin, D.; Jeong, W.; Csihony, S.; Gomez, E.; Balsara, N.; Hedrick, J.; Waymouth, R., *Angew. Chem. Int. Ed.* **2007,** *46*, 2627.
102. Shin, E. J.; Brown, H. A.; Gonzalez, S.; Jeong, W.; Hedrick, J. L.; Waymouth, R. M., *Angew. Chem. Int. Ed.* **2011,** *50*, 6388.
103. Jeong, W.; Shin, E. J.; Culkin, D. A.; Hedrick, J. L.; Waymouth, R. M., *J. Am. Chem. Soc.* **2009,** *131*, 4884.
104. Lee, C.-U.; Smart, T. P.; Guo, L.; Epps, T. H.; Zhang, D., *Macromolecules* **2011,** *44*, 9574.
105. Li, X.; Guo, L.; Casiano-Maldonado, M.; Zhang, D.; Wesdemiotis, C., *Macromolecules* **2011,** *44*, 4555.
106. Shin, E. J.; Jeong, W.; Brown, H. A.; Koo, B. J.; Hedrick, J. L.; Waymouth, R. M., *Macromolecules* **2011,** *44*, 2773.
107. Wohlfarth, C., In *Handbook of Chemistry and Physics*, 87th Edition ed.; Lide, D. R., Ed. CRC Press: Boca Raton, FL, 2006; p 135.
108. Jacobsen, H.; Cavallo, L., *ChemPhysChem* **2012,** *13*, 562.
109. M. J. Frisch, G. W. Trucks, H. B. Schlegel, G. E. Scuseria, M. A. Robb, J. R. Cheeseman, J. A. Montgomery, Jr. T. Vreven, K. N. Kudin, J. C. Burant, J. M. Millam, S. S. Iyengar, J. Tomasi, V. Barone, B. Mennucci, M. Cossi, G. Scalmani, N. Rega, G. A. Petersson, H. Nakatsuji, M. Hada, M. Ehara, K. Toyota, R. Fukuda, J. Hasegawa, M. Ishida, T. Nakajima, Y. Honda, O. Kitao, H. Nakai, M. X. Klene, X. Li, J. E. Knox, H. P. Hratchian, J. B. Cross, C. Adamo, J. Jaramillo, R. Gomperts, R. E. Stratmann, O. Yazyev, A. J. Austin, R. Cammi, C. Pomelli, J. W. Ochterski, P. Y. Ayala, K. Morokuma, G. A. Voth, P. Salvador, J. J. Dannenberg, V. G. Zakrzewski, S. Dapprich, A. D. Daniels, M. C. Strain, O. Farkas, D. K. Malick, A. D. Rabuck, K. Raghavachari, J. B. Foresman, J. V. Ortiz, Q. Cui, A. G. Baboul, S. Clifford, J. Cioslowski, B. B. Stefanov, G. Liu, A. Liashenko, P. Piskorz, I. Komaromi, R. L. Martin, D. J. Fox, T. Keith, M. A. Al-Laham, C. Y. Peng, A. Nanayakkara, M. Challacombe, P. M. W. Gill, B. Johnson, W. Chen, M. W. Wong, C. Gonzalez, J. A. Pople, Gaussian 03, Revision D-02, Gaussian, Inc., Pittsburgh PA, **2003**.
110. Parr, R. G.; Yang, W., *Density Functional Theory of Atoms and Molecules*, Breslow, R.; Goodenough, J. B., Eds. Oxford University Press: New York, 1989.
111. Becke, A. D., *J. Chem. Phys.* **1993,** *98*, 5648.
112. Becke, A. D., *Phys. Rev. A* **1988,** *38*, 3098.
113. Lee, C.; Yang, W.; Parr, R. G., *Phys. Rev. B* **1988,** *37*, 785.
114. Hariharan, P. C.; Pople, J. A., *Theor. Chem. Acc.* **1973,** *28*, 213.
115. Gonzalez, C.; Schlegel, H. B., *J. Chem. Phys.* **1989,** *90*, 2154.
116. Gonzalez, C.; Schlegel, H. B., *J. Phys. Chem.* **1990,** *94*, 5523.
117. Arduengo, A. J.; Dias, H. V. R.; Harlow, R. L.; Kline, M., *J. Am. Chem. Soc.* **1992,** *114*, 5530.
118. Kuhn, N.; Kratz, T., *Synthesis* **1993,** *1993*, 561.
119. Swamy, K. C. K.; Chandrasekhar, V.; Harland, J. J.; Holmes, J. M.; Day, R. O.; Holmes, R. R., *J. Am. Chem. Soc.* **1990,** *112*, 2341.
120. Perozzi, E. F.; Michalak, R. S.; Figuly, G. D.; Stevenson, W. H.; Dess, D.; Ross, M. R.; Martin, J. C., *J. Org. Chem.* **1981,** *46*, 1049.

Chapitre 4

Polymérisation par Transfert de Groupe des (Méth)acrylates d'alkyle Organocatalysée par la Tris(2,4,6-trimethoxyphenyl)phosphine (TTMPP)

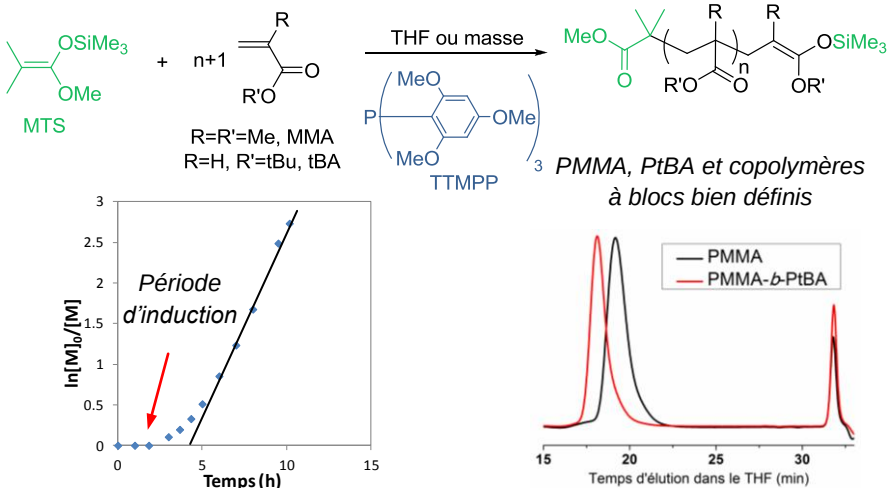

Mots clés: Organocatalyse, Phosphines, Polymérisation par transfert de groupe, Méthacrylate de méthyle, Acrylate de *tert*-butyle, Copolymérisation.

Keywords: Organocatalysis, Phosphines, Group transfer polymerization, Methyl methacrylate, *tert*-Butyl acrylate, Copolymerization.

Résumé: Plusieurs trialkyle phosphines commerciales ont été testées en tant que catalyseurs organiques pour la polymérisation par transfert de groupe (GTP) du méthacrylate de méthyle (MMA) et de l'acrylate de *tert*-butyle (*t*BA). Parmi elles, seule la tris(2,4,6-trimethoxyphenyl)phosphine (TTMPP) a permis de polymériser ces deux monomères de façon "vivante/contrôlée", dans le THF mais aussi en masse, en utilisant le 1-methoxy-2-methyl-1-[(trimethylsilyl)oxy]prop-1-ene (MTS) en tant qu'amorceur. Les masses des poly[alkyl(méth)acrylate]s obtenus sont en accord avec le ratio molaire initial $[monomère]_0/[MTS]_0$ et les dispersités sont <1.37 et <1.45 pour les réactions effectuées respectivement en masse et dans le THF. D'un point de vue général, un meilleur contrôle de ces polymérisations catalysées par la TTMPP a pu être noté avec les monomères méthacryliques par rapport aux acryliques. Un copolymère à blocs (poly(méthacrylate de méthyle)-*b*-poly(acrylate de *tert*-butyle)) avec un dispersité finale <1.2 et des masses molaires contrôlées a été synthétisé par GTP séquentielle catalysée par la TTMPP. L'évolution cinétique (premier ordre en monomère) présente une période d'induction, dont la durée dépend des conditions expérimentales utilisées. La tacticité des PMMAs obtenus (*mm/mr/rr* = 0.06/0.42/0.52) est très similaire à celle d'un PMMA synthétisé par polymérisation anionique. Ces deux dernières remarques sont en faveur de l'occurrence d'un mécanisme dissociatif pour la GTP du MMA catalysée par la TTMPP dans le THF. Ce mécanisme implique la formation d'une petite quantité d'espèces propageantes de type énolates au cours de la réaction. Cependant, les analyses par spectroscopie RMN ^{13}C et ^{29}Si, à température ambiante, d'un mélange équimolaire entre le MTS et la TTMPP n'ont pas permis l'observation de telles espèces.

This chapter describes the use of phosphines as potent organocatalysts for the group transfer polymerization of alkyl (meth)acrylates. These results have been published recently in Macromolecules.[1]

Chapter 4

Tris(2,4,6-trimethoxyphenyl)phosphine (TTMPP) as Potent Organocatalyst for Group Transfer Polymerization of Alkyl (Meth)acrylates

TABLE OF CONTENTS

Introduction

Group transfer polymerization (GTP) involves a silyl ketene acetal (SKA), typically 1-methoxy-2-methyl-1-[(trimethylsilyl)oxy]prop-1-ene (MTS), as an initiator, which is added onto an incoming (meth)acrylic monomer and transferred to the polymer chain end.[2-3] GTP traditionally utilizes a metal-free Lewis base catalyst (e.g., tris(dimethylamino)sulfonium bifluoride ($TASHF_2$), tetrabutylammonium fluoride (TBAF), Figure 1) activating the SKA in the case of methacrylics, while metal-based Lewis acids (e.g., AlR_2Cl, $ZnCl_2$) are employed with acrylic monomers. The repetition of the elementary addition reaction of the SKA to the (meth)acrylic substrate, referred to as the Mukaiyama-Michael reaction, allows for a "controlled/living" polymerization at room temperature (RT).

Whether the mechanism of GTP proceeds *via* an associative or a dissociative pathway has been the focus of an intense debate.[4-5] Moreover, the lack of a common catalyst for the GTP of both acrylic and methacrylic monomers quickly limited the application of this polymerization method to macromolecular engineering,[6-10] for instance, for the synthesis of all-acrylic block copolymers.[3,11]

In recent years, however, the scope of GTP has been broadened (see Figure 1) through the use of organic catalysts.[12] For instance, both Hedrick, Waymouth *et al.*[13] and our group[14-16] have reported that *N*-heterocyclic carbenes (NHCs) efficiently catalyze the GTP of both acrylics and methacrylics. NHCs have also enabled the synthesis of all-acrylic block copolymers *via* sequential GTP of both families of monomers.[17] Other organic catalysts can induce GTP in a "controlled/living" fashion, including Bronsted phosphazene bases, such as (*tert*-butylimino)tris{[tris(dimethylamino)phosphoranylidene]amino},phosphorane (*t*-BuP_4) or proazaphosphatrane 2,8,9-triisobutyl-2,5,8,9-tetraaza-1-phosphabicyclo[3.3.3]undecane (TiBP)[18-20] and strong Bronsted acids, such as bis(trifluoromethanesulfonyl)imide (Tf_2NH), pentafluorophenylbis(triflyl)methane ($C_6F_5CHTf_2$) or sulfonimide derivatives, and oxonium ($[H(Et_2O)_2]^+$) or ammonium ($[HN(Me_2)Ph]^+$) acids featuring a $[B(C_6F_5)_4]^-$ borate counteranion.[21-24] Chen *et al.* have also reported that $[Ph_3C]^+[B(C_6F_5)_4]^-$ is an efficient precatalyst for the GTP of various

(meth)acrylics, including renewable butyrolactone-based vinylidene monomers derived from a naturally occurring resource.[25-27]

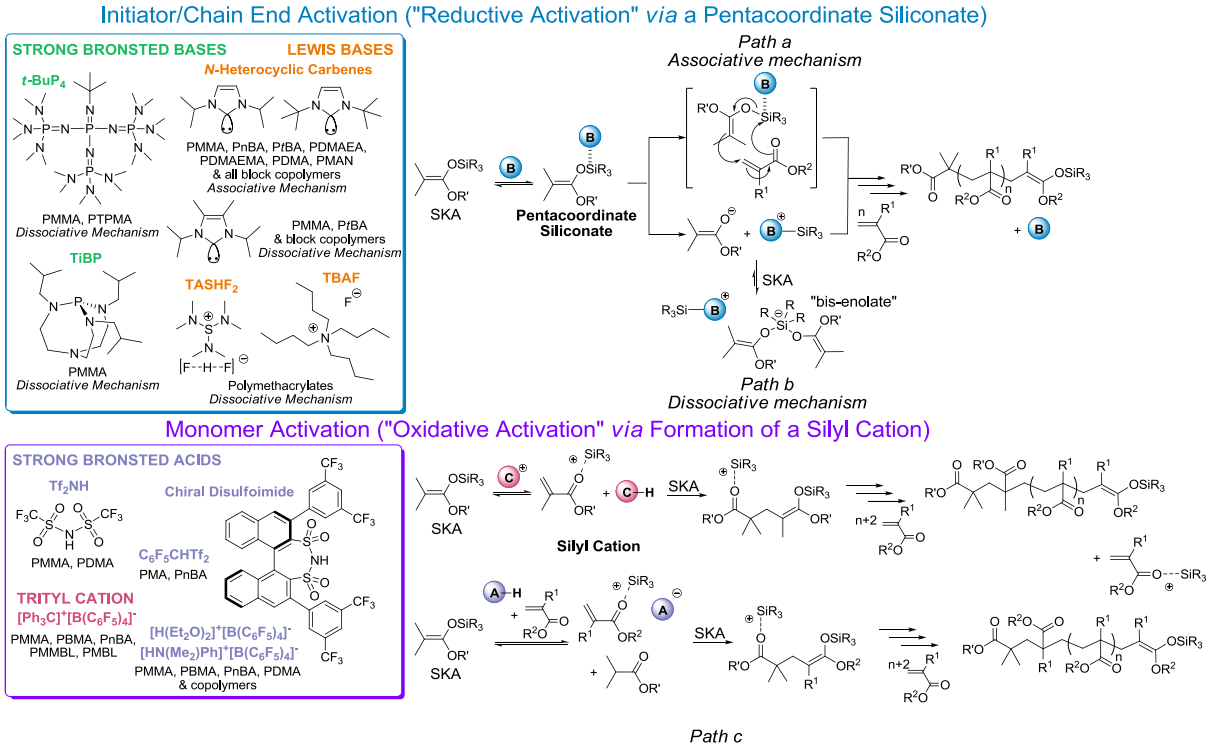

Figure 1. Overview of recent (pre)catalysts of group transfer polymerization of (meth)acrylics and related mechanisms: activated initiator/chain end mechanism *via* an associative (Path a) or a dissociative pathway (Path b), and the monomer activated mechanism (Path c, counter-anion are omitted).

Lewis or Bronsted bases, such as NHCs, *t*BuP$_4$ or TiBP, activate the SKA moiety of the initiator/chain ends *via* the formation of a pentacoordinated siliconate intermediate (Figure 1); this is referred to as the "reductive activation mechanism".[13,15,19] Further propagation can occur either *via* the generation of true enolates (dissociative pathway; Figure 1, Path b) or *via* a concerted-like mechanism (associative pathway; Figure 1, Path a). However, stating on the occurrence of that mechanism or the other is not straightforward. For instance, the NHC-catalyzed GTP has been reported to follow either the associative[15] or the dissociative[13] mechanism, depending on the substituents on the NHC backbone.

On the other hand, both strong Bronsted acids and $[Ph_3C]^+[B(C_6F_5)_4]^-$ are thought to generate silyl cations, by consumption of a small portion of the SKA initiator, which further activates the monomer (this is referred to as the "oxidative activation"; Figure 1, Path c).[21,23] This concept has been elegantly applied by Chen *et al.*[28] to a bis-SKA serving both as initiator/chain end and catalyst.

Here, we wish to evaluate the behavior of tri-alkyl phosphines as GTP catalysts. Indeed, NHCs and tri-alkyl phosphines have been often used for similar applications and, in particular, as potent ligands in organometallic chemistry.[29] Surprisingly, phosphines, in contrast to NHCs, remain seldom studied among organocatalysts used in polymerization reactions.[12] They can serve as metal-free initiators (but not catalysts) for the ring opening copolymerization of butyrolactone derivatives and epoxides,[30] or for the zwitterionic polymerization of butyl cyanoacrylate.[31] Only one report by Hedrick *et al.*[32] has employed PR_3 as true organocatalysts for the ring-opening polymerization of D,L-lactide.

Although NHCs are less and less considered as phosphines analogues in organometallic chemistry, mainly due to different steric properties and σ-donation capacities, the comparison between these two compounds can still be helpful.[33] Indeed, the potential of phosphines as organocatalysts in molecular chemistry is well documented.[34-35] For instance, phosphines efficiently activate C-Si and O-Si bonds.[36-40] In this regard, Matsukawa *et al.* have shown that, among several alkyl and aryl phosphines, tris(2,4,6-trimethoxyphenyl)phosphine (TTMPP) was the most efficient to catalyze Mukaiyama-aldol reactions.[37] TTMPP is a relatively strongly basic phosphine (pK_a=11.2)[41] compared, for instance to triphenylphosphine, Ph_3P (pK_a in CH_3NO_2 = 2.73).[42]

As Mukaiyama-Michael and Mukaiyama-aldol reactions have similarities, this has prompted us to consider different phosphines as GTP catalysts. We show here that only TTMPP enables to control the GTP of both methyl methacrylate and *tert*-butylacrylate. Synthesis of related block copolymers by sequential GTP is also presented.

1. Phosphines as catalysts for the GTP of methyl methacrylate

The 1-methoxy-2-methyl-1-[(trimethylsilyl)oxy]prop-1-ene (MTS)-initiated polymerization of MMA was first investigated in THF solution, at RT, using four different tris-alkyl phosphines as

catalysts (Scheme 1). Under these conditions, only TTMPP (10% mol. relative to MTS) proved efficient to trigger MMA polymerization (Table 1). The three other phosphines, Bu_3P ($pK_a(Bu_3P)$ in CH_3NO_2 = 8.43),[43] Cy_3P (pK_a in THF = 9.7)[44] and Ph_3P (pK_a in CH_3NO_2 = 2.73),[42] led to very poor conversion after 24 h without any control of the polymerization, as indicated by NMR analyses and SEC traces of the obtained PMMA's (runs 1-3). Using higher quantities of these three phosphines or increasing the temperature to 50 °C did not allow for a better control. In sharp contrast, TTMPP (pK_a = 11.2)[41] quantitatively afforded PMMA's exhibiting well-controlled molar masses (M_n= 3,000 and 10,600 g/mol) and dispersities ($D = M_w/M_n$) lower than 1.15 (SEC in THF calibrated with PS standards), when polymerizing MMA in THF using the following initial ratios: $[TTMPP]_0/[MTS]_0/[MMA]_0$ = 0.1/1/30 and 0.1/1/100, respectively (runs 4 and 5).

In particular, no signal was observed on the UV signal of the SEC trace at λ = 305 nm, a wavelength corresponding to the maximum of absorbance of β-keto-ester chain ends of PMMA generated by a backbiting termination reaction.[45] Such a side reaction, which results in a progressive loss of control, is frequently observed during the anionic polymerization of (meth)acrylics.[45] This attests that the TTMPP-catalyzed GTP of MMA proceeds with negligible extent –if any– of this backbiting reaction.

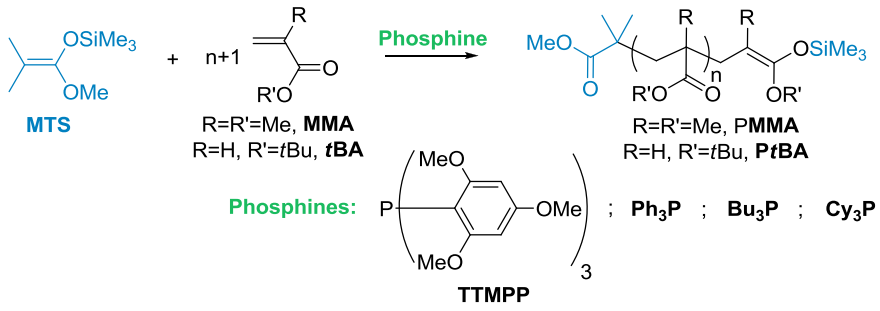

Scheme 1. Group transfer polymerization of MMA catalyzed by different phosphines and using MTS as initiator.

Surprisingly, polymerization reactions performed under the same conditions using toluene instead of THF did not yield any polymer at all (run 6). This result is in contrast to previous observations made with NHC catalysts and Bronsted bases such as *t*-BuP_4 and TiBP, which efficiently catalyze the

GTP of MMA both in THF and toluene.[15,19] It is worth mentioning, however, that a decrease of the catalytic efficiency of TTMPP was already noted when substituting toluene for THF, in the context of catalysis in molecular chemistry.[39-40]

Table 1. Group transfer polymerization of MMA in solution or in bulk at 25 °C catalyzed by different phosphines, in the presence of MTS as initiator.

Run	Solvent	Phosphine	$[P]_0/[MTS]_0/[MMA]_0$	time (h)	conv[a] (%)	$M_{n,theo}$[b] (g/mol)	$M_{n,SEC}$[c] (g/mol)	D[c]
1	THF	Bu_3P	0.1/1/30	30	4	-	bimodal	-
2	THF	Cy_3P	0.5/1/30	24	0	-	-	-
3	THF	Ph_3P	0.1/1/30	24	0	-	-	-
4	THF	TTMPP	0.1/1/30	13	100	3,000	3,000	1.13
5	THF	TTMPP	0.1/1/100	26	100	10,000	10,600	1.15
6	toluene	TTMPP	0.1/1/30	13	0	-	-	-
7	-	TTMPP	0.1/1/30	-	96	3,000	3,600	1.37
8	-	TTMPP	0.1/1/100	-	96	10,000	9,500	1.3
9	-	TTMPP	0.1/1/500	2	95	50,000	57,000	1.3
10	-	TTMPP	0.1/-/30	15	<1	-	-	-

[a] Determined by ^1H NMR in $CDCl_3$ (Figure S2). [b] Calculated as follows: $M_{n,theo} = ([MMA]_0/[MTS]_0) \times conv \times M_{MMA} + M_{MTS}$. [c] Determined by SEC in THF using PS standards.

Interestingly, TTMPP was also found to efficiently catalyze the polymerization of MMA in bulk. Under such solvent-less conditions, quantitative conversions were reached within a few hours with good control over the molar masses and dispersity. This is likely due to the relatively moderate catalytic activity of TTMPP compared to other nucleophiles used as GTP catalysts. NHCs, for instance, did not enable to control the GTP of methacrylics in bulk at RT.[46] Tetrabutylammonium bibenzoate[47] and tetrabutylammonium fluoride[48] allowed catalyzing the bulk GTP of 2-(dimethylamino)ethyl methacrylate and methyl or butyl methacrylates, respectively. A 30% discrepancy between obtained and targeted molar masses was, however, noted with dispersities ranging from 1.5 to 2.1. When TTMPP was dissolved in MMA overnight, followed by addition of the desired amount of MTS, PMMA's with M_n values in the range 3,600 to 57,000 g/mol were obtained (runs 7 to 9), molar masses being still controlled by the initial $[MTS]_0/[MMA]_0$ ratio (Figure 2 for experiments in bulk and Figure S1 for experiments in THF). Relatively low dispersities (<1.4) were noted, solvent-free conditions decreasing the ability of the monomer and polymer species to diffuse in

the polymerization medium. It is worth mentioning that polymerization experiments with low $[MTS]_0/[MMA]_0$ ratios proceeded immediately after MTS was added.

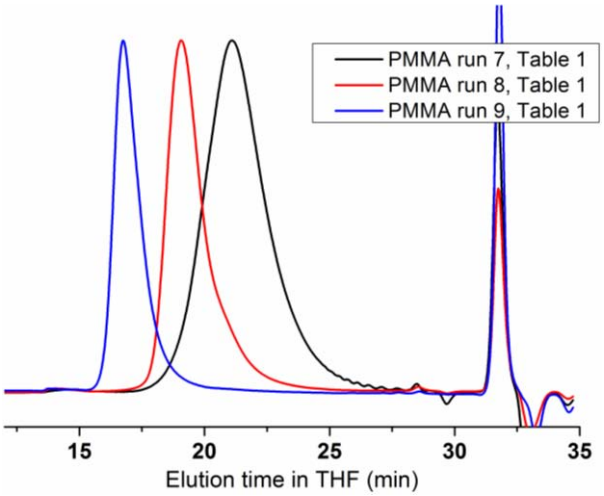

Figure 2. SEC traces (RI detector) of PMMA's obtained from the TTMPP-catalyzed GTP of MMA under solventless conditions (Table 1, runs 7-9).

2. TTMPP as catalyst for the GTP of *tert*-butyl acrylate

The TTMPP catalyzed-GTP of *tert*-butyl acrylate (*t*BA) in THF was next investigated. Corresponding experiments are summarized in Table 2. Unexpectedly, the TTMPP-catalyzed GTP of *t*BA was effective either at rather high concentrations in THF or under very dilute conditions, while intermediate concentrations led to a poor control. Solution experiments (runs 1-2) performed with an initial ratio $V_{THF}/V_{tBA0} = 1$ (corresponding to an initial concentration $[tBA]_0 = 7$ M), indeed, allowed for a good control of the polymerization of *t*BA. In contrast, increasing this ratio to 2 resulted in a loss of control, as evidenced by a bimodal distribution of corresponding SEC traces (run 3, Table 2), whereas a narrowly distributed P*t*BA was obtained using an initial $[tBA]_0$ of 0.47 M ($V_{THF}/V_{tBA0} = 15$). In the latter case, the kinetics of the reaction was obviously slower (run 4, Table 2).

Poly(*tert*-butyl acrylate)s (P*t*BA's) with M_n values equal to 3,100 and 7,800 g/mol (SEC in THF calibrated with PS standards) were obtained by GTP in THF within 2 h (Table 2, runs 1-2). Experimental molar masses were found in good agreement with expected values based on initial $[TTMPP]_0/[MTS]_0/[tBA]_0$ ratios. Dispersity values (D) were always close to 1.4, attesting to a slightly

lower control of the TTMPP-catalyzed GTP of *t*BA (see Figure 3 for the corresponding SEC traces), as compared to that discussed above for MMA. The much higher reactivity of *t*BA compared to MMA can explain this trend. As in the case of TTMPP-catalyzed GTP of MMA, no signal was yet noted on the UV signal of the SEC trace at the wavelength corresponding to the maximum of absorbance of P*t*BA chains terminated by backbiting reactions (λ = 260 nm, specifically for polyacrylate chains). In contrast, attempts to polymerize *t*BA in bulk (run 6, Table 2) were unsuccessful, presumably due to the poor solubility of TTMPP in this particular monomer. Thus, in general terms, control of the polymerization appeared to be more difficult with *t*BA as compared to MMA.

Table 2. Group transfer polymerization of *t*BA in THF at 25 °C catalyzed by TTMPP using MTS as initiator.

Run	Solvent	$[TTMPP]_0/[MTS]_0/[tBA]_0$	time (h)	conv[a] (%)	$M_{n,theo}$[b] (g/mol)	$M_{n,SEC}$[c] (g/mol)	D[c]
1	THF[d]	0.01/1/22	2	99	2,800	3,100	1.4
2	THF[d]	0.01/1/78	2	75	7,500	7,800	1.45
3	THF[e]	0.01/1/22	5	87	2,400	bimodal	-
4	THF[f]	0.01/1/22	60	80	2,300	2,100	1.12
5	THF[d]	0.1/-/23	17	29	-	-	-
6	-	0.1/1/23	17	0	-	-	-

[a] Determined by ^{1}H NMR in $CDCl_3$ (see Figure S3). [b] Calculated as follows: $M_{n,theo} = ([tBA]_0/[MTS]_0) \times conv \times M_{tBA} + M_{MTS}$. [c] Determined by SEC in THF using PS standards. [d] $[tBA]_0$ = 7 M. [e] $[tBA]_0$ = 3.5 M. [f] $[tBA]_0$ = 0.47 M.

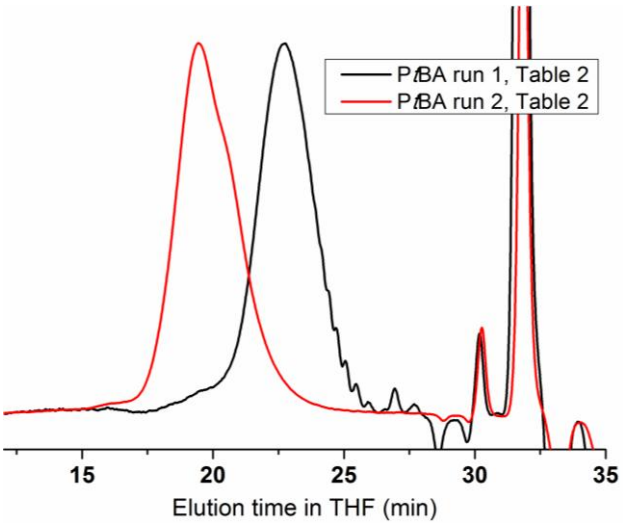

Figure 3. SEC traces (RI detector) of P*t*BA's obtained from the TTMPP-catalyzed GTP of *t*BA in THF (Table 2, runs 1-2).

3. Chain extension experiment and synthesis of PMMA-*b*-P*t*BA diblock copolymers

Chain extension experiments were next carried out so as to account for the "controlled/living" character of these TTMPP-catalyzed GTP's. Results are summarized in Table 3. First, MMA was polymerized in THF with an initial ratio $[TTMPP]_0/[MTS]_0/[MMA]_0$ = 0.1/1/120. After complete consumption of the monomer, a polymer denoted as PMMA(1^{st}), with M_n = 12,300 g/mol and D = 1.15 (SEC in THF *vs* PS standards) was obtained (run 1a, Table 3). Then, 135 eq. of MMA were added to the parent PMMA(1^{st}), affording PMMA(2^{nd}) with M_n = 22,600 g/mol and D = 1.16 (run 1b). Hence, SEC traces showed a shift to a higher M_n region after chain extension, with a monomodal distribution of the resulting PMMA(2^{nd}) (Figure 4a). Adding a higher amount of MMA (200 eq.) in another chain extension experiment led, however, to minute amounts of PMMA dead chains (<5%, see supporting info for SEC traces), most probably owing to the high viscosity of the initial solution ([PMMA] = 2.8 M, before chain extension).

Interestingly, adding *tert*-butyl acrylate (*t*BA, 95 eq.) to a parent PMMA derived by TTMPP-catalyzed GTP led to a structurally well-defined block copolymer, PMMA-*b*-P*t*BA, with M_n = 22,000 g/mol and D = 1.19 (run 2, Table 3 and Figure 4b). As depicted in Figure 5b, SEC trace of the compound obtained by this sequential GTP is monomodal, while its experimental molar mass (*vs* PS standards) is in relatively good accordance with the targeted value. Analysis by ^{1}H NMR spectroscopy of this PMMA-*b*-P*t*BA block copolymer confirmed the presence of characteristic protons of both blocks. The molar mass of the second block could thus be calculated, from the relative integration of characteristic signals due to PMMA and P*t*BA blocks, assuming that SEC provides a good estimate of the molar mass of the first PMMA block (Figure S4, for the corresponding ^{1}H NMR spectrum with all signals' assignment). Experimental molar masses of the PMMA-*b*-P*t*BA copolymer provided by SEC (22,000 g/mol) and by NMR (27,000 g/mol) were in relatively good agreement. Thus, the TTMPP-catalyzed GTP of MMA enables the synthesis of well-defined PMMA's that can serve as macroinitiators in both chain extension experiments and crossover to the polymerization of *t*BA for methacrylic-acrylic block copolymer synthesis.

Table 3. Chain extension experiments and synthesis of PMMA-*b*-P*t*BA block copolymers by sequential group transfer polymerization in THF at 25 °C in the presence of TTMPP (first PMMA block is grown using MTS as an initiator).

Run	Growing block	$[TTMPP]_0/[MTS]_0/[M]_0$	Cumulated time (h)	conv (%)[a]	$M_{n,theo}$ (g/mol)[b]	$M_{n,SEC}$ (g/mol)[c]	$Đ$[c]
1a	PMMA(1^{st})	0.1/1/120	30	100	12,000	12,300	1.15
1b	PMMA(2^{nd})	+ 135 eq. MMA	60	100	25,500	22,600	1.16
2a	PMMA(1^{st})	0.1/1/100	26	100	10,000	10,600	1.15
2b	P*t*BA(2^{nd})	+ 95 eq. *t*BA	60	100	22,000	22,000[d]	1.19

[a] Determined by ^{1}H NMR in $CDCl_3$. [b] Calculated as follows: $M_{n,theo} = ([MMA]_0/[MTS]_0) \times conv \times M_{MMA} + M_{MTS}$ for 1st block and $M_{n,theo} = ([M]_0/[MTS]_0) \times conv \times M_M + M_{1st\ block(SEC)}$ for 2nd block, where the monomer (M) is either MMA or *t*BA. [c] Determined by SEC in THF using PS standards. [d] $M_{n,NMR} = M_{1st\ block(SEC)} + M_{1st\ block(SEC)}$ = 27,000 g/mol.

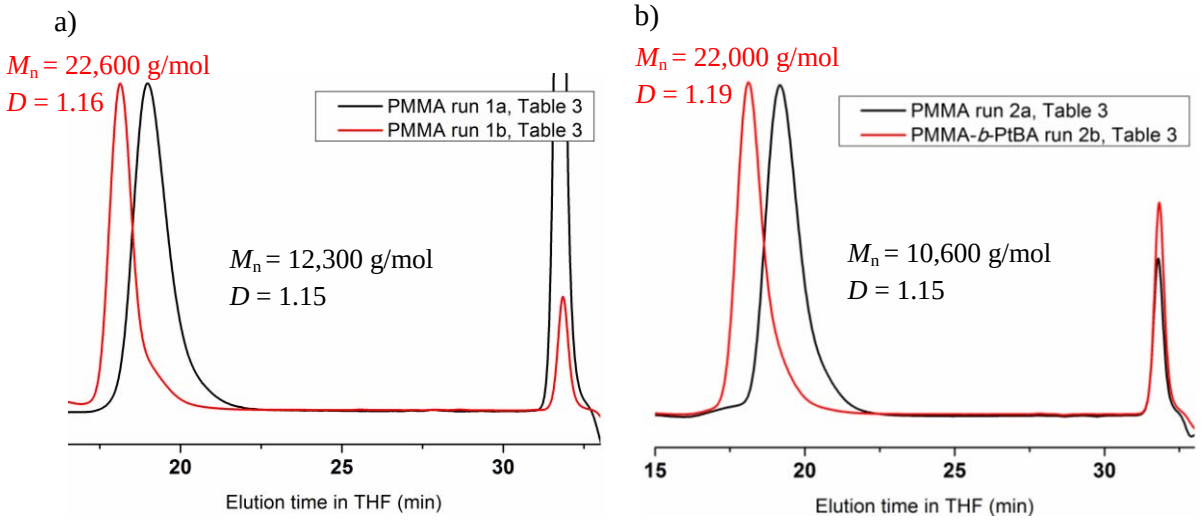

Figure 4. SEC traces (RI detector) of: a) Chain extension of PMMA obtained from the TTMPP-catalyzed GTP in THF (Table 3, run 1); b) PMMA-*b*-P*t*BA obtained from the TTMPP-catalyzed GTP in THF (Table 3, run 2).

4. Investigation of the mechanism and kinetic study

Control experiments in absence of MTS were performed with both MMA (run 10, Table 1) and *t*BA run 5, Table 2), in the presence of TTMPP. Under such conditions, very low conversion (<1%) was obtained after 15 h of reaction between TTMPP and MMA. In contrast, TTMPP alone allowed initiating the polymerization of *t*BA at high concentration ([TTMPP] = 14.6 mM). However, a much lower time scale was noted in this case, compared to the situation prevailing when TTMPP was

employed as a real catalyst ([TTMPP] = 0.19 mM, Table 2, run 5 *vs* run 1). These results indicate that MTS plays a key role in the polymerization process, which most probably proceeds *via* a GTP-type mechanism.

The MALDI-ToF mass spectrum of a TTMPP-derived PMMA obtained in THF with an initial $[MTS]_0/[MMA]_0$ ratio of 1/30 (run 4) is shown in Figure 5. A single population of peaks can be observed, with individual peaks being separated by *m/z* equal to 100.12 mass units, which corresponds to the molar mass of one MMA unit. The observed *m/z* values are in perfect agreement with the molar mass of a sodium-complexed PMMA whose silyl ketene acetal chain ends have been hydrolyzed during precipitation and/or by the ionization of the MALDI-ToF analysis. This result further supports that the TTMPP-catalyzed MMA polymerization occurs *via* a GTP process, the molar mass of the final polymer being well-controlled by the initial quantity of MTS.

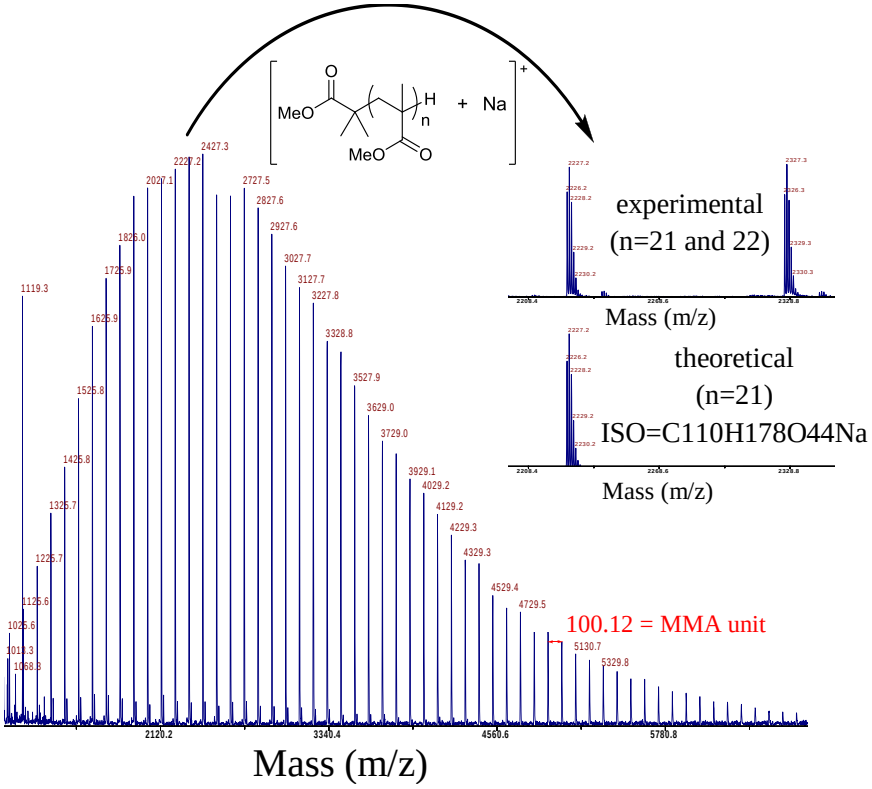

Figure 5. MALDI-ToF MS spectrum in reflector mode of PMMA ($[TTMPP]_0/[MTS]_0/[MMA]_0$ = 0.1/1/30 in THF; run 4, Table 1).

Investigation into the kinetics of the TTMPP-catalyzed GTP of MMA was also undertaken. To this end, it was assumed that MMA polymerizations were first-order in monomer concentration. An initial ratio $[TTMPP]_0/[MTS]_0/[MMA]_0 = 0.1/1/30$ was selected to easily monitor the polymerization kinetics within a relatively short period of time, while preserving the controlled character of the polymerization. Aliquots were taken out periodically and analyzed by ^{1}H NMR to determine the monomer conversion (Figure S1), and by SEC in THF to access experimental molar masses and dispersities.

As depicted in Figure 6a, the molar mass increases linearly with conversion, although experimental M_n values are higher than targeted ones, especially at low monomer conversion. SEC profiles are monomodal and relatively narrow regardless of the reaction time (Figure 6b). The first order kinetic plot clearly exhibits an induction period of about 2 h, after which a linear evolution can be observed (Figure 6c). This induction period may be ascribed to the occurrence of a dissociative GTP mechanism, involving the formation of dormant bis-enolate-type species (see path b, Figure 1). Relatively poor initiation efficiency also characterizes such a dissociative mechanism.[4,49-51] This could explain the discrepancy observed between experimental and expected M_n values during the TTMPP-catalyzed GTP of MMA (Figure 6a). Appearance of an induction period and difference between theoretical and experimental molar masses were already reported, for instance, in the NHC-catalyzed GTP of MMA, which followed a dissociative mechanism.[13] However, it has to be acknowledged that the poor agreement between experimental and targeted M_n values of polymers derived by TTMPP-catalyzed GTP of MMA might also be due to an inappropriate calibration of SEC in the low molar mass region. Monitoring the kinetics of the MTS-initiated TTMPP-catalyzed polymerization of *t*BA was also attempted. However, the polymerization proved much faster with this monomer, in comparison to MMA, so that the conversion could not be determined with accuracy.

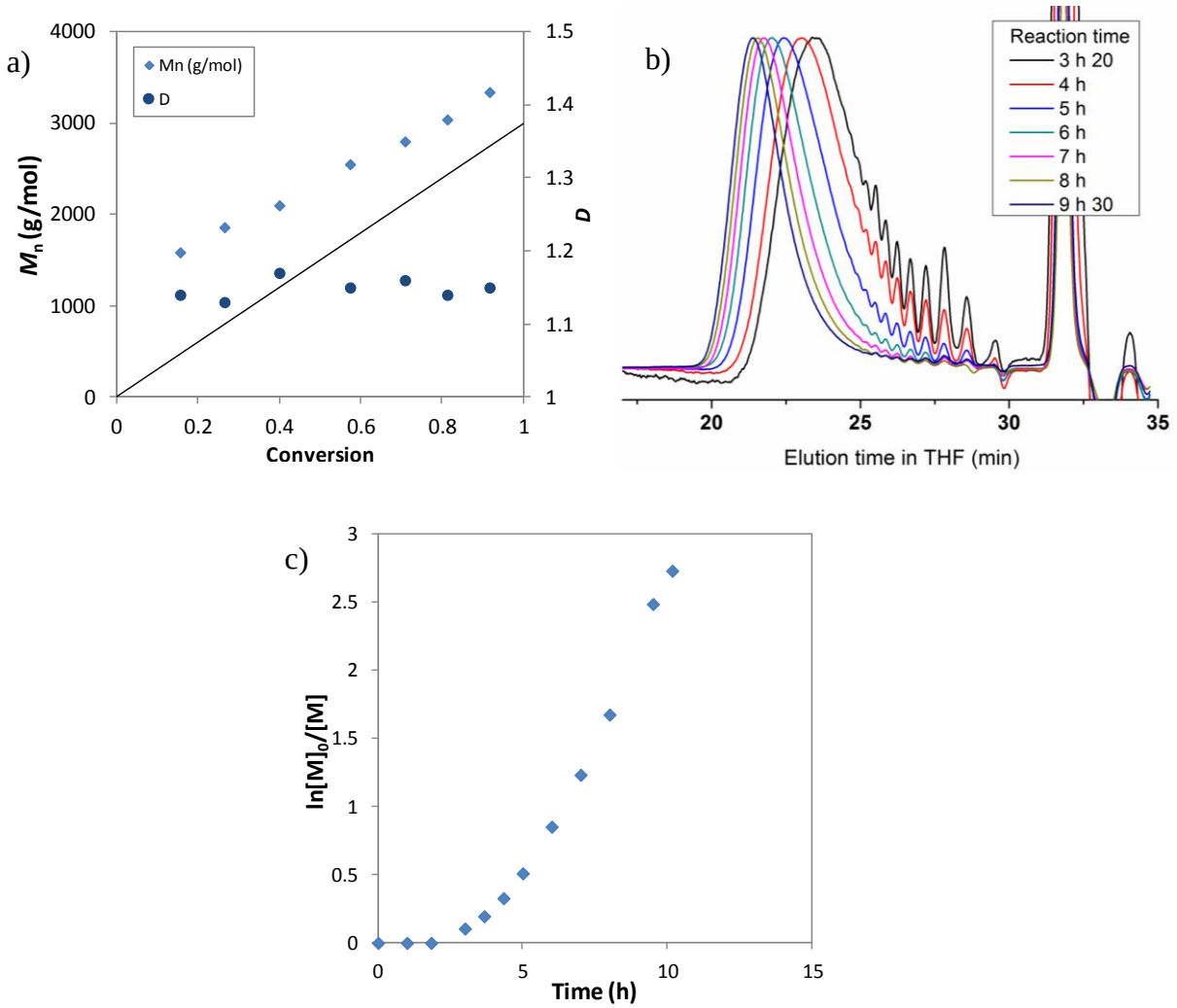

Figure 6. Kinetic study of the TTMPP-catalyzed GTP of MMA in THF ($[TTMPP]_0/[MTS]_0/[MMA]_0$ = 0.1/1/30, $[MMA]_0$ = 2.35M); a) Molar masses (M_n, in blue) and dispersities ($D = M_w/M_n$, in purple) (determined by SEC in THF calibrated with PS standards) *versus* conversion (determined by ^{1}H NMR in $CDCl_3$), Solid line represents theoretical M_n based on $[M]_0/[I]_0$ ratio; b) Corresponding SEC traces (RI detector) ; c) Corresponding first order kinetic plot.

A close look into a typical ^{1}H NMR spectrum of a TTMPP-derived PMMA allowed us to determine its tacticity: *mm/mr/rr* = 0.06/0.41/0.53 (Figure S5). This result is close to that observed from a PMMA synthesized using tris(dimethylamino)sulfonium difluorotrimethylsilicate ($TASF_2SiMe_3$) as a catalyst at 20 °C in THF (*mm/mr/rr* = 0.05/0.39/0.56).[52] Since $TASF_2SiMe_3$ is thought to catalyze GTP *via* a dissociative mechanism,[5,49] this observation is again in favor of the occurrence of such a mechanism when catalyzing GTP with TTMPP.

Previous studies have shown that $TASF_2SiMe_3$ form free enolates when mixed in a 1:1 ratio with MTS at RT.[15] Similar NMR analyses were thus performed here using an equimolar mixture between MTS and TTMPP in THF-d_8. However, ^1H, ^{13}C and ^{29}Si NMR spectra did not show any signal that could be attributable to enolate species, and did not provide any information about possible interactions between TTMPP and MTS (Figures S6-S8). However, as the formation of enolate-type species is likely reversible, such species might not be observable at the NMR timescale, measurements being performed at room temperature.

Conclusion

Among several commercially available trialkyl phosphines, namely tributylphosphine (Bu_3P), tricyclohexylphosphine (Cy_3P), triphenylphosphine (Ph_3P) and tris(2,4,6-trimethoxyphenyl)phosphine (TTMPP), only the latter one was shown to readily catalyze the group transfer polymerization (GTP) of both methyl methacrylate and *tert*-butyl acrylate, in the presence of 1-methoxy-2-methyl-1-[(trimethylsilyl)oxy]prop-1-ene (MTS) as initiator. Polymerizations could be conducted at room temperature in THF, but not in toluene where total inhibition was noted. Poly(methyl methacrylate)s and poly(*tert*-butyl acrylate)s of relatively low dispersities and experimental molar masses in close agreement with targeted values were obtained in this way. Overall, better control of these TTMPP-catalyzed polymerizations was noted with MMA as monomer compared to *t*BA. Poly(methyl methacrylate)-*b*-poly(*tert*-butyl acrylate) block copolymer could also be derived by sequential TTMPP-catalyzed GTP. The GTP of MMA could also be implemented in bulk (solvent-free conditions), while maintaining good control over molar masses and dispersities, likely due to the moderate activity of the TTMPP catalyst in contrast to other nucleophiles, such as *N*-heterocyclic carbenes. First-order kinetic plots revealed an induction period of a few hours during the GTP of MMA catalyzed by TTMPP in THF, which would be consistent with the occurrence of a dissociative mechanism. The obtained poly(methyl methacrylate)s exhibited a tacticity very similar to that of polymethacrylate chains grown from an anionic process, another argument in favor of such a dissociative mechanism. However, the presence of anionic enolate-type species could not be detected

by NMR spectroscopy at room temperature, from 1:1 mixtures between MTS and TTMPP. Current works in our group aim, in one hand, at exemplifying this practical method of control of (meth)acrylic polymerization to macromolecular engineering, through the synthesis of miscellaneous block copolymers and, on the other hand, at elucidating the exact mechanism when employing TTMPP in GTP.

Annexe: Supporting Information

Materials. All experiments were performed under a dry and inert atmosphere using standard Schlenk techniques. Tributylphosphine (Bu_3P; Aldrich, 99%), tricyclohexylphosphine (Cy_3P; Strem, 97%), triphenylphosphine (Ph_3P; Sigma, 98.5%) and tris(2,4,6-trimethoxyphenyl)phosphine (TTMPP; Sigma) were used as received. Methyl methacrylate (MMA; Sigma, 99%), *tert*-butylacrylate (*t*BA; Alfa, 99%) were distilled over CaH_2 into graduated burets and stored at low temperature. 1-Methoxy-2-methyl-1-[(trimethylsilyl)oxy]prop-1-ene (MTS; Sigma, 95%) was distilled over CaH_2 and stored into a Schlenk tube kept at -20 °C in a glovebox. Tetrahydrofuran (THF; technical grade) and toluene were distilled, respectively, over Na/benzophenone and polystyryl lithium prior to use.

Instruments. ^{1}H NMR (400 MHz) spectra of polymers were recorded on a Bruker AC-400 spectrometer in $CDCl_3$. ^{1}H, ^{13}C, ^{19}F and ^{29}Si NMR spectra of MTS/phosphine mixtures in a 1/1 ratio were performed in dry THF-d_8 in Young-tubes under inert atmosphere on the same instrument. Molar masses of polymers samples were determined by size exclusion chromatography (SEC) using a 3-column set of TSK gel TOSOH (G4000, G3000, G2000 with pore sizes of 20, 75 and 200 Å respectively, connected in series) calibrated with PS standards with THF as eluent (1 mL/min) and trichlorobenzene as a flow marker at 40 °C, using both refractometric and UV detectors (Varian). MALDI-ToF spectrometry was performed using a Voyager-DE STR (Applied Biosystems) spectrometer equipped with a nitrogen laser (337 nm), a delay extraction and a reflector. The instrument is equipped with a pulsed N_2 laser (337 nm) and a time-delayed extracted ion source. Spectra were recorded in the positive-ion mode using the reflectron and with an accelerating voltage of 20 kV. Samples were dissolved in THF at 10 mg/mL. The IAA matrix (Indole acrylic acid) solution was prepared by dissolving 10 mg in 1 mL of THF. A MeOH solution of cationization agent (NaI, 10 mg/mL) was also prepared. The solutions were combined in a 10:1:1 volume ratio of matrix to sample to cationization agent. One to two microliters of the obtained solution was deposited onto the sample target and vacuum-dried.

Group transfer polymerization of methyl methacrylate. In a typical procedure, 63.5 µL (3.13×10^{-4} mol) of MTS and 16.7 mg (3.13×10^{-5} mol) of TTMPP were added in a Schlenk tube in the glovebox. After removal of the Schlenk tube from the glovebox, 4 mL of THF were introduced under vacuum. After 5 min homogenization, 1 mL MMA (9.4×10^{-3} mol) was added drop by drop over 5 min at 25 °C. After 13 h at RT, the polymerization was quenched by exposure to air. An aliquot of the polymerization mixture was taken to determine the conversion by ^{1}H NMR in $CDCl_3$ (100%, Figure S2). Molecular characteristics were determined by SEC (Table 1): M_n = 3,000 g/mol, D = 1.23 (RI detection).

Group transfer polymerization of *tert*-butyl acrylate. In a typical procedure, 127 µL (6.26×10^{-4} mol) of MTS and 3.3 mg (6.20×10^{-6} mol) of TTMPP were added in a Schlenk tube in the glovebox. After removal of the Schlenk tube from the glovebox, 2 mL of THF were introduced under vacuum. After 5 min homogenization, 2 mL *t*BA (1.4×10^{-2} mol) was added drop by drop over 5 min at 25 °C. After 2 h at RT, the polymerization was quenched by exposure to air. An aliquot of the polymerization mixture was taken to determine the conversion by ^{1}H NMR in $CDCl_3$ (99%, Figure S3). Molecular characteristics were determined by SEC (Table 2): M_n = 3,100 g/mol, D = 1.4 (RI detection).

Polymerizations in solution using different catalysts or monomer were carried out using a similar procedure. Polymerizations in bulk were performed by rapid addition of MTS on a solution of phosphine in MMA which was previously allowed for stirring for overnight.

Synthesis of PMMA-*b*-P*t*BA block copolymers by sequential GTP. In a typical procedure, 63.5 µL (3.13×10^{-4} mol) of MTS and 16.7 mg (3.13×10^{-5} mol) of TTMPP were added in a Schlenk in the glovebox. After removal of the Schlenk tube from the glovebox, 12 mL of THF were introduced under vacuum. After 5 min homogenization, 3.3 mL MMA (3.1×10^{-2} mol) were added drop by drop over 10 min at 25 °C. After one day at RT, an aliquot of the polymerization mixture was withdrawn. The conversion was determined by ^{1}H NMR measurement in $CDCl_3$ (100%). The polymer was analyzed by SEC (RI detector): M_n = 10,600 g/mol, D = 1.15. Onto the living PMMA, 4.3 mL *t*BA (2.9×10^{-2} mol) were added dropwise over 15 min at 25 °C. After 1.5 days, the reaction was quenched. The

conversion was analyzed by ^{1}H NMR measurement in $CDCl_3$ (100%). Molecular characteristics of the copolymer were determined by SEC (see Table 3): M_n = 22,000 g/mol, D = 1.19 (RI detection).

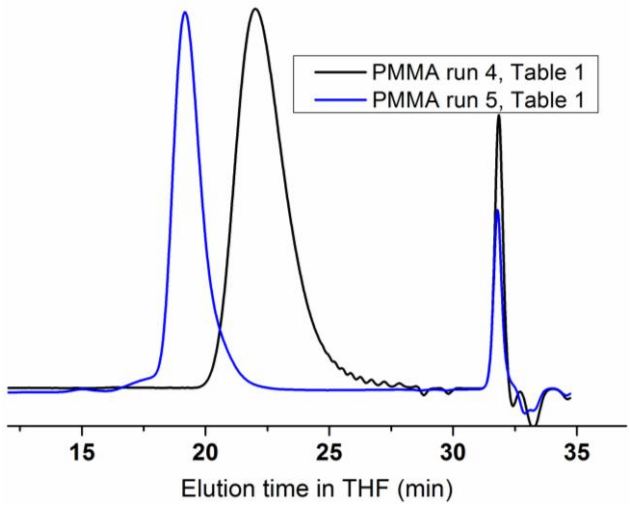

Figure S1. SEC traces (RI detector) of PMMA's obtained from the TTMPP-catalyzed GTP of MMA in THF (Table 1, runs 4-5).

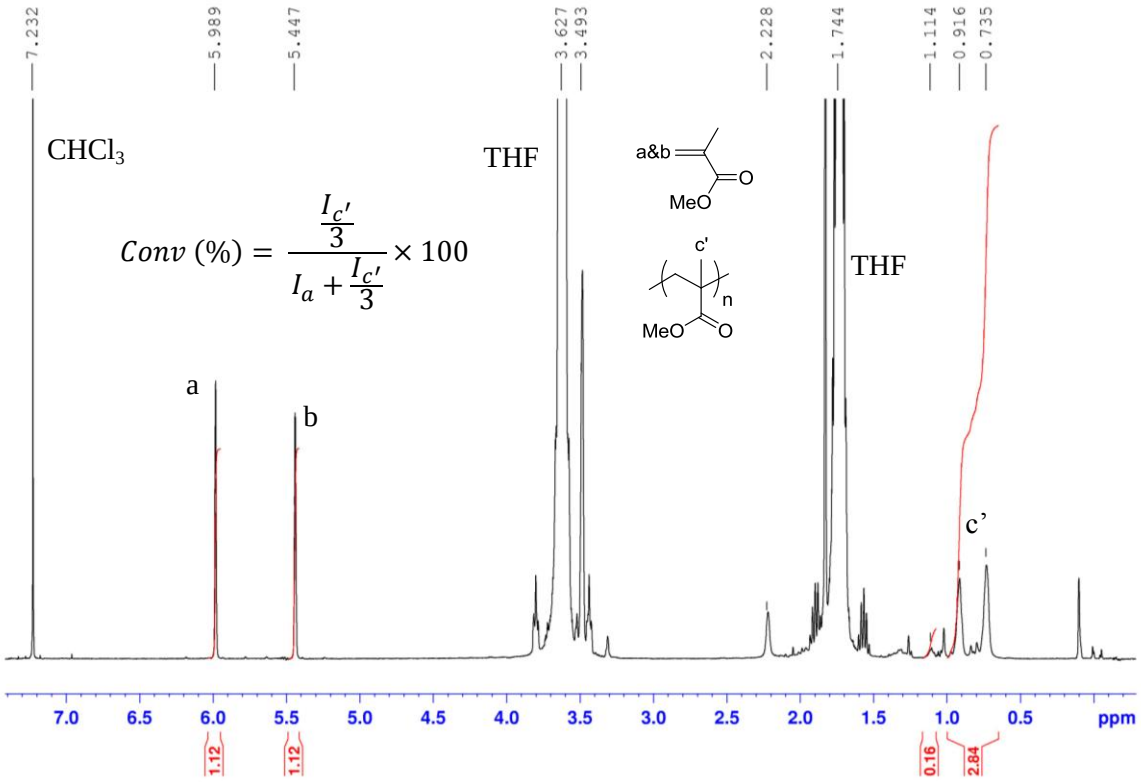

$$Conv\ (\%) = \frac{\frac{I_{c'}}{3}}{I_a + \frac{I_{c'}}{3}} \times 100$$

Figure S2. ^{1}H NMR spectrum in $CDCl_3$ to determine the conversion during GTP of methyl methacrylate in THF.

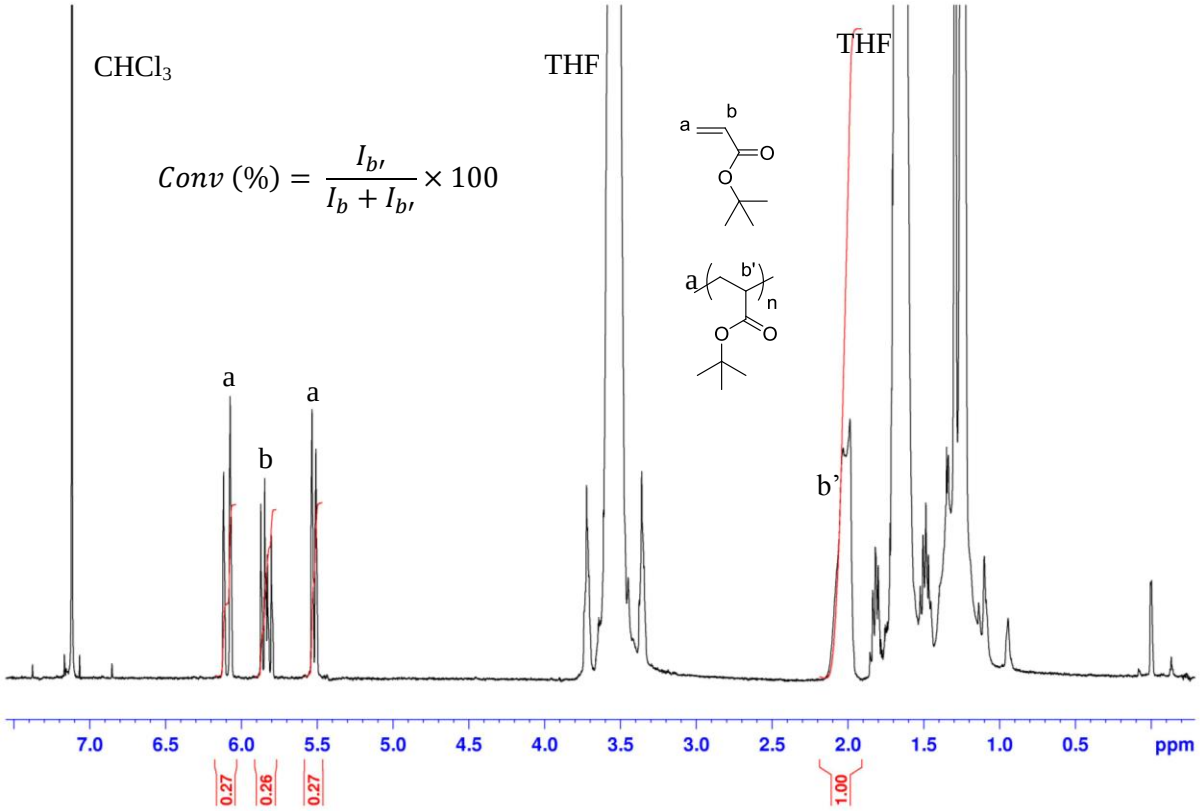

Figure S3. ^{1}H NMR spectrum in $CDCl_3$ to determine the conversion during GTP of *tert*-butyl acrylate in THF.

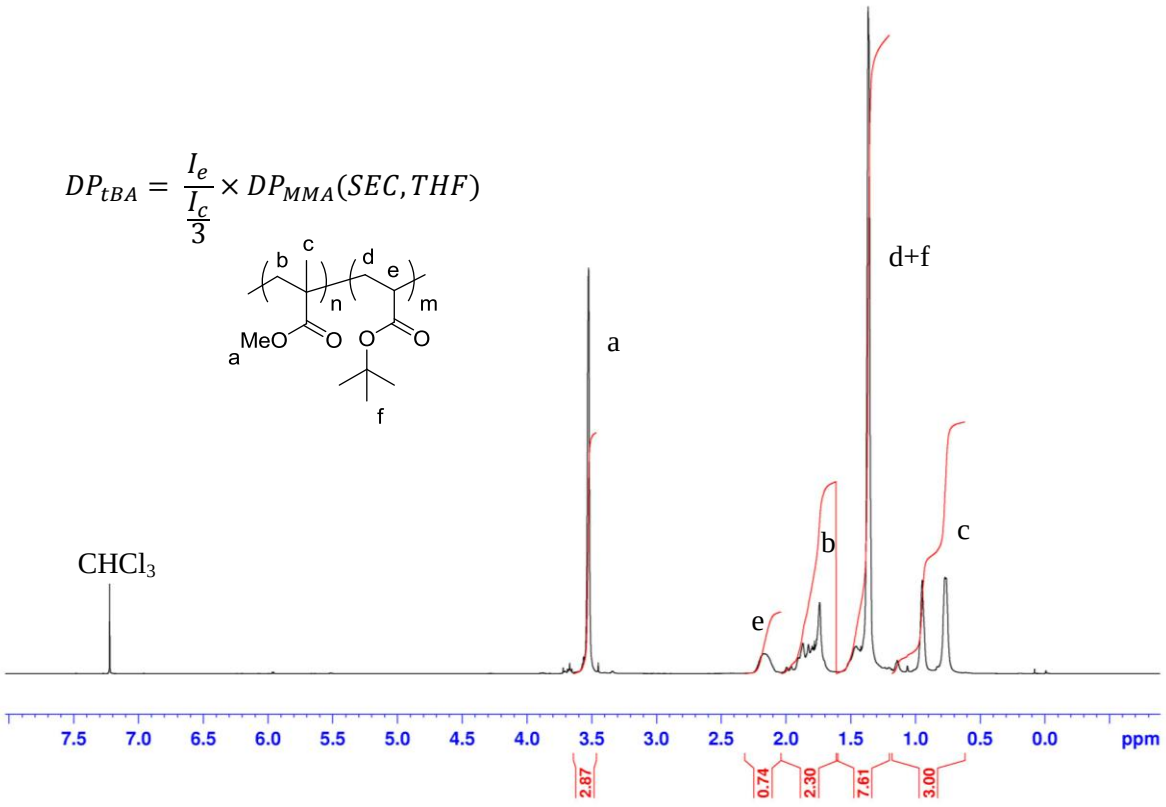

Figure S4. ^{1}H NMR spectrum in $CDCl_3$ of PMMA-*b*-P*t*BA synthesized by TTMPP-catalyzed GTP.

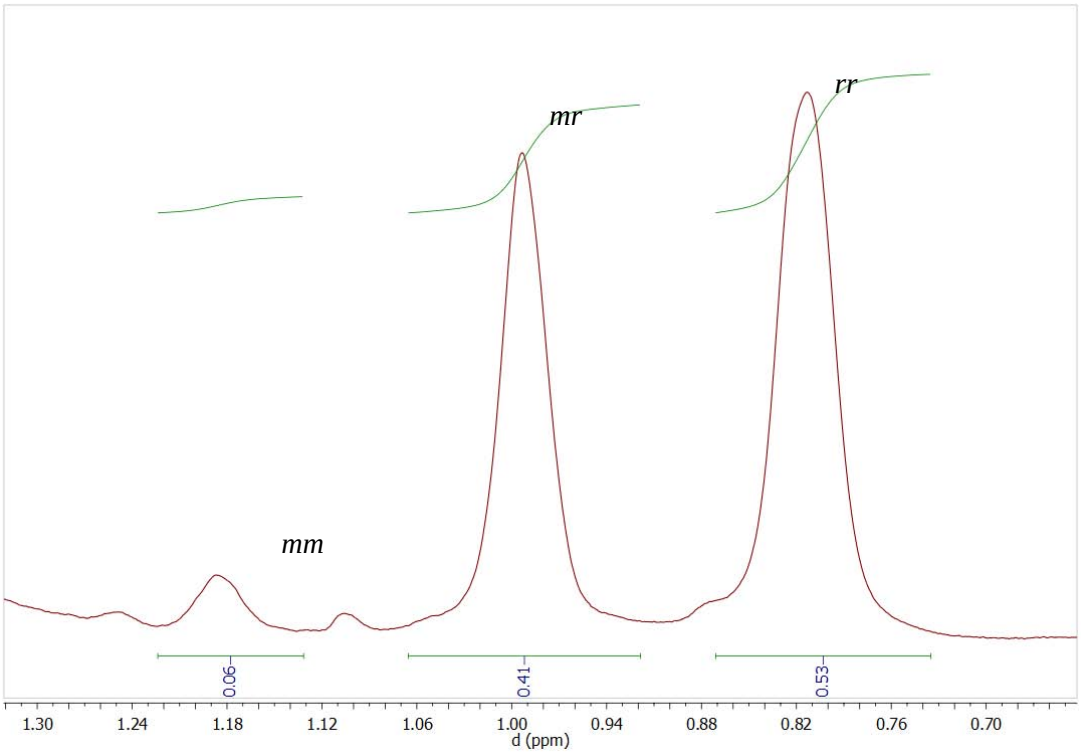

Figure S5. ^{1}H NMR spectrum of PMMA synthesized *via* TTMPP-catalyzed GTP.

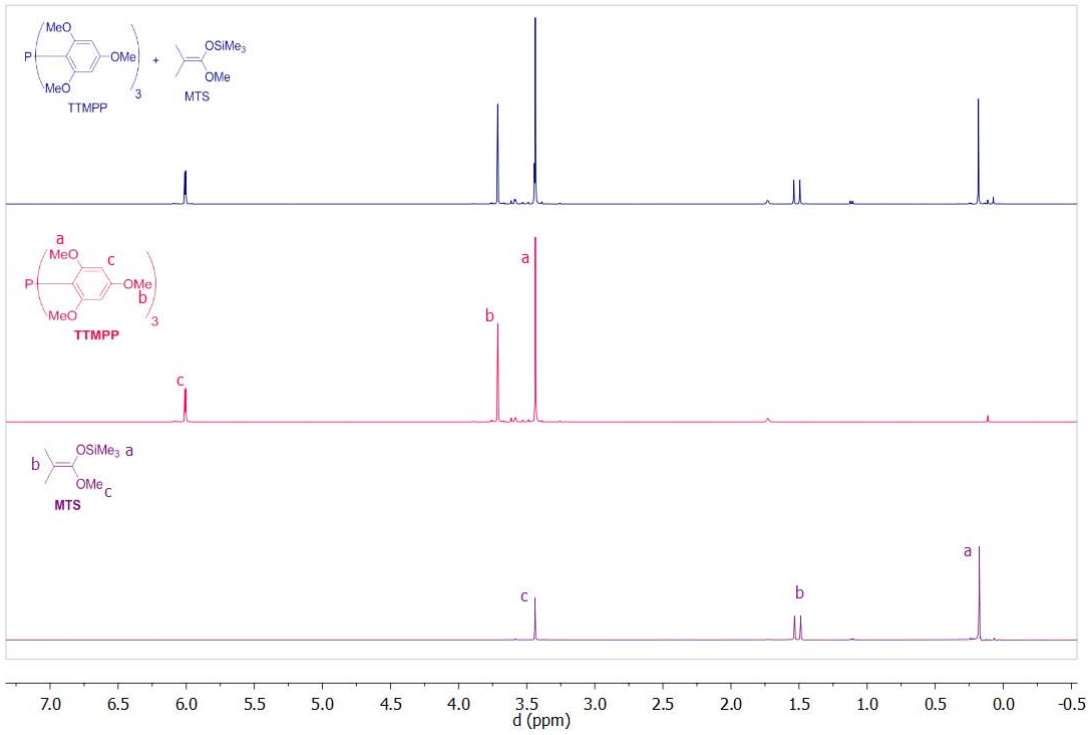

Figure S6. ^{1}H NMR spectra in THF-d_8 of (from bottom to top): MTS, TTMPP and 1/1 mixture between MTS and TTMPP.

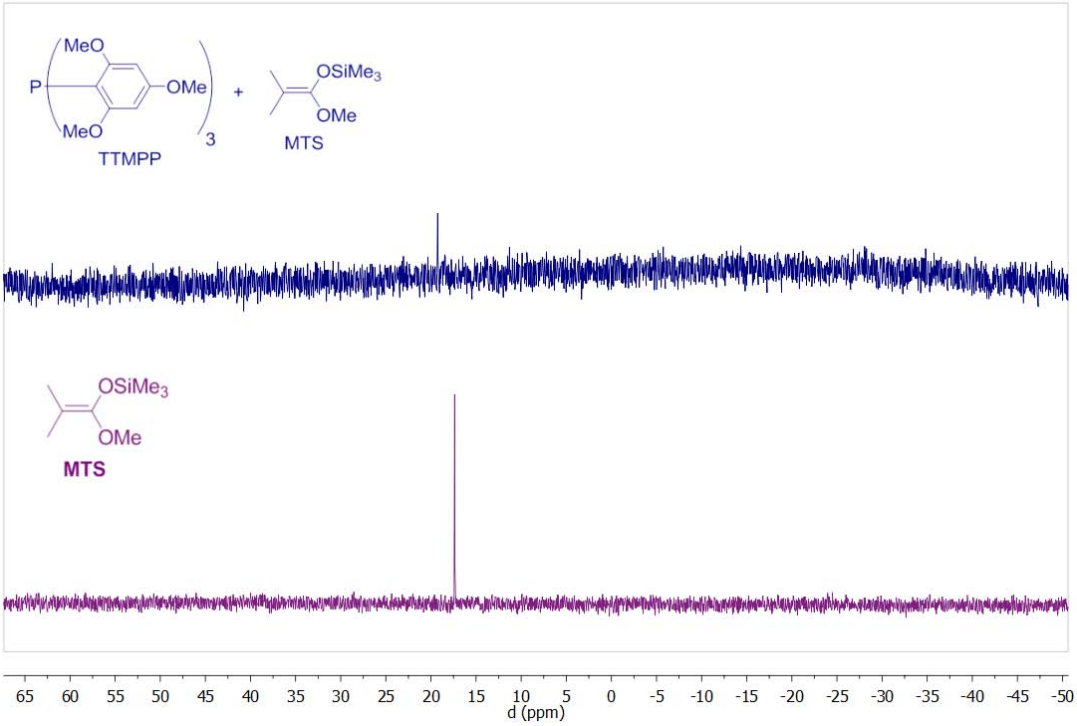

Figure S7. ^{29}Si NMR spectra in THF-d_8 of (from bottom to top): MTS and 1/1 mixture between MTS and TTMPP.

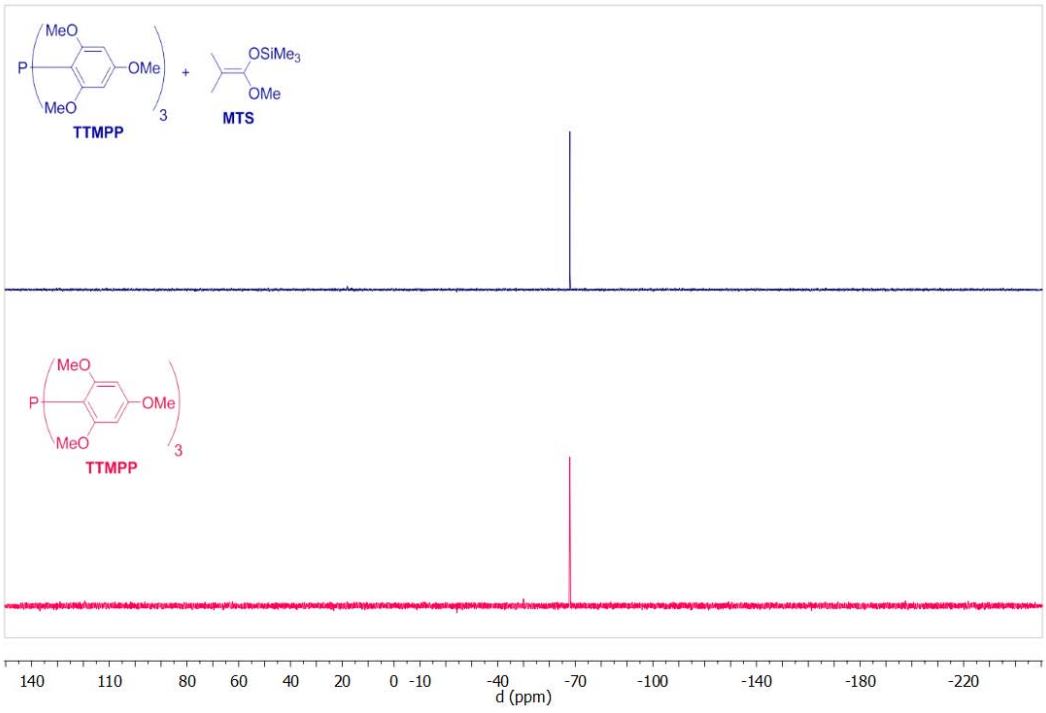

Figure S8. ^{31}P NMR spectra in THF-d_8 of (from bottom to top): TTMPP and 1/1 mixture between MTS and TTMPP.

References

1. Fevre, M.; Vignolle, J.; Heroguez, V.; Taton, D., *Macromolecules* **2012**, *45*, 7711.
2. Webster, O. W.; Hertler, W. R.; Sogah, D. Y.; Farnham, W. B.; RajanBabu, T. V., *J. Am. Chem. Soc.* **1983,** *105*, 5706.
3. Webster, O. W., *J. Polym. Sci., Part A: Polym. Chem.* **2000,** *38*, 2855.
4. Quirk, R. P.; Kim, J.-S., *J. Phys. Org. Chem.* **1995,** *8*, 242.
5. Webster, O. W., In *New Synthetic Methods*, Springer Berlin / Heidelberg: 2004; Vol. 167, p 257.
6. Pafiti, K. S.; Mastroyiannopoulos, N. P.; Phylactou, L. A.; Patrickios, C. S., *Biomacromolecules* **2011,** *12*, 1468.
7. Kassi, E.; Loizou, E.; Porcar, L.; Patrickios, C. S., *Eur. Polym. J.* **2011,** *47*, 816.
8. Butun, V.; Taktak, F. F.; Tuncer, C., *Macromol. Chem. Phys.* **2011,** *212*, 1115.
9. Iatridi, Z.; Mattheolabakis, G.; Avgoustakis, K.; Tsitsilianis, C., *Soft Matter* **2011,** *7*, 11160.
10. Ward, M. A.; Georgiou, T. K., *Soft Matter* **2012,** *8*, 2737.
11. Brittain, W. J., *Rubber Chem. Technol.* **1992,** *65*, 580.
12. Kiesewetter, M. K.; Shin, E. J.; Hedrick, J. L.; Waymouth, R. M., *Macromolecules* **2010,** *43*, 2093.
13. Scholten, M. D.; Hedrick, J. L.; Waymouth, R. M., *Macromolecules* **2008,** *41*, 7399.
14. Raynaud, J.; Ciolino, A.; Baceiredo, A.; Destarac, M.; Bonnette, F.; Kato, T.; Gnanou, Y.; Taton, D., *Angew. Chem. Int. Ed.* **2008,** *47*, 5390.
15. Raynaud, J.; Gnanou, Y.; Taton, D., *Macromolecules* **2009,** *42*, 5996.
16. Raynaud, J.; Liu, N.; Gnanou, Y.; Taton, D., *Macromolecules* **2010,** *43*, 8853.
17. Raynaud, J.; Liu, N.; Fevre, M.; Gnanou, Y.; Taton, D., *Polym. Chem.* **2011,** *2*, 1706.
18. Chen, Y.; Fuchise, K.; Narumi, A.; Kawaguchi, S.; Satoh, T.; Kakuchi, T., *Macromolecules* **2011,** *44*, 9091.
19. Kakuchi, T.; Chen, Y.; Kitakado, J.; Mori, K.; Fuchise, K.; Satoh, T., *Macromolecules* **2011,** *44*, 4641.
20. Hsu, J.-C.; Chen, Y.; Kakuchi, T.; Chen, W.-C., *Macromolecules* **2011,** *44*, 5168.
21. Kakuchi, R.; Chiba, K.; Fuchise, K.; Sakai, R.; Satoh, T.; Kakuchi, T., *Macromolecules* **2009,** *42*, 8747.
22. Fuchise, K.; Sakai, R.; Satoh, T.; Sato, S.-i.; Narumi, A.; Kawaguchi, S.; Kakuchi, T., *Macromolecules* **2010,** *43*, 5589.
23. Zhang, Y.; Lay, F.; García-García, P.; List, B.; Chen, E. Y. X., *Chem. Eur. J.* **2010,** *16*, 10462.
24. Takada, K.; Fuchise, K.; Chen, Y.; Satoh, T.; Kakuchi, T., *J. Polym. Sci., Part A: Polym. Chem.* **2012,** *50*, 3560.
25. Zhang, Y.; Chen, E. Y. X., *Macromolecules* **2007,** *41*, 36.
26. Zhang, Y.; Chen, E. Y. X., *Macromolecules* **2008,** *41*, 6353.
27. Miyake, G. M.; Zhang, Y.; Chen, E. Y. X., *Macromolecules* **2010,** *43*, 4902.
28. Zhang, Y.; Gustafson, L. O.; Chen, E. Y. X., *J. Am. Chem. Soc.* **2011,** *133*, 13674.
29. Crabtree, R. H., *J. Organomet. Chem.* **2005,** *690*, 5451.
30. Ohsawa, S.; Morino, K.; Sudo, A.; Endo, T., *Macromolecules* **2010,** *43*, 3585.
31. Cronin, J. P.; Pepper, D. C., *Makromol. Chem.* **1988,** *189*, 85.
32. Myers, M.; Connor, E. F.; Glauser, T.; Möck, A.; Nyce, G.; Hedrick, J. L., *J. Polym. Sci., Part A: Polym. Chem.* **2002,** *40*, 844.
33. Cesar, V.; Bellemin-Laponnaz, S., *Actualite Chimique* **2009,** *326*, 8.
34. Vedejs, E.; Diver, S. T., *J. Am. Chem. Soc.* **1993,** *115*, 3358.
35. Marinetti, A.; Voituriez, A., *Synlett* **2010**, 174.
36. Kobayasi, S.; Tsuchiya, Y.; Mukaiyama, T., *Chem. Lett.* **1991,** *20*, 537.
37. Matsukawa, S.; Okano, N.; Imamoto, T., *Tetrahedron Lett.* **2000,** *41*, 103.
38. Matsukawa, S.; Sekine, I., *Synth. Commun.* **2009,** *39*, 1718.
39. Matsukawa, S.; Sekine, I.; Iitsuka, A., *Molecules* **2009,** *14*, 3353.
40. Matsukawa, S.; Tsukamoto, K., *Org. Biomol. Chem.* **2009,** *7*, 3792.
41. Wada, M.; Higashizaki, S., *J. Chem. Soc., Chem. Commun.* **1984**, 482.
42. Allman, T.; Goel, R. G., *Can. J. Chem.* **1982,** *60*, 716.
43. Henderson, W. A.; Streuli, C. A., *J. Am. Chem. Soc.* **1960,** *82*, 5791.
44. Streitwieser, A.; McKeown, A. E.; Hasanayn, F.; Davis, N. R., *Org. Lett.* **2005,** *7*, 1259.
45. Baskaran, D., *Prog. Polym. Sci.* **2003,** *28*, 521.
46. Raynaud, J. *Thesis*, *Université Bordeaux1*, **2010**.
47. Yamasaki, E. N.; Patrickios, C. S., *Eur. Polym. J.* **2003,** *39*, 609.
48. Ballard, D. G. H.; Pickering, A.; Runciman, P. J. I. US Patent 5196489, 1993.
49. Quirk, R. P.; Ren, J., *Macromolecules* **1992,** *25*, 6612.
50. Quirk, R. P.; Bidinger, G. P., *Polym. Bull.* **1989,** *22*, 63.

51. Mueller, A. H. E., *Macromolecules* **1994,** *27*, 1685.
52. Sogah, D. Y.; Hertler, W. R.; Webster, O. W.; Cohen, G. M., *Macromolecules* **1987,** *20*, 1473.

Conclusion Générale et Perspectives

Ce travail de thèse visait à palier certaines difficultés liées à l'utilisation des carbènes *N*-hétérocycliques (NHCs) en tant que catalyseurs organiques de réactions de polymérisation. Comme premier objectif, nous souhaitions disposer de précurseurs de NHCs, faciles à synthétiser et à manipuler, notamment à l'air, et permettant de générer les NHCs dans des conditions douces. Un autre objectif était de développer une plateforme multitâche de catalyseurs organiques (non-métalliques) afin d'élargir le champ des monomères polymérisables par les NHCs. Enfin, nous souhaitions mettre en lumière le potentiel, encore peu exploité, des phosphines en tant que catalyseurs organiques de polymérisation.

Pour répondre au premier point mentionné, nous avons conçu de nouveaux précurseurs de NHCs, stables à l'air, et par conséquent facilement manipulables. Par simple échange d'anion d'un bromure d'azolium commercial avec $KHCO_3$, divers hydrogénocarbonates d'azolium, notés [NHC(H)][HCO_3], ont d'abord été synthétisés en une seule étape. En solution, ces espèces sont à l'équilibre avec leurs homologues carboxylates d'azolium (adduits zwittérioniques de NHC avec le CO_2, notés NHC-CO_2). L'étude en phase solide des composés [NHC(H)][HCO_3] a ensuite permis de mettre en évidence, pour la première fois, qu'il était possible de générer un NHC par chauffage d'un précurseur [NHC(H)][HCO_3].

Des calculs théoriques (DFT) ont permis d'étayer le fait que les NHCs sont générés depuis leurs précurseurs [NHC(H)][HCO_3] par perte formelle de H_2CO_3, *via* un mécanisme concerté mettant en jeu des barrières énergétiques faibles (<12 kcal/mol).

Ces précurseurs ont ensuite permis d'accéder très facilement, c'est-à-dire sans avoir besoin de travailler en conditions inertes, à divers complexes organométalliques (à base de Pd et d'Au), par transfert du NHC sur le substrat métallique. Enfin, le potentiel des [NHC(H)][HCO_3] comme précurseurs de NHCs a été confirmé et leur potentiel catalytique a été évalué et comparé avec celui des adduits NHC-CO_2 correspondants. Diverses réactions de chimie moléculaire (cyanosilylation, condensation de la benzoine et transestérification), ainsi que des réactions de polymérisation (ROP du lactide et GTP du méthacrylate de méthyle) ont ainsi pu être déclenchées en utilisant des

[NHC(H)][HCO_3] comme pré-catalyseurs, à température ambiante, plus probablement par un effet de solvatation.

Pour atteindre le deuxième objectif, nous avons tenté d'associer des NHCs à des co-activateurs non-métalliques (de type silane ou borane) pour induire des réactions de polymérisation par un effet de double assistance (acide/base de Lewis). La stratégie générale choisie ici a consisté à associer un acide de Lewis (spirosilane, SiR_4 ou tris(pentafluorophenyl)borane, $B(C_6F_5)_3$) à la base de Lewis NHC dans l'espoir que les deux entités agissent coopérativement par effet "push-pull". Dans cette partie de l'étude, plusieurs combinaisons entre acide de Lewis et NHC ont été testées. Les interactions au sein de ces "paires de Lewis" ont été systématiquement analysées.

Nous avons par exemple mis en évidence qu'avec des acides de Lewis de type silane, l'encombrement des substituants du NHC joue un rôle prépondérant sur la nature du composé d'addition formé (adduit "classique" acide/base de Lewis *vs.* paire de Lewis dite frustrée). Ces paires de Lewis ont alors été utilisées pour isoler l'intermédiaire présumé, dit "de Breslow", de la réaction de condensation de la benzoine.

Une paire de Lewis $B(C_6F_5)_3$/NHC, dont l'adduit "classique" a pu être caractérisé, a ensuite été employée pour la polymérisation zwitterionique du méthacrylate de méthyle. En jouant sur l'ordre d'addition des réactifs (solution de monomère activée par l'acide de Lewis ajoutée sur une solution de NHC), les interactions entre acide et base de Lewis ont pu être minimisées. En utilisant des conditions expérimentales spécifiques, la polymérisation présente un certain contrôle. Des analyses MALDI-ToF effectuées sur des PMMAs de faibles masses ont indiqué que la plupart des chaines, après terminaison, sont dotées d'un groupement imidazolium en position α.

L'étude cinétique a montré que cette méthode de polymérisation est caractérisée par une étape d'amorçage lente. Cette étape a ensuite été étudiée par RMN et des calculs théoriques (DFT) ont été réalisés, ce qui a permis de proposer qu'une quantité très faible d'espèces actives intervient au début de la réaction. Le rôle clé de l'acide de Lewis de type $B(C_6F_5)_3$ en tant qu'activateur de la polymérisation a cependant été confirmé.

La conception des paires de Lewis doit donc être adaptée à l'application visée (chimie

moléculaire, polymérisation des oxiranes ou des monomères moins polaires, etc…). Par exemple, aux vues des limitations déjà observées pour polymériser le méthacrylate de méthyle avec $B(C_6F_5)_3$, des composés possédant une acidité de Lewis plus forte sont certainement à considérer pour permettre d'activer de façon efficace les monomères non-polaires. Ces aspects sont actuellement traités dans un autre travail de thèse au laboratoire (dans le cadre d'un projet ANR démarré en 2011).

Enfin, dans la dernière partie de ce travail de thèse, le potentiel des phosphines à catalyser la polymérisation par transfert de groupe des (méth)acrylates d'alkyle a été évalué. Parmi toutes les phosphines testées, seule la tris(2,4,6-triméthoxyphényl)phosphine (TTMPP) a été en mesure de catalyser la polymérisation du méthacrylate méthyle (MMA) et de l'acrylate de *tert*-butyle (*t*BA). La réaction s'effectue à température ambiante, dans le THF ou en masse en utilisant le 1-méthoxy-2-méthyl-1-[(triméthylsilyl)oxy]prop-1-ène (MTS) en tant qu'amorceur. La polymérisation est "vivante/contrôlée" et un copolymère à blocs PMMA-*b*-P*t*BA a même pu être synthétisé par GTP séquentielle. La cinétique et la tacticité des PMMAs obtenus seraient en faveur d'un mécanisme dissociatif mais la RMN n'a pas permis l'isolation des espèces de type énolate mises en jeu dans ce mécanisme.

Ce travail de thèse offre donc des perspectives prometteuses pour permettre une utilisation plus variée des NHCs et des phosphines en tant que catalyseurs/activateurs organiques pour des réactions de chimie (macro)moléculaires). Enfin, aux vues de la valorisation grandissante des matériaux polymères synthétisés par organocatalyse, il est à prévoir que la communauté des polymeristes, comme l'a fait celle des chimistes organiciens avant elle, ne tardera pas à adopter ces organocatalyseurs de façon plus étendue dans les années à venir.

RESUME

Dans ce travail de thèse, plusieurs approches ont été développées pour permettre une utilisation plus variée des carbènes *N*-hétérocycliques (NHCs) et des phosphines en tant que catalyseurs/activateurs organiques.

Les précurseurs de NHCs étudiés dans un premier temps, c'est-à-dire les hydrogénocarbonates d'azolium, peuvent être synthétisés en une seule étape, à l'inverse des NHCs dont la synthèse et l'isolation sont souvent compliquées. Nous avons démontré que ces espèces sont stables à l'air et sont à l'équilibre en solution avec leurs homologues carboxylates d'azolium (adduits NHC-CO_2). Leur utilisation permet donc de faciliter la manipulation des NHCs tout en conservant une activité catalytique satisfaisante tant en synthèse moléculaire qu'en chimie des polymères.

Des paires de Lewis silane ou borane/NHC ont ensuite été employées afin d'augmenter le potentiel des NHCs pour des réactions "modèles" de chimie (macro)moléculaire par un effet de double assistance (acide/base de Lewis).

Enfin, une phosphine commerciale a été utilisée pour catalyser la polymérisation par transfert de groupe des (méth)acrylates d'alkyle de façon "vivante/contrôlée".

Mots-clés : Catalyse, Polymérisation, Carbènes *N*-hétérocycliques, Phosphines, Hydrogénocarbonates d'azolium, Carboxylates d'azolium, Paires de Lewis, Double assistance.

SUMMARY

In this thesis work, some points are adressed in order to broaden the scope of the application of *N*-heterocyclic carbenes (NHCs) as organic catalysts/activators.

The novel NHC precursors studied first, i.e. azolium hydrogen carbonates, are synthesized in a one-step undemanding process, in contrast to NHCs whose synthesis and isolation is often a tedious procedure. We then showed that these species are air-stable and are at the equilibrium, in solution, with their azolium-2-carboxylates homologues (NHC-CO_2 adducts). The use of such precatalysts thus allows facilitating the manipulation of NHCs, while maintaining an efficient catalytic activity in molecular chemistry as well as in polymer synthesis.

We then proposed to use NHCs in conjunction with organic Lewis acids (silanes or boranes) as a possible means to induce a cooperative dual activation mechanism (Lewis acid/base) in order to increase the potential of NHCs for "model" (macro)molecular reactions.

Finally, a commercial phosphine was used to trigger the group transfer polymerization of alkyl (meth)acrylates in a "controlled/living" fashion.

Keywords : Catalysis, Polymerization, *N*-heterocyclic carbenes, Phosphines, Azolium hydrogen carbonates, Azolium-2-carboxylates, Lewis Pairs, Dual activation.

Laboratoire de Chimie des Polymères Organiques
16 avenue Pey Berland
F-33607 Pessac